Development and *in vitro* evaluation of an alternative thermo-tolerant antimicrobial polymer for the prevention and treatment of bovine mastitis

by

Kevin Masterson (Hons) Biochemistry

Thesis submitted to

Faculty of Science and Health, Technological University of the Shannon Midlands Midwest (TUS)

In partial fulfilment of the requirements for the

Doctorate of Philosophy (PhD) Degree in Microbiology

Submitted

May 2023

Based on the research carried out under the supervision of

Professor Neil J Rowan, Dr Ian Major, and Dr Mark Lynch

with TUS Presidential Doctorate funding support

(AIT-2017-008).

I. Abstract

Despite advancements in veterinary medicine, bovine mastitis remains one of the most significant and prevalent diseases in Irish dairy herds. Raw milk represents one of Ireland's main food exports and as DAFM Food-Wise 2025 aims to increase food exports by 85%, coupled with the removal of the EU Milk Quota in March 2015, there is need for improved milk yields from Irish farms. Bovine mastitis is an inflammatory infection of the mammary gland, which is a major constraint on milk production, causing animals discomfort, health complications, production of poor-quality milk and when treated using conventional means, requires their removal from the herd. There are several prevention plans being implemented but the use of antibiotics remains the only recognised means of treatment, which requires a cool-off period to ensure no traces of antibiotics enter the food supply. Due to emerging antibiotic resistance, there is an ever-increasing demand for antibiotic-free treatments in all fields of medicine; thus, highlighting the need for developing new or alternative treatments targeting infectious diseases such as mastitis.

In this study, four thermo-tolerant bioactives (nisin, silver nitrate, zinc oxide and chitosan) were evaluated in order to determine their suitability as alternatives for antibiotics in the treatment of bovine mastitis. They will be assessed for their antimicrobial capabilities as well as their suitability for polymer incorporation through hot-melt extrusion (HME), which would greatly open their potential applications and uses. Well established methods in the evaluation of antibiotics and other antimicrobial compounds were utilised to allow comparisons with published literature and already well-established antimicrobials. Additional methods have also been implemented and developed to assess the antibiofilm capabilities of the bioactives, and other methods commonly used in pharmaceutical studies for determining combinational potential of the compounds in terms of a synergy assessment.

Methods: The four bioactives were first incorporated into a polymer matrix of PVP-VA64 through hot-melt extrusion (HME) as a means to access this novel route of therapeutic delivery. Broth microdilution assays were utilized to evaluate the microbial growth inhibition capabilities of each bioactive, before and after HME, and to determine their individual minimum inhibitory concentration (MIC) against four bacterial strains, *E. coli*, *S. aureus*, *S. epidermidis* and *P. aeruginosa*. Growth inhibition was determined by measuring absorbance

while secondary analysis was carried out by use of the extra-cellular dye, resazurin. MIC studies were conducted on a number of veterinary isolate strains, some of which have demonstrated antimicrobial resistance (AMR). The biofilm disruptive capabilities of each bioactive was assessed against *S. aureus* and *P. aeruginosa* biofilms. A novel protocol was developed to assess bioactive effects upon the three stages of biofilm development, attachment, growth, and maturity. Thereafter, the bioactives were assessed in arrangements of two, three and four drug combinations to determine their synergistic capabilities for inhibiting *E. coli*, *S. aureus* and *S. epidermidis* growth. The synergistic relationship between bioactive activity was evaluated by a new analytical system developed using the Python coding language, allowing for high-throughput evaluation and quantification.

In vitro experiments were then conducted in order to determine the cytotoxic and inflammatory potential of the bioactives against bovine mammary epithelial (BME) cells. To assess the bioactive cytotoxicity, BME cells were treated with each bioactive at a range of concentrations, and cell viability was determined by use of the MTT assay. Cells were also treated and assessed to determine their inflammatory response, by determining changes in the expression of the cytokines TNFα, IL-1β, IL-6 and IL-8. Relative expression was determined by use of RT-qPCR using β-actin as the reference housekeeping gene.

Results: The four bioactives were found to exhibit satisfactory antimicrobial inhibitory effects, before and after their incorporation into a polymer matrix against *E. coli*, *S. aureus*, *S. epidermidis* and *P. aeruginosa*. Bioactive studies against veterinary and reference strain bacterial isolates also exhibited promising findings in terms of addressing AMR. Assessment of the biofilm disruptive capabilities highlighted varying degrees of bioactive efficacy. Furthermore, this study generated novel data that will advance the field of biofilm innovation. The inclusion of a novel anti-attachment step in the anti-biofilm assessment process holds great potential as a pivotal source of data, informing future preventative measures against biofilms and biofilm-mediated infections. The novel anti-attachment step included in the present study generated important revealing the bioactives effect upon the initial stages of biofilm development. While some results varied greatly with some treatments (such as $AgNO_3$) causing notable decreases in biofilm growth against *P. aeruginosa*, but causing increased *S. aureus* biofilm growth, the study shows the import of considering such scenarios.

Synergistic combinational assessments yielded enormous amounts of data for the named bioactives tested, with the majority showing clear synergistic capabilities when combined. This data also exhibited interesting trends such as how therapeutic behaviour can change unpredictably depending upon the combination of bioactives used. Results show how two or more drugs can interact differently with each other when they are at the active site of treatment, and how their activity can change. While the primary intention is for positive therapeutic reinforcement of activity (i.e. synergy), certain bioactives were shown to inhibit each other (i.e. antagonism). While antagonistic interactions are not favourable, they are equally valuable data points to consider when preparing combinational therapies as these combinations can be reduced to limit such antagonism. The most interesting finding from this section involved the use of nisin, a lantibiotic unable to affect gram-negative bacteria, which was shown to have a definite effect when used in combination with other bioactives (primarily $AgNO_3$ and Chitosan) which was a hugely significant finding that carried the hypothesis of the combination studies. Previously used combination/synergy predictive models would claim there would be no effect between these compounds, whereas in the present study it was proven that there was an effect. This constitutes the first study that exploits a three-drug combinational study for these bioactives and the only four-drug conducted study of any therapeutic compounds.

Cytotoxic assessment of the bioactives reported negative effects when using $AgNO_3$ and ZnO with BME cells. Both $AgNO_3$ and ZnO were quite toxic to the cells *in vitro*, however as per results from other studies carried out during this project, both bioactives still hold great potential for inclusion in a final treatment solution. For example, combinational report much lower required concentrations of each which enables the potential of using sub-toxic concentrations of each compound that may still hold notable anti-microbial effect. Furthermore, inflammatory assessment revealed interesting effects upon cytokine expressions. $AgNO_3$ was noted to produce a strong anti-inflammatory response, as noted by the reduced expression of the pro-inflammatory cytokines, TNFα, IL-1β, IL-6 and IL-8. Reduced expression of such cytokines is a key indicator of reduced inflammation, which holds great promise for the treatment of inflammatory diseases, such as mastitis. Nisin, chitosan and ZnO also reduced the expression of some target cytokines. Notably, there was no major increase in expression of targeted cytokines using the aforementioned bioactives which indicates that

they did not elicit an inflammatory response in the cells. This too is an important characteristic required for treatment of inflammatory diseases.

The findings of this research were published in leading journals that will inform solutions for AMR crisis where this cross-cutting area aligns with the new TUS Strategic Plan 2023-2026.

II. Table of Contents

III. List of Tables & Figures

IV. List of Abbreviations

AM: Automatic Milking.

AMR: Antimicrobial Resistance.

BDCT: Blanket dry cow therapy.

BIs: Biofilm Associated Infections.

BME: Bovine Mammary Epithelial, 35

BMEM: Bovine Mammary Epithelial Proliferation Media.

BSA: Bovine Serum Albumin.

BTSCC: Bulk Tank Somatic Cell Count.

CD: Cell Death.

CM: Clinical Mastitis.

CMT: California Mastitis Test.

CNS: Coagulase-Negative Staphylococci.

EC: Electrical Conductivity.

FIC: Fractional Inhibitory Concentration.

GC: Growth Control, 38

GRAS: Generally Recognised as Safe.

HSA: Highest Single Agent.

IC: Imagery Cytometry.

IDF: International Dairy Federation.

IMI: Intramammary Infections.

IMM: Intramammary.

IRT: Infrared Thermography.

IV. List of Abbreviations

IU: International Units.

LPS: Lipopolysaccharide

MBC: Minimum Bactericidal Concentration.

MBEC: Minimum Biofilm Eradication Concentration.

MH: Mueller-Hinton.

MHB: Mueller-Hinton Broth.

MTT: Methylthiazolyldiphenyl-tetrazolium bromide.

NIRD: The National Institute for Research in Dairying.

NMC: National Mastitis Council.

NPs: Nanoparticles.

PVP/VA-64: poly-vinyl-pyrrolidone/vinyl acetate.

QS: Quorum Sensing.

ROS: Reactive Oxygen Species.

SC: Sterility Control

SCC: Somatic cell count.

SCM: Sub-clinical Mastitis.

SDCT: Selective Dry Cow Therapy.

SKU: Stock Keeping Unit

TFTC: Too Few To Count.

TNTC: Too Numerous To Count.

TSA: Tryptone Soy Agar.

TSE: Twin Screw Extruder.

Tv: Treatment Vehicle.

IV. List of Abbreviations

USST: Udder Skin Surface Temperature.

UT: Untreated.

WHO: World Health Organisation World Health Organisation.

V. Acknowledgements

I would like to thank my supervisors, Professor Neil J. Rowan (Lead), Dr. Ian Major, and Dr. Mark Lynch for their encouragement, help and guidance throughout this project. I was given the support and independence to develop the project beyond its original scope that allowed me to learn and to discover along its meandering journey.

Special thanks to my family for their support. To my parents Maura and David, brother Conor, the Lee and the Caitlin, for everything through the years that helped me get to where I am today. And to my sister Claire, who was another huge source of encouragement and guidance throughout my PhD, helping with so much whenever possible.

I hope the best to all my friends and colleagues who were with me during my time in the Hub. Thank you for all the help, support, nights out and making me feel like I wasn't only one who felt lost sometimes! And to all current and future post-graduates, I wish you all the best of luck!

A big thank you to all of my friends, near and far, for your encouragement and support over the years. Your company has been invaluable, and I wouldn't be who I am or where I am today without it.

Finally, I would like to thank the Technological University of the Shannon for funding this project through their President Seed initiative.

VI. Declaration

I hereby declare the work contained within this thesis, submitted to Technological University of the Shannon: Midlands Midwest for the degree of Doctorate of Philosophy, has not been accepted for the award of any other degree in any other higher education institute, and is entirely my own work and to the best of my knowledge, contains no work previously written or published by another party (except in the case of referenced material)

_____ _____

Kevin Masterson Date

Confidentiality Statement

All of the information in this thesis is confidential and shall not be disclosed to any further parties without the permission of the first author due to intellectual property constraints. Details of the information presented shall be decided upon with the members of the projects prior to public dissemination.

Chapter 1 Introduction

The dairy industry today represents one of the oldest agricultural-based industries while still holding huge significance throughout the world in terms of economics, employment and as a major source of food goods (Garvey, Curran, and Savage 2017). The value of the industry comes from its supply of highly nutritious foods, which is becoming increasingly more important as the global population continues to grow. While the continued development of the dairy industry's milk supply is vital for continued success, it is important to bear in mind the effects that an increased herd size may have, for example, towards the environment and also the indirect effects to other areas. In recent years there has been a large influx of investment and interest into the industry in order to maintain its growth to correlate with the increasing demand from the global market. This saw large scale expansion and proliferation of the industry Worldwide. Presently, as the scale of the industry is beginning to peak, the current focus for improvement lies on the development of a more sustainable industry, one that can meet and maintain the expected production growth while minimising cost and as such creating a more efficient industry. The Irish dairy industry has been a major supplier of raw cow milk to many countries within Europe, and with the abolishment of the European Union Milk Quota in March 2015, there has been a great influx of resources in-order to increase Ireland's milk output (Department of Agriculture Food and the Marine 2015; Donnellan, Hennessy, and Thorne 2015). These investments hold great potential returns for several reasons. Recent financial studies have given in-depth analysis of Irish farms over a ten-year period, from 2003 – 2013.(Thorne et al. 2015). This study of Irish agriculture, as led by Teagasc, reveals interesting financial trends of Irish farms compared by their main output, be it dairy, livestock or tillage. Dairy farms have reported lower solvency levels (which compares borrowed capital of a business to the owner's equity capital in the business) on average as compared to livestock and tillage. As well as this, dairy farms were found to be the most economically viable Irish farm systems over all others, when evaluated by returns on non-land capital being at least 5 percent and their ability to reimburse family labour at the minimum agricultural wage rate. However, the average level of debt on dairy farms was significantly higher than that of livestock farm. Considering the majority of loans taken by Irish farms were used for the development of buildings and as capital for their work force, it can

be no surprise that dairy farms require larger sums due to need for specialised equipment, housing and trained farm hands as well as additional expenditures in comparison to other farm systems.

A commonly faced challenge by dairy farmers is the upkeep of the herd's health, primarily in the prevention infectious disease which can spread quickly and unnoticed while having a huge impact on overall cost and profits of a farm. Although there have been huge efforts into management and prevention of such, mastitis remains one of the most prevalent and problematical diseases within dairy industries. While mastitis can be prevalent in all farm systems that house livestock, be it cattle or sheep, dairy farms have the greatest prevalence of mastitis and also show the largest impact on overall profits as a result for the disease. There have been a number of studies into the estimated costs of mastitis upon farms through direct costs (or failure costs), such as production losses, treatment and culling of the herd (Geary et al. 2012; Huijps, Lam, and Hogeveen 2008) but also into the costs involved its control and prevention (van Soest et al. 2016). Mastitis also has a major effect on the quality of produced milk, the quality of which can be quantitatively measured by a somatic cell count (SCC) of the milk which detects any cells that were shed from internal mammary gland extracellular layer due to damage or infection. Several EU regulations have been imposed in-order to keep SCC of raw milk from farms below a certain threshold. The value of milk falls dramatically as its average SCC/mL increases; thus it is in the best interest of dairy farmers to properly maintain the health of their livestock in order to maximise profits. To better understand intramammary infections (IMI) and the steps necessary for management of such, it's important to first understand the mammary system and the pathogens involved in infection.

1.1 Diagnosis

While diagnosis of CM can be quite straightforward due to the visible clinical signs, means of evaluation are still required as it is important to determine the severity of the infection and to established if it is a mastitic infection. In contrast, the asymptomatic nature of SCM necessitates routine monitoring of the herd and requires specialised tests for diagnosis. At present, there are various methods for the detection of mastitis that are as follows:

Visual Inspection: The initial step in diagnosis of mastitis involves visual inspection of the udder and milk produced. Inspection of this manner looks for heat, swelling, inflammation

and sensitivity of a quarter or the udder as a whole. The milk is also assessed by colour and consistency of state (whether it is of normal standard or watery). Visual inspection may only be reliable for determination of CM, it is still hugely important and should be carried out in regular intervals to allow for prompt response to mastitic occurrence (Contreras and Rodríguez 2011; Mainau, Temple, and Manteca 2014; Jones and Bailey 2009).

Field Tests: Conventional field testing gives a simplistic yet rapid means for the detection of mastitis. One of the most commonly used and readily accessible methods available to both farm-hands and veterinarians alike, is the California Mastitis Test (CMT) (Schalm and Noorlander 1957). This detects elevated levels of somatic cells in milk by addition of the CMT-Test reagent, disrupting their membranes causing the cells to rupture and coagulate forming a gel with viscosity that is proportional to cell numbers. The CMT is generally carried out on a paddle divided into four wells, one for each udder quarter, for holding the milk during the test. The reaction of each quarter is recorded on a scale of 0 – 3, 0 being no reaction, 3 being full positive reaction with a viscous gel formation. (Dingwell et al. 2003; Kaşikçi et al. 2012). However the interpretation of the results can be subjective to the individual performing the test and therefore can lead to false negatives/positives (Viguier et al. 2009)

Other established methods used include the measurement of electrical conductivity (EC) and pH of the milk and measurement of udder skin surface temperature (USST) (Langer et al. 2014; Viguier et al. 2009; Polat et al. 2010). The principle behind EC measurement is that the conductivity of milk increases during mastitic infection due to the changes in ionic concentrations as a result of damaged mammary tissue, leading to an increase of Na^+ and Cl^- ions. EC is commonly used in automatic milking (AM) systems as a detection tool for CM as it is simple and inexpensive, and when used in conjunction with other detection methods such as CMT or SCC, it can make for reliable SCM detection (Kamphuis et al. 2008; Kaşikçi et al. 2012).

Measurement of USST can also be indicative of infection within the mammary gland. Polat et al. demonstrated that infrared thermography (IRT) was sensitive enough to detect thermal changes on the udder skin caused by SCM, clarified by use of CMT and SCC (Polat et al. 2010)

Somatic Cell Counts: As previously mentioned one of the main methods for the diagnosis of mastitis, as well as being a measure of udder health and overall milk quality, is the somatic

cell content of milk (Jones et al. 1984; Dohoo and Meek 1982). An elevated SCC in milk is most commonly related to mastitis, both clinical and sub-clinical. This is due to the immune response to the infection, which causes mass gathering of leukocytes (predominantly neutrophils) as well as mammary epithelial cell detachment (exfoliation), which can occur as a defence against bacterial attachment or as a result of damage from the infection (Nagasawa et al. 2018). While the CMT gives only a rough indication to the presence of somatic cells, there are more quantitative methods available. Counting by direct microscopy is well established means of determining the SCC of milk and is also one of the most officially recognized methods. It does however hold a number of draw-backs, primarily that of inaccuracies as a result of human error in counting (Nielsen, Smyth, and Greenfield 1991; Frøsig 2017)

Technological advancements have allowed the development of automated counting by use of imagery cytometry (IC). By utilising fluorescence imaging, IC based instruments have become widely used in SCCs as they allow for rapid and reliable counts and can accommodate mass sample analysis. There are a number of IC-based equipment's available such as flow cytometers but also instruments made specifically for milk SCCs such as the NucleoCounter®, which is now widely used (Shah et al. 2006; Sumon, Ehsan, and Islam 2017; Javorová et al. 2013). An individual SCC of <100,000 cells/mL indicates a normal healthy cow, but it is widely accepted up to 150,000 cells/mL (O'Brien 2008).

While SCCs are generally carried out to determine individual infections, it is recommended procedure on dairy farms to carry out a bulk tank somatic cell count (BTSCC) at regular intervals (Savić, Mikulec, and Radovanović 2017). A BTSCC can give an indication to the presence of mastitic cows within a herd and also an estimate of what percentage of the herd is infected. For example a BTSCC of 100,000 to 200,000 cells/ml indicates that approximately 20% of the herd are infected, a BMSCC of 300,000 to 400,000 cells/ml indicates that approximately 40% of the herd are infected (O'Brien 2016). The European Union has set a regulatory limit of 400,000 cells/mL for raw cow's milk, after which they will enforce appropriate measures (Community 1984).

In vitro culture: Culturing of microorganisms present in affected milk is regarded as a gold standard test for the detection of IMI's and gives insightful information to the aetiology of the infection, allowing more specialised treatment (Bouchard, Roy, and Tremblay 2014). Culturing

the organisms is as simple as streaking a tryptone soy agar (TSA) plate with a sample of milk taken from the individual to be tested, or more specifically, from the quarter suspected to be infected. However, the implications in this method revolve around the actual causative pathogen of the IMI, whether it be bacterial, fungal or viral. Viral isolation is a more complex procedure and requires specialised facilities (Leland and French 1988). While fungal pathogens are more easily isolated, they require a longer incubation time before growth can be seen. Certain bacterial isolates will require additional growth supplements such as defibrillated sheep blood, in order to grow sufficiently. After a culture is established in the most suitable media, additional microbial and biochemical tests can be performed to identify the microorganism (Shelley, Deeth, and MacRae 1987). Proper identification of the pathogen is of great importance as it allows more efficient treatment, management and also prevention.

1.2 Bovine Mammary System and Infection

The bovine mammary system is collectively found in the udder which consists of four quarters (see Figure 1.1 for a cross-section illustration of two quarters), each containing a separate mammary gland composed of milk ducts, a gland cistern teat cistern and glandular tissue (or parenchyma) consisting of small, milk producing sacs known as alveoli (Nickerson and Akers 2011).While mammary tissue is present in all mammals, it's development into a mature gland does not initiate until puberty of female mammals and does not become fully productive until first conception (Knight, Wilde, and Peaker 1988). After parturition, a shift in the cow's hormones will trigger the alveoli to produce milk or lactate. Although lactation will continue normally for a time, the production of milk will eventually hit a peak after which it will decline steadily until lactation ends (Schmidt and Vleck 1974). Due to this, dairy farmers plan breeding times accordingly in order to achieve the highest potential milk yield. The period between calving is what's known as the "lactation cycle" and is divided into four phases: early lactation, mid lactation, late lactation and a dry period. While each lactation period can last up to 120 days, the dry period should ideally last 60 days (Moran 2015). The dry period is necessary as it allows the cows to recuperate, regain body fat supplies, regenerate secretory tissue and prepares for the next lactating cycle which can all lead to an overall increase in production (Cortes, Search, and Period 2018).

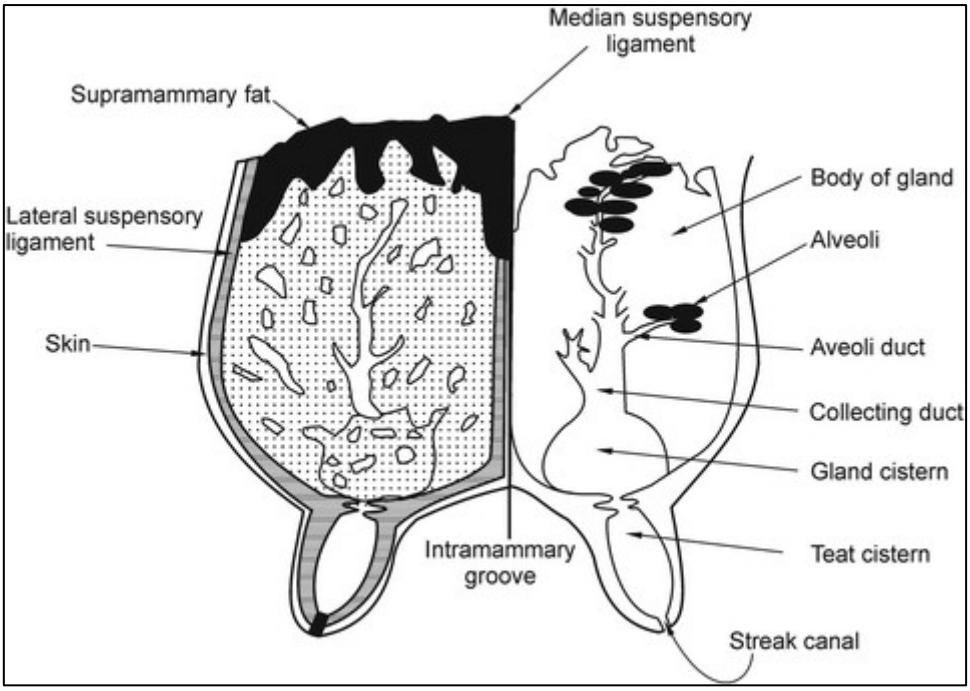

Figure 1.1 *Bovine Mammary Gland Cross-section.*
Cross-section illustration of two bovine mammary gland quarters, showing dermal layers (left) and internal system structure (right). (Alany et al. 2013)

One of the main goals of Irish, and indeed all dairy farmers is to increase and maintain their annual raw milk yield for enhanced profit. The general course of action to achieve such involves proficient management of the herd's lactation cycles as well as other influential factors such as nourishment, rearing, housing conditions and the general health and well-being of the herd as a whole (Ingvartsen, Dewhurst, and Friggens 2003). Maintenance of a herd's well-being can be the most challenging and problematic of such. Dairy farms worldwide commonly face issues that can have a direct impact on milk yield such as poor reproductive performance of cows, which increases calving interval and consequently lowers the average lactation length (Nebel and McGilliard 1993; Gröhn and Rajala-Schultz 2000); non-infectious diseases such as milk fever acidosis, ketosis (Rajala-Schultz, Gröhn, and McCulloch 1999); infectious diseases such as bluetongue, foot-and-mouth and mastitis (Wells, Ott, and Hillberg Seitzinger 1998; Fleischer et al. 2001). While each such condition can be quite harmful to production or herd sustainability, diseases of the mammary gland itself have the greatest potential impact on milk production if left unchecked. Mammary infections can have a direct effect on farm production by lowering milk quality but also causing indirect complications by necessitating the removal of infected cows from the line or in extreme cases, culling (George et al. 2008). It is therefore in the best interest of farmers to prevent ailments to their herd, or

to treat such promptly and appropriately, in order to maintain the highest possible performance, however this is not always possible. While it can be said that teat, udder and mammary gland disorders can be quite harmful in all aspects, they also greatly increase susceptibility of cows to bacterial infection within the udder, which can then lead to the onset of IMI, such as mastitis. Mastitis can have a major influence on milk production and quality, herd health and sustainability, thus affecting overall profits.

1.3 Mastitis

Mastitis is defined as inflammation of the parenchyma, regardless of the causative agent, and can be characterized by pathological changes of the glandular tissue itself as well as various physical and chemical changes to the milk produced. It primarily occurs as an immune response caused by bacterial invasion of the mammary gland but may also be caused by chemical or physical trauma of the udder and can affect one or more of the udder quarters simultaneously (Constable, Hinchcliff, Done, and Grünberg 2017). Mastitis can be further classified in terms of clinical signs, aetiological agents and its progression (i.e. mild, per-acute, acute, sub-acute or chronic) (Contreras and Rodríguez 2011).

Mastitis is referred to as clinical mastitis (CM) in cases where there are visual signs of infection, both on the udder itself and in the milk. The milk will have obvious signs of infection such as blood clots, discoloration and altered composition causing the milk to become watery (Mainau, Temple, and Manteca 2014). The more common indicators of CM on the udder include swelling, heat, increased sensitivity (hyperalgesia, allodynia) and bruising. In more extreme cases, systematic symptoms can develop such as fever, loss of appetite/anorexia, weakness and reduced rumen function (Bogni et al. 2011; Jones and Bailey 2009).

Sub-clinical mastitis (SCM) however has no visual symptoms and instead requires analysis of the produced milk in order to determine the quantity of somatic cells present, a key identifying agent of both CM and SCM (Björk 2013; A. J. Bradley 2002). Due to the difficulty in diagnosing SCM, it is considered more serious than CM and is responsible for much greater losses within the dairy industry (Islam et al. 2011). Due to its inconspicuous nature, it can quickly spread throughout a herd if left unchecked and prolonged infections can develop into clinical cases (Constable, Hinchcliff, Done, and Grunberg 2017; Saglam et al. 2017). Depending on the causative pathogen, there is also the threat of the infection being allowed to produce

a biofilm layer which can greatly complicate the matter due to the protective nature of biofilms against immunological responses, antibiotic treatments and can also play a role in reoccurrence (Melchior 2011; Melchior, Vaarkamp, and Fink-Gremmels 2006; Gomes, Saavedra, and Henriques 2016).

1.4 Aetiology

Mastitis is a complex disease caused by numerous pathogens of varying origins, with different patterns of infection. While over 135 different micro-organisms, including bacteria, fungi and viruses, have been isolated from bovine IMI's, the majority of infections are of bacterial origins. The more commonly faced bacteria are staphylococci, streptococci and Gram-negative bacteria (Thompson-Crispi et al. 2014).

Bacteria associated with mastitis can be classified by their primary source and mode of transmission as being either contagious or environmental. Contagious bacteria are transmitted through contact, which primarily occurs by indirect means, from an infected udder. For example, after a cow that carries a contagious infection is milked, the bacteria can be passed on through the machinery or by the handling of the farmer if proper hygiene and disinfection is not followed. The most predominant contagious bacteria in most countries, including Ireland is *Staphylococcus aureus* which primarily causes SCM (Bogni et al. 2011). Another well-known pathogen is *Streptococcus agalactiae* however it is mainly associated with individual herds and it's occurrence is generally associated with inadequate milking procedures (Barrett et al. 2005).

Environmental pathogens arise from the cow's surroundings such as housing, bedding and manure. They are regarded more opportunistic in nature, invading individuals with weakened defences or at certain stages of lactation. Common species that fall under this classification are coliforms (such as *Escherichia coli*) and certain streptococci such as *Streptococci uberis* and *Streptococci dysgalactiae* (Jones and Bailey 2009; Thompson-Crispi et al. 2014; A. J. Bradley 2002). While *S. dysgalactiae* is classified as an environmental pathogen, it's pathogenic traits are more that of a contagious strain in terms of infection and transmission, but it's main reservoir is the environment (Bogni et al. 2011).

Another group of bacteria commonly identified in cases of mastitis are teat skin-associated opportunistic pathogens, primarily coagulase-negative staphylococci (CNS) bacteria. While

CNS bacteria have been known to be implicated with mastitis, they were held in very low regard until recently where they have been identified as one of the leading causes of SCM on many farms (Vanderhaeghen et al. 2015). Of particular interest is *Staphylococcus epidermidis* which is one of the most frequently isolated CNS species from SCM. The most notable characteristic of *S. epidermidis* is that it is of human origin, found on the skin. Therefore it is assumed that its origin is from improper hygiene and sanitation of farmers themselves (Thorberg et al. 2006).

1.5 Epidemiology

There are a number of factors that influence the risk of mastitis which can relate to the host, its farm environment. While incidence of CM or SCM can vary according to these factors, the prevalent pathogen in reported cases also varies.

Host factors

The most significant factors that can influence susceptibility to mastitis are the age and parity of the cow, which affect herds globally. A number of studies have shown the correlation between increasing age of a cow and the occurrence of mastitis. One study reported cows above the age of seven years holding highest prevalence of SCM with a notable trend of it increasing with age (Tripura et al. 2014). A separate study reported cows in age groups of 3 – 5 years and 6 – 10 years had infection prevalence rates of 65% and 93.2% respectively (Zeryehun, Aya, and Bayecha 2013). Advancing parity shows a trend of increasing SCM prevalence, with studies showing it to be significantly higher in cows above second parity, which can be associated with weakened host immune systems (Tripura et al. 2014; Jamali et al. 2018; Sarker et al. 2013). Mastitis incidence has also been related to lactation periods. Young, primparous cows hold high prevalence of CM in early lactation while older animals have higher prevalence during middle or late lactation cycles (McDougall et al. 2009; Green et al. 2007). Breed of cow has also been noted to play a factor in mastitis prevalence. Islam *et al.* reported crossbreed and local breed cows screened for SCM had prevalence rates of 37.5% and 24.61% repectively (Islam et al. 2011). The condition of the outer udder also plays a huge influence on a cow's susceptibility to invading pathogens. The streak canal is the opening of the teat which acts as the main entry point of pathogens into the mammary gland. The condition of the teat end holds huge influence against initial invasion of pathogens and can

become damaged due to improper milking and external trauma that can be caused by feeding calves (Jones and Bailey 2009).

Environment

General farm condition can play a hugely influential role in the occurrence of mastitis. The milking parlour holds the greatest danger for the transmission of contagious pathogens. (Deb et al. 2013). Milking a mastitic cow can transfer bacteria onto the teat cups and even the hands of the individuals, which in-turn will put the next cow into great danger of contact with the bacterial contaminants. Cows kept in housing are at a greater threat to environmental pathogens, such as *E. coli* and *S. dysgalactiae*, found in bedding and manure (Argaw 2016). Those most at risk of such infections are in the older age range (>7 years) and those following calving (Berry and Meaney 2005)

Size of herd and individual exposure is also noted to correlate with mastitis incidence, primarily that of contagious aetiology but also environmental. Larger herds make it more difficult for inspection and diagnosis of mastitis, especially SCM. Mixed herds of different age, parity and health increases overall incidence of infection, as individuals with low risk of infection are in constant proximity with high-risk individuals. Animals with mastitis of contagious origins are now exposed to healthy individuals, increasing risk of transmission (Mekonnen et al. 2017). Following the establishment of major movements and societies to publicise mastitis and through the implementation of programs, such as the five-point plan, the incidence rates of mastitis have dropped significantly over the last number of decades. In the UK, the average annual rate of mastitis (measured in number of cases per 100 cows over a 12 month period) fell from 150 cases per 100 cows/year in the 1960s, to ~30 cases per 100 cows/year in the last decade (AHDB Dairy 2018). Other sources have reported that the current average cases in individual herds range from 10% to 12% of the herd, however higher incidence rates (up to 65%) have been recorded in some exception (Constable, Hinchcliff, Done, and Grünberg 2017). Such abnormally high incidence rates can be accredited to a number of factors that are specific to individual farms, which will be discussed in chapter 1.8.

In recent years the occurrence of CM has fell greatly, which can be accredited previously mentioned improvements in herd management and preventative measures against the disease. However, SCM has since overtaken as the dominant form of mastitis. The ability to

recognize CM more straightforwardly allows the needed steps to be taken in its treatment, whereas the clinically symptomless SCM lacks this advantage. As well as this, reports have shown that cows with previous cases of CM hold a greater possibility of developing SCM which can be due to ineffective treatments of the CM. Surviving bacterial strains may then cause the onset of chronic SCM (Sarker et al. 2013).

1.6 Pathology

Development of mastitis is a complex process occurs in three stages: invasion, infection and inflammation. These stages are summarised in Figure 1.2.

Invasion of the teat end by a pathogen species is the first step towards the development of mastitis. The streak canal can be described to as the first line of defence against mastitis, acting as a mechanical and anti-microbial barrier (Burvenich et al. 2000). Teat end damage, known as hyper-callosity, can occur as a result of improper milking methods, badly maintained milking machinery and damage from suckling calves or any external trauma to the teat. This compromises the teats defences which leads to the streak canal becoming more prone to invading bacteria (Jones and Bailey 2009).

Infection describes the establishment of the pathogen within the mammary gland, allowing for rapid multiplication and further invasion of mammary tissue by migration of pathogenic cells into the gland cistern and ultimately towards the alveoli. At this point it could be said that an IMI has established and while it does not mark the onset of mastitis, there are certain invading pathogens such as coliform bacteria, that can produce endotoxins leading to systematic signs of infection with little to no inflammatory response (Constable, Hinchcliff, Done, and Grünberg 2017).

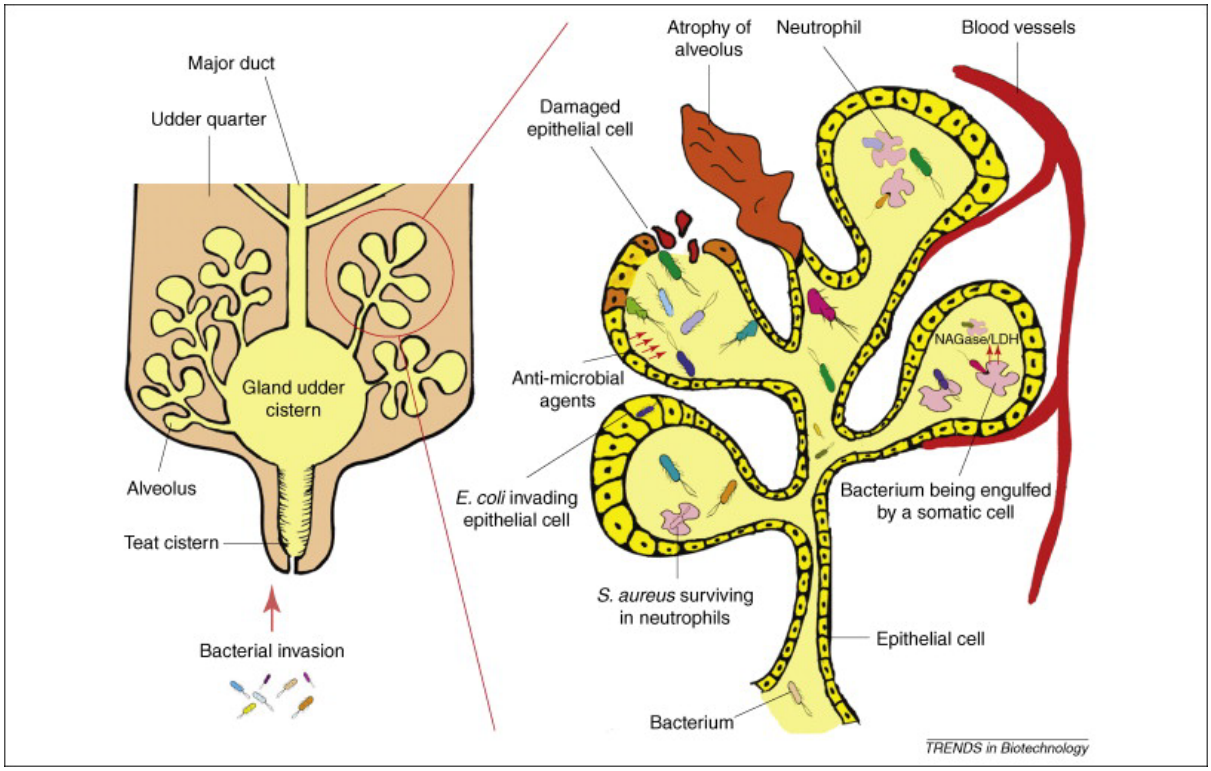

Figure 1.2 *Bacterial Invasion of bovine mammary gland.*
Cross section overview of a bovine mammary gland quarter and an enlarged view of alveoli following bacterial invasion. Bacteria breach the streak canal and colonize the gland udder cistern before advancing towards the alveoli. Bacterial invasion of the alveoli is the primary source of damage and pathology of mastitis. Here bacteria can colonise epithelial cells by invasion or attachment, which can then propagate biofilm formation. Epithelial lining can become damaged through bacterial toxin secretion and as an indirect effect of the inflammatory response (Viguier et al. 2009).

Inflammation is the key mark for the onset of mastitis, resulting in both clinical and sub-clinical symptoms, which depends on the invading pathogen species and the level of infection (Contreras and Rodríguez 2011; George et al. 2008). This occurs following invasion of pathogen which then elicit a host immune response. The main leukocyte involved mastitis defence are neutrophils, which are present in a healthy mammary gland in quite low numbers (<11% of all leukocytes). If the pathogen is able to bypass this initial defence, they then migrate to the alveoli and into the glandular tissue (intracellular invasion), leading to colonisation of the tissue. It is here that their effects are most prominent, due to newly produced bacteria and also through secretions such as cell wall components, metabolic by-products and endotoxins (Constable, Hinchcliff, Done, and Grünberg 2017). Secretion of such by-products leads to recruitment of additional leukocytes from the bloodstream to the site of infection. If this immune response is unsuccessful, inflammation will continue to evolve

leading to neutrophil migration between cells of the parenchyma. Prolonged occurrence of this rapid recruit of immune cells, referred to as leukocyte extravasation or diapedesis, results can cause severe damage to the secretory tissues which in turn leads to exfoliation of the cells (Nagasawa et al. 2018; Reshi et al. 2015). This provoked leukocyte recruitment, coupled with the detached epithelial cells is what leads to the increased SCC in milk released from mastitis infected glands.

1.7 Management

The management of infectious diseases revolves around their control and prevention, likewise to mastitis. Over the years, there have been great movements in the understanding and control of mastitis, with the establishment of the National Mastitis Council (NMC) in the United States being regarded as the starting point (Middleton et al. 2014). The NMC in cooperation with the International Dairy Federation (IDF) became an international hub for farmers and veterinary researchers to collaborate towards improvement of udder health. The National Institute for Research in Dairying (NIRD) was a similar organization based in the United Kingdom, and undertook a similar imitative, focusing on development of hygienic practises (Hillerton and Booth 2018). The result of this movement is what's known as the "Five-Point Control Plan", a simple five step program aimed at the reduction of CM and SCM through the control of contagious pathogens. Through the cooperation of international organizations the five-point plan was circulated through the dairy industry undergoing several trials, and developed into a system that farmers could understand and utilise (Hillerton and Booth 2018). The five-point control plan is as follows:

1) Teat and udder disinfection. Disinfection of the teat and udder is critical in eliminating bacterial pathogens. Use of teat dipping post-milking has a significant effect in the prevention of pathogen transmission between cows. As well as correct disinfection of the cow, it is vital that farmers themselves following proper hygienic practise to prevent spreading of bacteria on their person (i.e., hand, clothes)

2) Proper installation and maintenance of milking equipment. Milking machines should meet functional standards and only be used upon correctly prepare udders. This ensure the udder and teat are not exposed to unnecessary pathogens and are not damaged during milking, which greatly increases susceptibility to infection.

3) Dry cow management and therapy. The role of dry period is a valuable opportunity to improve udder health, as the risk of infection is greatest at the beginning and the end of the dry period. The most commonly used method is dry cow therapy, which aims to eliminate existing infections and to prevent new infections through use of intramammary (IMM) antimicrobial infusion. The two major variants are Blanket dry cow therapy (BDCT) which involves treatment of every quarter of every cow with long-acting antimicrobials, and Selective Dry Cow Therapy (SDCT) which requires identification and treatment of only infected cows/quarters or those of highest risk.

4) Appropriate use of lactation therapy. Since the commercialisation of antimicrobial agents in the 1950's, they have been used for the treatment of mastitis and still remain the primary method today. They are generally administered through IMM or parenteral routes, although as a general rule they should not be used unless deemed necessary by a trained veterinarian. The treatment strategy for antimicrobial use depends on a number of factors such as whether the mastitis is sub-clinical or clinical and the overall health status of the herd.

5) Culling of chronically infected cows. Culling is a necessary step for the removal of problematic animals. Such animals are those that exhibit recurrent CM, have a record of chronic mastitis coupled with additional illnesses (e.g., severe fibrosis) and/or have a high S. aureus prevalence are most commonly recommended for culling.

While the five-point plan was hugely successful at arms where it was properly utilised, however it is ineffective for the control of mastitis from environmental pathogen origin (R. Gill et al. 1990). As further studies were carried out in mastitis management and as our understanding of the topic advanced additional points were added to the five-point plan.

6) Maintenances of an appropriate environment. Sufficient cleanliness of the animal's environment is essential in preventing infection from contagious and opportunistic environmental pathogens. Basic farm management, such as merely changing bedding regularly and building adequate housing, can have a great impact on the spread of mastitis within a herd. Proper protection from severe climate conditions is also recommended as exposure to such can weaken the immune system, thus increasing chances of infection.

7) Good record keeping. Proper record keeping is necessary to keep track of mastitis cases within a herd. Such information is important in order to assess possible risk factors that may

be associated with mastitis incidents and to also keep track of steps taken or yet to be carried out in treatments. Although a simplistic step, its value is becoming more and more evident in recent years, due mainly to the fact of antibiotic misuse.

8) Monitoring udder health status. Although not included in early control programs for mastitis, it is now seen as the third key principle for the control of mastitis. Since the employment of the SCC on bulk milk tanks, there have been noticeable improvements in herd udder health. While monitoring overall herd health is important and can give quick indication to possible infections within, it is also necessary to monitor udder health on an individual. This can be achieved by use of cow side diagnostics and bacterial culturing of milk samples.

9) Periodic review of the udder health management program. With changes in technology and the aetiology of mastitis, it is important to periodically review management programs to ensure the most effective treatments and technologies are implemented.

10) Setting goals for udder health status. Realistic targets are important to identify shortfalls related to milk quality and general health. They should be achievable while still maintaining sufficient economic significance and as such, it is important to balance performance with profit.

It is now expected that dairy farms follow at-least six points of this ten-point plan in order to tackle the threat of environmental pathogen-related mastitis which, since the implementation of the five-point plan, has overtaken contagious mastitis in prevalence. The remaining 4 points, however, are considered necessary procedure in the optimised control of mastitis globally.

While the development and implementation of these plans has seen dramatic reduction in mastitis occurrence and BTSCC, there are a number of downfalls to their current structure as well as issues faced due to factors such as improper employment by farmers.

1.8 Impact and Costs

Mastitis at present holds great influence on the dairy industry as whole, from the international market to small independent farms and can have either a direct or an indirect effect to certain areas.

Direct impacts of mastitis involve areas that are influenced from the disease itself. This includes the effect on individual cow and herd health, quality and quantity of milk production as well as costs of veterinary care. The effect on individual cow refers to general well-being and as with any disease, mastitis (specifically CM) has several detrimental effects. In clinical cases, the costs of mastitis add up from discarded milk, labour needed to manage and veterinary costs for treatment. In extreme cases with recurrent infections, culling is the advised course of action. As previously mentioned, the SCC of milk is a key method for the detection of mastitis, but it is also a means of qualifying the milk. There are SCC restrictions implemented globally by various controlling bodies in order to keep SCC of dairy producers in check. In Europe, milk received from a dairy farm whose herd has an average SCC above 100,000 cells/mL has milk quality penalties applied (O'Brien 2016). Mastitis can also been linked to infertility, which can have huge impact on profits of a farm considering it will lead to fewer offspring and also as a result, lowered milk production (Metcalfe 2016). Milk production is also directly affected due to damaged secretory cells as a result of the inflammatory response and from toxin secretions from certain pathogens (Seegers, Fourichon, and Beaudeau 2003).

Indirect impacts are areas affected following the disease. Such areas can range from losses due to taking cows out of milking rotation, culling of animals, disposal of milk due to raised SCC or the presence of antimicrobials. At present, the only effective means of treatment for mastitis are antibiotics, however there are a number of issues with this. Due to recent incentives to reduce use and public exposure to antimicrobials (as a result of the increasing prevalence of antibiotic resistance) cows that have undergone antimicrobial therapy are removed from milking for 3 – 4 weeks to ensure there are no antimicrobial residues remaining in their system. This also requires the need of a trained professional to administer treatment (Krömker and Leimbach 2017). Occasionally, even after such periods the SCC and/or levels of antimicrobials will be too high and must be disposed of, leading to further loses.

1.9 Antibiotics and Mastitis

Mastitis has been the subject of intense research interest, particularly in recent years, which has positively informed real improvements in disease detection, management and prevention. However, the primary means of therapy still rely heavily on the use of antibiotics. While the effectiveness of using antibiotics remains high, there is an increasing trend where

antibiotic therapy is insufficient. However, success rates for treating cases of mastitis involving intracellular invasive pathogens with antibiotics, such as *S. aureus*, have been reported to be approximately 10 – 30% (Gomes and Henriques 2016b). A major contributor to antimicrobial resistance (AMR) found in staphylococci species, is their ability to form biofilms, a mechanism that mastitic bacteria utilise successfully to prolong the infection and to hurdle therapeutic treatments. Due to the relevance and impact of biofilms in mitigating effectiveness of mastitic counter-treatments, it is important to understand physiological characteristics that govern its' formation and persistence.

A major mechanism of resistance seen in such complex systems are biofilms, which form a protective, physical barrier around mixed communities of bacteria preventing molecules from interacting with their targets. Biofilm formations are quite common in nature and also in various medical fields, the majority of which occur on foreign bodies (such as medical devices, implants and catheters) but may also develop on natural surfaces (e.g. plaque formations on teeth, endocarditis in the heart and mastitis in mammary glands) (Melchior 2011; Marsh 2004; Nallapareddy et al. 2006).

1.1.1. Biofilm: Characteristics and Formation

Biofilms are the product of close-knit bacterial communities which cooperate in order to increase their survivability. While bacteria are seen as fully self-sufficient organisms, they have the ability to communicate with one another through quorum sensing (QS), a basic form of inter-cellular signalling that allows the ability to recognise population densities. There are a number of example activities that are accomplished through such communication, such as bioluminescence production, exoenzyme secretion and biofilm formation (Solano, Echeverz, and Lasa 2014). Biofilm formation can be described in a stepwise manner, the reported number of which varies but follows the basic structure as such; 1) attachment, 2) growth, 3) maturation and 4) detachment, after which the cycle repeats (see Figure 1.3).

The initial step involves a primary bacteria species adhering to a surface and establishing a micro-colony. During this stage, the biofilm formation process is still reversible as the cells are still exposed to external threats (Stoodley et al. 2002). Following colony formation, begins irreversible attachment of the bacteria to the surface and formation of the biofilm matrix.

This is initiated through QS and exposure to external stress factors (De la Fuente-Núñez et al. 2013). The bacterial colony excretes an extracellular matrix, consisting of a glutinous substance known as exopolysaccharide (EPS) which can comprise of a variety of compounds such as polysaccharides, lipids, proteins and nucleic particles (Stoodley et al. 2002; Bjarnsholt et al. 2013; Jolivet-Gougeon and Bonnaure-Mallet 2014). This matrix can account for 90% of biofilm mass and aids bacterial endurance, giving physical protection and providing the basic structure of the biofilm (Sutherland 2001; Sun et al. 2013). In the majority of cases, biofilms are regarded as multispecies with the initial EPS formation being produced by several bacterial micro colonies which ultimately combine into the mature biofilm. The initial secretion is primarily activated in response to a high bacterial population density, as determined through QS which identifies QS signal molecules in the extracellular environment (Solano, Echeverz, and Lasa 2014).

During the growth stage, the biofilm expands and bacteria within multiply. However, nutrients are prioritised for use in developing the extracellular matrix rather than production of new cells. As the biofilm develops, it matures and begins to gain structure. The structure, as well as composition of the biofilm, varies depending on the primary species. For example, *Pseudomonas aeruginosa* forms mushroom like micro-colonies while *Streptococcus pneumoniae* is known to form tower-like assemblies After irreversible attachment, the biofilm initiates growth. Nutrients are prioritised for use in developing the extracellular matrix rather than production of new cells, however if needed the bacteria have the capacity to produce digestive enzymes which can break down the matrix for use. As the biofilm develops, it matures and begins to gain structure. The structure, as well as composition of the biofilm, varies depending on the primary species. For example, *Pseudomonas aeruginosa* forms mushroom like micro-colonies while Streptococcus pneumoniae is known to form tower-like assemblies (Wilkins et al. 2014). A major component common to many biofilms formations, are interspersed water channels which allow for transport of nutrients within the biofilm, but also allowing for a basic form of transport to take in nutrients and remove waste (de Beer et al. 1994). With a distinct structure and water channels established, the biofilm is now mature. At this point, it is possible for a secondary bacterial species to adhere to this initial biofilm and begin developing a secondary biofilm.

The final stage involves detachment of small segments of the biofilms and/or release of bacterial cells from the matrix. This process is aided by the production of saccharolytic enzymes by interior microbial communities, which lyse the EPS matrix. During this stage, cells upregulate expression flagella production in-order to encourage motility of released cells (Jamal et al. 2018). These planktonic cells may then relocate and colonise other surfaces, giving further indication of the advanced pathology of biofilm associated infections (BIs) (Wilkins et al. 2014).

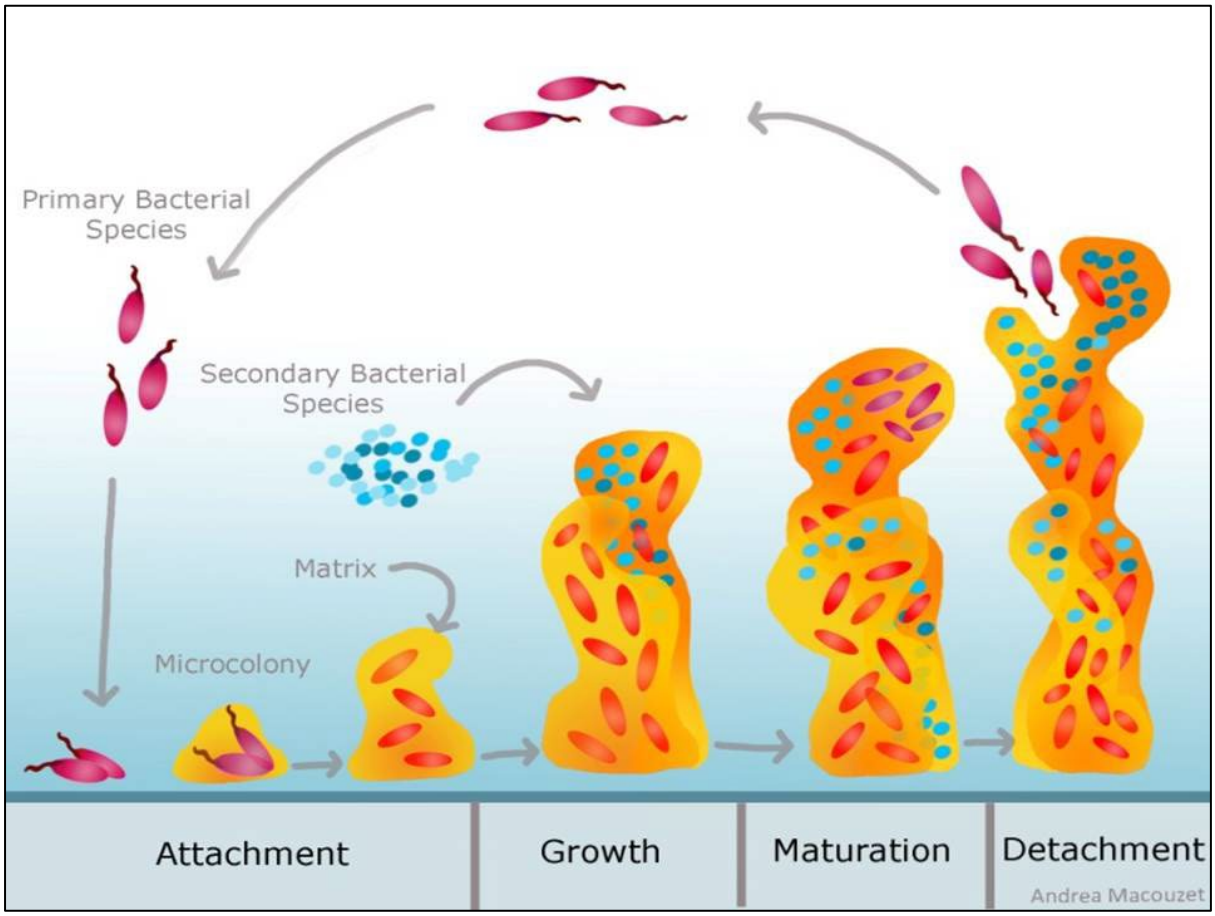

Figure 1.3 Stages of Biofilm Formation
Biofilm development can be commonly described in four stages: 1) Attachment, 2) Growth, 3) Maturation and 4) Detachment. Bacteria adhere (reversibly) to surface, form a micro-colony and produce a glue-like substance known as exopolysaccharide (EPS). Following EPS production, they are irreversibly attached, allowing for the biofilm to grow. During this stage, the biofilm develops a definite structure and inter-channel waterways. The protruded structure also gives opportunity for a secondary bacterial species to form a biofilm upon the initial biofilm. After maturation of the biofilm, bacterial cells are detached and dispersed out of the extracellular matrix, allowing further colonisation and biofilm production (Jacques 2013)

1.1.2. Biofilm Mediated Resistance

Biofilm formations are quite common in various medical fields, the majority of which occur on foreign bodies (such as medical devices, implants and catheters) but may also develop on natural surfaces (e.g. plaque formations on teeth, endocarditis in the heart and mastitis in mammary glands) (Melchior 2011; Marsh 2004; Nallapareddy et al. 2006). It is estimated that a majority of all bacterial infections have been found to be associated with biofilm formations (Jamal et al. 2018). As such, BIs are frequently encountered and yield numerous challenges which greatly impede the successful treatment of infections. As previously mentioned, biofilms confer a higher level of resilience to the containing bacterial species against external threats which can come in the form of the hosts immune response, antimicrobial compounds from other unrelated bacteria or medical treatments (e.g., antibiotics).

1.1.3. Mechanisms of Biofilm Mediated Resistance

There are a number of different means through which biofilms can increase anti-microbial resistance of microorganisms. While biofilm composition and structures can vary between bacterial species, the general mechanisms remain consistent. There are several well-known mechanisms that aid in AMR, including hindered permeability due to the EPS matrix structure, altered bacterial physiology/phenotype due to genotypic alterations which can prevent interaction with target ligands, high density cell populations, QS and also multi-drug efflux pumps.

While the EPS matrix is known to hinder antibiotic diffusion, slowing its migration towards the cells within the biofilm, it is primarily enzymes within the matrix that produce the greatest defence by altering or degrading the antibiotics. One such class of enzymes are β-lactamases (Jolivet-Gougeon and Bonnaure-Mallet 2014; Hall and Mah 2017). Multi-drug efflux pumps are also a commonly faced resistance mechanism which effectively remove antimicrobial compounds from the internal environment of a biofilm. These pumps, coupled with the biofilms internal water channels, establish an effective means of drug removal.

High-density cell populations provide greater means for bacteria to improve their defence. Through QS, they can assess when their numbers reach critical levels, and response by activating certain genes which in term produce toxins and enzymes. These compounds aid in the infection pathology but also in eliminating threats such as host immune cells or

antimicrobial compounds which can be degraded by certain enzymes (Høiby, Bjarnsholt, Givskov, Molin, Ciofu, et al. 2010). The close proximity of such numerous bacteria also gives greater accessibility for horizontal gene transfer between microbes, thus enhancing the overall populations survivability.

1.10 Global Concerns Regarding AMR

There is a pressing need to develop new or alternative antimicrobial compounds to combat the global threat of antimicrobial resistance (AMR) that has caused a depletion in efficacy to front line therapeutics for human and animal intervention. The World Health Organisation (WHO) released a report in 2014 summarising the global prevalence of AMR species and called for immediate action to counteract this "antibiotic resistance crisis" (WHO 2014). This initial report has led to the establishment of many important initiatives, such as the global action plan of 2015, the Interagency Coordination Group (IACG) on Antimicrobial Resistance in 2016, which also lead to the formation of a multi-partner trust fund in collaboration with the Food and Agriculture Organization (FAO), and the World Organisation for Animal Health (OIE), named the One Health Global Leaders Group on antimicrobial resistance in 2019 (World Health Organistaion 2015; "New Multi-Partner Trust Fund Launched to Combat Antimicrobial Resistance Globally" 2019; World Health Organistaion 2020; Interagency Coordination Group on Antimicrobial Resistance 2019). With this mass support, a resurgence in the development of antibiotics has seen many new agents being produced in order to cope with the increasing occurrence of AMR (World Health Organization 2019).

Antibiotic usage in agriculture is reported to be a major contributor to the rise in antibiotic resistant bacteria through introduction of antimicrobial residues to the food chain as well as AMR pathogens themselves (Economou and Gousia 2015). While a number of countries have implemented policies for efficient therapy methods in order control unnecessary antimicrobial usage, the need for alternative therapies still are in high demand (Valde et al. 2004).

While newly developed antibiotics are crucial to counteract the global rise in AMR, it has been reported that the dependence on their use and their subsequent misuse to be one of the major factors leading to the increase in AMR bacterial species, with history showing that resistant bacterial species emerge within 15 years of an antibiotic being mass produced and

distributed publicly (Aminov 2010; Ventola 2015). Antibiotic use in the agricultural sector has also been identified as a major contributor to AMR on a global scale through introduction of antimicrobial residues to the food chain as well as AMR pathogens themselves (Watkins and Bonomo 2016; Economou and Gousia 2015). The misuse of antibiotics is hugely prevalent and difficult to regulate on farmlands, allowing antibiotic residues to enter our food supply through animal products, where the correct procedure and withdrawal periods are not followed. While the majority of antibiotics used in animals are not used in human medicine, many antibiotics have similar frameworks and targets (Manyi-Loh et al. 2018). As such, AMR bacteria that arise from such areas can still lead to bacteria resistant to even the most effective human used antibiotics (Economou and Gousia 2015).

1.11 Alternatives

There are a number of different alternatives currently under study for treatment of infectious diseases such as mastitis. There are a number of antibiotic alternatives currently under investigation such as vaccines, phages, and various organic and inorganic compounds, however such alternatives hold limitations in treating bacterial infections.

1.11.1 Vaccines

Immunisation against bovine mastitis has been a long sought-after solution with very limited results. A number of vaccines were produced for *S. aureus* based mastitis, none of which showed promising results due to limited efficiency (Gomes and Henriques 2016b). However, a vaccine for coliform mastitis has been developed with promising success rates. The *E. coli* J5 vaccine composes of whole antigens derived from the *E. coli* J5 variant strain and was proven to reduce the number of coliform mastitis by ~75% (Wilson and González 2003) The main difficulty in establishing an effective vaccine is due to the complex aetiology of mastitis and other such biofilm-associate infections.

1.11.2 Bacteriophages

The use of bacteriophages for the treatment of bacterial pathogens has been a topic of controversy for some years. Bacteriophages, or simply phages, are viruses that target and invade bacterial cells, eliminating the pathogen (Wittebole, De Roock, and Opal 2014). There

have been a number of bacteriophages developed for the use against mastitis such as Phage K, MSA6 and $CHAP_K$ which show great promise as treatments for the elimination of staphylococci species.(J. J. Gill et al. 2006; Fenton et al. 2013; O'Flaherty et al. 2005; Kwiatek et al. 2012). Phage therapy does hold a number of limitations such as their degradation/inactivation by host immune systems and their specificity. For mastitis treatment and indeed other biofilm based infections, a wide-spectrum antimicrobials is required, however there have been studies conducted using cocktails of bacteriophage species (Porter et al. 2016; Breyne et al. 2017).

Both vaccines and bacteriophages have a narrow spectrum of effect and are generally tailored per bacterial species, leading to increased costs and higher probability of inefficacy versus infections with more complex aetiology (Gomes, Saavedra, and Henriques 2016; Breyne et al. 2017; Porter et al. 2016).

1.11.3 Organic Compounds

Naturally produced, organic compounds with antimicrobial properties are an area of great interest in the treatment for mastitis for a number of reasons. Due to their natural sources, such compounds are biologically safe with no effect towards the individual cow and as well as this, any residues or particles remaining in the milk are acceptable.

Chitosan is a widely studied compound derived from chitin, an organic polysaccharide, in the shell of crustaceans. Chitosan is a polysaccharide-based polymer, produced from the deacetylation of chitin, a major component in shells of crustaceans (Kyoon et al. 2002). Chitosan is a well-studied compound used in the biomedical and food packaging sectors. The exact mechanism of chitosan's antimicrobial properties are still unknown, but it is thought to interact with cellular wall lipids, causing destabilization (Qin et al. 2006). There are reports claiming that chitosan requires acidic solution in order to confer its antimicrobial properties (Hamdine, Heuzey, and Bégin 2005; Romanazzi et al. 2009). Chitosan has already been involved in a number studies, exhibiting its effect against mastitis bacterial pathogens and also its use to encapsulate alternative treatments, such as nitric oxide (Moon et al. 2007; Cardozo et al. 2014; Asli et al. 2017)

Antimicrobial peptides are also accumulating great interest in the field of alternative antimicrobial treatments. Nisin is one such polypeptide with an already well-established

status as an antimicrobial with a good number of studies involving its effect against various bacterial strains. Nisin is a lantibiotic, a group of poly-cyclic polypeptide antibiotics produced by Gram negative bacteria in order to attack other Gram-negative bacteria. Lantibiotics act by binding with great affinity to bacterial cell wall components such as lipid II, a precursor molecule in cell wall synthesis. They are divided into two categories based upon their mode of action after lipid II binding, Type A eliminate bacteria by rapid pore formation and Type B inhibits peptidoglycan synthesis (Hasper et al. 2006; Willey and van der Donk 2007). Nisin is a type A lantibiotic produced by *Lactococcus lactis*, a lactic acid bacterium commonly used in dairy processing as fermentation initiators. As such, these bacteria and their compounds have a well-established use in the food industry (J. Wu, Hu, and Cao 2007). There are different variants of nisin identified, with nisin A being the first such form of nisin discovered and studied. The other variants are nisin Z, F, Q and U which differ slighting in their primary structure giving them slightly altered modes of actions. This gives the facility for bioengineering of nisin variants (J. M. Shin et al. 2016). Nisin and its variants have also been studied for their effect against mastitis derived bacteria and have shown great promised against normally treatment resistant bacteria (J. Wu, Hu, and Cao 2007; Delves-Broughton 1996). The use of lantibiotics as treatment for mastitis has been a topic of great interest for many years and some nisin-based treatments are already developed such as Mast out, a IMM infusion product containing nisin and Wipe Out, a wipe soaked in antimicrobial solution containing nisin (Bogni et al. 2011). Another area showing great interest in antimicrobial organic compounds is that of active food packaging. This involves the incorporation of active compounds into packaging materials. Both chitosan and nisin have been studied for this purpose and have showed promising results which could pave the way for the use of such bioactive incorporated materials in mastitis treatment (Bastarrachea et al. 2015).

1.11.4 Inorganic Compounds

There are a number of compounds that have been used in the treatment of bacterial infections for many years. Metal and metal oxides, such as gold, silver, titanium oxide (TiO_2), zinc oxide (ZnO) have been extensively studied for their antimicrobial effect (Beyth et al. 2015). Nanoparticles (NPs) have been a topic of increasing interest following recent advancements in nanotechnology and due to their unique functional and physiochemical

properties. A number of NPs forms of well-established antimicrobials have been developed and extensively studied for their antibacterial properties, such as chitosan, silver, zinc oxide.

ZnO is an inorganic compound, approved as generally recognised as safe (GRAS) by the FDA, and a widely used ingredient in a number of different, everyday products (U.S. Food & Drug Administraion 2019). While its major applications make use of its different characteristics, such as its ability to block ultra violet (UV) light in sun block, its pigmentation used in paints, or as a nutrient supplement in foods, recently there is considerable research looking to various ways of utilising its antimicrobial abilities (Beyth et al. 2015). The antibacterial properties of ZnO have been well studied, and it's mechanism of action involves the destabilisation of microbial membranes upon direct contact, the production of reactive oxygen species (ROS) and the release of Zn^{2+} ions (Pasquet, Chevalier, Pelletier, et al. 2014). ZnO has been shown to utilise three major mechanisms to confer its antimicrobial abilities; 1) the release of antimicrobial ions (Zn^{2+}), 2) destabilisation of the outer membrane via electrostatic interactions, 3) the production of reactive oxygen species (ROS) (Pasquet, Chevalier, Pelletier, et al. 2014). ZnO NPs have also been shown to exhibit greater antimicrobial effects, due to their reduced structural size which allows more effective interactions with bacteria cells (Padmavathy and Vijayaraghavan 2008). They have been used in studies for their effects against mastitis in sheep, buffalos and also cows (Anju Manuja 2015; A. Hassan et al. 2014; Alekish et al. 2018).

Silver and its various compounds have been used for the disinfection of medical, water purification and for the treatment of burns and wounds. The earliest uses of silver as an antimicrobial can be dated as far back as the 11^{th} century BC, with noted cases of water being kept in silver containers in-order to keep it potable. There are later reported uses of silver for the treatment of ailments such as eye inflammation of new-born infants and topical cleaning of burn wounds (Balazs et al. 2004; Atiyeh et al. 2007). It was not until the late 19^{th} century AD that the first medicinal studies involving silver were carried out, noting its ability to eradicate freshwater *Spirogyra* (Russell and Hugo 1994). In the 1960s, studies were carried out into the characteristics of silver and its mechanisms. Silver salts were implemented, due to their stability as a carrier system leading to the common usage of Silver nitrate ($AgNO_3$)(Atiyeh et al. 2007). However, as the development of antibiotics progressed, the needed use of silver and its salt derivatives for their antimicrobial abilities were gradually

made redundant in medicine. With the recent need of antibiotic alternatives, silver and $AgNO_3$ have been under recent reassessment, with noted successes in several areas such as biomedical devices and dentistry (Gao et al. 2018; Balazs et al. 2004).

Silver NPs have also been studied for their effective antibacterial effect. Silvers mode of action is similar to that of other inorganic metals which interact with the cell membrane and cause disruption through production of free radicals, allowing the NPs to transverse into the cell where they continue producing reactive species (Prabhu and Poulose 2012). Saied *et al.* conducted a study using silver NPs as a treatment against *S. aureus* samples taken from cows suffering with SCM, which showed the treatment to be highly effective (Saied, Fatemeh, and Azizollah 2011).

Although there has been comprehensive research and expansion in our knowledge of bovine mastitis and its management, it still remains a major problem to dairy farms globally. While antibiotics remain the most widely used method of treatment, there is a rising need for alternative therapies in order to improve dairy production but also to remove antibiotics from the food chain. There are a number of alternatives to antibiotic use that hold great promise for use in agriculture. While individual treatments, such as nisin and silver, are displaying significant results in the treatment of mastitis originated pathogens, the greatest potential lies within the possible synergy of such compounds.

1.11.5 Processing Methods

Alternative methods used to challenge AMR bacteria and biofilm formations in medical fields include producing polymer-based materials and coatings that release antibiotics into surrounding tissues and fluids in order to prevent a build-up of bacterial cells in the area, and thus stopping initial attachment and formation of the biofilm (Costerton 2005). Such methods, and other polymer based applications, require the use of antimicrobials that are suitable for processing and polymer incorporation through techniques such as hot-melt extrusion (HME), which necessitates the capacity to withstand thermal processing while retaining bioactivity (Simões, Pinto, and Simões 2019). HME is a commonly widely used in the area of pharmaceuticals as it allows the production of biologically active polymers with various formulations, dosage forms, and can enhance the physical properties of the bioactive component (such as increased water solubility, improved stability and shelf-life, and aiding

bioavailability) (Patil, Tiwari, and Repka 2016). HME is carried out using a device known as an extruder. There are various arrangements of extruders available, which also vary in size and abilities, but the principal part of every extruder is the screw, housed in a heated barrel, which blends the materials along the length of the barrel, pushing the materials towards a die from which the final extrudate exits. The type of die also determines the shape of the final product. Extruder assemblies can have a single screw (SSE), twin-screws (TSE) or multiple screws (MSE) which will alter how the materials are blended and thus their final properties (Rajadhyax et al. 2021). The process of HME for producing pharmaceutical materials involves combining and feeding of the active drug with a chosen polymer carrier into the barrel at a constant rate, with the screw rotating at a chosen speed, which carries and blends the materials along the length of the barrel which is heated to a chosen temperature, usually above the glass transition temperature (Tg) of polymers and many times even above the melting temperature (Tm)(Tambe et al. 2021). Melting of the ingredients results in mixing at the molecular level along the screw within the barrel, to produce extrudates with excellent content uniformity and improved quality.

There are a wide variety of polymers available which can be used for HME, which can vary greatly in their characteristics and properties, which ultimately influences the final pharmaceutical product (Thakkar et al. 2020). Commonly used polymers for HME include polyethylene oxide (PEO), polyethylene glycol (PEG), hydroxypropyl cellulose (HPC) and polyvinylpyrrolidone (PVP0), but there are also formulations which combine different polymers and additives to enhance their properties (Tambe et al. 2021). One such polymer of recent widespread use and research in pharmaceuticals is Kollidon® VA-64 (PVP/VA64), a co-polymer of poly-vinyl-pyrrolidone and vinyl acetate (VA) at a 6:4 ratio. PVP/VA64 has excellent stability through extrusion processing with good flowability and can be used in a variety of roles, depending on the application. In pharmaceuticals, it is used as a dry binder in tablets, as a matrix former in amorphous solid dispersion and as retarding and film-forming agents. Its properties as a carrier allows increased water solubility and bioavailability, while being non-toxic and biocompatible (Ding et al. 2019; Akram et al. 2022)

Traditional antibiotics unfortunately have quite low thermal stability, excluding them as possible candidates for HME applications (Wylie et al. 2021). Antimicrobials suitable for such

processing would support their use in areas requiring controlled delivery of an antimicrobial effect, such as active packaging, biomedical devices and subdermal implants.

1.12 Concluding Statements

Global awareness of AMR has been significantly increasing since the release of the WHO report in 2017, which has seen major research into novel antibiotics, alternative therapies and alternative treatments. Bovine mastitis has been a key infectious disease in agriculture and food industries for many years, which has been found to hold many prominent effects throughout. While the rise in AMR and mastitis are not generally associated with one another, it can be argued that both of these occurrences can have definite interlinking effects. The lenient approach towards agricultural antibiotic usage is being progressively restrained, which may hold important down-stream effects upon AMR stemming from the unnecessary antibiotic exposure to wild type bacterial species. However while this may help in managing the rate of AMR, it will cause inconvenience to those who work in these sectors, which may cause huge losses in production and capital. As previously mentioned, one of the most viable solutions to both problems is the discovery of effective alternatives of antibiotics for use against bovine mastitis. The most ideal candidates would hold effect against a range of bacterial species, including AMR strains, while having no effect upon livestock or the dairy products produced. While there are a number of possible and even unknown candidates for such, it would be most prudent to choose a small number of already known antimicrobials, with documented effects, and assess these upon the bacterial species most commonly associated with mastitis and AMR. Such compounds, which were already previously mentioned, include silver nitrate ($AgNO_3$), nisin, chitosan and zinc oxide (ZnO). While their antimicrobial abilities have been documented in previous studies, they were not assessed on par with that of antibiotics testing methods. Furthermore, a major avenue of novel antimicrobial research involves assessing combinations of previously established treatments, which has not yet been carried out with these four compounds. Such studies could reveal many interesting mechanisms, areas and possibilities involving these compounds and the plethora of other, similar compounds still yet to be investigated. The main areas of research in which the four aforementioned bioactives are being investigates would benefit greatly from the currently proposed studies, and visa versa. Their established antimicrobial activity, previous inclusion in polymer matrices through food packaging research, as well as their GRAS

status holds great capacity for their use in the current project with the aim to develop an alternative antimicrobial for a complex bacterial disease such as mastitis, incorporating polymer processing and synergistic analysis.

Chapter 2 Aims & Hypothesis

2.1. Project Aim

To design, develop and test (*in vitro*) a potential alternative bioactive-based treatment for targeting pathological bacteria involved in bovine mastitis, in order to limit or remove the reliance on front-line antibiotics where acquired microbial resistance is at global crisis point.

2.2. Project objectives

a. To access the antimicrobial effect of four chosen bioactives, silver nitrate, zinc oxide, nisin and chitosan (individually and in combination) against major mastitis-associated bacterial pathogens, namely *Escherichia coli, Staphylococcus aureus, P. aeruginosa* and *Staphylococcus epidermidis*.
b. To design and incorporate the bioactives compounds into appropriate polymer carriers using hot-melt extrusion, after which they will be reassessed to determine their activity post-process.
c. To assess the anti-biofilm capabilities of the bioactives against chosen biofilm forming bacteria, related to bovine mastitis.
d. The determine the *in vitro* cytotoxic and inflammatory effects of the bioactives against mammalian cells, representative of the area in which mastitis occurs.

2.3. Overall Hypothesis

That food-safe, bioactive compounds can be used for the novel treatment of bacterial pathogens that exhibit antibiotic resistance through intrinsic mechanisms, evolutionary traits and biofilm formations, while having no adverse effect upon patient health.

2.4. Specific Hypothesis

That the four selected bioactive compounds (silver nitrate, zinc oxide, nisin and chitosan) will eliminate four major bacterial pathogens attributed to causing mastitis, namely *E. coli, S. aureus, P. aeruginosa* and *S. epidermidis* .

Chapter 3 Materials & Methods

3.1 Bacterial Cell Culture

Escherichia coli (NCTC 12241, aka ATCC 25922) was obtained from Public Health England (Culture Collections, Public Health England, SP4 0JG, UK). *Pseudomonas aeruginosa* (ATCC 27853) and *Staphylococcus aureus* (ATCC 29213) from American Type Culture Collection (LGC Standards, Middlesex, United Kingdom). *Staphylococcus epidermidis* (ATCC 35984) was purchased from DSMZ (Braunschweig, Germany). Strains arrived as lyophilized cultures in glass ampoules, which were recovered as per ATCC protocol (Kaftanoglu 2015). Once a successful plate culture was established, individual colonies were used to inoculate Microbank™ vials (Pro-Lab Diagnostics, Merseyside, CH62 3QL, UK) as per their documentation (Pro-lab Diagnostics 2012). The vials were then stored at -80°C until use. Prior to use, the required bacterial strain was revived from frozen by streaking a bead taken from the desired microbank on tryptone soy agar (TSA) to prepare a subculture. Using sterilised forceps, a single bead was taken from the micro bank under aseptic conditions and placed on a TSA plate. The bank was immediately sealed and put back in -80˚C storage to avoid thawing of the remaining beads. Using sterile, disposable inoculating loops, the bead was streaked on a small section to one side of the plate. The forceps were again sterilised and used to remove the bead which was put to autoclave waste. The inoculated section of the plate was then streaked across the plate for isolation, to result in individual colonies. Figure 3.2 shows a basic example of the streaking pattern used. The plate was then incubated at 37˚C for 24 hours. The resulting subculture can then be used to inoculate secondary subcultures for use in inoculum preparation, in-order to minimise freeze/thawing of microbanks. The initial subculture plate was wrapped in parafilm and stored at 2 – 8°C for up to 2 weeks.

3.2 Inoculum Preparation

Inoculum preparation methods were adapted from previously published protocols (Wiegand, Hilpert, and Hancock 2008; Harrison et al. 2010)

3.2.1 Colony Suspension

Several bacterial colonies of similar morphology were taken from the prepared, secondary subculture plates and suspended growth broth. The suspension was vortexed vigorously

completely disperse bacterial cells through the broth. 1 mL of suspension was transferred to a cuvette and its turbidity measured by reading the absorbance at 625nM (Abs_{625}) using a Jenway® 6300 Spectrophotometer (Jenway® Equipment, Staffordshire, ST15 OSA, UK) which was blanked using fresh broth. A reading between 0.08 – 0.13 Abs_{625} represents a 0.5 McFarland standard, giving approximately a 1 x 10^8 cfu/mL suspension. The turbidity of the bacterial suspension was adjusted to that of a 0.5 MacFarland standard, either by suspending additional colonies if too low, or by diluting the suspension with additional broth. The resulting suspension is to be used within 30 mins of being prepared.

3.2.2 Broth Growth

Several bacterial colonies of similar morphology were taken from the prepared, secondary subculture and suspended in appropriate growth broth. The bacterial suspension was incubated in a rotary incubator at 37°C, 120 RPM. Bacterial growth was monitored by taking 1 mL aliquots from the suspension and measuring the absorbance at 625 nM (Abs_{625}). Absorbance was measured hourly until a reading ≥0.25 Abs_{625} was noted, which represents approximately 3 x 10^8 cfu/mL. This liquid culture can then be diluted to prepare appropriate inoculum.

3.1. Isolation and characterisation of veterinary zoonotic strains

Bacterial isolates including *Escherichia coli*, Methicillin-resistant *Staphylococcus aureus* (MRSA), Vancomycin Resistant Enterococci (VRE), *Listeria monocytogenes* and *Acinetobacter baumannii* were obtained from diagnostic testing of canine, equine and farm animals manifesting with conditions such as bacteraemia, renal infection, open wound infections, and mastitis. Collected samples of infection or disease in the form of urine, blood material, milk and swabs were provided by registered veterinary personnel in sterile containers (Cruinn Diagnostics, Dublin, Ireland). Liquid samples were immediately inoculated onto nutrient agar and incubated at 37°C for 24 hours. Swabs were inoculated in nutrient broth and incubated at 37°C for up to 24 hours under rotary conditions (125 RPM) before streaking onto nutrient agar plates.

Individual colonies were re-streaked for isolation and pure isolated colonies inoculated into nutrient broth for further biochemical characterization. Colonies were identified based on their morphological characteristics, biochemical profile, and growth on selective agars,

specifically CHROMagar™ Acinetobacter (CHROMagar™, Paris, France), Harlequin™ E. coli/Coliform Medium, Harlequin™ Listeria Chromogenic Agar, Baird Parker agar (LabM, Cruinn Diagnostics Ltd., Dublin, Ireland) and BBL™ Enterococcosel™ Agar (Becton, Dickinson and Company, Dublin, Ireland). Identity was confirmed via polymerase chain reaction (PCR). Specifically, a single colony of each bacterial test isolate was subcultured in nutrient broth and incubated overnight at 37°C. Genomic DNA was directly extracted using the GenElute™ Bacterial Genomic kit (Sigma-Aldrich/Merck, Merck Life Science Limited, Co. Wicklow, Ireland) according to the manufacturer's instructions. The bacterial primers ITS_8F (5'-AGAGTTTGATCCTGGCTCAG -3') and ITS_U1492R (5'- GGTTACCTTGTTACGACTT -3') (Sigma-Aldrich/Merck) were used for amplification of 16s rRNA gene. PCR was performed in a total reaction volume of 20 µL, containing 17 µL red Taq 1.1x master mix (VWR, Dublin, Ireland) 1 µL ITS_8F, 1 µL ITS_U1492R and 1 µL of pure genomic DNA eluate. DNA amplification was performed in a thermocycler (VWR, Dublin, Ireland) using the recommended parameters. Following DNA amplification, the PCR products were examined by electrophoresis on a 1% w/v agarose gel run at 120 volts for 50 min. Successful reactions were sent to Source Bioscience (Waterford, Ireland) for clean-up and gene sequencing of products. Strains were stored long term in 20% glycerol at -20℃ and short term in nutrient broth at 5℃. Identity of strains was confirmed via Gram stain and selective agars prior to each experimental set up.

3.3 Antibiotic resistance profile of veterinary isolates

Antibiotic resistance profiles were established using CHROMagar™ agars selective for Extended Spectrum Beta-Lactamase (ESBL), vancomycin-resistant enterococci (VRE) and Methicillin-resistant Staphylococcus aureus (MRSA)(CHROMagar™, Paris, France) and a range of antibiotic susceptibility disks (ThermoFisher Scientific, Ireland) as per European Committee for Antibiotic Susceptibility Testing (EUCAST) guidelines (European Committe on Antimicrobial Susceptibility Testing (EUCAST) 2021). Specifically, colonies of an overnight bacterial culture suspended in sterile saline at a density of 0.5 McFarland (ca. 1 x 10^8 cfu/mL) were overlaid on to Mueller-Hinton agar (MHA) (4 mm) in 90 mm circular petri plate as per the EUCAST disk diffusion method. An antibiotic inoculated disk was placed in the centre of the plate and incubated inverted for 18 hours at 37°C. Antibiotics used during profiling include Streptomycin, Vancomycin, Chloramphenicol, Erythromycin, Ampicillin, Amoxicillin /

Clavulanic acid, Cefpodoxime, Cefotaxime, Aztreonam, Doripenem, Meropenem, Ciprofloxacin, Levofloxacin, Colistin, Doxycycline.

Zones of inhibition were measured and used to determine the bacterial species resistance profile. The absence of a zone of inhibition denotes complete resistance (R) of the species against the tested antibiotic. Susceptible species were graded as being completely susceptible (S), or as having intermediate susceptibility (I), based on the ability of the test drug to produce a zone diameter according to EUCAST zone diameter guidelines. MRSA and VRE, which are listed as high importance, were assessed for resistance to vancomycin and quinolones amongst other therapeutics. Isolates that tested positive on CHROMagar™ ESBL and displayed resistance to the extended-spectrum cephalosporin group of antibiotics were selected for phenotype confirmation of ESBL production. ESBL detection and characterisation are recommended for public health and infection control purposes ((European Committe on Antimicrobial Susceptibility Testing (EUCAST) 2021)). This was carried out by placing cefpodoxime (10µg) and cefpodoxime/clavulanate (10µg/1µg) discs on an inoculated MHA plate, 30mm apart. Plates were then incubated overnight at 37°C. The test shows positive ESBL production if the inhibition zone diameter is 5 mm larger with clavulanate than without.

3.4 Plate Drop-count

In order to determine the bacterial concentration of a sample, the drop-count method was utilised as follows. Suspensions of the bacteria sample were prepared in sterile PBS at appropriate dilutions. Five drops of the bacterial suspension (10 µL) were dropped onto TSA plate and allowed to dry into the plate (approx. 1 hour). Figure 3.1 shows an example of a drop plate layout, with four separate sections each containing five 10 µL drops. Once the drops had dried, plates were inverted and incubated overnight. Following incubation, the number of individual colonies per drop were counted. Drops containing more than 40 colonies were regarded too numerous to count (TNTC) while those with less than 3 were regarded too few to count (TFTC). The total sum of colonies was determined and then the mean calculated. The cfu/mL was then determined using the following equation:

$$cfu/mL = Mean \times Dilution\ Factor \times 100$$

Where the *Mean* is the average number of colonies per drop, per dilution.

3.5 Bioactive Sample Preparation

Silver Nitrate ($AgNO_3$) (SKU: S8157, CAS: 7761-88-8), nisin, 2.5% (SKU: N5764, CAS: 1414-45-5), Chitosan, low molecular weight (SKU: 448869, CAS: 9012-76-4), Zinc Oxide (ZnO), nanopowder: <100 nm particle size (SKU: 544906, CAS: 1314-13-2) were purchased from Sigma-Aldrich/Merck.

$AgNO_3$ was prepared by dissolving in a solution of 28% (v/v) Poly(ethylene glycol), average molecular weight 400 (PEG-400) and 26% (w/v) d-sorbitol (Boekema 2018). The sample was vortexed to ensure complete solubility. The solution was then filter sterilised using a 0.2 µm syringe filter. The solution was aliquoted into 1.5 mL centrifuge tubes and stored at 4°C in a covered container to prevent light exposure. $AgNO_3$ preparation was carried out as quickly as possible to limit oxygen and light exposure.

Nisin was dissolved in a solution of 400 mM sodium chloride (NaCl), pH 3.25. The solution was sterilised by autoclaving, after which it was briefly centrifuged to settle precipitate. The supernatant was then taken as the active nisin solution. Nisin solution was stored at 4˚C and was prepared fresh every 7 – 10 days.

Chitosan was weighed and added to a container with 1% (v/v) acetic acid (AcOH). The container was sealed, and the solution then put to stir overnight at 50˚C to ensure complete solubilisation. The solution was then adjusted to pH 5.5 with 0.4 M sodium hydroxide (NaOH) in a dropwise manner. This preparation was then sterilised by autoclaving and allowed to cool to room temperature before use.

ZnO was suspended in dH_2O and then vortexed vigorously. The suspension was sterilised by autoclaving. Due to the nature of the suspension, it required vigorous agitation directly before use to ensure a uniform mixture.

3.6 Bioactive-loaded Polymer Processing

Each bioactive compound was incorporated into a polymer matrix by hot-melt extrusion (HME). The polymer carrier used was Kollidon® VA-64 (poly-vinyl-pyrrolidone/vinyl acetate, PVP/VA64), chosen as it has excellent stability throughout extrusion processing, good flowability, and can act as a solubilizer, dispersant, crystallization inhibitor and matrix former.

PVP/VA64 was purchased from BASF (BASF SE Headquarters, Ludwigshafen am Rhein, Germany). The bioactive and PVP/VA64 powders were weighed separately and combined in a container, preparing a stock of 100 g, with a minimum bioactive concentration of 1% (w/w). This is done as a concentration lower than 1% (w/w) is not suitable for HME, due to the nature of the extrusions blending process. The combined powders were thoroughly blended to ensure a uniform mixture. The bioactive/polymer mixtures, as well as a neat stock of PVP/VA64, were then dried in an air-flow oven for 24 hours at 60°C to remove all moisture which would alter the melting properties of the powders. The HME was carried out using a table-top twin-screw extruder, PRISM TSE-16-TC (Twin bore diameter: 16mm, screw diameter: 15.6 mm, channel depth: 3.3 mm, barrel length: 384 mm) (See Figure 3.5). A strand shaped die was used, to produce strands or filament like polymer products. The extruder was allowed to heat to 140˚C before use. The prepared PVP/VA64 stock was first fed through the extruder to coat the screws and barrel, and to ensure that the instrument was sufficiently clean before use. The sample mixtures were steadily fed manually into the hopper, which was gradually brought into the feed of the extruder, which was run at a screw speed of 100 RPM chosen to ensure uniform blending without being overly abrasive upon polymer or bioactives. The hopper was not allowed to run empty, but kept approximately 20% full, which allowed a free flow into the feed at the chosen screw speed, while not allowing the samples to sit too long as they may melt before entering the screw barrel. The samples were allowed to run and were examined exiting the die until an evident visual colour or physical change in the polymer was observed, indicating the presence of the bioactive. After an evident visual change in extruded polymer product was observed, it was allowed to run for short period after which processed samples were collected. When running multiple samples, the extruder was flushed thoroughly with stock PVP/VA64 between samples to remove residual material that may remain in the barrel from the previous sample. A clean screw and barrel was confirmed once the flushed stock polymer returned to its original colour/form.

3.7 Bioactive-loaded Polymer Preparation

The bioactive-loaded polymers were ground to fine powder using a mortar and pestle, after which they were put to solution. The bioactive-loaded polymers were dissolved in their corresponding bioactives solvent (section 3.4), apart from the $AgNO_3$ loaded PVP/VA64 polymer which was dissolved in dH_2O. Prepared samples were then sterilised by autoclaving,

which also aided in their complete solubilisation. A sample of PVP/VA64 (both pre-HME and post-HME) was also prepared in dH_2O as well as any other solvents that were used with the bioactives and assessed.

3.8 Minimum Inhibitory Concentration Assay

All steps were conducted under aseptic conditions or in closed systems. The antimicrobial properties of the bioactive solutions were assessed in terms of their minimum inhibitory concentration (MIC). The MIC refers to the lowest concentration of the solution required to inhibit bacterial growth, where growth is determined by an increase in broth turbidity and inhibition determined by no increase in turbidity, as determined by measuring absorbance. The MIC Assay procedure was adapted from a previously published protocol (Wiegand, Hilpert, and Hancock 2008). A secondary streak of the desired bacterial species was prepared 24 hours prior to the assay on an appropriate agar plate (see section 3.1). All bioactive concentrations are expressed in µg/mL in-order to keep comparable and uniform reporting of MICs.

3.8.1 Broth Microdilution Assay

Broth microdilution assays were carried out in a flat bottom 96-well plates (untreated) against three chosen bacterial strains, *E. coli*, *S. aureus* and *S. epidermidis*. Before use, microplate lids were treated using a hydrophilic coating (20% (v/v) isopropyl alcohol (IPA), 0.5% (v/v) Triton-X100)(Brewster 2003). The lid was exposed to this solution for 15 – 30 seconds. It was then drained and left to stand in an upright position until dry. 60 µL of Mueller-Hinton broth (MHB) was aliquoted to each well. 60 µL of antimicrobial solution to be tested was added to the wells of column 1 and serially diluted (1:2) along the plate to column 10. Each treatment was carried out with minimum of 2 technical replications (i.e., at least 2 wells in each column) allowing for up 4 different treatments to be assayed in a single 96-well plate. Where necessary, a treatment vehicle (T_v) was also included to assess any effects that the solutions maybe have (excluding the bioactive itself). The T_v concentrations were prepared in-order to mirror that of the treatment solutions.

A bacterial inoculum was prepared by colony suspension, as previously described (See Chapter 3.2.1). The inoculum was adjusted to a bacterial concentration of 1×10^6 cfu/mL. 60 µL of this inoculum dilution was added to each treatment well, giving a final in-well

concentration of 5 x 10^5 cfu/mL. 60 µL MH broth was aliquoted to the wells in column 11 along with 60 µL of the inoculum solution, acting as the negative treatment control, which is also referred to as a growth control (GC). 120 µL MH broth was aliquoted to the wells of column 11 to act as the positive treatment control, a blank control and also as the sterility control (SC). Final in well volume for all wells was 120 µL, with inoculated wells having a cell density of 5 x 10^5 cfu/mL (see Figure 3.3 for general microdilution layout). Following inoculation, a 10 µL sample was taken from the GC and diluted in 990 µL PBS (Total 1:100 dilution), from which a 100 µL aliquot was taken and further diluted in 900 µL PBS (Total 1:1000 dilution). These dilutions were used in-order to determine the actual in-well bacterial cell density of the plate, by utilising the drop-plate count method (see Chapter 3.3). Absorbance of the plate was then measured by using a BioTek® Synergy HT microplate reader with Gen5 Microplate Reader Software (Version 2.01.14) (BioTek® Instruments GmbH, Bad Friedrichshall, Germany). The plate was read with an endpoint absorbance read at 625 nM and results were recorded as time-point 0 (t = 0). This allowed measurement of any turbidity caused by treatments and will be used for later calculations. The plate was placed in a container to aid evaporation prevention. Container was placed on a rotary incubator at 120 RPM, 37˚C for 18 hours.

Following incubation, the plates were removed, and their wells were observed for growth as determined by visible turbidity. In order to quantify this turbidity (i.e., growth), the plate absorbance was read (variable shake, 1 minute. endpoint absorbance read at 625 nm). Results were recorded as timepoint 18 (t = 18). An additional growth check was carried out by use of the extra-cellular metabolic dye, resazurin (commonly sold under the name alamarBlue™). Resazurin was added to each well, giving a final concentration of 10 µg/mL. The fluorescence was read using a Synergy HT microplate reader (Excitation: 528/20, Emission: 590/35) immediately to give a reading at t = 0. Plates were then incubated at 37°C, and fluorescence was read after 1 hour. Wells were also observed for colour change (blue to pink) which denoted bacterial metabolic activity. The well absorbance and fluorescence values were averaged and the % Inhibition for each treatment column was determined, relative to the averaged GC values. The t = 0 values were used as a blank and so removed from all relative well values. The MIC was determined as the lowest concentration of a treatment to cause 95 – 100% inhibition (allowing for minor discrepancies). Absorbance values were used as the

principal data for determining MIC, while the fluorescence values were utilised as confirmatory aids.

3.9 Biofilm Inhibition and Reduction Assays

Anti-biofilm potential of each bioactive and bioactive-loaded polymer was carried out using two chosen bacterial strains, *P. aeruginosa* and *S. aureus*, per methods adapted from previously published protocols (O'Toole 2011; Harrison et al. 2010; Innovotech 2015; Bueno 2011). The bioactive compounds were assessed in terms of their ability to inhibit bacterial attachment (attachment inhibition) and biofilm development (biofilm inhibition) and for their ability to eliminate an already developed biofilm (biofilm reduction). Biofilm assays were carried out in Thermo Scientific™ Nunc™ 96-well plates using Thermo Scientific™ Nunc™ Immuno TSP peg lids. Plate wells and lid pegs were coated with a bovine plasma solution before use. Bovine plasma (citrated and lyophilized) (Product code: P4639) was purchased from Merck. Thermo Scientific™ Nunc™ flat-bottom plates (non-treated) (Product code: 10000571) and Thermo Scientific™ Nunc™ Immuno TSP lids (Product code: 10429962) were purchased from Thermo Fisher Scientific (Fisher Scientific, Dublin, Ireland). The bovine plasma was reconstituted in sterile PBS to the marked volume, giving a 100% solution. The solution was diluted to 1% solution in PBS. 120 µL of 1% bovine plasma was aliquoted to each well and the TSP lid was placed on the plate, submerging the pegs in the 1% bovine plasma solution in the wells. The plate was then incubated at 4°C overnight. Resulting plates and peg lids were used the following biofilm assay protocols. The bovine plasma solution was not aspirated from wells too soon in order to avoid drying of the well walls or lid pegs. The following assays were carried out in matching approaches, apart from the stage at which the bioactive treatments are introduced.

3.9.1 Attachment Inhibition

100 µL of each treatment solution was added to corresponding wells of column 1 in the plate. 50 µL of BHI broth was added to the remaining wells, with 100 µL added to column 12 to act as the positive/sterility control (SC) having only BHI broth. 50 µL of each treatment was serially diluted across the plate from column 1 – 10. Bacterial inoculum was prepared as per the broth growth method (section 3.2.2). The inoculum was adjusted and 50 µL was added to each well in columns 1 – 11, to result with an in-well bacterial cell density of 1 x 10^6 cells/mL. Column

11 was to act as the negative/growth control (GC), having just bacteria and no treatment. The pegs were inserted into the wells and the plate was incubated at 37°C for 1 hour.

Following attachment, well contents were aspirated, and wells and pegs were washed twice with 120 µL PBS to remove loosely attached bacteria. 100 µL fresh BHI broth was added to each well and the pegs were placed back in the wells, and the plate was incubated under static conditions at 37°C overnight for 24 hours to allow biofilm growth. Following overnight incubation, the peg lid was removed, and the well contents removed. The wells and pegs were washed twice with PBS. 120 µL resazurin solution (10 µg/mL) was added to each well of the biofilm plate, and to each well of a new, sterile 96-well plate. The biofilm plate was closed with a standard 96-well plate lid, and the lid pegs were placed into the wells of the new plate. The fluorescence of both plates was measured using a Synergy HT microplate reader (Excitation: 528/20, Emission: 590/35) for time-point 0 (t = 0) and the plates were covered and incubated at 37°C, 120 RPM. Fluorescence was then measured each hour until a noticeable fluorescence signal was measured in every well, or up to a max incubatory period of 5 hours. Plates and pegs were then carried on for crystal violet (CV) staining. From this point, there was no need to keep conditions sterile and aseptic. The plate was emptied, and the wells and pegs were washed with dH_2O. The biofilms were heat-fixed by putting the biofilm plate and peg lid to a 60°C oven overnight. Following heat-fixing, 120 µL for 0.1% CV solution was added to each well of the biofilm plate and the pegs were placed into the wells. The plate was left to incubate at room temperature (RT) for 10 – 15 mins. The CV was disposed of, and the wells and pegs were washed in dH_2O 2 – 3 times or until no more CV was being evidently washed off. At this point, formed biofilms were evident by purple staining on the pegs or around the well edges. They were then left to air dry in a fume hood. The CV was then solubilised using 30% acetic acid (AcOH), by adding 120 µL to each well of the biofilm plate, and to each well of a separate 96-well plate for the peg lid. Both plates were incubated under rotation for at least 30 mins to allow complete solubilisation. Plates and pegs were observed for complete solubilisation of the CV (as evident from any remaining purple rings on the pegs or on the edges of the wells). If CV was not completely solubilised, they were incubated for a further 30 mins. Absorbance of each plate was read (590 nM). Resazurin conversion readings were used quantify bacterial numbers within the biofilm of each well/peg by determining the % reduction of cell numbers by comparing the fluorescence readings against those from the

GC (0% reduction). The CV absorbance was used to quantify the physical biofilm formed on the pegs/wells by comparing the absorbance of the treatments to the of the GC (100% growth) and SC (0% growth). These readings can then be used to determine attachment inhibition by reduced cell counts or biofilm formation.

3.9.2 Biofilm Inhibition

Bacterial inoculum preparation, initial attachment and biofilm growth was carried out as per section 3.9.1, with the following modification: following the aspiration and wash steps carried out after initial attachment, 200 µL of each treatment solution was added to corresponding wells of column 1 in the plate. 100 µL of BHI broth was added to the remaining wells. 100 µL of each treatment was serially diluted across the plate from column 1 – 10. Wells in columns 11 and 12 were left without treatments. The pegs were re-inserted into the plate, and the plate was incubated under static conditions at 37°C overnight for 24 hours to allow biofilm growth in conjunctions with treatment exposure. Following incubation and biofilm growth, the peg lids and plate wells were washed and analysed by use of resazurin solution, and then subsequently using CV as per section 3.9.1. Resazurin conversion readings were used to quantify bacterial cell numbers within formed biofilms on each well/peg and the CV absorbance was used to quantify the physical biofilm formed on the pegs/wells as previously done. These readings were then expressed in terms of percentage biofilm growth inhibition.

3.9.3 Biofilm Reduction

Bacterial inoculum preparation, initial attachment and biofilm growth was carried out as per section 3.9.1 and 3.9.2, with the following modification: following overnight incubation, the peg lid was removed, the wells contents aspirated, and the wells and pegs were washed with PBS. 200 µL of each treatment solution was then added to corresponding wells of column 1 of a separate 96-well plate. 100 µL of BHI broth was added to the remaining wells. 100 µL of each treatment was serially diluted across the plate from column 1 – 10. Wells of columns 11 and 12 were left without treatments. Contents of this plate was then transferred to the biofilm growth plate. The pegs were re-inserted into the plate, and the plate was then incubated under static conditions at 37°C for 24 hours overnight. Following incubation, the peg lids and plate wells were washed and analysed by use of resazurin solution, and then CV

as previously described. Results were used to determine final % reduction of internal bacterial numbers (resazurin) or reduction of the physical biofilm (CV).

3.10 Combination Assays

In order to determine any interactions that may occur between the bioactive compounds while in treatment, a number of drug-combination assays were carried out. Combination assays were carried out in a similar approach as to that of the broth microdilution assays, using untreated, flat bottom 96-well plates, with a number of alterations depending on the final number of treatments to be assessed. The chosen bacterial species were *E. coli*, *S. aureus* and *S. epidermidis*.

3.10.1 2-Drug Combination Assay

2-Drug combination assays were prepared in an 8x8 checkerboard layout, which covered the wells in columns 1 – 8, rows A – H. This layout allowed for a total of 64 combinations on one plate, 8 concentrations of Drug A versus 8 concentrations of Drug B. Dilutions of drug A and B were prepared in Mueller-Hinton broth (MHB) to a concentration four times higher (4X) than the highest desired in-well concentration. This final in-well concentration of each drug should be calculated after determining the MIC value and should be equal to twice (2X) that of the MIC. Normal broth microdilution assay will also be carried out (as per 3.7.1) as a control to ensure the individual treatments and bacteria to be tested are performing nominally.

A sterile, flat bottom (F-bottom) 96-well plate (untreated) was labelled Plate 1 (treatment plate). Lids were treated with a hydrophilic coating (20% (v/v) IPA, 0.5% (v/v) Triton-X100) (Brewster 2003). The lid was exposed to the solution for 10 – 15 seconds after which it was drained and left standing in an upright position until dry.

60 µL of the prepared drug A dilution was aliquoted to each well in column 1. 30 µL of MHB was aliquoted to the remaining wells of the checkerboard within Plate 1 (columns 2 – 8). 30 µL was taken from column 1 and serial diluted (1:2) across the plate, from column 1 – 7, leaving column 8 with only MHB.

A separate, sterile round bottom (U-bottom) 96-well plate (untreated) was labelled plate 2 (dilutions plate). 60 µL of MHB was aliquoted to each well in the first 7 rows of the checkerboard on plate 2 (Row A – G). 120 µL of drug B was aliquoted to the wells in row H. 30

µL was taken from wells in row H and serial diluted (1:2) up the plate, from row H - B, leaving row A with only MHB.

The prepared dilutions of drug B were then transferred to plate 1 by transferring 30 µL from each well to the corresponding wells of plate 1, starting from row A (i.e. starting at the lowest concentration) (Figure 3.5). This transfer results in a 1:2 dilution of drug A and drug B. The bacterial inoculum was then prepared via the colony suspension method (see chapter 3.2.1). 60 µL of MHB was added to each well in column 9 for use as a negative treatment control/growth control (GC), and 120 µL to wells in column 10 to act as positive treatment control/sterility control (SC). 60 µL of prepared inoculum was added to all wells of the checkerboard in plate 1 (i.e., all wells within column 1 – 8, row A – H) resulting in an additional 1:2 dilution of drug A and drug B, for a total dilution of 1:4. 60 µL of the inoculum was also added to wells of column 10, the GC. See Figure 3.6 for a final plate layout. Final in-well bacterial cell density equals 5 x 10^5 cfu/mL, with a final volume of 120 µL. Following inoculation, a 10 µL sample was taken from a random well of the GC and diluted 1:100 and 1:1000, and then plated following the drop-count technique (see Chapter 3.3) in order to determine the final in-well cell density.

Absorbance of the plate was read using a Synergy HT microplate reader (endpoint rea:625nm, with 5 second variable shake) to give an initial reading for timepoint 0 (t = 0). The plate was placed in a container to prevent evaporation. Container was placed on a rotary incubator at 120 RPM, 37 ˚C for 18 hours. Following incubation, absorbance of plate was read (t = 18). Resazurin was then added to each well giving a final concentration of 50 µg/mL. Fluorescence was read (Excitation: 528/20, Emission: 590/35) and plates were incubated for an additional 1 hour, after which the fluorescence was read again. Comparison of absorbances was used to determine bacterial growth inhibition and was expressed in terms of % Inhibition. The fluorescent readings were used as a secondary means of identifying inhibition.

3.10.2 3-Drug Combination Assay

3-Drug combination assays were carried out in a 6x6 checkerboard layout. The size of the checkerboards was reduced in-order to facilitate the number of drug combinations without requiring the use of excessive amounts of plates and reagents, while also having enough test combinations to properly assess a range of concentrations and combinations. To equally

assess the combinational effect of a third treatment, drug C, six such checkerboards were prepared combining drug A and drug B, with each individual checkerboard having a single concentration of drug C being applied. This setup allows for 6 concentrations of drug A, drug B and drug C to be assessed in combination (6x6x6) for a total of 216 combinations. The experiment was split across three 96-well plates, allowing for two 6x6 checkerboards per plate. A broth microdilution assay was also carried out (as per 3.7.1) as a control to ensure the individual treatments and bacteria to be tested are performing nominally. The procedure for preparing a 6x6x6 setup was as follows.

A broth microdilution assay was also carried out using drug A, B and C (as per 3.7.1) in tandem with the 3-Drug combination assay, as a control to ensure that the individual treatments and bacteria being tested are performing nominally. Working stock dilutions of drug A and drug B were prepared in MHB to a concentration five times (5X) greater than the highest desired in-well concentration. Three flat bottom (F-bottom) 96-well plates (untreated) were labelled plate 1, 2 and 3 (treatment plates). The lids were treated using a hydrophilic coating (as per 3.9.1) and allowed to dry. Two 6x6 checkerboards (CB) were designated on each plate, one within columns 1 – 6, rows A – F and the other within columns 7 – 12, rows A – F, and assigned an identity number (Plate 1: CB1, CB2. Plate 2: CB3, CB4. Plate 3: CB5, CB6). 60 µL of drug A dilution was added to each well in the first column of each CB, 30 µL MHB was added to the remaining wells. 30 µL of drug A was taken from the first column of the CB and serial diluted along the CB, excluding the last column, leaving those wells with only MHB. This was repeated in all six CBs.

In a separate U-bottom 96-well plate, a serial dilution of drug B was carried out in two CBs. 300 µL of drug B was added to the wells of row F. 150 µL of MHB was added to the remaining wells. Drug B was serial diluted from row F – row B. Row A was left with just MHB. 30 µL of each dilution was transferred to the corresponding wells in each CB of each treatment plate, starting at the lowest concentration, resulting in a 1:2 in-well dilution of drug A and B. Five stock dilutions of drug C were prepared in broth to a concentration 2.5X greater than the desired in-well concentrations. 60 µL of drug C was added to each corresponding CB in each treatment plate, while only adding MHB to the wells of CB6, resulting in a 1:2 in-well dilution of drug A, drug B, and drug C.

The bacterial inoculum was then prepared via the colony suspension method (see chapter 3.2.1). 120 µL of MHB was added to each well in row G for use as a negative treatment control/growth control (GC), and 150 µL to wells in row H to act as positive treatment control/sterility control (SC). 30 µL of prepared inoculum was added to all wells of each CB in each plate resulting in an additional 4:5 dilution of drug A and drug B, for a total dilution of 1:5. 30 µL of the inoculum was also added to wells of row F, the GC. See Figure 3.7 for final plate layout. Final in-well bacterial cell density equals 5 x 10^5 cfu/mL, with a final volume of 150 µL. Following inoculation, a 10 µL sample was taken from a random well of the GC and diluted 1:100 and 1:1000, and then plated following the drop-count technique (see section 3.3) in order to determine the final in-well cell density.

Absorbance of each plate was read using a Synergy HT microplate reader (endpoint absorbance read:625nm, with 5 second variable shake) to give an initial reading for timepoint 0 (t = 0). The plates were placed in a container to prevent evaporation. Container was placed on a rotary incubator at 120 RPM, 37 ˚C for 18 hours. Following incubation, absorbance of plate was read (t = 18). Resazurin was then added to each well giving a final concentration of 50 µg/mL. Fluorescence was read (Excitation: 528/20, Emission: 590/35) and plates were incubated for an additional 1 hour, after which the fluorescence was read again. Comparison of absorbances was used to determine bacterial growth inhibition and was expressed in terms of % Inhibition. The fluorescent readings were used as a secondary means of identifying inhibition.

3.10.3 4-Drug Combination Assay

4-Drug combination assays were carried out in a 4x4 checkerboard layout, expanding upon the 3-Drug layout and reasoning. A 4x4 sized checkerboard holds a number of disadvantages over a larger 6x6 or 8x8 checkerboard, primarily the fact that it cannot accommodate enough combinations to give a full model of the possible combinational interactions. However, if performed following a 2-Drug or 3-Drug assay, key concentrations noted from these assays can be selected and utilised within the 4-Drug assay for further investigation. As such, the following 4-Drug assay layout should be used as a follow-on study rather than an initial combinational study, due to such limitations. Likewise, with the chosen 3-Drug assay layout, the 4-Drug assay layout allowed for a reduced experimental size and faster setup. The layout was designed in such a way that four 4x4 checkerboards (CBs) are set up within four 96-well

plates. Each CB will have drug A combined with drug B. Each of these four CBs will then have a different concentration of drug C added. To all CBs within each plate, a difference concentration of drug D will be added. The resulting system will yield a 4x4x4x4 combination (totalling in 256 combinations).

A broth microdilution assay was also carried out using drug A, B, C and D (as per 3.7.1) in tandem with the 4-Drug combination assay, as a control to ensure that the individual treatments and bacteria being tested are performing nominally. Three dilutions of each test treatment, drug A, drug B, drug C and drug D were prepared in MHB at a concentration 5X greater than the final desired in-well concentration. This was done in order to account for all dilutions steps from addition of the treatments and inoculum. Four flat bottom (F-bottom) 96-well plates (untreated) were labelled plates 1 – 4 (treatment plates). The lids were treated using a hydrophilic coating (as per 3.9.1) and allowed to dry. Four 4x4 CBs were designated on each plate, CB1 (columns 1 – 4, rows A – D), CB2 (columns 5 – 8, rows A – D), CB3 (columns 1 – 4, rows E – H) and CB4 (columns 5 – 8, rows E - H). 30 µL of each drug A dilution was added to each well in the corresponding column of each CB, 30 µL MHB was added to the remaining wells. 30 µL of drug B was added to each well in the corresponding column of each CB, 30 µL MHB was added to the remaining wells. 30 µL of the drug C dilutions were added to the wells of each corresponding CB on each plate, with 30 µL of MHB added to the wells of each CB4. 30 µL of the drug D dilutions were added to all treatment wells on their corresponding plates, with 30 µL MHB added to the treatment wells of plate 4.

The bacterial inoculum was then prepared via the colony suspension method (see chapter 3.2.1). 122 µL of MHB was added to each well in column 9 for use as a negative treatment control/growth control (GC), and 150 µL to wells in column 10 to act as positive treatment control/sterility control (SC). 30 µL of prepared inoculum was added to all wells of each treatment well in each plate, and 30 µL was also added to wells of column 9, the GC. See Figure 3.8 for final plate layout. Final in-well bacterial cell density equals 5 x 10^5 cfu/mL, with a final volume of 150 µL. Following inoculation, a 10 µL sample was taken from a random well of the GC and diluted 1:100 and 1:1000, and then plated following the drop-count technique (see section 3.3) in order to determine the final in-well cell density.

Absorbance of each plate was read using a Synergy HT microplate reader (endpoint read:625nm, with 5 second variable shake) to give an initial reading for timepoint 0 (t = 0).

The plates were placed in a container to prevent evaporation. Container was placed on a rotary incubator at 120 RPM, 37 ˚C for 18 hours. Following incubation, absorbance of plate was read (t = 18). Resazurin was then added to each well giving a final concentration of 50 µg/mL. Fluorescence was read (Excitation: 528/20, Emission: 590/35) and plates were incubated for an additional 1 hour, after which the fluorescence was read again. Comparison of absorbances was used to determine bacterial growth inhibition and was expressed in terms of % Inhibition. The fluorescent readings were used as a secondary means of identifying inhibition.

3.10.4 Analysis of Results for Determination of Synergy/Antagonism

Results from drug combination assays were analysed to determine drug interactions in terms of synergy or antagonism, by use of the *synergy* python package (D. J. Wooten and Albert 2021). Input data for synergy was prepared in Excel using the concentration of each drug (µg/mL), and the % growth. Input data contained an individual column for the concentration of each drug ("drug1.conc", "drug2.conc", "drug3.conc" and "drug4.conc"). For analysis using the Bliss model, the reported response was expressed in terms of % growth. The response was input under the column "effect" and was expressed as a decimal fraction of 1 (i.e., 100% growth = 1.0, 50% = 0.5, 0% = 0.0). Data was then exported as an .csv file. The synergy package was opened and run using PyCharm (version 2020.2), a python integrated development environment (IDE). Following the synergy documentation, input data was imported and analysed. The Bliss model was used due to its simplicity, which was advantageous for analysing the more complex inputs of the 3-drug and 4-drug assays.

3.11 Establishing BME Cell Stock

Bovine mammary epithelial (BME) cells (Cat. No. ME-BN-501) and bovine mammary epithelial proliferation media (BMEM) (Cat. No. BNM-02) were purchased from AvantiCell Science Limited (AvantiCell Science Limited, Scotland). All flasks were surfaced treated with 0.2% gelatin solution for 1 hour before use to aid cell attachment. BME cells were acquired as a frozen vial and immediately put to liquid nitrogen storage upon receipt. To establish an adequate cell stock, the cells were removed from storage and grown as follows; cells were taken from liquid nitrogen (LN_2), quickly thawed, and added to 15mL of warmed (37°C) bovine mammary epithelial proliferation media (BMEM). The cell suspension was added to a T-75

flask, placed on a flat surface for 5 minutes to allow cell attachment, and then incubated (37°C, 5% CO_2). Cell growth was checked every 24 hours. Once cells had grown to ~80% confluency, they were then split into two T-175 tissue culture flasks and allowed grow again. Once both flasks reached ~80% confluency they were split, suspended in freezing media (90% foetal bovine serum, 10% dimethyl sulfoxide (DMSO)) and divided into separate cryogenic storage vials at 1 x 10^6 cells. The tubes were put into a Mr. Frosty™ freezing container and stored at - 80°C for 24 hours. They were then transferred to LN_2 for long term storage.

3.12 Cell Viability Assay

Effect of bioactives upon BME cells was determined by use of a cell viability assay. All steps carrier out in sterile conditions were appropriate. Prior to experiment, all flasks and plates were surfaced treated with 0.2% gelatin solution for at least 1 hour to aid in cell attachment. A vial of BME cells was taken from previously prepared stock in LN_2 storage and grown in a T-75 flask to ~80% confluency. Cells were passaged again before use. Cells were split and used to seed a 96-well microplate at 5 x 10^3 cells/well. Cells were allowed to fully attach and reach ~80% confluency before use. Media was aspirated from all wells and 100 µL of fresh media added. 100 µL of bioactive solution was added wells of column 1. 100 µL was taken and serially diluted across the plate (column 1 – column 10). Columns 11 and 12 were left without treatment (negative and positive control respectively). Treatments were carried out in duplicates. Treatment vehicles (T_v) of the bioactives were also added to assess any additional effects that may be caused by the solutions used to prepare the treatments. Plates were incubated for 18 hours (5% CO_2). Following incubation, media was aspirated from all wells. A solution of 0.5% Methylthiazolyldiphenyl-tetrazolium bromide (MTT) was prepared in BMEM and 100 µL added to wells of column 1 – column 11. 100 µL stock BMEM was added to column 12. Plate was incubated for 3 – 4 hours, until MTT was metabolized by the cells, which was indicated by a dark purple colour observable in cells of the negative control, indicating presence of formazan crystals. Media was aspirated from wells and 100 µL DMSO was added to each well to solubilise the cells and formazan crystals. Plate was placed on a rotary incubator (37˚C) for 30 minutes or until all crystals were solubilised. Plate absorbance was read (endpoint read: 540 nm). Absorbance readings were used to determine percentage cell viability by comparing absorbances of treatment wells against absorbances of the negative control. Cytotoxicity of bioactives was assessed by determining the lowest concentrations

which caused ≥70% cell death (IC70) as per international standards guideline document, ISO 10993-1:2018 (International Organization for Standardization 2018).

Cell images were taken using Olympus CKX41 inverted light-microscope with a IS300, 3.0 MP camera attachment. (Olympus Life Science, Hamburg, Germany), using TSView Imaging Software (Version 7.3.1.7).

3.13 Cellular Immune Response Assay

The immune response of BME cells to each bioactive compound was determined by measuring gene activity using reverse transcriptase, quantitative polymerase chain reaction (RT-qPCR.).

3.13.1 BME Cell Treatment

All steps carried out in sterile conditions. All flasks and plates were surface treated using 0.2% gelatin solution to aid in cell attachment. BME cells were taken from LN_2 stock, grown, and passaged twice before use. A 24-well tissue culture plate was seeded with 500 µL of BME cells at $5x10^4$ cells/mL ($2.5x10^4$ cells/well). Cells were mixed gently by pipetting to prevent accumulation in the centre of the wells. The plate was then rocked gently back and forth, and then placed on a solid flat surface for 5 mins to allow dispersed attachment. Cells were constantly monitored under microscope to ensure an even dispersion. Cells were then incubated (37˚C, 5% CO_2) until ~80% cell confluency was observed in wells.

Lipopolysaccharide (LPS) from Escherichia coli O111:B4 (Merck, product number: L2630) was reconstituted in UltraPure™ DNase/RNase free, distilled water (uH_2O)(Thermo Fisher Scientific, product code:11538646) to a concentration of 4 mg/mL. A stock dilution of LPS was prepared in media to a concentration of 10 µg/mL and was further diluted in media as needed. Media was aspirated from wells and the cells were then pre-treated for 1 hour with 500 µL of 50 ng/mL LPS.

Stock solutions of each bioactive treatment were prepared to a concentration so as to give a final in-well concentration equal to the highest concentration that does not cause any noticeable effects upon the cell viability (as determined previously). Stock solutions of the polymer PVP/VA64 were also prepared. All stock solutions were prepared to double the concentration (2X), as they will be added as a co-treatment with LPS. Following 1-hour LPS

pre-treatment, media was aspirated and 250µL of each treatment dilution was added to their corresponding wells, along with 250µL of 100ng/mL LPS to give a final in-well concentration of 50 ng/mL LPS. Cells were the incubated for 24 hours (37˚C, 5% CO_2), after which they were taken for RNA extraction and isolation.

3.13.2 RNA Extraction & Isolation,

All steps carried out in appropriate area for RNA preparations, with consistent cleaning of area and items using RNase AWAY surface decontaminator (Thermo Fisher Scientific). All samples, materials (plates, tubes) and reagents were kept on ice were possible. Media was aspirated from all wells of plate and cells were gently washed with ultrapure, RNase-free water (uH_2O) twice. While working in a fume hood, 500 µL of TRIzol was added to each well to solubilize the cells and extract nuclear material. Cells were completely solubilized by gently mixing and were allowed to incubate at room temperature (RT) for 5 minutes. Contents of each well were transferred to individual 1.5 mL centrifuge tubes. 0.1 mL chloroform was added to each tube. Tubes were mixed vigorously for 15 seconds using a vortex and then allowed to incubate for 2 – 3 mins at RT. Using a refrigerated centrifuge, tubes were spun at 12,000xg, 4°C for 15 mins, the resulting sample was divided into 3 layers (if no clear divide was formed, tubes were centrifuged for an additional 5 – 10 mins). The upper, clear aqueous phase containing the extracted RNA was carefully aspirated and transferred to a new 1.5 mL centrifuge tube.

RNA was precipitated by adding 250 µL IPA to each tube and allowing them to incubate for 10 mins at RT. Tubes were centrifuged for 10 mins at 12,000 xg, 4°C forming an invisible RNA pellet at the base of the tube. Supernatant was discarded and the pellet resuspended in 500 µL 75% ethanol. Tubes were vortexed briefly and centrifuged at 7500 xg, 4°C for 5 mins. Supernatant was discarded as much as possible. Tubes were left out to allow pellets to air dry, taking care not to let the pellet dry completely. Pellet was resuspended in uH_2O. RNA yield and purity was determined by use of a Picodrop™ CUBE (Pico100) microliter UV/Vis spectrophotometer and the accompanying Picodrop software. The software was set to measure RNA and was blanked using uH_2O. A 2 µL aliquot of each sample was read. The software automatically calculates RNA yield and purity. Purity was determined by the 260/280nm absorbance ratio method which was automatically calculated by the Picodrop software, giving purity in ng/mL.

3.13.3 cDNA Template Synthesis

All steps carried out in appropriate area for RNA preparations, with consistent cleaning of area and items using RNase AWAY. All steps were performed on ice were possible. Using RNA yields calculated from previous step, samples were prepared for cDNA synthesis. Appropriate dilutions were determined for each experimental replicate in order to prepare 12µL of each RNA sample containing the same amount of RNA in each (calculated in relation to the lowest yielding sample). A reverse transcriptase (RT) master mix (MM) was prepared from a Transcriptor First Strand cDNA Synthesis Kit (Roche). At least 10µL of MM is required per reaction, with each reaction containing RT buffer, dNTP mix (100mM), RT random primers, RT, RNase inhibitor and uH_2O, prepared as per manufacturers guidelines. A stock MM was prepared with excess for all reactions to be carried out. 10µL of each RNA sample was transferred to a separate tube of a thermal cycler 8-tube strip. 10µL of RT MM was added to the bottom of each tube. The tube strip was capped and briefly centrifuged to collect all contents at the bottom of each tube. The tubes were placed in a Applied Biosystems™ MiniAmp™ thermal cycler and with the following conditions. Reaction volume: 20µL. Step 1: 25°C for 10 mins. Step2: 37°C for 120 mins. Step 3: 85°C for 5 mins. Step 4: 4°C indefinitely. After run was completed, tubes were removed from the thermal cycler and were either used immediately for PCR or stored at -14°C.

3.13.4 qRT-PCR

All steps carried out in appropriate area for RNA preparations, with consistent cleaning of area and items using RNase AWAY. All samples, materials (plates, tubes) and reagents were kept on ice were possible. Primers were reconstituted with uH_2O, as per their individual documentation, to 100 µM. 10 µM stocks of each primer were prepared, to avoid recurrent freeze/thawing of the original primer stocks. 1:10 dilutions of each cDNA template were prepared, with excess being prepped for all reactions to be carried out (number of genes x number of replicates). A PCR MM was prepared using KiCqStart Sybr Green master mix (Sigma-Aldrich/Merck) as per the kit protocol, containing KiCqStart Sybr Green, forward primers, reverse primers and uH_2O. 4 µL of the prepared cDNA templates were added to individual wells of a LightCycler® 96-well plate in duplicate. 4 µL of uH_2O was also added to separate wells (in duplicate) to act as the non-template control (NTC). 16 µL of the PCR MM was then added to each corresponding well (depending on the gene/primer). Plate was sealed

using the accompanying sealing foils. Plates were centrifuged for 5 mins to ensure all reaction contents were collected at the base of each well. Plate was then loaded into a Roche LightCycler® 96 System and run with the following conditions. **Preincubation**: 95°C for 300 seconds. **2-Step Amplification** (60 cycles): 95°C for 5 seconds. 58°C for 15 seconds. 72°C for 10 seconds (single acquisition). Results were analysed using Roche LightCycler® 96 software (version 1.1.0.1320). Relative Quantification was determined by analysing the target gene of interest against the reference gene, β-actin.

3.14 Statistical Analysis

Results were analysed and statistical significance calculated by use of GraphPad Prism 8.0.1 for Windows (GraphPad Software, San Diego, California, USA. www.graphpad.com). Results from MIC testing of bioactives and their polymer processed forms for each bacterial strain were analysed for significance. Significant changes in MIC before and after polymer extrusion were determined by use of a two-way ANOVA with Sidak multiple comparisons test and expressed in terms of a P value, following the APA style.

For toxicology results, significance between treatment and treatment vehicle (T_v) effects versus bovine mammary cells was determined by use of a two-way ANOVA model with Sidak multiple comparisons test and expressed in terms of a P value, following the APA. For the analysis of zinc oxide (in which there was no treatment vehicle), significance was determined by use of a Wilcoxon signed-rank test (non-parametric statistical hypothesis test) with the hypothetical value = 100. This was chosen to represent the hypothesis that the compound would have no effect upon the cells, thus resulting in 100% cell viability.

3.15 Figures

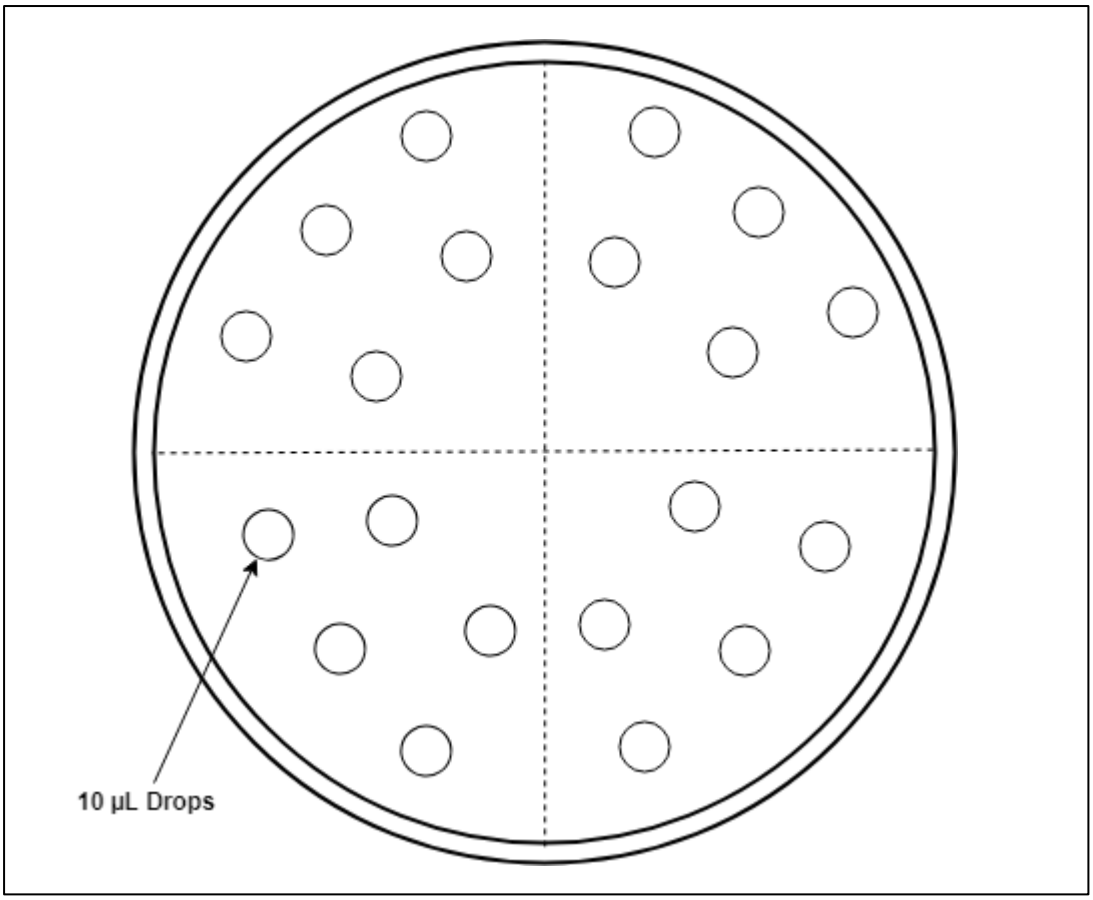

Figure 3.1 *Layout of Drop-count plates*.
Plates were divided into quarters to allow for 4 separate counts. Each circle represents a 10 µL drop of the diluted sample, with five drops per section.

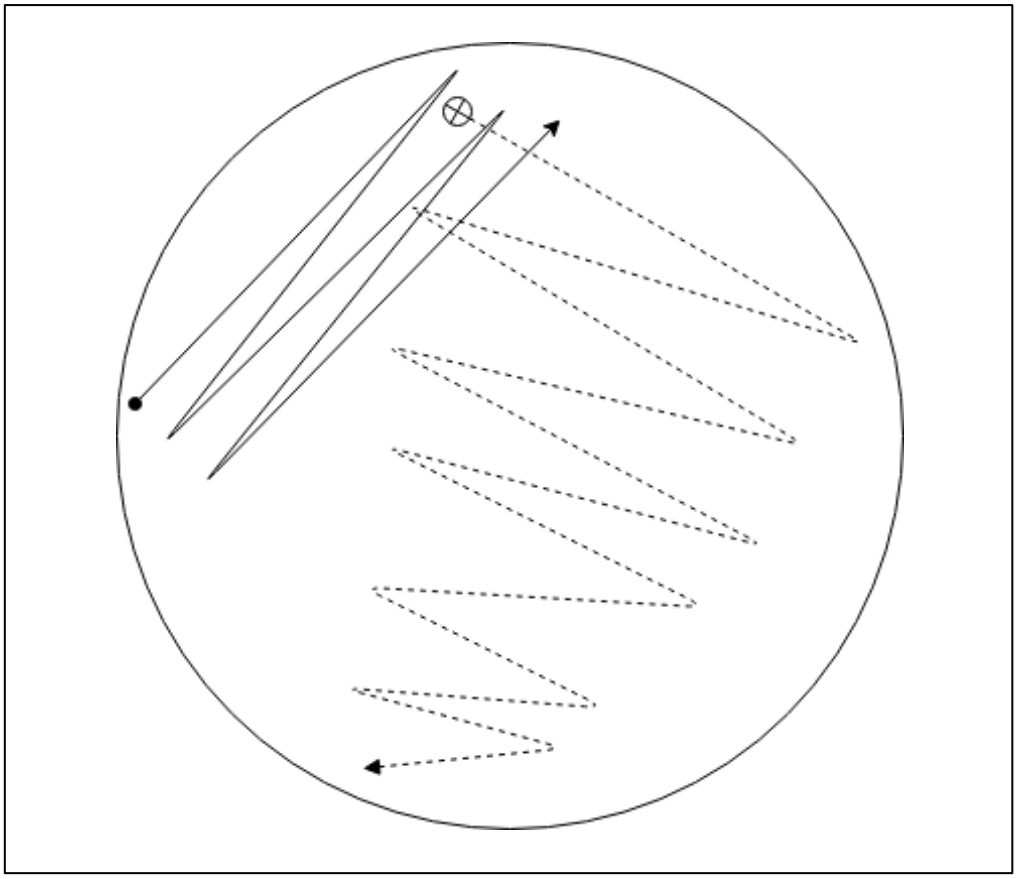

Figure 3.2 *Streak Plate Pattern*.
Streaking pattern used to isolate colonies of bacterial species. Solid line represents initial streak made using microbead. Dotted lines represent streak taken from initial streak in order to isolate colonies of the bacteria.

Drug X — Serial Dilution 1:2

	1	2	3	4	5	6	7	8	9	10	11	12
A	X	X/2	X/4	X/8	X/16	X/32	X/64	X/128	X/256	X/512	GC	SC
B	X	X/2	X/4	X/8	X/16	X/32	X/64	X/128	X/256	X/512	GC	SC
c	X	X/2	X/4	X/8	X/16	X/32	X/64	X/128	X/256	X/512	GC	SC
D	X	X/2	X/4	X/8	X/16	X/32	X/64	X/128	X/256	X/512	GC	SC
E	X	X/2	X/4	X/8	X/16	X/32	X/64	X/128	X/256	X/512	GC	SC
F	X	X/2	X/4	X/8	X/16	X/32	X/64	X/128	X/256	X/512	GC	SC
G	X	X/2	X/4	X/8	X/16	X/32	X/64	X/128	X/256	X/512	GC	SC
H	X	X/2	X/4	X/8	X/16	X/32	X/64	X/128	X/256	X/512	GC	SC

Figure 3.3 Broth Microdilution Assay Layout.
Example layout used in a 96-well microplate during a broth macrodilution assay. Example shows only a single drug assay. X represents drug concentration. GC: Growth Control (negative control), SC: Sterility Control (positive control).

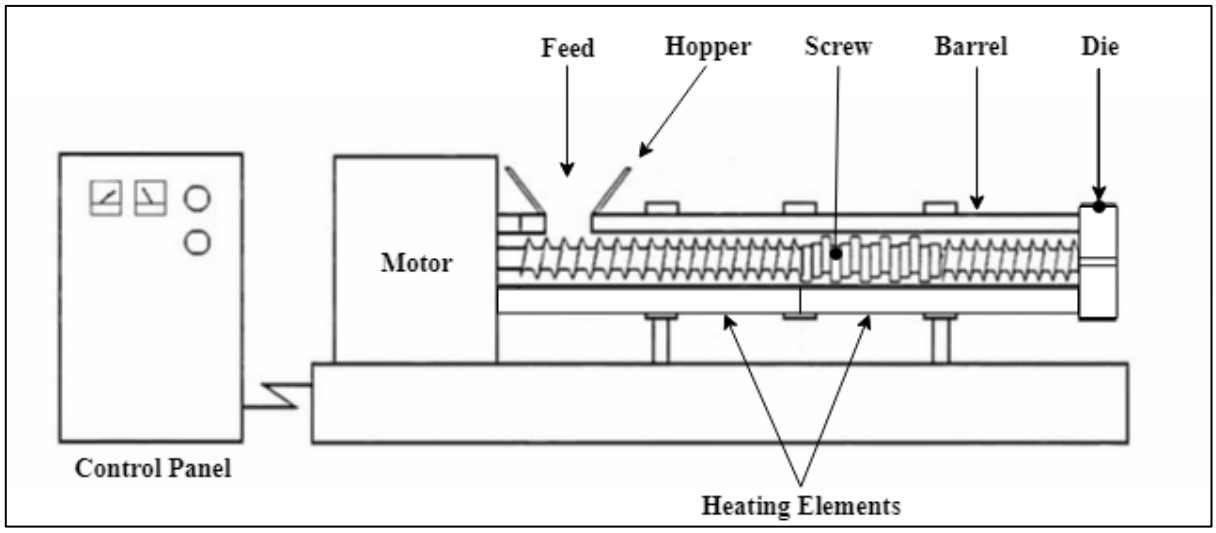

Figure 3.3 *Twin-Screw Extruder Schematic*.
Common layout of a twin-screw extruder alike to that of the PRISM TSE 16 TC. Control Panel is used to set barrel temperature, feed speed, screw speed and also monitor torque pressure being exhibited (Expressed in %). Prepare sample is feed into the barrel via the hopper where it is taken along the barrel by the twin-screw system. During the extrusion, the samples are sheared and mixed, and forced through a die at the end of the barrel. The shape of the die can determine the final extruded product shape (e.g., tape or string). Heating elements keep the barrel at a fixed temperature during processing. Figure adapted from (Mehuys 2004)

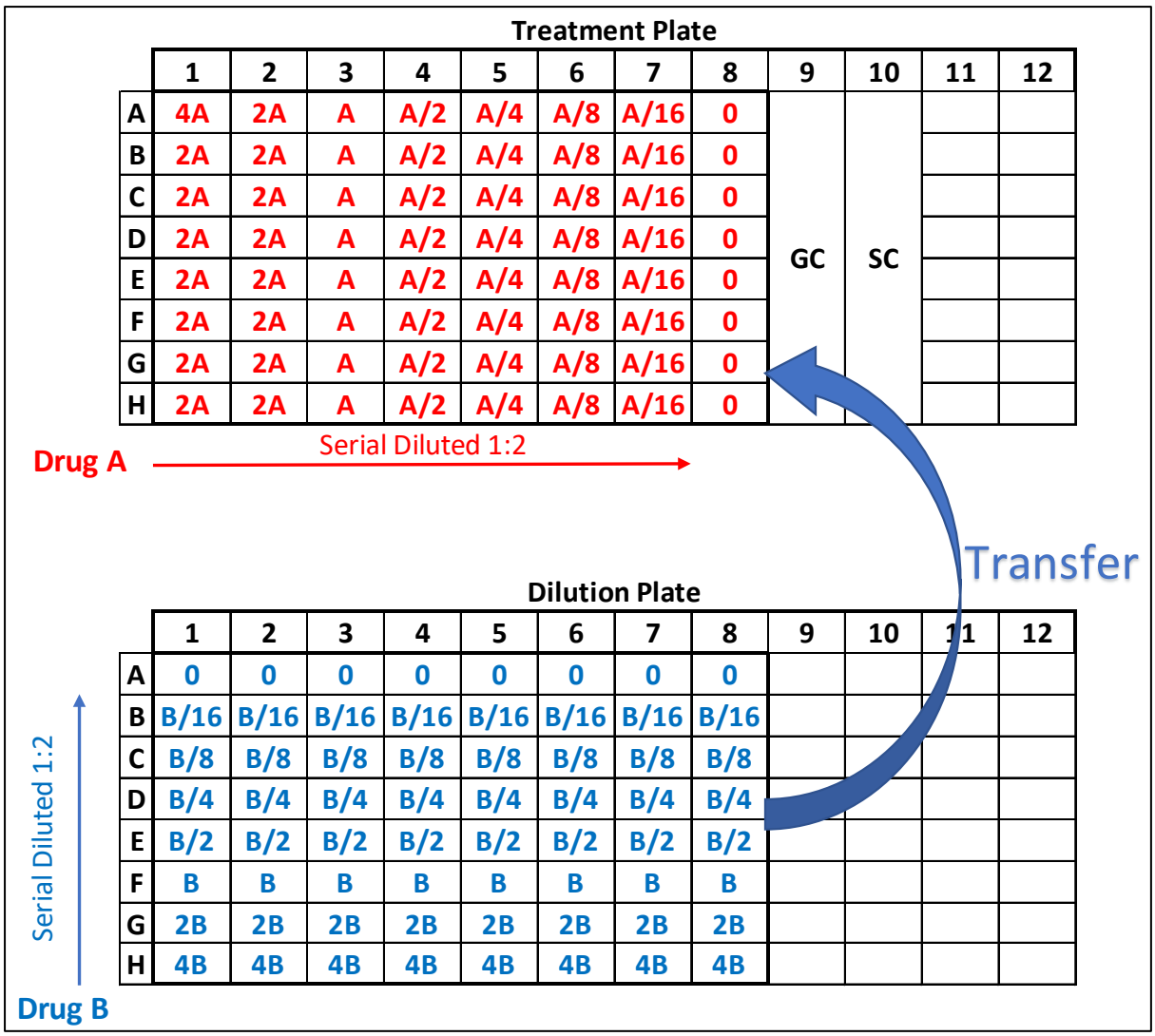

Figure 3.4 Drug Combination Set Up.
Layout of 2-drug combination treatment plate and dilution plate before transfer step. **A** refers to concentration of Drug A, **B** refers to the concentration of Drug B, showing the dilution factor of each following the serial dilution. **GC**: Growth Control, **SC**: Sterility Control.

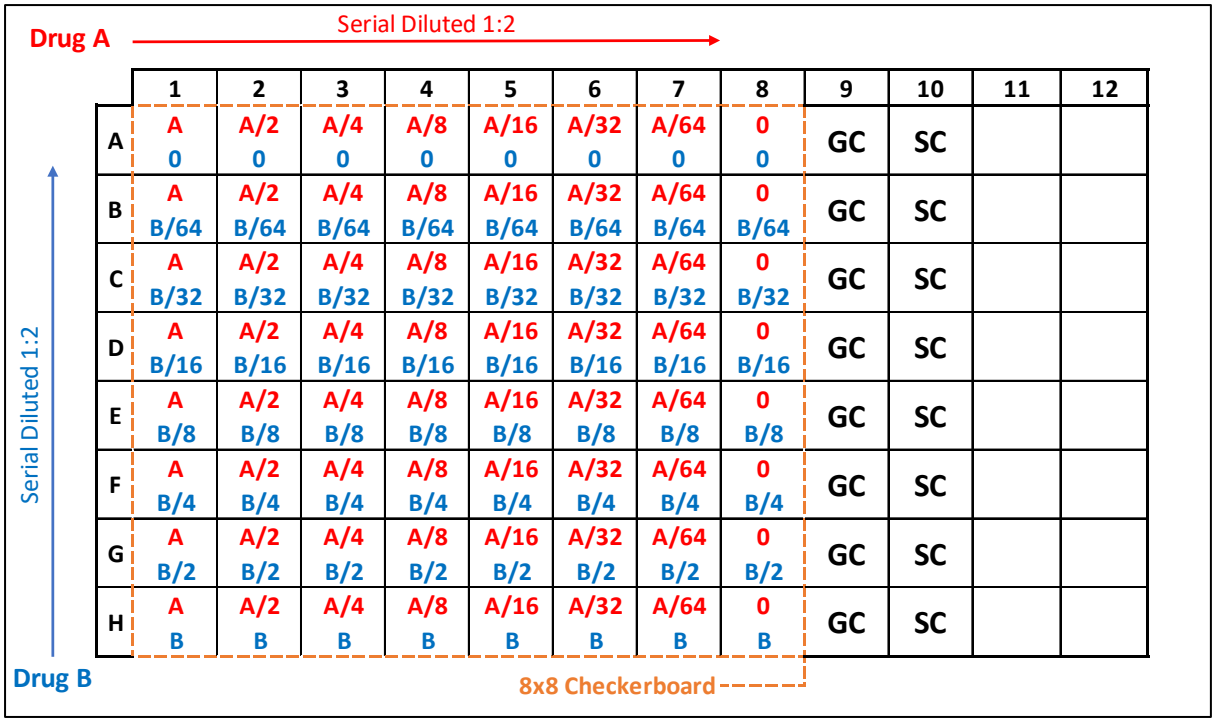

	1	2	3	4	5	6	7	8	9	10	11	12
A	A 0	A/2 0	A/4 0	A/8 0	A/16 0	A/32 0	A/64 0	0 0	GC	SC		
B	A B/64	A/2 B/64	A/4 B/64	A/8 B/64	A/16 B/64	A/32 B/64	A/64 B/64	0 B/64	GC	SC		
C	A B/32	A/2 B/32	A/4 B/32	A/8 B/32	A/16 B/32	A/32 B/32	A/64 B/32	0 B/32	GC	SC		
D	A B/16	A/2 B/16	A/4 B/16	A/8 B/16	A/16 B/16	A/32 B/16	A/64 B/16	0 B/16	GC	SC		
E	A B/8	A/2 B/8	A/4 B/8	A/8 B/8	A/16 B/8	A/32 B/8	A/64 B/8	0 B/8	GC	SC		
F	A B/4	A/2 B/4	A/4 B/4	A/8 B/4	A/16 B/4	A/32 B/4	A/64 B/4	0 B/4	GC	SC		
G	A B/2	A/2 B/2	A/4 B/2	A/8 B/2	A/16 B/2	A/32 B/2	A/64 B/2	0 B/2	GC	SC		
H	A B	A/2 B	A/4 B	A/8 B	A/16 B	A/32 B	A/64 B	0 B	GC	SC		

Figure 3.5 *Drug Combination Assay Final Layout*.
Final layout of 96-well plate for a 2-Drug combination assay. **A** refers to concentration of Drug A, **B** refers to the concentration of Drug B, showing the dilution factor of each following the serial dilution, transfer step and addition of inoculum. The 8x8 checkboard is labelled with dashed lines. **GC**: Growth Control, **SC**: Sterility Control.

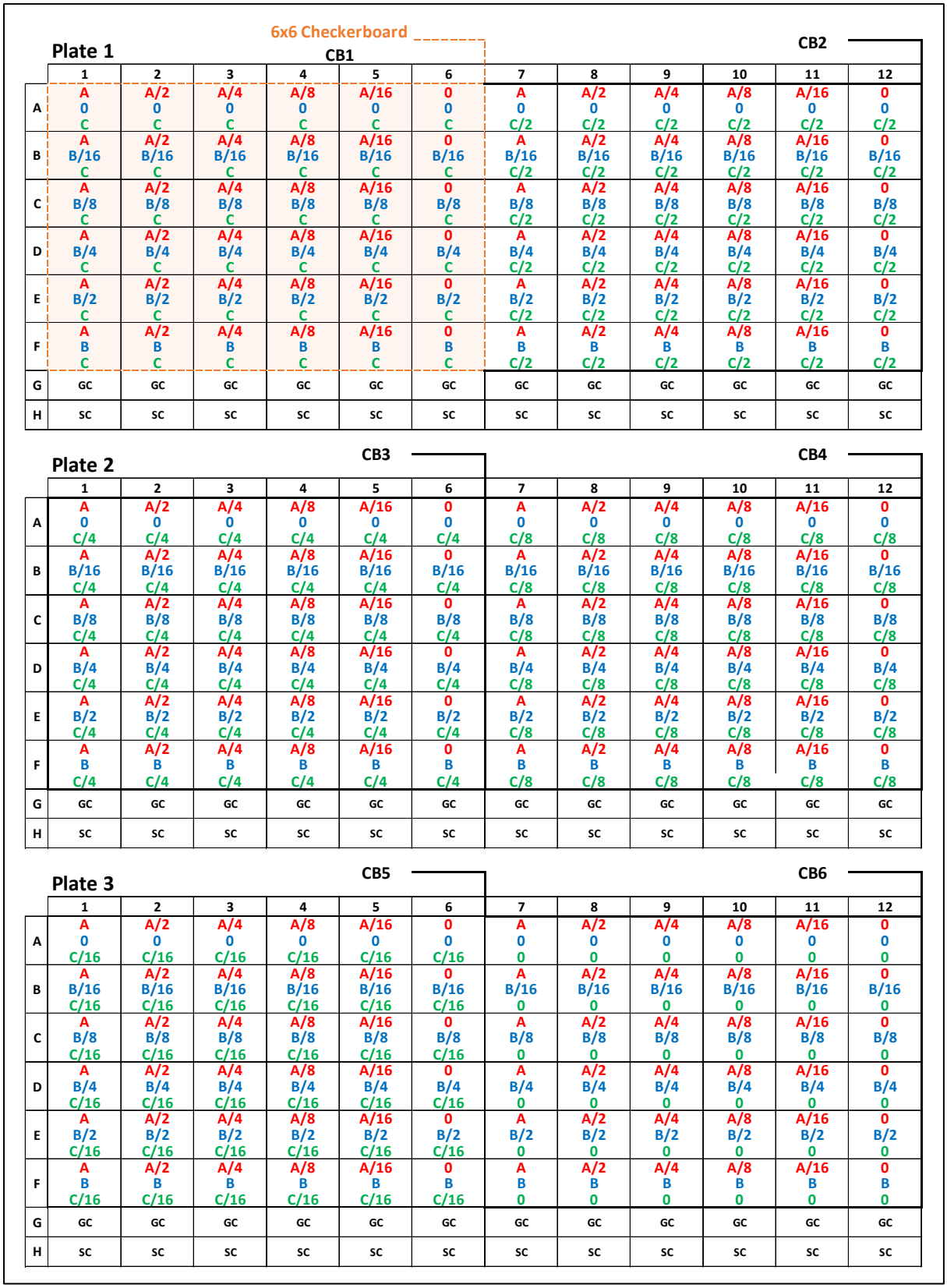

Figure 3.6 *Drug Combination Assay Final Layout*.
Final 96-well plate layout for a 3-Drug combination assay. A refers to concentration of Drug A, B refers to the concentration of Drug B, C refers to the concentration of Drug D, showing

the dilution factor of each following the serial dilution, transfer steps and addition of inoculum. GC: Growth Control, SC: Sterility Control.

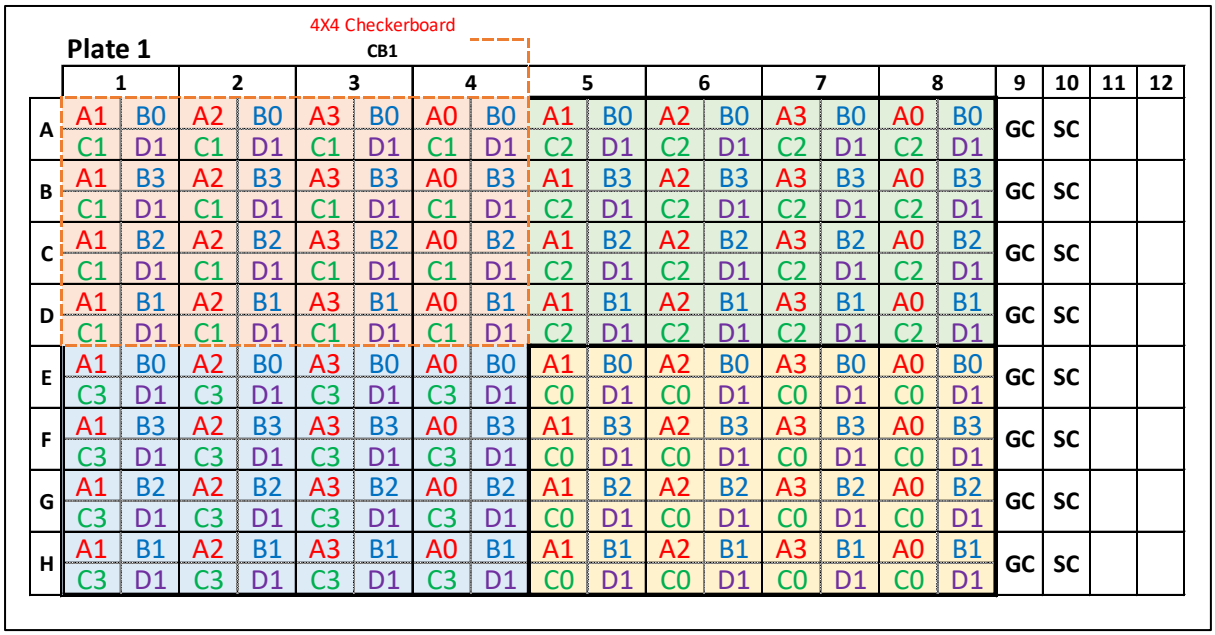

	1		2		3		4		5		6		7		8		9	10	11	12
A	A1	B0	A2	B0	A3	B0	A0	B0	A1	B0	A2	B0	A3	B0	A0	B0	GC	SC		
	C1	D1	C1	D1	C1	D1	C1	D1	C2	D1	C2	D1	C2	D1	C2	D1				
B	A1	B3	A2	B3	A3	B3	A0	B3	A1	B3	A2	B3	A3	B3	A0	B3	GC	SC		
	C1	D1	C1	D1	C1	D1	C1	D1	C2	D1	C2	D1	C2	D1	C2	D1				
C	A1	B2	A2	B2	A3	B2	A0	B2	A1	B2	A2	B2	A3	B2	A0	B2	GC	SC		
	C1	D1	C1	D1	C1	D1	C1	D1	C2	D1	C2	D1	C2	D1	C2	D1				
D	A1	B1	A2	B1	A3	B1	A0	B1	A1	B1	A2	B1	A3	B1	A0	B1	GC	SC		
	C1	D1	C1	D1	C1	D1	C1	D1	C2	D1	C2	D1	C2	D1	C2	D1				
E	A1	B0	A2	B0	A3	B0	A0	B0	A1	B0	A2	B0	A3	B0	A0	B0	GC	SC		
	C3	D1	C3	D1	C3	D1	C3	D1	C0	D1	C0	D1	C0	D1	C0	D1				
F	A1	B3	A2	B3	A3	B3	A0	B3	A1	B3	A2	B3	A3	B3	A0	B3	GC	SC		
	C3	D1	C3	D1	C3	D1	C3	D1	C0	D1	C0	D1	C0	D1	C0	D1				
G	A1	B2	A2	B2	A3	B2	A0	B2	A1	B2	A2	B2	A3	B2	A0	B2	GC	SC		
	C3	D1	C3	D1	C3	D1	C3	D1	C0	D1	C0	D1	C0	D1	C0	D1				
H	A1	B1	A2	B1	A3	B1	A0	B1	A1	B1	A2	B1	A3	B1	A0	B1	GC	SC		
	C3	D1	C3	D1	C3	D1	C3	D1	C0	D1	C0	D1	C0	D1	C0	D1				

Figure 3.7 *Drug Combination Assay Final Layout*.
Final 96-well plate layout for one of four plates prepared for a 4-Drug combination assay showing the drug concentration of each of the four test compounds within each well. A refers to concentration of Drug A, B refers to the concentration of Drug B, C refers to the concentration of Drug C, D refers to the concentration of Drug D. Each column contains different concentration of drug A, each row has a different concentration of drug B, each 4x4 checkerboard contains different concentration of drug C, and each plate contains a different concentration of drug D, with the example plate shown having concentration 1 (D1). GC: Growth Control, SC: Sterility Control.

Chapter 4 Antimicrobial Determination of Bioactives

3.1. Introduction

The use of antibiotics in medicine has taken a hesitant approach in recent years due to their misuse being observed in various sectors, particularly agriculture, which has had a significant influence on increasing levels of bacteria with antimicrobial resistance (AMR). The monitoring and documenting of AMR is a vital phase in controlling its emergence and instigating future actions. Simply differentiating which drugs to which bacteria are susceptible , and to which they are resistant , is essential to clinicians, where susceptibility results guide treatment options. The emergence of *S. aureus* strains displaying intermediate susceptibility (VISA) or full resistance (VRSA) to vancomycin, is currently a significant threat to public health and safety where they are associated with hard-to-treat nosocomial infections globally. The evidence of varying levels of resistance in these veterinary isolates contributes to the association between the veterinary use of antibiotics and emergence/proliferation of antibiotic resistance. In conjunction with monitoring resistance profiles, discovery of a bacterial strain's sensitivity to antibiotics or antibiotic alternatives is another major phase in monitoring and controlling the threat of AMR.

Mastitis is an inflammatory disease that develops primarily as response to bacterial invasion of the mammary gland and subsequent infection of the epithelial tissue. Current veterinary treatment of bovine mastitis relies heavily on the use of antibiotics to eliminate the infection (Barlow 2011; Melchior 2011; More, Clegg, and McCoy 2017; Royster and Wagner 2015). Due to regulations within the food and animal industries, the use of antibiotics requires that animals are withdrawn from milking for a period of up to four weeks in-order to allow all residual antibiotics to pass from the animal (Seegers, Fourichon, and Beaudeau 2003). While the misuse of antibiotics is hugely prevalent on farmlands, it is difficult to regulate (Poizat et al. 2017). Allowing antibiotic residues to enter our food supply has a major influence on the rise of AMR harbouring bacteria species, that are directly linked to both humans and animals alike (Economou and Gousia 2015; Manyi-Loh et al. 2018). While the significance of this issue is being addressed by the implementation of stricter regulations and guidelines in agricultural

settings, the use of antibiotics themselves need be addressed as well (Andrew J. Bradley and Green 2004; Gomes and Henriques 2016a; Breyne et al. 2017).

Currently, there are limited options suitable as antibiotic alternatives for the treatment of livestock, discussed previously in Chapter 1.11. As a result, there is a need for the development of alternative therapies that not only have excellent antibacterial qualities, but also enable for the animal to be returned to production lines more quickly without risk of introducing residual medications into the food chain. In the following study, we present four antimicrobial bioactives compounds, silver nitrate ($AgNO_3$), zinc oxide (ZnO), chitosan and nisin, as potential antibiotic alternatives for use in agricultural settings and against AMR bacteria.

$AgNO_3$ is a commonly studied silver salt derivative which has seen raised interest in recent times as an antimicrobial (Russell and Hugo 1994; Atiyeh et al. 2007; Prabhu and Poulose 2012; Gao et al. 2018; Balazs et al. 2004). While the use of silver derivatives does hold environmental concerns, especially in aquatic ecosystems, studies have found that they may only have effect upon soil-based bacteria and a rather minor or short lived effect upon aquatic life with exposure to high doses (Clark et al. 2019; Schlich et al. 2018). Furthermore, the use of silver nanoparticles were found to have much greater detrimental effect in comparison to $AgNO_3$ at similar levels of silver exposure (Rahmatpour et al. 2017).

ZnO is a commonly used ingredient in cosmetics and other areas that is categorised as generally recognised as safe (GRAS) by the FDA, and has recently elicited interest in its antimicrobial abilities (U.S. Food & Drug Administraion 2019; Beyth et al. 2015). ZnO has been shown to utilise three major mechanisms to confer its antimicrobial abilities; 1) the release of antimicrobial ions (Zn^{2+}), 2) destabilisation of the outer membrane via electrostatic interactions, 3) the production of reactive oxygen species (ROS) (Pasquet, Chevalier, Pelletier, et al. 2014). Studies have shown that ZnO in the form of nanoparticles (ZnO-NPs) exhibit a considerably greater antimicrobial effect, which can be accredited to the higher surface area yielded by the substantially smaller particles, and the fact that they allow for higher concentrations in a smaller area (Padmavathy and Vijayaraghavan 2008). Zinc oxide (ZnO) and silver nitrate ($AgNO_3$) also have previous use in cosmetics and external wound treatments due to their antibacterial properties (Atiyeh et al. 2007; Archana et al. 2015; Gao et al. 2018).

Chitosan is a linear polysaccharide-based polymer, produced from the deacetylation of chitin, a major component in shells of crustaceans (Kyoon et al. 2002). Chitosan is a well-studied compound used in the biomedical and food packaging sectors. While recent studies involve its use as a carrier for other antimicrobial products, chitosan itself has been reported to exhibit its own antibacterial properties through interactions with bacterial cell wall lipids, causing destabilization (Qin et al. 2006). Nisin is a polycyclic antimicrobial peptide, produced by lactic acid bacteria such as *Lactococcus lactis*, and classified as a bacteriocin (McAuliffe, O., Ross, R. P., Hill 2001; Cleveland et al. 2001; Jozala, Celia, and Novaes 2015). Unlike traditional antibiotics, which are secondary metabolites, bacteriocins are ribosomally synthesized peptides, sensitive to degradation by proteases and generally harmless to the non-prokaryotic organisms (Yang et al. 2014). The primary mechanism of nisin is its ability to target and bind the lipid-II, intramembrane-bound molecule of bacteria, inhibiting cell wall formation and leading to the destabilisation and destruction of the cell (Hasper et al. 2006; Willey and van der Donk 2007).Both nisin and chitosan are designated by the FDA as GRAS compounds, and have previously been investigated for use in active food packaging due to their established antimicrobial abilities, while having no toxic effects upon mammalian cells (Bastarrachea et al. 2015; Moon et al. 2007; Cardozo et al. 2014; Asli et al. 2017; J. Wu, Hu, and Cao 2007).

The four bioactives will to be evaluated following standard antimicrobial protocols used to assess antibiotic efficacy (M. P. Weinstein 2012; Zgoda and Porter 2001). they will be assessed to determine their minimum inhibitory concentration (MIC) against four commercially available bacteria strains, *Escherichia coli*, *Staphylococcus aureus*, *Pseudomonas aeruginosa* and *Staphylococcus epidermidis*. These four strains are regarded as standard strains for use antimicrobial testing and they are also major pathogens associated with various diseases, including bovine mastitis. Each strain represents a different pathological aspect of mastitic bacterial (*E. coli* being an environmental pathogen, *S. aureus* a contagious pathogen, *S. epidermidis* opportunistic and *P. aeruginosa* biofilm forming) (A. J. Bradley 2002; Jones and Bailey 2009; Park et al. 2014). *S. epidermidis* also falls into a bacterial group known as coagulase-negative staphylococci (CNS) bacteria, which have been identified as the leading pathogen of many modern cases of sub-clinical mastitis (SCM) (Vanderhaeghen et al. 2015). Additionally, to investigate the bioactives efficacy against wild-type and AMR bacterial strains,

a number of veterinary isolates will also be included in the bioactives assessment. The veterinary strains will be collected from local farm animals, isolated, identified and then assessed.

While treatment efficacy is undeniably an important factor in the development of novel therapies, another vital consideration is that of a delivery system with which to administer the treatment effectively (Nicholas, Michelle, and Kathryn 2014; Gruet et al. 2001; Alany et al. 2013). Many drugs and active ingredients have very poor solubility, making it difficult to use them as effect treatments (Vipul et al. 2013; Nouraei 2018; Malcolm et al. 2003). Another issue faced is that of non-specific interactions that may cause adverse side-effects, or even a lack of efficacy due to the inability to successfully deliver the drug to the intended target site (Salahpour Anarjan 2019). A common approach in the pharmaceutical industry for developing such delivery systems involves the incorporation of the active pharmaceutical ingredient (API) within a polymer matrix . Hot-melt extrusion (HME) is a commonly used, and widely recognised method for the production of such drug-polymer combinations (Sarode et al. 2013; Simões, Pinto, and Simões 2019). Although HME is a very convenient and easily applied method for drug development, it does necessitate that the active compound holds the capacity to withstand thermal and physical processing, maintaining bioactivity post-process (Simões, Pinto, and Simões 2019). Traditional antibiotics have low thermal stability, thus excluding them as possible candidates for HME applications (Wylie et al. 2021). HME has seen growing use in the area of pharmaceuticals as it allows the production of biologically active polymers with various formulations, dosage forms, and can enhance the physical properties of the bioactive component (such as increased water solubility, improved stability and shelf-life) (Patil, Tiwari, and Repka 2016). In order to determine each bioactives processing potential and suitability, they will also be assessed by incorporating them into a polymer matrix by HME and then re-assessing their antibacterial capabilities. By comparing their MIC both before and after HME, it will be possible to determine any loss of bioactivity. Kollidon® VA-64 (PVP/VA64) will be assessed as the polymer base. PVP/VA64 is a co-polymer consisting of Vinylpyrrolidone-vinyl acetate, commonly used as soluble binder for granulation and as dry-binder in direct compression technology (H. He, Yang, and Tang 2010). PVP/VA64 was chosen due to its low melting temperature, allowing lower processing temperatures which would ensure minimal heat damage to the bioactives. It is also readily soluble in water and as

well as this, extruded PVP/VA64 has a very solid, yet brittle, composition allowing it to be ground to a powder for easier solution preparation of the prepared bioactive-loaded polymers.

4.1 Aims & Hypothesis

The aim of this study is to assess the antimicrobial ability of four bioactive compounds which will be tested against four standard bacterial species and five isolated wild-type bacterial species associated with recurring cases of mastitis, and to then assess their abilities following incorporations into a polymer, in order determine their suitability as antibiotic alternatives.

It is hypothesised that the four bioactives will inhibit growth of the test bacterial species, and hold activity following polymer incorporation, validating their part in future research as an antimicrobial bioactive-loaded polymer.

4.2 Results

4.2.1 Resistance profile of veterinary isolates

Resistance profiles were established in accordance with the WHO priority pathogen list for veterinary isolates MRSA, VRE, *L. monocytogenes*, with critically important *E. coli (isolate)*, and *A. baumannii* also being assessed for resistance to 3rd generation cephalosporins and carbapenems, amongst other drug classes (Table 4.1). *A. baumannii* and *E. coli (isolate)* both exhibited resistance to vancomycin and ampicillin, with ESBL activity, which was confirmed, with the bacteria exhibiting zones of 15 mm and 20 mm vs Cefpodoxime discs, and 23 mm and 28 mm vs Cefpodoxime + clavulanic acid discs, respectively. *E. coli* also demonstrated resistance to amoxicillin/clavulanic acid. *E. coli (isolate)* and *A. baumannii* displayed intermediate susceptibility to an array of antibiotics including streptomycin (10mm, 15mm), erythromycin (9mm, 9mm), and chloramphenicol (21mm, 9mm) respectively. MRSA give clear indication of resistance to streptomycin and 3rd generation cephalosporins, with intermediate susceptibility to vancomycin (16mm), tetracycline (11mm), and erythromycin (22mm). The high priority pathogen VRE demonstrates clear resistance to streptomycin, cephalosporins and quinolones, with low susceptibility to the macrolide erythromycin (7mm) and full susceptibility to tetracyclines (doxycycline, 30mm). *L. monocytogenes* displays resistance to ampicillin, erythromycin, and cephalosporins. The MIC of an array of antibiotics

was determined against each veterinary isolate of MRSA, VRE, *E. coli (isolate)* and *A. baumannii* (

Table 4.2).

4.2.2 Minimum Inhibitory Concentration Assays

The mean minimum inhibitory concentration (MIC) of each bioactive, before and after HME, are presented in Table 4.3 (MIC versus collection cultures) and Table 4.4 (MIC versus Veterinary isolates).

- **Silver Nitrate ($AgNO_3$)**

$AgNO_3$ held a notable inhibitory effect against each tested strain, both before and after polymer processing by HME, while its treatment vehicle (T_v) of 28% (v/v) PEG-400, 26% (w/v) d-sorbitol held no effect at any concentration. $AgNO_3$ MIC values ranged between 4.88 – 36.46 µg/mL while values of the $AgNO_3$ polymer ($AgNO_3$-PVPVA) ranged between 6.51 – 104.17 µg/mL. Figure 4.1 presents the mean MIC (µg/mL) of $AgNO_3$ and $AgNO_3$-PVPVA for each bacterial strain as a bar graph for ease of comparison. MIC values post HME increased overall, representing a loss of antibacterial effect due to the polymer incorporation, however only the increase in MIC versus *S. aureus* was considered significant ($P<0.01$). While there was no change in MIC values versus *L. monocytogenes* and *A. baumannii*, there were reductions in MIC values versus *E. coli* and *S. epidermidis,* indicating increases in efficacy, however they were not considered significant ($P>0.05$).

- **Chitosan**

Chitosan effectively inhibited the growth of all tested bacterial strains before and after HME with PVPVA64. Chitosan MIC values ranged between 156.25 – 1250 µg/mL, with Chitosan-PVPVA MIC values ranging between 156.25 – 1666.67 µg/mL. The Chitosan T_v held noticeable effect at the higher concentration of 0.25% acetic acid (AcOH), which is equivalent to a chitosan concentration of 2500 µg/mL. VRE was found to be more resistant to chitosan's inhibitory effects in comparison to other tested species, both before and after HME. Mean MIC values of chitosan before and after HME with PVPVA are presented in Figure 4.2 for comparison. Chitosan-PVPVA exhibited the greatest loss of activity (as determined by increase in MIC values) versus *A. baumannii* (1.6-fold increase) and *P. aeruginosa* (1.5-fold increase), however these increases were not found to be significant ($P>0.05$). While MIC values versus *S. aureus*, *L. monocytogenes* and the *E. coli (isolate)* were lowered 1.33-fold (416.67 → 312.5 µg/mL), 1.5-fold (234.38 → 156.25 µg/mL) and 1.5-fold (234.38 → 156.2

µg/mL) respectively, showing an increase in efficacy, these were not considered significant (P>0.05).

- **Zinc Oxide (ZnO)**

ZnO effectively inhibited the growth of *E. coli*, *S. aureus* and *S. epidermidis*, with MIC values of 312.50 µg/mL, 156.25 µg/mL and 104.17 µg/mL respectively. *P. aeruginosa* reported an above average MIC of 1250 µg/mL (Table 4.3). Established MIC values against veterinary isolate strains were found to be higher than those against the standard culture strains (Table 4.4). *A. baumannii* and *E. coli* (isolate) reported mean MIC values of 364.58 µg/mL and 520.83 µg/mL respectively. *L. monocytogenes* reported a higher mean MIC of 937.50 µg/mL. MRSA required higher concentrations to inhibit growth, reporting a MIC of 2291.67 µg/mL. VRE reported the highest mean MIC of 3125.00 µg/mL.

Results indicate ZnO to have its antimicrobial abilities hindered against most bacterial species by the HME process, as MIC values were observed to increase against *E. coli* (520.83 µg/mL), *S. aureus* (520.83 µg/mL), *S. epidermidis* (156.25 µg/mL), *E. coli* (isolate) (1145.83 µg/mL), *L. monocytogene* (3333.33 µg/mL), VRE (11250.00 µg/mL) and MRSA (3020.83 µg/mL). However, efficacy was noted to increase against *P. aeruginosa* (1041.67 µg/mL) and *A. baumannii* (208.17 µg/mL).

- **Nisin**

Nisin effectively and consistently inhibited the growth of the tested Gram-positive bacteria, *S. aureus*, *S. epidermidis*, MRSA, VRE and *L. monocytogenes,* with pre-HME MIC's ranging between 3.91 – 15.6 µg/mL and post-HME MIC's ranging between 1.95 – 15.63 µg/mL. The HME process had a notable impact on the effect of nisin, indicated by significant changes in MIC values (Figure 4.4). Nisin was less effective versus *S. aureus* following HME, reporting a mean MIC of 15.63 µg/mL which represents a 4-fold increase of nisin required to inhibit growth (P<0.001). In contrast, nisin was found to be more effective versus MRSA, VRE and *L. monocytogenes* after HME, reporting 4-fold, 8-fold and 6.4-fold decreases in MIC values respectively (P<0.01). While there was a slight increase in nisin MIC versus *S. epidermidis* following HME, it was not considered significant (P>0.05). No MICs were recorded versus *E. coli*, *P. aeruginosa, E. coli* (isolate) or *A. baumannii* before or after HME, with concentrations up to 30mg/mL being tested.

4.3 Discussion

In the present study, four bioactive compounds, silver nitrate ($AgNO_3$), chitosan, zinc oxide (ZnO) and nisin were presented and assessed for their antibacterial abilities under conditions equal to that of antibiotic testing. While $AgNO_3$ is reported as being water soluble at concentrations up to 1M at 20˚C, it was found that while in solution with dH_2O, $AgNO_3$ would precipitate out as a heavy, white precipitate when added to bacterial growth broth. Exposure to air and light caused the precipitate to discolour to a dark brown, indicating oxidation of $AgNO_3$. Assessment of various solvents (such as phosphate buffered saline (PBS), 0.1M Sodium Hydroxide (NaOH), 0.1M Hydrochloric acid (HCL)) suggested that it was the salt content of the growth broth causing precipitation. Dissolving the $AgNO_3$ in a solution of 28% (v/v) PEG-400 and 26% (w/v) d-sorbitol was successful in avoiding these issues. Use of this $AgNO_3$ preparation showed stable solubility with the carrier exhibiting no effects against bacterial strains. Previous studies evaluating and comparing $AgNO_3$ and silver nanoparticles (AgNPs) reported $AgNO_3$ mean MIC values of 85.5 µg/mL against *E. coli* and 55.5 µg/mL against *S. aureus*, which closely resemble MIC values determined in the present study (Salman 2017; Lima et al. 2019). Another study investigating the antibacterial and cytotoxic properties of $AgNO_3$, reported MIC values of 6 µg/mL versus *E. coli* and *S. aureus*, which are notably lower than MIC values reported here (20.83 and 36.46 µg/mL respectively) (Mulley, Jenkins, and Waterfield 2014). A seperate study of $AgNO_3$ and AgNPs versus *P. aeruginosa* reported a MIC of 10 µg/mL, which closely resembles the MIC reported here (4.88 µg/mL)(Königs, Flemming, and Wingender 2015). The present study has found that $AgNO_3$ not only holds antibacterial ability following HME, but also exhibited an increase in efficacy versus *E. coli* (which saw a 2-fold decrease in the MIC) and *S. epidermidis* (1.5-fold decrease). However, there were also decreases in efficacy observed versus *S. aureus* (2.86-fold increase in MIC), *P. aeruginosa* (1.33-fold increase), MRSA (1.5-fold increase), VRE (1.5-fold increase) and *E. coli* (isolate) (2-fold increase), although only the decreased efficacy versus *S. aureus* was considered significant ($P<0.001$). To best knowledge, the present study represents the only such study that examines polymer extruded $AgNO_3$, which makes it difficult to determine the reasoning behind the altered antibacterial efficacy. Further studies are required to analyse $AgNO_3$ and its polymer form in order to assess its alternate composition and structure.

However, in terms of its antibacterial ability, both before and after HME, $AgNO_3$ has shown satisfactory inhibition, with a broad-spectrum of effect.

Chitosan has been under continuous study for its applications as a polymer and also as an antimicrobial bioactive. Previous studies have determined chitosan to be most soluble in organic acids and that it also exhibits an antimicrobial effect only within an acidic pH (Kyoon et al. 2002; Romanazzi et al. 2009). 1%(v/v) acetic acid (AcOH) was found to be the most effective solvent, as it completely dissolved the chitosan at all desired ranges for testing. A pH between 5.0 – 5.5 was determined to be most appropriate, allowing solubility of the chitosan while also being within a tolerable acidic range for the bacterial test species, reducing interference with antimicrobial results. Reported antimicrobial abilities of chitosan vary significantly, with studies showing MIC values higher than those presented here (ranging between 625 – 1250 µg/mL), while other studies reported slightly lower MIC value of 100 µg/mL versus *E. coli* and *S. aureus* (Zaghloul 2015; Aliasghari et al. 2016; Shanmugam, Kathiresan, and Nayak 2016). The lower MIC reported by Shanmugam et. al is quite significant in comparison to the values presented here (156.25 µg/mL vs *E. coli*, 416.67 µg/mL versus *S. aureus*). While the present study utilised commercial chitosan, as did the other cited studies, the group of Shanmugam et. al extracted and produced their own chitosan, which could explain the difference in abilities. Modifications of chitosan have also been shown to increase its antibacterial potential, however in comparison to values reported in the present study, the modifications do not hold much significance, particularly with the additional preparation steps required (M. A. Hassan et al. 2018). HME processing had only a minor impact upon chitosan's antibacterial abilities, and while there were increases in MIC values versus *P. aeruginosa*, VRE and *A. baumannii,* the changes in efficacy were not considered significant. Overall, the MIC values reported here are consistently lower than those from other studies demonstrating effect bacterial inhibition, and as well as this, the HME process had no significant effects on chitosan's efficacy.

While ZnO is reported to be soluble in strong solvents (such as formic acid, sulphuric acid), it was prepared as a suspension as dissolving it in such solvents would interfere with antimicrobial testing due to their strength which would themselves hold toxic effect upon bacterial cells and skew results. Furthermore, one of the primary mechanisms of ZnO is its structure, which interacts with bacterial membranes, forms reactive oxygen species and also

peroxides (Xie et al. 2011). A number of studies have examined ZnO-polymers in terms of bacterial number reduction (by determining reduction of colony forming units, CFUs); however, the present study assesses microbial growth inhibition and MIC determination. Regardless, the results presented can be compared to show clear indication that ZnO can be effectively incorporated into a polymer medium and while there is clear loss of effect, the polymer processed materials retain most of ZnO's activity. A separate study involving ZnO extrusion with the polymer polylactic acid (PLA), noted hindered diffusion of ZnO from the extruded polymer, which could explain the reduced efficacy observed in the current study, as this would greatly interfere with its antimicrobial activity (Pantani et al. 2013).

Following incorporation into a PVP/VA64 polymer, most MIC values saw an increase. The ZnO suspension held varying degrees of efficacy, while effectively inhibiting growth of the four ATCC strains, it showed low efficacy against *P. aeruginosa* and, to some extent, *E. coli*. It was seen most effective against *S. aureus* and *S. epidermidis*. This can be accounted for by the bacteria's intrinsic resistance and pathological strengths. Gram-negative bacterium, such as *P. aeruginosa*, have multiple, thin layers of membrane combined with an inner peptidoglycan cell wall-layer, which present formidable barrier for therapeutics. Gram-positive bacteria, such as *S. aureus* and *S. epidermidis*, comprise of a single, outer cell membrane under a thick peptidoglycan layer that has actually been shown to enable therapeutics by aiding their absorption into the cell. Furthermore, *S. epidermidis* is a well-known opportunistic, biofilm forming bacteria recognised as an etiological agent in complex device-mediated infection in healthcare and in veterinary practice. It generally exhibits low resistance to antimicrobials while in planktonic forms, requiring biofilm formation to become more resistant, thus justifying its lower MIC compared to *E. coli* and even *S. aureus*. The resistance of VRE to ZnO may be accounted for by its alternative peptidoglycan synthesis, which alters the bonding potential of its outer peptidoglycan layer, preventing ZnO from interacting and penetrating the bacteria cell (Ahmed and Baptiste 2018).

The most suitable nisin solvent was determined by considering two major parameters, salt content and pH. The chosen 400mM NaCl concentration was previously reported to confer the highest solubility of nisin (Abts et al. 2011). The acidity of the solution was adjusted to a range of pH 3.2 – 3.3, as previous studies have shown nisin to be most stable at this range, while also conferring its highest antibacterial activity (Rollema Hs et al. 1995; Yamazaki et al.

2000). The solution was sterilised by autoclaving, as the nitrocellulose composition of a 0.2µm filter would cause non-specific binding of the nisin peptide, lowering the final nisin concentration of the solution. The stability conferred by the altered pH was vital for this step to ensure there was no degradation of the peptide from autoclaving. Due to the production process of commercially purchased nisin, the chemical composition contains a number of by-products. The potency of nisin in commercial stocks is expressed in terms of international units (IU). As such, the actual concentration of nisin is calculated as follows:

$$1\text{g Commercial Nisin Powder} = 1 \times 10^6 \text{ IU} = 25\text{mg Nisin}$$

$$[1\text{IU} = 0.025\mu\text{g Nisin}]$$

Nisin had no effect against *E. coli, P. aeruginosa* or *A. baumannii* as these bacterial strains are Gram negative. Nisin cannot carry out its antibacterial mechanisms versus Gram negative bacteria due to the presence of the outer membrane, which acts as a physical barrier preventing nisin from reaching the inner membrane and interacting with its target, the intramembrane molecule lipid II (Brötz et al. 1998; AlKhatib et al. 2014; Wiedemann et al. 2001). Nisin has been a topic of considerable research in terms of its antibacterial abilities, however these studies all vary in their results. A 2018 study of nisin Z, a variant of nisin, reported MIC values against *S. aureus* (10µg/ml) and *S. epidermidis* (9.17µg/ml) which were marginally higher than the MICs reported here (3.91µg/ml versus both strains) (Lewies, Plessis, and Wentzel 2018). The variants nisin A and nisin Z, differ by a single amino acid and are reported to only hold differing solubility characteristics. A more recent study at Kagoshima University reported MIC values (3.2 – 6.4 µg/mL versus *S. aureus*) comparable to the value reported in the present study (3.91 µg/mL), while following similar preparation steps (Kawada-Matsuo et al. 2019). Another study reported MIC values of 1mg/mL against *Enterococcus* species, which is significantly higher than concentrations reported presently (15.6 µg/mL versus VRE) (Tong et al. 2014). Variation of MIC values may be a consequence of the different preparation protocols. Some literature reports using a dilute acid in-order to dissolve the nisin after which the solution is sterilised by autoclaving or filtration. Other studies have reported the need of a specific salt content in-order to stabilise nisin in solution, without which would increase its susceptibility to the damaging effects of the autoclaving process (Rollema Hs et al. 1995; Yamazaki et al. 2000).

Many studies involving nisin are concerned with its incorporation into materials for use in food packaging, and as an anti-spoilage material (Imran et al. 2014; T. Jin and Zhang 2008; Yamazaki et al. 2000). Other areas include its use as an active component or as a coating on processed polymer films (Cutter, Willett, and GRSiragusa 2001; Hanušová et al. 2010). Various polymers have been investigated as a potential carrier for nisin, such as polylactic acid (PLA), nitrocellulose (NC), methylcellulose (MC), polyethylene oxide (PEO), and even chitosan (Cha et al. 2003; Han et al. 2017; Tony Jin et al. 2009). Many of these studies have reported increased antimicrobial activity following polymer incorporation.

However, many of the methods utilised are time-consuming, requiring mixing of the components in a liquid form and then drying before processing. The incorporation of nisin into a polymer by extrusion has also been documented, although is reported that the heat and shear forces of the process have negative effects upon the antimicrobial abilities of nisin (Gharsallaoui et al. 2016). The present study represents the first known to extrude nisin using the PVPVA64 co-polymer. Results indicate successful incorporation of nisin into the polymer while also retaining activity and even showing increased efficacy against MRSA, VRE and *L. monocytogene*. While nisin was seen to lose potency following incorporation versus *S. aureus* and *S. epidermidis*, it still holds an impressive effect in growth inhibition. Additionally, several advantages over previous studies can be noted in that the preparation was combined using dry stocks, the product was processed in a much shorter timespan with a prolonged shelf. Many of the additional components of the commercial nisin powder are intentionally left within its composition in-order to increase the compounds shelf life. However once in solution, it was observed to lose potency after 7 – 10 days. The Nisin-PVP/VA64 polymers were observed to hold same level of potency for up to 30 days following solution preparation. This could be accredited to the polymer supporting the nisin's polycyclic structure stability (Jung 1991; Gut, Blanke, and Van Der Donk 2011; Fang et al. 2017). Results from this study demonstrates nisin's ability to inhibit bacterial growth in a similar capacity as before (in relation to *S. aureus)* or, in some cases, to even higher degree in relation to *Enterococcus* species tested.

Overall, results of the MIC broth assays gave positive indication to the microbial inhibitory properties of $AgNO_3$, chitosan, ZnO and nisin, versus commercially sourced and wild-type bacteria, including antibiotic resistant strains. In terms of effective treatment dose, $AgNO_3$

and nisin held the greatest efficiency to lowest concentration. Chitosan had equally consistent results across bacterial strains and, along with $AgNO_3$, was the least negatively affected following HME with PVP/VA64. While ZnO demonstrated promising inhibitory effects pre-HME, it exhibited the most significant loss of activity post-HME. While it is unlikely that the heat from the polymer process caused this loss of potency (as ZnO has a melting temperature of 1,975° C), it is possible that the shearing effect of the twin-screw extruder may have denatured it. Although it is much more likely that the polymer itself bound too strongly to the ZnO molecules, preventing it from freely interacting with bacterial cells.

In conclusion, the four bioactives show great promise as antibacterial agents and for their use in the project and inclusion in further research towards the project aim. The bioactives demonstrated their antibacterial capabilities and their compatibility for polymer processing, both central characteristics of alternative compounds in terms of this project. While their efficacy against planktonic bacteria has been demonstrated, focus should now lie upon determining their effect against more resilient forms of bacteria commonly faced in various infections and diseases, such as biofilms. While a number of the presently assessed bacterial strains are classified as biofilm forming, they were not assessed as biofilms. In order to accurately determine the effect of the chosen bioactives versus established biofilm bacteria, an experimental system must be set up to stimulate biofilm growth and then test the formed biofilms. Further experimentation will be carried out to determine the bioactives ability to inhibit biofilms and their ability to eradicate already formed biofilms.

4.4 Tables

Table 4.1 EUCAST cut-off of antibiotics versus veterinary isolates.

			Zone Diameter of Bacterial Species (mm)				
Drug Class	**Antibiotic**	**Conc. (µg/disc)**	***A. baumannii***	***E. coli (isolate)***	**MRSA***	**VRE***	***L. monocytogenes***
Aminoglycoside	Streptomycin	10	15	10	R	R	11
Glycopeptide	Vancomycin	30	R	R	16	R(12)	13
Chloramphenicol	Chloramphenicol	30	9	21[24]	22(18)[24]	20	27
Macrolide	Erythromycin	15	9	9	15(18)[26]	7	15(25)
Penicillin	Ampicillin	10	R	R	R	15	10(16)
Penicillin-like	Ampicillin/ clav	20:10	25	14(19)	11	24	25
Cephalosporins	Cefpodoxime	10	10	20(21)	R	15	R
	Cefotaxime	5	16	16(17)	R	R	R
Monobactam	Aztreonam	30	32	25(21)	-	-	-
Carbapenems	Doripenem	10	29	22[9]	16	25	38
	Meropenem	10	25(15)	23(16)	30	12	30(26)
Quinolones	Ciprofloxacin	5	30(21)	36(22)	28(24)	R(15)	10
	Levofloxacin	5	32(20)	31[33](19)	29(22)	R(15)	26
Polymyxin	Colistin	10	13	12[9]	-	-	-
Tetracycline	Doxycycline	30	10	12	11	30	40

*WHO high priority pathogens
R complete resistance to antibiotic
() EUCAST 2020 cut-off zone diameter (mm) for antibiotic resistance for certain species and antibiotic. Zones below this are deemed resistant.
[] EUCAST 2019 cut-off zone diameter (mm) for antibiotic resistance for certain species and antibiotic. Zones below this are deemed resistant.

Table 4.2 Antibiotic Minimum Inhibitory Concentrations for Veterinary Isolates.
N=3

		Bacterial species			
		A. baumannii	***E. coli (isolate)***	***MRSA***	***L. monocytogenes***
Antibiotic (µg/mL)	**Streptomycin**	8	4	R	16
	Vancomycin	R	256	1	0.5
	Erythromycin	32	R	1	16
	Azithromycin	4	8	8	32
	Amoxicillin	256	128	256	4
	Ceftazidime (3rd)	64	16	32	R
	Cefotaxime (3rd)	128	16	32	R
	Ceftriaxone (3rd)	64	4	32	R
	Cefepime (4th)	64	2	32	16
	Aztreonam	256	8	-	-
	Meropenem	0.5	0.125	32	16
	Doxycycline	16	64	128	8
	Tetracycline	128	128	128	16
	Ciprofloxacin	0.125	0.25	0.25	2
	Levofloxacin	0.25	0.25	0.25	2

Table 4.3 Mean Minimum Inhibitory Concentrations (MIC) against ATCC culture collection strains.
N=3

		Bacterial Species			
		E. coli (ATCC 25922)	*S. aureus* (ATCC 25913)	*S. epidermidis* (ATCC 35984)	*P. aeruginosa (ATCC* 27853*)*
Bioactive MIC (µg/mL)	**$AgNO_3$**	20.83	36.46***	15.63	4.88
	$AgNO_3$ -PVPVA	10.42	104.17***	10.42	6.51
	Chitosan	156.25	416.67	208.33	416.67
	Chitosan-PVPVA64	208.33	312.50	208.33	625.00
	ZnO	312.5	156.25**	104.17	1250
	ZnO-PVPVA64	520.83	520.83**	156.25	1041.67
	Nisin	No MIC [(a)]	6.833**	4.885	No MIC [(a)]
	Nisin-PVPVA64	No MIC [(a)]	19.53**	8.3	No MIC [(a)]

[(a)] Up to 125µg/mL tested
** P < 0.01
*** P < 0.001

Table 4.4 Mean Minimum Inhibitory Concentrations versus Veterinary Isolates.
N=3

		Veterinary Isolate				
		MRSA	VRE	*L. monocytogenes*	*E. coli (isolate)*	*A. baumannii*
Bioactive (µg/mL)	$AgNO_3$	20.83	20.83	15.63	15.63**	13.02
	$AgNO_3$-PVPVA	31.25	31.25	15.63	31.25**	13.02
	Nisin	15.6**	15.6**	12.5**	No MIC(a)	No MIC(a)
	Nisin-PVPVA	3.9**	1.95**	1.95**	No MIC(a)	No MIC(a)
	Chitosan	208.33	1250	234.38	234.38	260.42
	Chitosan-PVPVA	260.42	1666.67	156.25	156.25	416.67
	ZnO	4583.33**	No MIC(b)	937.5	390.63	364.58
	ZnO-PVPVA	25000**	No MIC(b)	937.5	1562.5	208.17

(a) Up to 5000 µg/mL tested
(b) Up to 30000 µg/mL tested
** $P < 0.01$

4.5 Figures

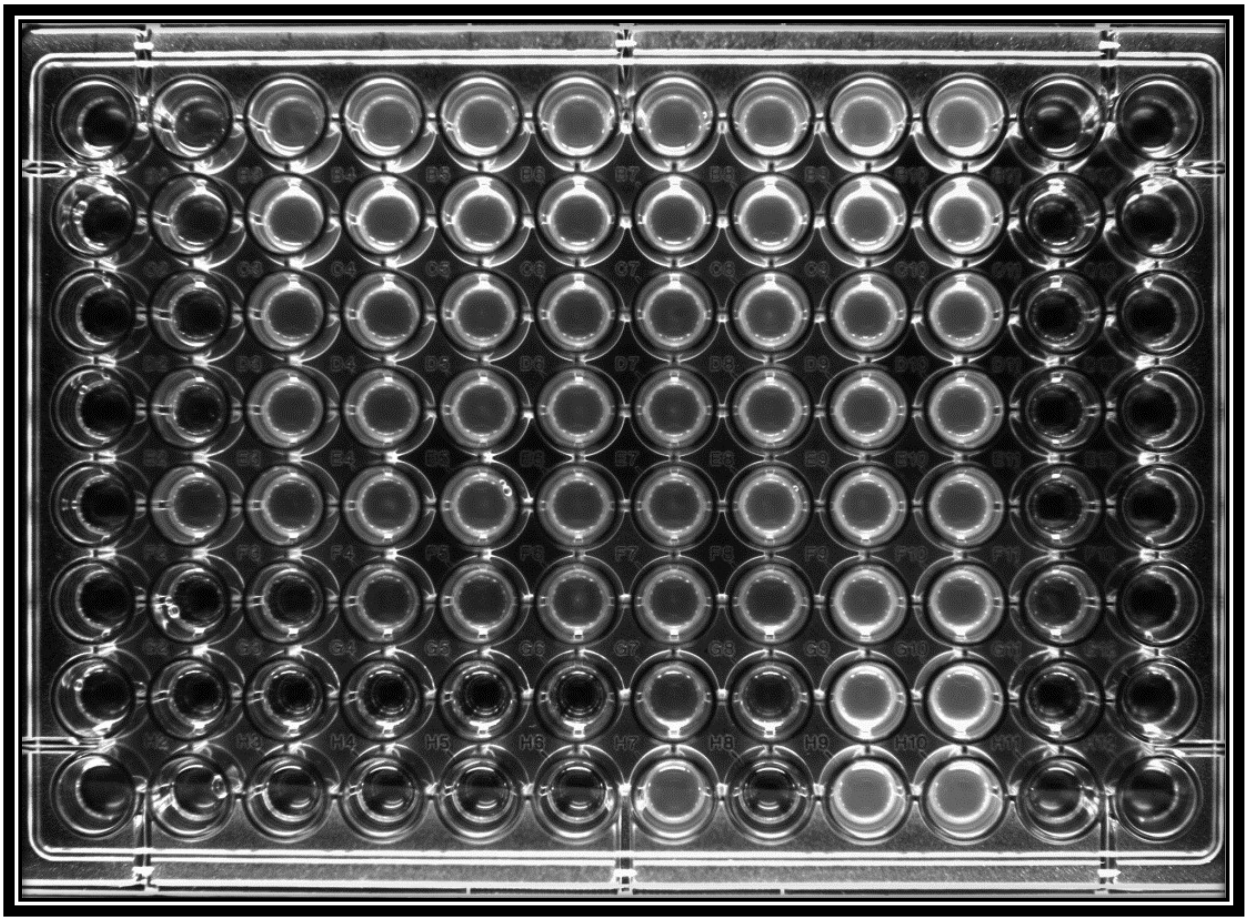

Figure 4.1 Broth Microdilution Example.
Image of a 96-well microplate following a MIC microdilution assay using Nisin and Silver nitrate against S. aureus. (t = 18). Columns 1 – 8 Treatment wells, Column 9, 10: Growth Control, Column 11, 12: Sterility Control.

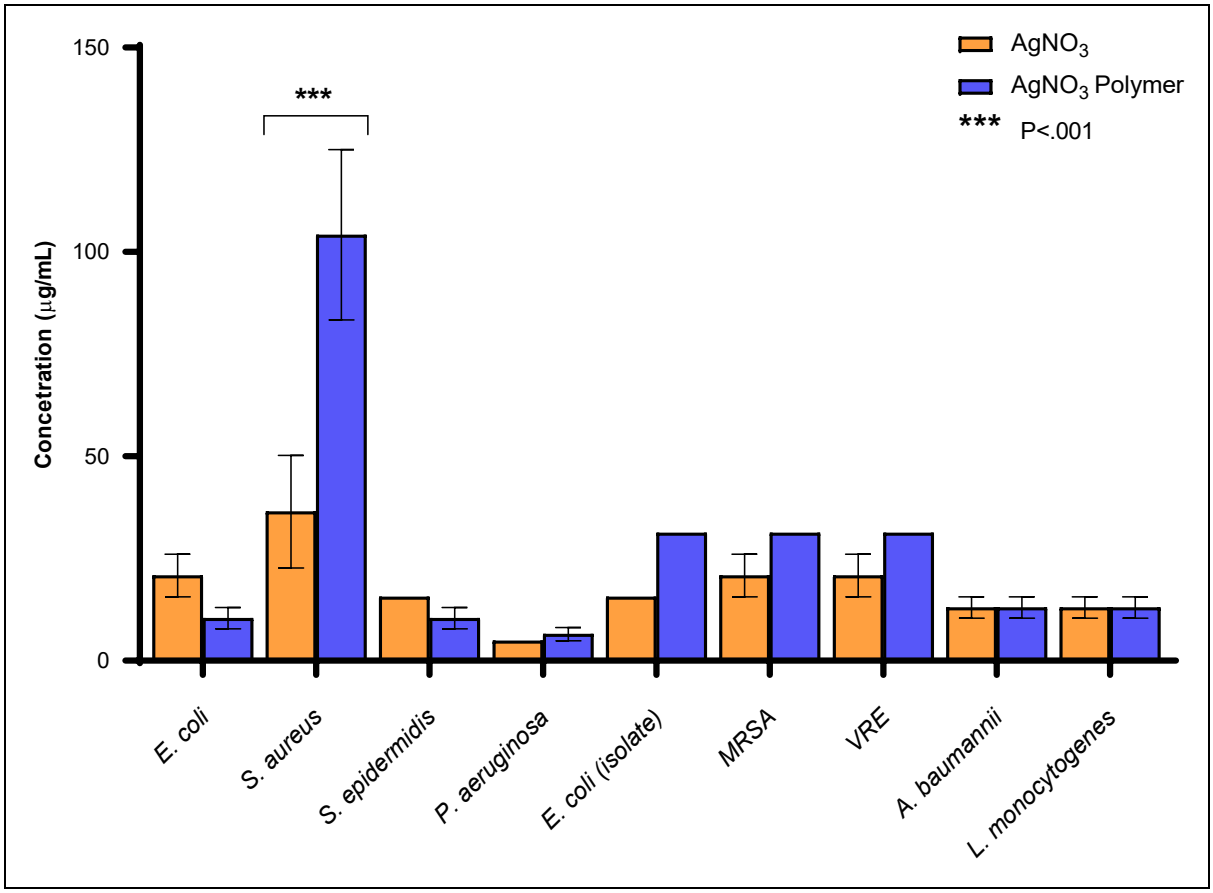

Figure 4.2 Mean Minimum Inhibitory Concentration of Silver Nitrate and Silver Nitrate Polymer.
Bars represent the mean minimum inhibitory concentration (MIC) of silver nitrate (AgNO3) and AgNO3 polymer, with concentrations expressed in µg/mL, against each tested bacterial strain. Error bars represent standard error of the mean (SEM). Significant changes in MIC values before and after polymer incorporation were determined by use of two-way ANOVA, with Sidak's multiple comparisons test, and expressed in terms of P value following the APA style. N = 3

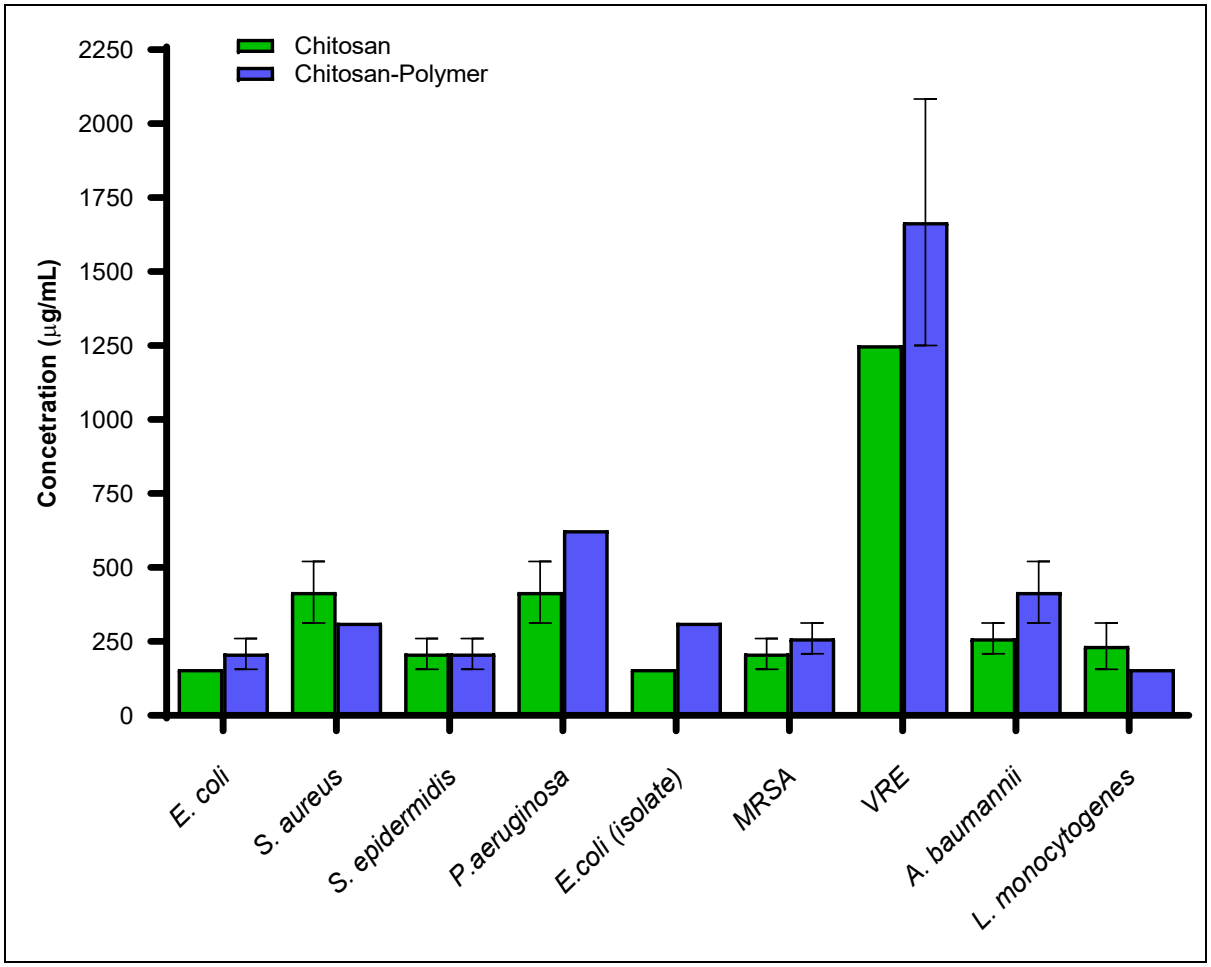

Figure 4.3 *Mean Minimum Inhibitory Concentration of Chitosan and Chitosan Polymer*. Bars represent the mean minimum inhibitory concentration (MIC) of chitosan and chitosan polymer, with concentrations expressed in µg/mL, against each tested bacterial strain. Error bars represent standard error of the mean (SEM). Results were assessed for significant changes in MIC values before and after polymer incorporation by use of a two-way ANOVA, with Sidak's multiple comparisons test. N = 3

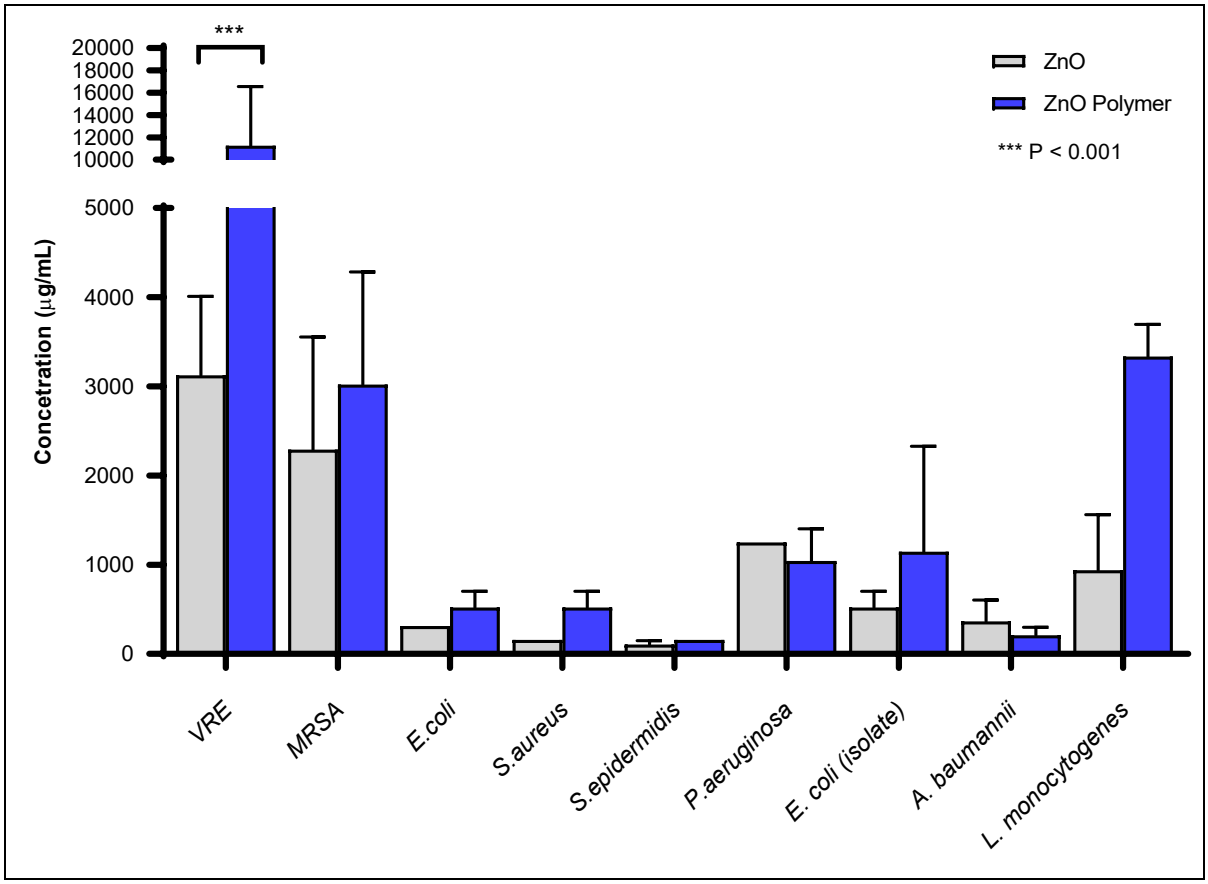

Figure 4.4 *Mean Minimum Inhibitory Concentration of Zinc Oxide and Zinc Oxide Polymer.* Bars represent the mean minimum inhibitory concentration (MIC) of zinc oxide (ZnO) and ZnO polymer, with concentrations expressed in µg/mL, against each tested bacterial strain. Error bars represent standard error of the mean (SEM). Significant changes in MIC values before and after polymer incorporation were determined by use of two-way ANOVA, with Sidak's multiple comparisons test, and expressed in terms of P value following the APA style. N = 3

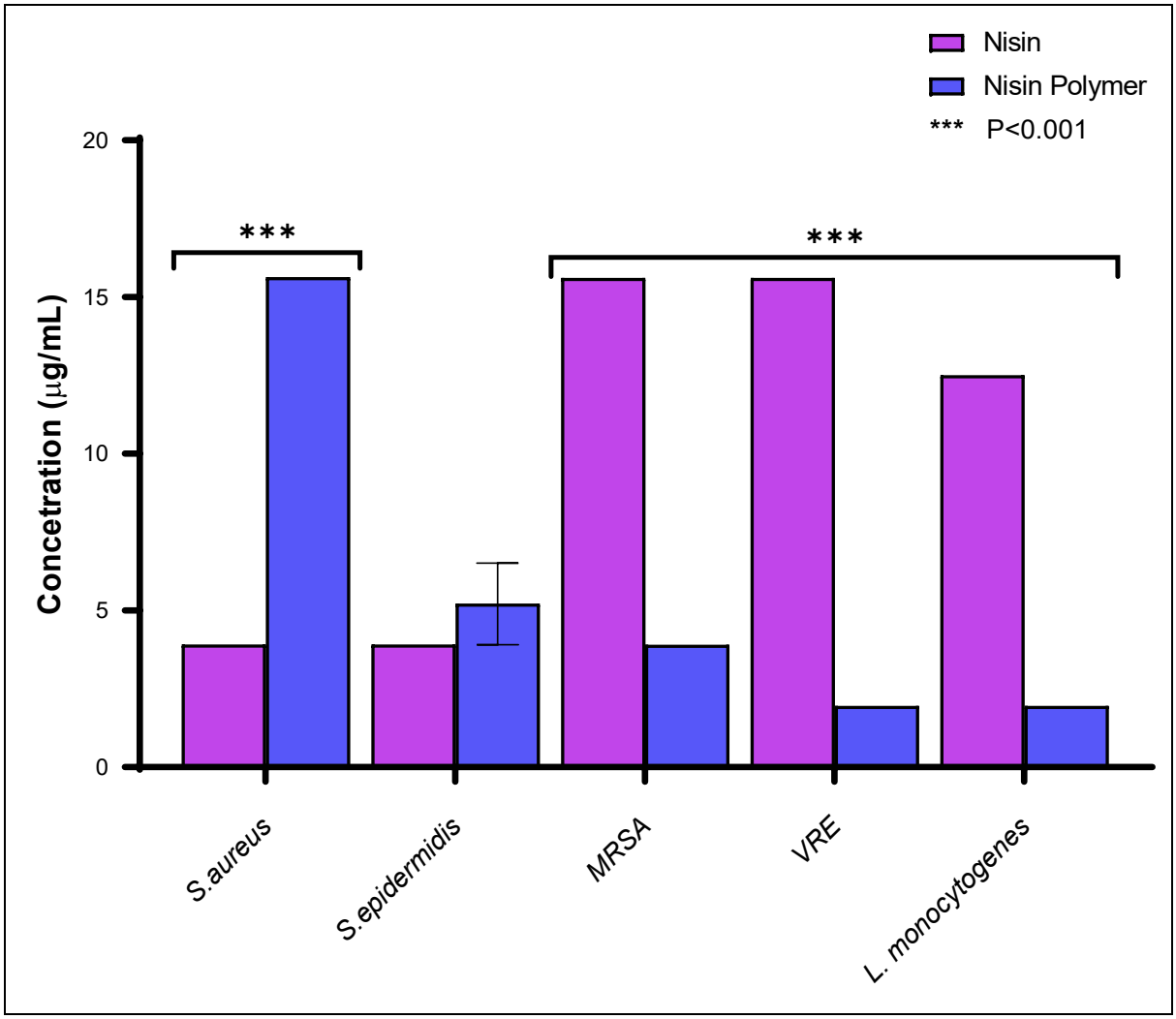

Figure 4.5 *Mean Minimum Inhibitory Concentration of Nisin and Nisin Polymer*
Bars represent the mean minimum inhibitory concentration (MIC) of nisin and nisin polymer, with concentrations expressed in µg/mL, against each tested bacterial strain. Error bars represent standard error of the mean (SEM). Significant changes in MIC values before and after polymer incorporation were determined by use of two-way ANOVA, with Sidak's multiple comparisons test, and expressed in terms of P value following the APA style. N = 3

Chapter 5 Assessment of Biofilm Disruption Capabilities

5.1 Introduction

As the threat of antibiotic resistance continues to globally rise, there is greater precedence on the development of alternative treatments to counteract this danger. As previously mentioned, the occurrence of antibiotic resistance can arise from a number of different bacterial mechanisms. The aim of much research recently has been to develop new antibiotics and alternative treatments as a countermeasure to bacterial species that have developed direct resistance to current antibiotics (such as MRSA and VRE), and also as pre-emptive measures against emerging antibiotic resistance. While novel antibiotics are crucial in this regard, this approach only address two major mechanisms of antibiotic resistance: modifying the drug target and inactivation of the drug (Jolivet-Gougeon and Bonnaure-Mallet 2014; Høiby, Bjarnsholt, Givskov, Molin, and Ciofu 2010). The other major resistance mechanisms, which are limiting drug uptake and drug efflux, cannot be counteracted through new antibiotic developments as these physical activities can prevent any and all antibiotics or treatments regardless of their drug target or mechanism. These resistance mechanisms are primarily associated with biofilm formations, which function as physical barriers against treatments, but can also efflux any treatments that do manage to infiltrate the biofilm itself, before they can interact with the internal bacterial population.

As previously reported in the present project, four chosen bioactives ($AgNO_3$, nisin, chitosan and ZnO) were assessed for their efficacy against a number of different bacterial strains, both test strains and isolated wild-type veterinary strains, including a number of AMR strains. The bioactives were found to effectively inhibit bacterial growth of these strains, before and after incorporation into the PVP-VA polymer carrier. With regards to the overall project aim, it is important that the test compounds hold efficacy against various strains of bacteria related to common infections and diseases. However, as the primary goal is to discover and develop treatments targeting AMR, it is vital to assess the bioactives against such, which holds difficulty due to the novelty of the bioactives use in this respect, as it becomes challenging to identify bacteria which hold resistance to these bioactives. Additionally, considering the

bioactives mechanisms of action, none of the currently known resistant bacterial strains would hold similar resistance to the chosen bioactives, excluding those boasting physical immunity such as that seen with Gram negative bacteria against nisin. However, antimicrobial resistance conferred by biofilm formations does not regard the mechanism of the treatment applied and can neutralise the efficacy of a variety of different antimicrobials. As such, a treatment able to elude biofilm mediated resistance (BMR) or that could have an effect upon the actual biofilm formations themselves would have significant benefit in the development of new approaches against BMI and AMR bacteria, which rely on BMR for survival. Furthermore, due to the broad-spectrum resistance owing to the physical biofilm formations, it can be reasoned that this resistance would also hold against the bioactive test compounds chosen for this study.

Anti-biofilm assays have been used for a number of years to determine antimicrobial efficacy against various biofilm forming bacteria. As the formation of biofilms occur through a number of stages, assays have been developed to evaluate treatments used at the principal stages of biofilm development, while remaining relative to the already well-established MIC assays (Azeredo et al. 2017). Currently the primary method used to assess an antimicrobials effect upon a biofilm is to first determine the lowest concentration required to inhibit biofilm formation, known as the minimum biofilm inhibitory concentration (MBIC), and the second to determine the lowest concentration required to remove an already developed biofilm, known as the minimum biofilm eradication concentration (MBEC) ((Coenye et al. 2018; Ceri et al. 2001). Currently, a new method of anti-biofilm assessment will be introduced which could provide valuable data for developing antibiofilm materials while remaining close in procedure to the previously mentioned MBIC and MBEC methods. While the MBEC primarily focuses on assessing potential removal of an established biofilm, the MBIC focuses on preventing biofilm growth caused by bacteria which have attached to a surface and can be considered preventative rather than treatment. Building upon the MBIC approach, a proposed method to determine the minimum concentration of an antimicrobial that can inhibit primary bacterial attachment to a surface, which we have named the minimum attachment inhibitory concentration (MAIC). As primary attachment is considered the most crucial point of biofilm formation, the ability to prevent this stage would completely counteract any biofilm development.

In order to determine the anti-biofilm capabilities of the chosen bioactives, $AgNO_3$, nisin, chitosan and ZnO will be assessed against two chosen bacterial strains, *S. aureus* and *P. aeruginosa*, which are known biofilm-forming species and are also representative of both Gram positive and negative bacterial strains respectively. While there are numerous publications of various biofilm assays, the primary focus of studies in this present project is to determine the minimum biofilm inhibition concentration (MBIC) and minimum biofilm eradication concentration (MBEC) for these novel bioactive combinations. While the focus remains the same, the methods can vary between studies which in turn, can lead to incomparable results. While there are some standardised test methods (Harrison et al. 2010), these protocols omit what can be considered vital conditions for biofilm testing. In addition to these points, there have been no biofilm studies with attention drawn upon the initial attachment of bacteria, which can be considered the most essential stage of biofilm development. With these considerations, the procedures used in the present study have been developed to incorporate what can be considered important test conditions and parameters of assessment, in-order to determine the most successful conditions for both producing biofilms and also for assessing the effect of treatments (Harrison, Turner, and Ceri 2005; Colomer-Winter, Lemos, and Flores-Mireles 2019; O'Toole 2011; Bueno 2011; Mah 2014). Furthermore, while definite endpoints such as the MBIC and MBEC are standard in clinical biofilm research, the methods utilised in the present study cannot conform to these strict end points. Rather than defining the lowest concentration that can inhibit biofilm growth or eradicate a mature biofilm, the current study can report the effects of each bioactive against bacterial attachment, biofilm inhibition and biofilm eradication in a dose-response fashion.

Initial coating of test surfaces has been previously carried out in a number of other studies, which show success in promoting bacterial attachment and thus, stimulating biofilm formations (Wagner, Aytac, and Maria Hänsch 2011; Chutipongtanate and Thongboonkerd 2010). Studies of initial biofilm mechanisms and development have established the importance of a number of proteins involved in initial bacterial attachment. The main protein identified, fibrinogen, is a blood plasma protein found which can be found throughout the body, in a number of different fluids including urine. This protein has been associated with major sites of biofilm formations on biomedical devices in the body, including stent valves in the heart and urinary catheters, and as such, is commonly utilised in such attachment studies.

While fibrinogen is undoubtedly the primary protein involved in attachment, other plasma-based proteins cannot be overlooked for their involvement. While some studies recognise this concept by utilising more complete attachment solutions, such as artificial urine, the present study opted for the use of blood plasma (Wagner, Aytac, and Maria Hänsch 2011). While the cost of blood plasma is significantly lower than alternate solutions, it also includes the entire array of proteins and other components involved in bacterial attachment which gives a more in-depth analysis closer to natural attachment observed in medical biofilms.

The bioactives will be assessed both in stock form and also after incorporation into a polymer carrier. They will be tested across a range of serially diluted concentrations, facilitated by use of 96-well plates which allow for screening of many different concentrations in replicate. Furthermore, the present study will utilise the peg lids for additional biofilm growth. Use of 96-well plates and also of peg lids in biofilm studies has been documented for a number of years, however, there have been no studies carried out which use both methods simultaneously. The present study is, to best knowledge, the first which has developed and carried out a standard test method which uses both the well walls of a 96-well plate and also the intruding pegs of a peg lid, as surfaces for the growth of biofilms. The two methods are to be then compared as to determine their individual efficacy for this biofilm analysis, and to establish any patterns in bacterial attachment.

Results will be determined by use of crystal violet (CV) staining of biofilm formations to assess physical treatment effects, and extracellular resazurin conversion to assess metabolically active cell numbers within the biofilm. The use of CV staining has been a primary method of biofilm analysis, as the physical structure of biofilm formations have strong binding affinity towards CV stain. It was determined that standardised staining methods utilised in this study, with adequate washing and solubilisation of the dye, followed by absorbance readings are effective means at quantifying the physical mass of a formed biofilm. The basic relationship of this measurement revolves around the concept that a large biofilm will bind a higher amount of CV compared to a smaller biofilm, while systems with no biofilm will not bind any CV whatsoever. Larger amounts of solubilised CV will produce a greater absorbance reading which can then be compared to internal controls (e.g. a growth control of 100% growth, a negative growth control of 0% growth, i.e. blank) of a system, allowing for basic inhibition or reduction measurements using readings from test samples.

While CV has well documented use in such studies, resazurin-based biofilm assessments has not been frequently used over the past number of years, but there has been a surge of interest in recent years (Sandberg et al. 2009; Peeters, Nelis, and Coenye 2008; Cruz, Shah, and Tammela 2018). The inclusion of resazurin in this study was due to its ability of in-directly measuring the metabolic activity of cells, hence allowing in-direct measurement of cell viability (Rampersad 2012; Cruz, Shah, and Tammela 2018). It is hypothesised that while a chosen antimicrobial may have no effect upon the physical biofilm structure or its integrity, the compound may still hold effect upon the internal bacterial population of a biofilm. While this has become a well-documented theory, the primary means of assessing internal biofilm bacteria populations involves disruption of the biofilm structure (normally via physical means such as sonication) and then subsequent growing of the extracted biofilm population on agar to perform a cell count, however, there have been a number of drawbacks to this method identified. The process involved in initiating and producing biofilms requires that the bacterial cells undergo a number of genetic and physical alterations which causes it to differ from its previously planktonic form, and as such, will not grow to the same standard on agar or in broth (Hall and Mah 2017; Madsen et al. 2012). This can cause issues in reading the efficacy of treatments as plate counts from such extractions are compared to normal, planktonic bacteria plate counts. Another issue is the means by which the bacteria are extracted from the biofilm wherein sonication of the biofilm being the most commonly used method, this process can cause major stress to the bacterial cells which in turn can cause their growth behaviours to change. As well as this, sonication has been found to vary in its efficacy to remove all cells from the biofilm (Rosa et al. 2019). These issues can lead to misreads of anti-biofilm treatment efficacy due to lower numbers of viable treated cells being determined and thus over-estimating a treatments efficacy. The use of resazurin bypasses these issues by allowing measurement of bacteria population health without causing stress or disruption to the cells or biofilms. Furthermore, as resazurin staining does not disrupt biofilm formations, this assessment can be carried out prior to CV staining which in turn allows for greater amounts of data to be generated from a single set of samples. The only identified drawback from use of such indirect measurements, is that it is unable to estimate the actual number of viable bacterial cells within the biofilm. As such, the measurements gained are used in conjunction with measurements from in-system controls such as the 100% growth control and negative growth controls, where comparison allows determination of a treatments effect

in terms of a percentage. Furthermore, the measurement is based upon the conversion rate of resazurin in such a way that a higher number of cells will convert a greater amount of resazurin (and thus producing a greater signal) in a shorter amount of time. In order to accurately measure differences, resazurin conversion will be monitored in an hourly manner. A specific time-point will be chosen at which all measurements are to be compared and results established.

5.2 Aims & Hypothesis

The aim of this study is to assess the anti-biofilm ability of four bioactive compounds both before and after incorporation into a polymer carrier. The bioactives will be tested against a number of bacterial species associated with biofilm mediated infections, in order determine their suitability as alternative treatments against AMR bacterial species.

It is hypothesised that the individual bioactives will prevent biofilm development by inhibiting initial bacterial attachment or by interrupting the actual formation. Additionally, the bioactives will exhibit effective reductions against already established biofilm formations.

5.3 Results

5.3.1 Crystal Violet Biofilm Analysis

- **Attachment Inhibition**

$AgNO_3$

$AgNO_3$ demonstrated effective attachment inhibition against *P. aeruginosa* at concentrations between 312.5 – 1250 µg/mL on lid pegs, as determined by the absence of biofilm formations (Figure 5.1). Lower concentrations resulted in increased bacterial attachment (~25%). $AgNO_3$-PVP varied greatly with no clear indication whether it impedes or enhances bacterial attachment on the pegs. $AgNO_3$ was effective at inhibiting attachment in plate wells as determined by reduced biofilm formations at all concentrations, with the highest reduction at 625 µg/mL (~75%). $AgNO_3$-PVP demonstrated effective attachment inhibition at concentrations between 78.13 – 625 µg/mL, with reductions between 50 – 100% against P. aeruginosa on plate wells.

$AgNO_3$ was not effective against *S. aureus* bacterial attachment on lid pegs (Figure 5.1) or in plate wells and was seen to greatly increase biofilm formations in rising concentrations (up to 200%) on plate wells. $AgNO_3$-PVP was also seen to cause increased biofilm formations as concentrations increased, with biofilm production seen to rise up to 125% in plate wells and up to 300% on lid pegs. Lower concentrations of $AgNO_3$ and $AgNO_3$-PVP were noted to cause slight inhibition up to 30% on lid pegs and up to 25% in plate wells.

Nisin

Both nisin and nisin-PVP demonstrated weak attachment inhibition properties against *P. aeruginosa* on peg lids at concentrations below 23.44 μg/mL, with inhibition % ranging between 10 – 40% (Figure 5.3). At higher concentrations nisin's attachment inhibition abilities fall, with some replicates showing a slight increase of attachment. Higher concentrations of nisin-PVP resulted in increased bacterial attachment (up to 75% at 187.5 μg/mL). Results against *P. aeruginosa* on plate wells exhibited more consistent results with nisin and nisin-PVP causing inhibition of approximately 25% in concentrations between 187.50 – 0.73 μg/mL (Figure 5.3). A slight increase in attachment was noted at the highest test concentration (375 μg/mL) for both nisin (~25% increase) and nisin-PVP (~15% increase).

Nisin demonstrated effective attachment inhibition against *S. aureus* on lid pegs (Figure 5.3), with inhibition of up to 75% at concentrations of 46.88 – 93.75 μg/mL. Nisin-PVP was shown to have moderate inhibitory effect, with inhibition of up to 50% at concentrations between 5.86 – 46.88 μg/mL. However, the highest test concentration of nisin-PVP (187.5 μg/mL) was seen to promote attachment up to 55 – 60%. Results against *S. aureus* on plate wells were inconsistent (Figure 5.3). Nisin only demonstrated notable inhibition at higher concentrations of 46.88 – 187.5 μg/mL with attachment inhibition between 25 – 50%. Nisin-PVP was not effective at inhibiting attachment and was seen to promote bacterial attachment up to 25% at 93.75 – 187.5 μg/mL.

Chitosan

Chitosan had no major inhibitory effect against *P. aeruginosa* on lid pegs, with peak inhibition of 30% at 78.13 μg/mL (Figure 5.5). Chitosan-PVP was seen to cause slight inhibition at lower concentrations (19.53 – 312.5 μg/mL) similar to chitosan (20 – 30% inhibition). At higher concentrations, chitosan-PVP was causing a notable increase in bacterial attachment (average 50% increase). Chitosan held similar inhibitory effect against *P. aeruginosa* on plate wells

(Figure 5.5) at all concentrations, with inhibition up to 30% seen at concentrations between 39.06 – 312.5 μg/mL. Chitosan-PVP also held similar inhibitor effect between 19.53 – 156.26 μg/mL with inhibition reaching 30%. Chitosan-PVP was also seen to promote attachment at the highest concentration of 2500 μg/mL (approximately 20% increase), however this was much lower in comparison to its effect against *P. aeruginosa* on the lid pegs.

Chitosan and chitosan-PVP demonstrated very poor attachment inhibitory properties against *S. aureus* on lid pegs (Figure 5.5). There was no attachment inhibitory effect of chitosan at any concentration tested. However, there was a notable increase in attachment at concentrations of 156.25 – 2500 μg/mL, which appeared to escalate linearly with the concentration (50 – 250%). Similar effect was seen with chitosan-PVP, but to a much larger extent, with attachment increasing from 75 – 800% at concentrations between 156.25 – 2500 μg/mL.

Chitosan and chitosan-PVP also demonstrate poor attachment inhibition against *S. aureus* on plate wells (Figure 5.5). Chitosan promoted bacterial attachment (up to 70%) at concentrations between 9.77 – 156.25 μg/mL. There was a slight inhibitory effect at concentrations between 312.5 – 1250 μg/mL, however these were not noteworthy. Chitosan-PVP held similar effect, with attachment increases of up to 50% at concentrations between 9.77 – 156.25 μg/mL. This increase in attachment was seen to reduce as concentrations increased, down to a 15% increase at 2500 μg/mL.

ZnO

ZnO demonstrated low attachment inhibitory properties against *P. aeruginosa* on lid pegs (Figure 5.7). While inhibition was seen to increase with ZnO concentrations, it did not reach higher than approximately 45% at 5000 μg/mL. ZnO-PVP was seen to cause an increase of bacterial attachment at all concentrations, with increases of up to 50% at 156.25 and 1250 μg/mL. ZnO against *P. aeruginosa* on plate wells (Figure 5.7) demonstrated an increase of attachment at higher concentrations (up to 50% at 5000 μg/mL), with minor inhibitory effects at lower concentrations (up to 20% at concentrations between 9.77 – 78.13 μg/mL). ZnO-PVP demonstrated similar properties to ZnO, with inhibition of up to 20% at concentrations between 9.77 – 78.13 μg/mL. Higher concentrations of ZnO-PVP had no noteworthy effect overall, except at 5000 μg/mL which appeared to cause a varying increase of attachment.

ZnO exhibited notable increases in *S. aureus* attachment on lid pegs (Figure 5.7), with a peak increase of 120% at 76.13 µg/mL. ZnO-PVP was also seen to cause a large increase in bacterial attachment, with increases 100% at 1250 µg/mL and up to 250% at 2500 µg/mL. Results against *S. aureus* on plate wells (Figure 5.4D) exhibited a clear linear increase of bacterial attachment with ZnO concentration increase. ZnO was shown to increase bacterial attachment at all concentrations, up to 150% at 1250 – 2500 µg/mL. ZnO-PVP also demonstrated a linear increase of bacterial attachment, up to 125% at 2500 µg/mL.

- **Biofilm Inhibition**

AgNO3

$AgNO_3$ held highly effective biofilm inhibition against *P. aeruginosa* on lid pegs (Figure 5.9) with complete inhibition at concentrations 156.25 – 1250 µg/mL. Concentrations below this held no notable inhibitory effect and was seen to promote biofilm at concentrations between 9.77 – 39.06 µg/mL with increases of up to 75%. $AgNO_3$-PVP also exhibited effective biofilm inhibition with complete inhibition at 312.5 – 1250 µg/mL. Concentrations between 78.13 – 156.25 µg/mL reported inhibition between 25 – 75%. Similar to $AgNO_3$, concentrations between 9.77 – 39.06 µg/mL was seen to promote biofilm growth with an increase of up to 50%. Effects against *P. aeruginosa* on plate wells (Figure 5.9) were comparable to those seen against *P. aeruginosa* on lid pegs. $AgNO_3$ and $AgNO_3$-PVP exhibited near complete inhibition at concentrations between 312.5 – 1250 µg/mL. At 156.25 µg/mL, $AgNO_3$ caused mean inhibition 80% whereas $AgNO_3$-PVP caused 50%. At concentrations between 9.77 – 78.13 µg/mL, both $AgNO_3$ and $AgNO_3$-PVP held no noteworthy inhibitory effect but were noted to cause slight increases in biofilm formations.

$AgNO_3$ exhibited moderate inhibition against *S. aureus* on lid pegs (Figure 5.9), with mean inhibition values of 50 – 75% at concentrations between 156.25 – 1250 µg/mL. Concentrations between 4.88 – 78.13 µg/mL displayed varying degrees of inhibition, with mean values of approximately 25%. $AgNO_3$-PVP held notable inhibition at concentrations between 156.25 – 625 µg/mL, with mean inhibitory values of approximately 70%. Lower concentrations between 4.88 -78.13 µg/mL exhibited a major increase of biofilm production, with mean increases of 300 – 550%. There was no notable effect at 1250 µg/mL. Effects of $AgNO_3$ against *S. aureus* on plate wells (Figure 5.9) were quite distinct in comparison to effects against *S. aureus* on lid pegs. Mean biofilm inhibitions of approximately 40% were noted at

concentrations of $AgNO_3$ between 156.25 – 625 µg/mL, while concentrations between 4.88 – 39.06 µg/mL exhibited increases in biofilm growth of up to 100%. $AgNO_3$-PVP held similar inhibitory effects at concentrations 156.25 – 625 µg/mL, however at lower concentrations there was only a slight increase in biofilm formation noted.

Nisin

Nisin held no notable inhibitory effect against *P. aeruginosa* on lid pegs (Figure 5.11), while nisin-PVP held only a slight inhibitory effect (between 20 – 25%) at 0.79 – 1.46 µg/mL. Both treatments were noted to cause an increase in biofilm formation. At concentrations ranging between 11.72 – 187.5 µg/mL, nisin caused increases of 15 – 35% while at 375 µg/mL, an increase of up to 200% was noted. At concentrations between 23.44 – 375 µg/mL, nisin-PVP caused biofilm growth increases of 25 – 45%. Nisin demonstrated more effective biofilm growth inhibition against *P. aeruginosa* on plate wells (Figure 5.11), with inhibition values of approximately 20% at concentrations of 0.73 – 23.44 µg/mL. Concentrations between 46.88 – 187.5 µg/mL held no notable effect, whereas at 375 µg/mL, nisin was seen to cause a 100% increase in biofilm growth. Nisin-PVP exhibited an increase of biofilm growth at all test concentrations, which increased linearly with concentrations (up to 75% increase at 375 µg/mL).

Nisin displayed notable inhibition against *S. aureus* on lid pegs (Figure 5.11) at concentrations between 1.46 – 93.75 µg/mL, with peak inhibition (70%) between 11.72 – 46.88 µg/mL. Nisin-PVP also showed effective inhibition at all test concentrations, with highest inhibition values (70 – 75%) seen at 5.86 – 23.44 µg/mL. Nisin did not demonstrate effective inhibition against *S. aureus* on plate wells (Figure 5.11), with the highest inhibition values (45 – 50%) seen at 4.688 – 93-75 µg/mL. Mid-range concentrations (5.86 – 23.44 µg/mL) varied greatly. Nisin-PVP exhibited an overall growth increase across the test concentrations (up to 40% at 46.88 µg/mL), with only a slight inhibitory effect at 187.5 µg/mL.

Chitosan

Chitosan exhibited low inhibitory effects against *P. aeruginosa* on lid pegs (Figure 5.13) across all test concentrations, with a max inhibition of approximately 25% at 78.13 ug/mL. Chitosan-PVP displayed low inhibitory effects (20 – 25%) at concentrations from 19.53 – 312.5 µg/mL, with noted increases of biofilm growth at concentrations of 1250 µg/mL (mean 15%) and 5000 µg/mL (mean 50%). Chitosan against *P. aeruginosa* on plate wells (Figure 5.13) demonstrated

low inhibition (25 – 30%) at concentrations between 9.77 – 312.5 μg/mL. At concentrations between 625 – 2500 μg/mL, increased biofilm growth was seen, with increases up to 70% at 1250 μg/mL. Chitosan-PVP did not exhibit any notable inhibition but was seen to increase biofilm growth on plate wells at concentrations between 19.53 – 2500 μg/mL, with mean increases of 80% at 1250 – 2500 μg/mL.

Chitosan displayed major increases to biofilm growth against *S. aureus* on lid pegs (Figure 5.13), with increases observed at concentrations 78.13 – 2500 μg/mL, up to 3500% at 1250 μg/mL. Chitosan-PVP also displayed substantial increases in biofilm formations at concentrations 19.53 – 2500 μg/mL, with highest increases of 2000% between 1250 – 2500 μg/mL. Chitosan was seen to promote increased biofilm formations against *S. aureus* on plate wells (Figure 5.13) at all test concentrations. The increase was observed to increase linearly with treatment concentration from 78.13 – 1250 μg/mL, with increase peaking at approximately 850%. Results of treatments at 2500 μg/mL also displayed majorly increased biofilm formations, with an increase of approx. 750% being reported. Chitosan-PVP was also seen to promote biofilm formations, similarly to chitosan, in a linear trend across all concentrations with a peak increase of approx. 600% at 2500 μg/mL.

ZnO

ZnO demonstrated moderate biofilm inhibition against *P. aeruginosa* on lid pegs (Figure 5.15), with inhibition of up to 50% at 5000 μg/mL. ZnO-PVP also exhibited moderate-high biofilm inhibition across all test concentrations with a peak mean inhibition of approx. 75% at 5000 μg/mL. ZnO did not report any notable inhibition against *P. aeruginosa* on plate wells (Figure 5.15) but was observed to cause an increase in biofilm formation at concentrations between 312.5 – 2500 μg/mL (up to 80% increase at 2500 μg/mL). Similarly, ZnO-PVP did not inhibit growth at any test concentrations but was seen to promote biofilm formation between 312.5 – 2500 μg/mL, with a peak increase of 60% at 1250 μg/mL.

Results of ZnO against *S. aureus* on lid pegs (Figure 5.15) have shown it to not be an effective inhibitor of biofilm growth, with only one concentration (156.25 μg/mL) reporting notable inhibition (50%). It was also shown to promote biofilm growth at concentrations between 9.77 – 39.06 μg/mL up to 50% and at concentrations between 625 – 1250 μg/mL up to 90%. ZnO-PVP did not report inhibition at any test concentrations but did demonstrate major biofilm growth stimulation. Mean growth promotion ranged from 150% at 2500 μg/mL to

1500% at 312.5 µg/mL. ZnO was also seen to increase biofilm growth against *S. aureus* on plate wells (Figure 5.15), with increases of 25 – 50% at concentrations between 9.77 – 156.25 µg/mL and increases of 150 – 400% at concentrations between 312.5 – 2500 µg/mL. ZnO-PVP exhibited slight biofilm growth inhibition at 156.25 µg/mL, but was otherwise comparable to ZnO, with high biofilm growth at 312.5 µg/mL (125%), 625 µg/mL (300%), 1250 µg/mL (150%) and 2500 µg/mL (100%).

- **Biofilm Reduction**

$AgNO_3$

Results against *P. aeruginosa* on lid pegs (Figure 5.17) show that $AgNO_3$ was effective on reducing biofilm formations at higher concentrations, with % reduction of 95% at 1250 µg/mL and 70% at 625 µg/mL. A lower reduction of 20% was observed at 312.5 µg/mL. Lower concentrations had no notable reduction, however there was an increase in biofilm formation observed at lower concentrations, most notably at 78.13 µg/mL (50%). $AgNO_3$-PVP demonstrated to be very effective, with biofilm reductions of 85% at concentrations between 156.25 – 1250 µg/mL, 50% at 78.13 µg/mL and 25% at 39.06 µg/mL. However, a biofilm formation increases of approx. 35% (mean) was observed at 19.53 µg/mL. There was no notable effect at 9.77 µg/mL.

$AgNO_3$ held much more effective reduction ability against *P. aeruginosa* on plate wells (Figure 5.17) with reductions of approaching 95% at 312.5 – 1250 µg/mL, 75% at 156.25 µg/mL, and 60% at 78.13 µg/mL. Lower concentrations 9.77 – 39.06 µg/mL also reported reductions of 25%. $AgNO_3$-PVP also exhibited notable biofilm reduction comparable closely to $AgNO_3$, with biofilm reductions of 95% at 156.26 – 1250 µg/mL and 65% at 78.13 µg/mL. Lower concentrations of 9.77 – 39.06 µg/mL also reported reductions of 25%.

Against *S. aureus* on lid pegs (Figure 5.17), was effective at reducing biofilm formations, with reductions of 60 – 75% between 39.06 – 2500 µg/mL, and reduction of 40% at 5000, 19.53 and 9.77 µg/mL. $AgNO_3$-PVP was also effective at reducing *S. aureus* biofilms on lid pegs, with reductions of 50 – 70% at concentrations between 156.25 – 2500 µg/mL, 45 – 50% at 9.77 and 19.53 µg/mL, and 20 – 25% at 39.06 and 78.13 µg/mL. There was no notable effect of $AgNO_3$-PVP at 5000 µg/mL.

$AgNO_3$ was quite effective at reducing *S. aureus* biofilm formations on plate wells (Figure 5.17), with reductions of 75% at 78.13 – 1250 µg/mL, 50% at 19.53 – 39.06 µg/mL and 20% at 9.77 µg/mL. $AgNO_3$-PVP was not as effective at reducing biofilms, with the highest reductions (50%) reported between 78.13 – 156.25 µg/mL, with % biofilm reduction seen to drop as the concentration of $AgNO_3$-PVP increased or decreased.

Nisin

Nisin reported mixed effects against *P. aeruginosa* on lid pegs (Figure 5.19) exhibiting biofilm reduction of 13% at 187.5 µg/mL, 27% at 93.75 µg/mL, 16% at 23.44 µg/mL, 9.4% at 2.93 µg/mL, 17% at 1.46 µg/mL and 16% at 0.73 µg/mL. Increases in biofilm formations were reported with 30% increase at 375 µg/mL and 18% at 46.88 µg/mL. There was no notable effect upon biofilm formations at 11.72 and 5.86 µg/mL. Nisin-PVP also reported mixed results, with reductions of 41% at 375 µg/mL and 27% at 187.5 µg/mL. Increased biofilm formations were reported with 23% increase at 46.88 µg/mL, 15% at 23.44 µg/mL, and increases of 25 – 45% at 0.73 – 5.86 µg/mL.

Nisin also reported varying results against *P. aeruginosa* on plate wells (Figure 5.19), with reductions of 9% at 93.75 µg/mL, 9 – 17% at 0.73 – 11.72 µg/mL. Notable increases in biofilm formations were reported with increases of 74% at 375 µg/mL, and 31% at 187.5 µg/mL. Nisin-PVP exhibited very minor effects upon biofilm formations with reductions of 11 – 13% at 23.44 and 375 µg/mL, while there was slight increase in biofilm formations of ~12% at 0.73, 1.46 and 187.5 µg/mL. There were no notable effects at all other test concentrations.

Nisin demonstrated effective biofilm reduction against *S. aureus* on lid pegs (Figure 5.19) with 44% reduction at 187.5 µg/mL, 68 – 70% at 46.88 – 93.75 µg/mL, 78% at 23.44 µg/mL, 82% at 11.72 µg/mL, 67% at 5.86 µg/mL and 33 – 45% at 0.73 – 2.93 µg/mL. Nisin was also seen to enhance biofilm formations with an increase of 71% at 375 µg/mL. Nisin-PVP also reported moderate reduction of biofilms across the treatment range, with reductions of 44 – 47% at 187.5 – 375 µg/mL, 25% at 46.88 µg/mL, 54% at 23.44 µg/mL 50% at 5.86 µg/mL, 20% at 2.93 µg/mL and 60 – 63% at 0.79 – 1.46 µg/mL. There were no notable effects at concentrations of 11.72 or 93.75 µg/mL.

Nisin had moderate biofilm reduction against *S. aureus* on plate wells (Figure 5.19) with reductions of 44% at 187.5 µg/mL, 61% at 93.75 µg/mL, 71% at 46.88 µg/mL, 55 – 56% at

11.72 – 23.44 μg/mL, 67% at 5.86 μg/mL, 48.5 – 53% at 0.73 – 2.93 μg/mL. There was no notable effect at 375 μg/mL. Nisin-PVP also exhibited moderate biofilm reduction with 62% reduction at 375 μg/mL, 57% at 187.5 μg/mL, 53% at 93.75 μg/mL, 43% at 46.88 μg/mL, 21% at 23.44 μg/mL, 34% at 11.72 μg/mL, 29% at 5.86 μg/mL, 32% at 2.93 μg/mL, 30% at 1.46 μg/mL and 29% at 0.73 μg/mL.

Chitosan

Chitosan had no notable effect at any test concentration against *P. aeruginosa* biofilms grown on lid pegs (Figure 5.21). Chitosan-PVP was seen to enhance biofilm formations on lid pegs at concentrations between 19.53 – 1250 μg/mL, with mean increases of 15 – 30%. There was notable biofilm reduction at 5000 μg/mL, with a 57% reduction being recorded.

Chitosan exhibited varying results against *P. aeruginosa* biofilm formations on plate wells (Figure 5.21). Lower concentrations (19.53 – 625 μg/mL) reported reductions between 4 – 27%, peaking at 78.125 – 156.25 μg/mL. There was an increase in biofilm formations seen at 1250 μg/mL (17% increase) and 2500 μg/mL (5% increase). The highest reduction, however, was seen at 5000 μg/mL, with a reduction in biofilm formations of 41%. Chitosan-PVP was seen to increase biofilm formations on plate wells by 10 – 17% at concentrations between 39.06 – 625 μg/mL. Reductions in biofilm formations were noted at higher concentrations of 1250 μg/mL (6%), 2500 μg/mL (30%) and 5000 μg/mL (40%).

S. aureus biofilm formations displayed dramatic increases in physical formations on peg lids following treatments of chitosan (Figure 5.21). Concentrations of 156.25 – 5000 μg/mL chitosan demonstrated increases of biofilm formations between 638 – 4152%, with peak increases seen at concentrations of 156.25 μg/mL (1101%) 312.5 μg/mL (2204%), 625 μg/mL (4152%) and 1250 μg/mL (2596%). Lower concentrations of chitosan were observed to have lesser effect, with a 11% increase at 39.06 μg/mL. Also, there was moderate reduction exhibited against biofilm formations at 19.531 μg/mL (48% reduction) and 78.13 μg/mL (3.7% reduction). Chitosan-PVP also exhibited extreme increases of physical biofilm formations on lid pegs, with the highest increases seen to occur at mid-test range concentrations. A reported biofilm increase of 369% was seen at the lowest test concentration (19.53 μg/mL) and increased linearly with increasing chitosan concentration, to a peak of 4679% at 312.5 μg/mL, which then decreased linearly, and chitosan concentration increased, to a biofilm increase of 708% at 5000 μg/mL.

S. aureus biofilms on plate wells were also seen to substantially increase overall when treated with chitosan (Figure 5.21). The lowest test concentration of 19.53 μg/mL saw biofilm reductions of 22%. Concentrations between 39.06 – 1250 μg/mL demonstrated increases in biofilm formations, that increased linearly with the concentration of chitosan, from 54% at 39.06 μg/mL to 795% at 1250 μg/mL. 2500 μg/mL also demonstrated a considerable increase of biofilm formations (640%). 5000 μg/mL did not hold any notable effect upon the *S. aureus* biofilms. Chitosan-PVP caused an increase of biofilm formations at all test concentrations. An increase of 489% was seen at the lowest test concentration(19.53 ug/mL) which increased linearly with chitosan-PVP concentration to a peak increase of 1395% at 312.5 μg/mL. The noted increase in biofilms was seen to decline above this concentration, from 1363% at 625 μg/mL to 81% at 5000 μg/mL.

ZnO

ZnO reported low reduction of *P. aeruginosa* biofilms grown on lid pegs at all test concentrations (Figure 5.23). There was no notable effect at lowest test concentration (19.53 μg/mL). Concentrations between 39.06 – 2500 μg/mL exhibited mean reductions of 15 – 29%. A reduction of 12% was noted at 5000 μg/mL. ZnO-PVP was seen to have increased reduction compared to ZnO. While there was no notable effect at the lowest test concentration (19.53 μg/mL), there was low – high reductions observed at other concentrations, which increased overall as the concentration of ZnO-PVP increased (19% at 39.06 μg/mL increasing to 64% at 5000 μg/mL).

ZnO held low – moderate reductions of *P. aeruginosa* biofilms grown on plate wells at all test concentrations (Figure 5.23). Lowest reduction was seen at 19.53 μg/mL (9% reduction). Concentrations 39.06 – 1250 μg/mL demonstrated increasing reductions of 22 – 42%. Reductions were observed to slightly decrease at 2500 μg/mL (38%) and 5000 μg/mL (27%). ZnO-PVP held low – moderate reductions against *P. aeruginosa* biofilms, with reduction of 25% at 78.13 μg/mL increasing to 52% at 5000 μg/mL. There was no notable effect at 19.53 – 39.06 μg/mL.

ZnO demonstrate moderate – high reduction of *S. aureus* biofilm formations on lid pegs at all test concentrations (Figure 5.23). High reductions (74 – 80%) were observed at concentrations of 625 – 5000 μg/mL, and the highest reduction (84%) was recorded at 39.06 μg/mL. ZnO-PVP effects varied greatly against *S. aureus* biofilms on lid pegs. The greatest reduction (43%) was

recorded at the lowest concentration (19.53 µg/mL), which then decreased as concentrations increased (41% at 39.06 µg/mL, 7% at 78.13 µg/mL, 5% at 156.25 µg/mL). There was a sharp change in effect at 312.5 µg/mL, which exhibited an 150% increase in biofilm formations. There was no notable effect at 625 µg/mL. There were also a strong increase in biofilm formations at the highest test concentrations, with increases of 67% at 1250 µg/mL, 190% at 2500 µg/mL and 91% at 5000 µg/mL.

ZnO held greatly varying effects upon *S. aureus* biofilm formations on plate wells (Figure 5.23). There was low – moderate reductions observed at 19.53 µg/mL (37%), 78.13 µg/mL (61%), 2500 µg/mL (23%) and 5000 µg/mL (42%). However, there were very high increases in biofilm formations observed at concentrations of 312.5 µg/mL (162%) and 625 µg/mL (144%). ZnO-PVP also held varying effects, with lower concentrations (19.53 – 78.13 µg/mL) exhibiting moderate inhibition (30 – 35%). Higher concentrations were seen to cause significant increases in biofilm formations (346% at 312.5 µg/mL, 462% at 625 µg/mL, 293% at 1250 µg/mL, 160% at 2500 µg/mL, 177% at 5000 µg/mL).

5.3.2 Resazurin Biofilm Analysis

- **Attachment Inhibition**

Results were observed to determine the degree to which each treatment inhibited or prevented bacterial attachment to lid pegs or plate well walls. Resazurin conversion indirectly represents the number of metabolically active bacteria within formed biofilms. Resazurin conversion is measured at the chosen time-point, and the amount converted by bacteria within each treated biofilm is compared to that which is converted by untreated biofilm bacteria. As such, lower conversion represents a lower population of metabolically active bacteria within the biofilm, which in turn can represent a lower number of bacteria that initially attached (i.e., a greater number of bacteria that were hindered in initial attachment or completely prevented from attaching to the treated surfaces).

AgNO3

$AgNO_3$ reported varied results against *P. aeruginosa* bacterial attachment on lid pegs (Figure 5.2). At the lowest test concentrations (9.77 – 19.53 µg/mL), a slight increase in biofilm populations was observed (12 – 18% increase). There was a greater increase observed (36 – 40%) at 39.06 – 78.13 µg/mL. At concentrations of 156.25 µg/mL, $AgNO_3$ reported a slight

reduction in biofilm populations, whereas concentrations of 312.5 – 2500 reported reductions of 84 – 85%. $AgNO_3$ -PVP did not cause any notable reduction of bacterial attachment, however it was reported to cause an increase in final biofilm populations (9 – 49% increases), indicating higher initial attachment.

$AgNO_3$ reported reductions against *P. aeruginosa* on plate wells at all concentrations (Figure 5.2). Lower concentrations of 9.77 – 156.2 µg/mL were seen to cause reductions of 8 – 23%. Higher concentrations of 312.5 – 2500 µg/mL reported reductions of 80 – 83%. $AgNO_3$ -PVP did not report reduced biofilm populations but did report an increase of populations at all test concentrations. Noteworthy increases ranged from 24% at 78.125 µg/mL and 312.5 µg/mL, up to 65% at 625 µg/mL, 72% at 1250 µg/mL and 118% at 2500 µg/mL.

$AgNO_3$ had no notable effect against *S. aureus* on lid pegs at lower concentrations between 4.88 – 19.53 µg/mL (Figure 5.2). There were slight reductions (8 – 10%) observed at concentrations between 39.06 – 78.13 µg/mL. Higher concentrations (156.25 – 625 µg/mL) reported reductions of 18 – 26%. Results of $AgNO_3$ -PVP against *S. aureus* on lid pegs reported no reduction in biofilm populations but did cause major increases in biofilm populations. Reported increases were observed to increase as treatment concentrations increased, from 16% at 4.88 µg/mL to a peak of 90% at 625 µg/mL, however these increases were not proportional to concentration increases.

There was no notable effect of $AgNO_3$ against *S. aureus* biofilm populations on plate wells at any test concentration (Figure 5.2). $AgNO_3$ -PVP also had no major effects, although it was seen to cause an increase of 13% in resazurin conversion at 625 µg/mL.

Nisin

Nisin v *P. aeruginosa* lid pegs

Nisin pre-treatments were noted to cause an increase in final biofilm populations at all test concentrations against *P. aeruginosa* on lid pegs (Figure 5.4). There was no clear trend in observed responses, with concentrations between 0.73 – 93.75 µg/mL reporting increases of 2 – 11%. There was a greater increase of 30% seen at the highest test concentration of 187.5 µg/mL. Nisin-PVP also exhibited conversion increases of 1 – 7% at concentrations between 0.73 – 5.9 µg/mL and 46.86 – 93.75 µg/mL. There were slight decreases of 5 – 9% observed

at 11.72 – 23.44 µg/mL. Similarly to nisin, there was a notable increase of 36% at the highest test concentration (187.5 µg/mL).

P. aeruginosa plate wells

Nisin did not reduce bacterial attachment of *P. aeruginosa* on plate wells but was observed to cause a slight increase at all concentrations (8 – 22% increase between 0.73 – 187.5 µg/mL) (Figure 5.4). Nisin-PVP was also ineffective at inhibiting *P. aeruginosa* bacterial attachment and was noted to cause major increases at all test concentrations (37 – 70% increases between 0.73 – 187.5 µg/mL).

S. aureus lid pegs

Nisin caused attachment inhibition against *S. aureus* on lid pegs, which was observed to increase with treatment concentration (Figure 5.4). Inhibition ranged between 15% at 0.37 µg/mL and to a peak of 94% at 97.75 µg/mL, with slightly less inhibition (89%) at 187.5 µg/mL. Nisin-PVP was ineffective at inhibiting *S. aureus* attachment on lid pegs at all concentrations and was also observed to cause a notable increase of 65% attachment at 187.5 µg/mL.

S. aureus plate wells

Nisin was effective at inhibiting attachment on plate wells at higher concentrations but also had a slight inhibitory effective at lower concentrations (Figure 5.4). Concentrations of 0.37 – 48.88 µg/mL caused inhibition of 6 – 9%. There was moderate inhibition of 43% seen at 93.75 µg/mL, and high inhibition of 83% at 187.5 µg/mL. Nisin-PVP exhibited a slight inhibitory effect (6 – 15%) at concentrations of 0.37 – 93.75 µg/mL, however there was a slight increase in attachment (10% increase) seen at 187.5 µg/mL.

Chitosan

Chitosan held low-moderate inhibitory effects against *P. aeruginosa* attachment on peg lids (Figure 5.6). There was close inhibition (19 – 34%) observed at all test concentrations 19.53 – 5000 µg/mL. Chitosan-PVP demonstrated similar results, with inhibition of 23 – 32% at

concentrations between 19.53 – 2500 µg/mL, however there was a slight increase in attachment (14% increase) observed at 5000 µg/mL.

Chitosan displayed similar results against *P. aeruginosa* on plate wells at lower concentrations (Figure 5.6). Attachment inhibition of 16 – 31% was reported for concentrations between 19.53 – 1250 µg/mL. Inhibition decreased to 6% at 2500 and -1% at 5000 µg/mL. Chitosan-PVP held varying effects. The largest inhibitory effect (22%) was noted at the lowest test concentration (19.53 µg/mL), which then decreased to 7% at 39.06 µg/mL and 0% at 78.13 µg/mL. Inhibition then increased to 19% at 156.25 µg/mL, but then decreased to 13% at 312.5 – 625 µg/mL. At higher concentrations, an increase in attachment was noted, with a 10% increase at 1250 µg/mL, 36% increase at 2500 µg/mL and a 198% increase at 5000 µg/mL.

Chitosan had a weak inhibitory effect against *S. aureus* attachment on lid pegs (Figure 5.6). Very slight inhibition (5%) was noted at the lowest test concentration (9.77 µg/mL). Inhibition was seen to range between 15% - 25% at concentrations of 19.53 – 625 µg/mL. The largest inhibition was noted at concentration so 1250 µg/mL (29%) and 2500 µg/mL (31%). Chitosan-PVP had very minor inhibitory effect (4 – 9%) against *S. aureus* on lid pegs at concentrations between 9.8 – 156.25 µg/mL. Higher concentrations exhibited an increase in bacterial attachment, which increased with concentration (4% at 312.5 µg/mL, 17% at 625 µg/mL, 40% at 1250 µg/mL, 108% at 2500 µg/mL).

Chitosan had very little effect against *S. aureus* bacterial attachment on plate wells at all test concentrations (19.53 – 2500 µg/mL) with inhibition ranging between 5 – 11% (Figure 5.6). Chitosan-PVP displayed a slight increase in inhibition (10 – 13%) at lower concentrations (19.53 – 312.5 µg/mL) and at 1250 µg/mL (12%). However, there was an increase in attachment (15% increase) noted at 2500 µg/mL.

ZnO

Zinc oxide (ZnO) held no inhibitory effect against *P. aeruginosa* on lid pegs and was instead seen to cause an increase in bacterial attachment (Figure 5.8). This attachment was seen to increase with treatment concentration (4% increase at 19.53 µg/mL to 55% increase at 5000 µg/mL). ZnO-PVP displayed a greater increase to bacterial attachment, peaking with an 86% increase at 1250 µg/mL.

While ZnO held slight attachment inhibition against *P. aeruginosa* on plate wells at some concentrations (12% inhibition at 39.06 µg/mL, 8% at 156.25 µg/mL, 8% at 312.5 µg/mL, 14% at 625 µg/mL), there was also attachment increase at other concentrations (13% increase µg/mL, 1% at 78.13 µg/mL, 11% at 1250 µg/mL, 9% at 2500 µg/mL, 9% at 5000 µg/mL) (Figure 5.8).

ZnO had minor effect against *S. aureus* attachment on lid pegs, with slight increases in attachment (5 – 13%) at concentrations between 9.77 – 312.5 µg/mL, and slight inhibition (10 – 13%) at 625 – 1250 µg/mL (Figure 5.8). Results of ZnO-PVP reported slight increases in attachment (13 – 29%) and concentrations of 9.77 – 312.5 µg/mL, and 1250 – 2500 µg/mL. There was minor inhibition (6%) observed at 625 µg/mL.

ZnO caused a minor increase in attachment (3 – 12% increases) at all test concentrations (19.53 – 2500 ug/mL) against *S. aureus* on plate wells (Figure 5.8). ZnO-PVP caused slight increase of attachment at lower concentrations (1 – 3% at 19.53 – 156.25 µg/mL). There was slight attachment inhibition noted at 312.5 µg/mL (4% inhibition) and 1250 µg/mL (7% inhibition), while there was a minor increase at 2500 µg/mL (16% increase).

- **Biofilm Inhibition**

Resazurin conversion was measured via fluorescence following overnight incubation of attached bacteria with each treatment. Measurements were also taken from untreated bacteria which were allowed grow unhindered under equivalent conditions. Readings of treated and untreated biofilms were compared to calculate % inhibition of biofilm development, as determined by reduced conversion of resazurin (i.e., biofilms having fewer metabolically active bacterial cells).

AgNO3

$AgNO_3$ had varying effect against *P. aeruginosa* biofilm bacteria on lid pegs (Figure 5.10). There was a notable increase in bacterial numbers at the lowest test concentrations (39% increase at 9.77 µg/mL and 15% increase at 19.53 µg/mL). The measured responses at 39.06 µg/mL and 78.13 µg/mL varied greatly but reported mean inhibition values of 4% and 31% respectively. There was effective inhibition (83 – 86%) recorded at concentrations between 156.25 – 2500 µg/mL. $AgNO_3$-PVP also held varying result, especially at lower concentrations

(9.77 – 156.25 μg/mL) which saw high variance (Figure 5.10). There was an increased response noted at concentrations of 9.77 μg/mL (4% increase), 19.53 μg/mL (13% increase), 39.06 μg/mL (21% increase) and 78.13 μg/mL (20% increase). Higher concentrations reported inhibition at 156.25 μg/mL (32% inhibition), 312.5 μg/mL (71% inhibition), 625 μg/mL (88% inhibition), 1250 μg/mL (88% inhibition) and 2500 μg/mL (83% inhibition).

$AgNO_3$ demonstrated an overall inhibitory effect against *P. aeruginosa* bacteria on plate wells (Figure 5.10). There was a minor increase (5% increase) recorded at 9.77 μg/mL, while higher concentrations caused an increasingly greater inhibitory effect. There was minor inhibition recorded at 19.53 μg/mL (3% inhibition), which increase at 39.06 μg/mL (16% inhibition), 78.13 μg/mL (34% inhibition), 156.25 μg/mL (72% inhibition), 312.5 μg/mL (79% inhibition), 625 μg/mL (75% inhibition), 1250 μg/mL (79% inhibition) and 2500 μg/mL (78% inhibition). $AgNO_3$-PVP caused inhibition at all test concentrations against *P. aeruginosa* on plate wells (Figure 5.10). There was minor inhibition at lower concentrations of 9.77 μg/mL (8% inhibition), 19.53 μg/mL (4% inhibition), 39.06 μg/mL (6% inhibition) and 78.13 μg/mL (9% inhibition). There was an increase of inhibition above this concentration, with 156.25 μg/mL (26% inhibition), 312.5 μg/mL (63% inhibition), 625 μg/mL (65% inhibition), 1250 μg/mL (66% inhibition) and 2500 μg/mL (55% inhibition).

$AgNO_3$ had little effect against *S. aureus* biofilm bacterial growth on lid pegs at lower concentrations but did exhibit effective inhibition at higher concentrations (Figure 5.10). Concentrations between 4.88 – 39.06 μg/mL had very minor effect (-4 – 1% inhibition). Higher concentrations displayed an increase of inhibition, at concentrations of 78.13 μg/mL (27% inhibition), 156.25 μg/mL (72% inhibition), 312.5 μg/mL (82%) and 625 μg/mL (82%). $AgNO_3$-PVP demonstrated comparable performance against *S. aureus* on lid pegs (Figure 5.10). Lower concentrations resulted in minor increase in response, with 3% increase at 4.88 μg/mL, 4% increase at 9.77 μg/mL, 6% increase at 19.53 μg/mL and 3% increase at 39.06 μg/mL. Higher concentrations caused increasing levels of inhibition with results showing 27% inhibition at 78.13 μg/mL, 73% inhibition at 156.25 μg/mL, 83% inhibition at 312.5 μg/mL and 86% inhibition at 625 μg/mL.

$AgNO_3$ caused minor inhibition of *S. aureus* biofilm bacterial growth on plate wells at lower concentrations but demonstrated moderate inhibition at higher concentrations (Figure 5.10). There was minor inhibition at 4.88 μg/mL (5% inhibition), 9.77 μg/mL (5% inhibition), 19.53

µg/mL (12% inhibition) and 78.13 µg/mL (6% inhibition). There was negligeable increase at 39.06 µg/mL (2% increase). There was moderately high inhibition exhibited at 156.25 µg/mL (58% inhibition), 312.5 µg/mL (68% inhibition) and 625 µg/mL (74% inhibition). $AgNO_3$-PVP effects varied against *S. aureus* biofilms on plate well, causing increased responses at lower concentrations but demonstrating effective inhibition at higher concentrations (Figure 5.10). Increased responses were recorded at concentrations of 4.88 µg/mL (13% increase), 9.77 µg/mL (17% increase), 19.53 µg/mL (4% increase), 39.06 µg/mL (6% increase) and 78.13 µg/mL (6% increase). At higher treatments, inhibition was noted to increase beside concentration, with $AgNO_3$-PVP causing inhibition at 156.25 µg/mL (57% inhibition), 312.5 µg/mL (76% inhibition) and 625 µg/mL (87% inhibition).

Nisin

Nisin held no inhibitory effect against *P. aeruginosa* on lid pegs at any concentration but was seen to cause a moderate to large increase in biofilm bacteria response (Figure 5.12). Lower concentrations did cause a low – moderate increase in response at concentrations of 0.73 µg/mL (21% increase), 1.47 µg/mL (28% increase), 2.93 µg/mL (16% increase), 5.86 µg/mL (12% increase), 11.72 µg/mL (36% increase), 23.44 µg/mL (36% increase) and 46.88 µg/mL (38% increase). There was a greater increase produced at 93.75 µg/mL (53% increase) and 187.5 µg/mL (147% increase). Nisin-PVP caused slight inhibition of biofilm development at lower concentrations of 0.73 µg/mL (8% inhibition), 1.47 µg/mL (8% inhibition), 2.93 µg/mL (7% inhibition), 5.86 µg/mL (16% inhibition), 11.72 µg/mL (13% inhibition), 23.44 µg/mL (13% inhibition) and 46.88 µg/mL (5% inhibition) (Figure 5.12). There was a slight increase produced at 93.75 µg/mL (1% increase) and 187.5 µg/mL (13% increase).

Nisin had very minor inhibitory effect against *P. aeruginosa* on plate wells and was seen to cause minor increases in biofilm development across a range of concentrations (Figure 5.12). There were increases in biofilm activity observed at lower concentrations of 0.37 µg/mL (18% increase), 0.73 µg/mL (15% increase), 1.47 µg/mL (9% increase), 2.93 µg/mL (8% increase), 5.86 µg/mL (7% increase) and 11.72 µg/mL (9% increase), and also at high concentrations of 93.75 (9% increase) and 187.5 µg/mL (13% increase). There was very minor inhibition caused at concentrations of 23.44 µg/mL (2% inhibition) and 46.88 µg/mL (2% inhibition)

Nisin caused effective inhibition of *S. aureus* biofilm development on lid pegs, which increased with treatment concentration (Figure 5.12). There was minor-moderate inhibition at lower concentrations of 0.37 μg/mL (9% inhibition), 0.73 μg/mL (5% inhibition), 1.47 μg/mL (6% inhibition), 2.93 μg/mL (11% inhibition), 5.86 μg/mL (33% inhibition), 11.72 μg/mL (19% inhibition) and 23.44 μg/mL (18% inhibition). Inhibition rose at 46.88 μg/mL (39% inhibition), 93.75 μg/mL (59% inhibition) and to a peak at 187.5 μg/mL (93% inhibition). Nisin-PVP was not effective at inhibiting *S. aureus* biofilms on lid pegs (Figure 5.12). There was little to no inhibition at low concentrations of 0.37 μg/mL (9% inhibition), 0.73 μg/mL (0% inhibition), 1.47 μg/mL (0% inhibition), 2.93 μg/mL (1% inhibition), 5.86 μg/mL (12% inhibition), 11.72 μg/mL (16% inhibition) and 23.44 μg/mL (13% inhibition), 46.88 μg/mL (21% inhibition), 93.75 μg/mL (16%). There was a minor increase in biofilm development at 187.5 μg/mL (28% increase).

Nisin caused minor inhibition of *S. aureus* biofilms on plate well at lower concentrations of 46.88 μg/mL (21% inhibition), 23.44 μg/mL (12% inhibition), 11.72 μg/mL (14% inhibition), 5.86 μg/mL (14% inhibition), 2.93 μg/mL (11% inhibition), 1.46 μg/mL (11% inhibition), 0.73 (12% inhibition) and caused moderate – high inhibition at concentrations of 93.75 μg/mL (37% inhibition) and 187.5 μg/mL (61% inhibition) (Figure 5.12). Nisin-PVP exhibited minor inhibition at concentrations of 0.73 μg/mL (12% inhibition), 1.46 μg/mL (11% inhibition), 2.93 μg/mL (8.5% inhibition), 5.86 μg/mL (9% inhibition), 11.72 μg/mL (9% inhibition), 23.44 μg/mL (10% inhibition), 46.88 μg/mL (0% inhibition) and 187.5 μg/mL (9% inhibition) (Figure 5.12). There was a slight increase in response at 93.75 μg/mL (2% increase).

Chitosan

Chitosan caused minor inhibition against *P. aeruginosa* biofilms on lid pegs at lower concentrations of 19.53 μg/mL (13% inhibition), 39.06 μg/mL (10% inhibition), 78.13 μg/mL (8% inhibition) and 156.25 μg/mL (15% inhibition) (Figure 5.14). There was minor – major increases in biofilm activity at concentrations of 312.50 μg/mL (18% increase), 625 μg/mL (33% increase), 1250 μg/mL (85% increase), 2500 μg/mL (97% increase) and 5000 μg/mL (52% increase). Chitosan-PVP had moderate inhibitory effects at concentrations of 19.53 μg/mL (40% inhibition), 39.06 μg/mL (35% inhibition), 78.13 μg/mL (29% inhibition), 156.25 μg/mL (26% inhibition) and 312.50 μg/mL (25% inhibition) (Figure 5.14). There was minor inhibition at 625 μg/mL (13% inhibition). Higher concentrations caused very minor – moderate increases

in biofilm activity, seen at concentrations of 1250 µg/mL (1% increase), 2500 µg/mL (2% increase) and 5000 µg/mL (23% increase).

Chitosan had varying effect against *P. aeruginosa* biofilm development on plate wells (Figure 5.14). There was moderate inhibition at lower concentrations of 19.53 µg/mL (20% inhibition), 39.06 µg/mL (13% inhibition) and 78.13 µg/mL (21% inhibition), with only minor inhibition at 156.25 µg/mL (8% inhibition). There were moderate increases seen at 312.5 µg/mL (23% increase) and 625 µg/mL (41% increase) which then rose causing major increases at 1250 µg/mL (99% increase) and 2500 µg/mL (145% increase). Chitosan-PVP caused increases in biofilm development, which increased with concentration (Figure 5.14). Minor increases occurred at 19.53 µg/mL (6% increase), 39.06 µg/mL (4% increase), 78.13 µg/mL (12% increase) and moderate – high increases at 156.25 µg/mL (32% increase) and 312.50 µg/mL (60% increase). Major increases were recorded at higher concentrations of 625 µg/mL (90% increase), 1250 µg/mL (148% increase) and 2500 µg/mL (177% increase).

Chitosan had mixed effects against *S. aureus* biofilm development on lid pegs (Figure 5.14). There was very minor inhibition/increases occurring at lower concentrations of 9.77 µg/mL (0% inhibition), 19.53 µg/mL (5% inhibition), 39.06 µg/mL (3% inhibition) and 78.13 µg/mL (2% increase). There was low – moderate increases observed at concentrations of 156.25 µg/mL (25% increase), 312.5 µg/mL (49% increase), 625 µg/mL (56% increase) and 1250 µg/mL (47% increase). There was moderate inhibition at 2500 µg/mL (31% inhibition). Chitosan-PVP had very minor effects against *S. aureus* biofilms on lid pegs (Figure 5.14). There was minor inhibition at lower concentrations of 9.77 µg/mL (12% inhibition), 19.53 µg/mL (5% inhibition), 39.06 µg/mL (3% inhibition) and 78.13 µg/mL (4% inhibition) and 156.25 µg/mL (2% inhibition) and also at higher concentration of 1250 µg/mL (4% inhibition). There was minor increases at other concentrations of 312.5 µg/mL (2% increase), 625 µg/mL (5% increase) and 2500 µg/mL (8% increase).

Chitosan demonstrated weak inhibition against *S. aureus* biofilms on plate wells, at all concentrations of 9.77 µg/mL (9% inhibition), 19.53 µg/mL (12% inhibition), 39.06 µg/mL (9% inhibition), 78.13 µg/mL (10% inhibition), 156.25 µg/mL (15% inhibition), 312.5 µg/mL (14% inhibition), 625 µg/mL (21% inhibition), 1250 µg/mL (11% inhibition) and 2500 µg/mL (5% inhibition) (Figure 5.14). Chitosan-PVP exhibited weak inhibitory activity at lower concentrations of 9.77 µg/mL (9% inhibition), 19.53 µg/mL (9% inhibition), 39.06 µg/mL (14%

inhibition), 78.13 µg/mL (9% inhibition), 156.25 µg/mL (7% inhibition), 312.5 µg/mL (11% inhibition), 625 µg/mL (6% inhibition) and 1250 µg/mL (7% inhibition), but caused a minor increase at the highest concentration of 2500 µg/mL (12% increase) (Figure 5.14).

ZnO

ZnO exhibited no biofilm inhibitory effect versus *P. aeruginosa* on lid pegs, causing moderate increases in biofilm formations at all test concentrations of 19.53 µg/mL (27% increase), 39.06 µg/mL (56% increase), 78.13 µg/mL (51% increase), 156.25 µg/mL (48% increase), 312.5 µg/mL (40% increase), 625 µg/mL (58% increase), 1250 µg/mL (59% increase), 2500 µg/mL (52% increase) and 5000 µg/mL (40% increase) (Figure 5.16). ZnO-PVP demonstrated mixed effects against *P. aeruginosa* biofilms growing on lid pegs, with minor inhibition at concentrations of 78.13 µg/mL (10% inhibition), 312.5 µg/mL (5% inhibition) and 5000 µg/mL (3% inhibition). There were low – moderate increases in biofilm formations seen at other test concentrations of 19.53 µg/mL (8% increase), 39.06 µg/mL (10% increase), 156.25 µg/mL (6% increase), 625 µg/mL (12% increase), 1250 µg/mL (23% increase) and 2500 µg/mL (12% increase) (Figure 5.16).

Similar effects were observed against *P. aeruginosa* biofilms growing on plate wells, with low increases seen at test concentrations of 19.53 µg/mL (11% increase), 39.06 µg/mL (28% increase), 78.13 µg/mL (6% increase), 156.25 µg/mL (13% increase), 312.5 µg/mL (28% increase), however inhibition was noted to rise at concentrations of 625 µg/mL (61% increase), 1250 µg/mL (40% increase), 2500 µg/mL (108% increase) and 5000 µg/mL (132% increase) (Figure 5.16). ZnO-PVP demonstrated varied effects, with minor inhibitions observed at lower concentrations of 19.53 µg/mL (7% inhibition), 39.06 µg/mL (10% increase) and 78.13 µg/mL (8% increase), and moderate increases in biofilm growth observed sat all other test concentrations of 156.25 µg/mL (21% increase), 312.5 µg/mL (38% increase), 625 µg/mL (59% increase), 1250 µg/mL (40% increase), 2500 µg/mL (35% increase) and 5000 µg/mL (45% increase) (Figure 5.16).

There was low – moderate increases in *S. aureus* biofilm growth noted on lid pegs, following treatment with ZnO at concentrations of 9.77 µg/mL (32% increase), 19.53 µg/mL (18% increase), 39.06 µg/mL (31% increase), 78.13 µg/mL (20% increase), 156.25 µg/mL (30%

increase), 312.5 µg/mL (46% increase) and 625 µg/mL (12% increase). Higher concentrations were noted to exhibit inhibition, at concentrations of 1250 µg/mL (17% inhibition) and 2500 µg/mL (42% inhibition). ZnO-PVP exhibited slight biofilm growth increases at lower concentrations against *S. aureus* biofilms on lid pegs, with increases noted at 9.77 µg/mL (5% increase), 19.53 µg/mL (8% increase) and 39.06 µg/mL (8% increase) (Figure 5.16). Inhibition was noted at higher test concentrations of 78.13 µg/mL (6% inhibition), 156.25 µg/mL (5% inhibition), 312.5 µg/mL (7% inhibition) 625 µg/mL (33% inhibition), 1250 µg/mL (55% inhibition) and 2500 µg/mL (77% inhibition) (Figure 5.16).

ZnO exhibited varied effects against *S. aureus* biofilm growth on plate wells, with minor increases at concentrations of 9.77 µg/mL (4% increase), 19.53 µg/mL (5% increase), 39.06 µg/mL (6% increase), 78.13 µg/mL (8% increase), 625 µg/mL (8% increase) and 1250 µg/mL (5% increase), and minor inhibition in biofilm growth at concentrations of 156.25 µg/mL (10% inhibition), 312.5 µg/mL (3% inhibition) and 2500 µg/mL (12% inhibition)(Figure 5.16).

ZnO-PVP held very comparable trends against *S. aureus* biofilm growth on plate wells, with minor increases at concentrations of 9.77 µg/mL (15% increase), 19.53 µg/mL (5% increase), 39.06 µg/mL (6% increase), 78.13 µg/mL (8% increase), 625 µg/mL (8% increase) and 1250 µg/mL (5% increase), and minor inhibition of biofilm growth at concentrations of 156.25 µg/mL (2% inhibition), 312.5 µg/mL (18% inhibition) and 2500 µg/mL (15% inhibition)(Figure 5.16).

- **Biofilm Reduction**

AgNO3

There was clear reduction caused by $AgNO_3$ against *P. aeruginosa* biofilms on lid pegs, with reduction being noted at 19.53 µg/mL (2% reduction) and rapidly increasing with concentrations of 39.06 µg/mL (17% reduction), 78.13 µg/mL (94% reduction), 156.25 µg/mL (97% reduction), 312.5 µg/mL (97% reduction), 625 µg/mL (98% reduction), 1250 µg/mL (98% reduction) and 2500 µg/mL (98% reduction) (Figure 5.18). $AgNO_3$-PVP demonstrated similar reduction abilities, with reductions at 78.13 µg/mL (32% reduction), 156.25 µg/mL (67% reduction), 312.5 µg/mL (92% reduction), 625 µg/mL (92% reduction), 1250 µg/mL (94%

reduction) and 2500 μg/mL (92% reduction), however there was noted increases in biofilm formation at lower concentrations of 9.77 μg/mL (20% increase), 19.53 μg/mL (11% increase) and 39.06 μg/mL (2% increase) (Figure 5.18).

$AgNO_3$ was also very effective at reducing *P. aeruginosa* biofilms grown on plate wells, with reductions seen at all test concentrations of 9.77 μg/mL (14% reduction), 19.53 μg/mL (25% reduction), 39.06 μg/mL (16% reduction), 78.13 μg/mL (72% reduction), 156.25 μg/mL (80% reduction), 312.5 μg/mL (79% reduction), 625 μg/mL (80% reduction), 1250 μg/mL (80% reduction) and 2500 μg/mL (79% reduction) (Figure 5.18). $AgNO_3$-PVP was noted more effective at lower concentrations against *P. aeruginosa* biofilms on plate wells, with reductions at 39.06 μg/mL (30% reduction), 78.13 μg/mL (51% reduction), 156.25 μg/mL (62% reduction), 312.5 μg/mL (81% reduction), 625 μg/mL (80% reduction), 1250 μg/mL (81% reduction) and 2500 μg/mL (77% reduction), while there was a minor increase in biofilm formations noted at 9.77 μg/mL (15% increase) (Figure 5.18).

$AgNO_3$ exhibited notable reduction against *S. aureus* biofilms on lid pegs, which was seen to correspond with higher concentrations of treatment (Figure 5.18). While the lowest test concentration exhibited minimal effects (4% increase at 9.77 μg/mL), reduction was seen as concentrations rose from 19.53 μg/mL (6% reduction) to 39.06 μg/mL (30% reduction), 78.13 μg/mL (78% reduction), 156.25 μg/mL (93% reduction), 312.5 μg/mL (95% reduction), 625 μg/mL (96% reduction) and 1250 μg/mL (98% reduction). $AgNO_3$-PVP also demonstrated effective reductions, but only at higher concentrations of 78.13 μg/mL (41% reduction), 156.25 μg/mL (90% reduction), 312.5 μg/mL (97% reduction), 625 μg/mL (98% reduction) and 1250 μg/mL (96% reduction) (Figure 5.18). Lower treatments were noted to cause increases in biofilm formations, at concentrations of 9.77 μg/mL (41% increase), 19.53 μg/mL (62% increase) to 39.06 μg/mL (31% increase).

Results against *S. aureus* biofilms on plate wells presented similar efficacy of $AgNO_3$ in reducing biofilm formations in moderate – high concentrations (Figure 5.18). Minor increases in biofilm formations were reported at lower concentrations of 9.77 μg/mL (17% increase), 19.53 μg/mL (13% increase) to 39.06 μg/mL (12% increase), but moderate – high reductions were then reported at concentrations above 78.13 μg/mL (77% reduction), 156.25 μg/mL (92% reduction), 312.5 μg/mL (93% reduction), 625 μg/mL (92% reduction) and 1250 μg/mL (96% reduction). $AgNO_3$-PVP demonstrated similar efficacy against *S. aureus* biofilms on plate

wells, with no reduction or increases at lower concentration of 9.77 μg/mL (9% reduction), 19.53 μg/mL (23% increase) to 39.06 μg/mL (0%), and increasing reduction at higher concentrations of 78.13 μg/mL (58% reduction), 156.25 μg/mL (91% reduction), 312.5 μg/mL (93% reduction), 625 μg/mL (94% reduction) and 1250 μg/mL (95% reduction) (Figure 5.18).

Nisin

Nisin exhibited no reduction against *P. aeruginosa* biofilms on lid pegs, and was recorded to cause an increase in biofilm formations at all test concentrations of 0.73 μg/mL (22% increase), 1.46 μg/mL (20% increase), 2.93 μg/mL (21% increase), 5.86 μg/mL (30% increase), 11.72 μg/mL (17% increase), 23.44 μg/mL (4% increase), 46.88 μg/mL (16% increase), 93.75 μg/mL (29% increase), 187.5 μg/mL (16% increase) (Figure 5.20). Nisin-PVP exhibited no reduction against *P. aeruginosa* on lid pegs, but was observed to cause moderate – high increases in biofilm formations at concentrations of 0.73 μg/mL (44% increase), 1.46 μg/mL (53% increase), 2.93 μg/mL (48% increase), 5.86 μg/mL (47% increase), 11.72 μg/mL (47% increase), 23.44 μg/mL (71% increase), 46.88 μg/mL (97% increase), 93.75 μg/mL (73% increase), 187.5 μg/mL (84% increase) (Figure 5.20).

There was similar efficacy of nisin against *P. aeruginosa* biofilms formed on plate wells, with mean increases in biofilm formations at 0.73 μg/mL (17% increase), 1.46 μg/mL (22% increase), 2.93 μg/mL (26% increase), 5.86 μg/mL (13% increase), 11.72 μg/mL (30% increase), 23.44 μg/mL (6% increase), 46.88 μg/mL (0%), 93.75 μg/mL (4% increase), however there was a minor reduction observed at 187.5 μg/mL (3% reduction) (Figure 5.20). Nisin-PVP displayed similar efficacy at 0.73 μg/mL (30% increase), 1.46 μg/mL (25% increase), 2.93 μg/mL (21% increase), 5.86 μg/mL (21% increase), 11.72 μg/mL (16% increase), 23.44 μg/mL (14% increase), 46.88 μg/mL (10% increase), 93.75 μg/mL (9% increase), 187.5 μg/mL (10% increase) (Figure 5.20).

Nisin demonstrated very effective reduction against *S. aureus* biofilms formed on lid pegs, with reduction values rising steadily with concentrations 0.73 μg/mL (15% reduction), 1.46 μg/mL (12% reduction), 2.93 μg/mL (17% reduction), 5.86 μg/mL (21% reduction), 11.72 μg/mL (37% reduction), 23.44 μg/mL (48% reduction), 46.88 μg/mL (56% reduction), 93.75 μg/mL (64% reduction), 187.5 μg/mL (80% reduction) and 375 μg/mL (87% reduction) (Figure 5.20). Nisin-PVP did not report comparable results, with moderate – low increases in biofilm formations noted at 0.73 μg/mL (26% increase), 1.46 μg/mL (25% increase), 2.93 μg/mL (29%

increase), 5.86 µg/mL (11% increase), 11.72 µg/mL (22% increase), 23.44 µg/mL (19% increase) and 46.88 µg/mL (5% increase), however there were minor reductions at 93.75 µg/mL (2% reduction), 187.5 µg/mL (7% reduction) and 375 µg/mL (4% reduction) (Figure 5.20).

Nisin held similar efficacy against *S. aureus* biofilms formed on plate wells, with steadily increasing reductions at concentrations of 0.73 µg/mL (3% reduction), 1.46 µg/mL (7% reduction), 2.93 µg/mL (9% reduction), 5.86 µg/mL (32% reduction), 11.72 µg/mL (22% reduction), 23.44 µg/mL (29% reduction), 46.88 µg/mL (56% reduction), 93.75 µg/mL (81% reduction) and 187.5 µg/mL (90% reduction) (Figure 5.20). Nisin-PVP did not exhibit as effective reduction of biofilms, but had consistent reduction across the treatment range at concentrations of 0.73 µg/mL (10% reduction), 1.46 µg/mL (6% reduction), 2.93 µg/mL (13% reduction), 5.86 µg/mL (11% reduction), 11.72 µg/mL (12% reduction), 23.44 µg/mL (12% reduction), 46.88 µg/mL (20% reduction), 93.75 µg/mL (26% reduction) and 187.5 µg/mL (39% reduction) (Figure 5.20).

Chitosan

Chitosan exhibited varying effects against *P. aeruginosa* biofilms on lid pegs, causing minor reductions in viable cell counts at lower concentrations of 19.53 µg/mL (23% reduction), 39.06 µg/mL (14% reduction) and 78.13 µg/mL (14% reduction) (Figure 5.22). There were no noteworthy effects at test concentrations of 156.25 µg/mL (2% reduction), 312.5 µg/mL (3% increase), 625 µg/mL (6% increase) or 2500 µg/mL (5% increase). There was a minor increase in response at 1250 µg/mL (14% increase). There was high variance noted at 5000 µg/mL (±55) but reported a mean response of 6% reduction. Chitosan-PVP reported varied results against *P. aeruginosa* biofilm bacteria on lid pegs, with minor reductions at 19.53 µg/mL (6% reduction) and 39.06 µg/mL (2% reduction) and causing slight increases at higher concentrations of 78.13 µg/mL (7% increase), 156.25 µg/mL (14% increase), 312.5 µg/mL (12% increase), 625 µg/mL (15% increase), 1250 µg/mL (12% increase) (Figure 5.22). There were moderate reductions reported at 2500 µg/mL (24% reduction) and 5000 µg/mL (54% reduction).

Chitosan exhibited minor reductions in biofilm cell counts against *P. aeruginosa* on plate wells at low concentrations of 39.06 µg/mL (16% reduction), 78.13 µg/mL (7% reduction) and 156.25 µg/mL (14% reduction) (Figure 5.22). Higher concentrations of chitosan were observed to cause an increase in biofilm cell counts which increased with concentration, from 312.5 µg/mL (16% increase) to 625 µg/mL (42% increase), 1250 µg/mL (43% increase), 2500 µg/mL (54% increase) and 5000 µg/mL (69% increase). Chitosan-PVP held varying effect against *P. aeruginosa* biofilm bacteria on plate wells, with minor – moderate increases noted at 39.06 µg/mL (5% increase), 78.13 µg/mL (15% increase), 156.25 µg/mL (21% increase), 312.5 µg/mL (17% increase), 625 µg/mL (23% increase) and 1250 µg/mL (5% increase), with moderate reductions observed at higher concentrations of 2500 µg/mL (15% reduction) and 5000 µg/mL (38% reduction) (Figure 5.22).

Chitosan caused low – moderate reductions in *S. aureus* biofilm cell counts formed on lid pegs at all test concentrations of 19.53 µg/mL (16% reduction), 39.06 µg/mL (17% reduction), 78.13 µg/mL (18% reduction), 156.25 µg/mL (36% reduction), 312.5 µg/mL (38% reduction), 625 µg/mL (36% reduction), 1250 µg/mL (20% reduction), 2500 µg/mL (42% reduction) and 5000 µg/mL (49% reduction) (Figure 5.22). Chitosan-PVP held varying effect, causing minor – moderate increases in biofilm viability at 19.53 µg/mL (11% increase), 39.06 µg/mL (11% increase), 78.13 µg/mL (32% increase), 156.25 µg/mL (21% increase), 312.5 µg/mL (21% increase), 625 µg/mL (27% increase) and 1250 µg/mL (21% increase) (Figure 2.23C). There was moderate – high reductions also noted at high concentrations of 2500 µg/mL (43% reduction) and 5000 µg/mL (36% reduction).

Chitosan caused low reductions against *S. aureus* biofilms on plate wells at concentrations of 19.53 µg/mL (4% reduction), 39.06 µg/mL (19% reduction), 78.13 µg/mL (22% reduction), 156.25 µg/mL (21% reduction), 312.5 µg/mL (15% reduction) and 625 µg/mL (14% reduction) (Figure 5.22). There was no noteworthy effect produced at 1250 µg/mL (1% increase) and a minor increase at 2500 µg/mL (11% increase). At higher concentrations, there was moderate reduction observed at 5000 µg/mL (32% reduction) and high reduction at 10000 µg/mL (71% reduction). Chitosan-PVP exhibited reductions at all test concentrations against *S. aureus* biofilms on plate wells (Figure 5.22). There were low – moderate reductions observed at concentrations of 19.53 µg/mL (10% reduction), 39.06 µg/mL (19% reduction), 78.13 µg/mL (17% reduction), 156.25 µg/mL (23% reduction), 312.5 µg/mL (27% reduction), 625 µg/mL

(27% reduction), 1250 µg/mL (18% reduction) and 2500 µg/mL (8% reduction) (Figure 5.22). Greater reductions were noted at 5000 µg/mL (35% reduction) and 10000 µg/mL (51% reduction).

ZnO

ZnO exhibited only minor reduction against *P. aeruginosa* biofilms on lid pegs at lower concentrations of 19.53 µg/mL (7% reduction), 39.06 µg/mL (15% reduction), 78.13 µg/mL (1% reduction) (Figure 5.24). There were varying degrees of biofilm cell propagation noted at concentrations of 156.25 µg/mL (17% increase), 312.5 µg/mL (17% increase), 625 µg/mL (6% increase), 1250 µg/mL (9% increase), 2500 µg/mL (4% increase) and 5000 µg/mL (34% increase). ZnO-PVP caused minor reductions at 39.06 µg/mL (16% reduction), 78.13 µg/mL (9% reduction) and 5000 µg/mL (3% reduction) (Figure 5.24). There were moderate increases of biofilm cell counts at 19.53 µg/mL (22% increase), 156.25 µg/mL (16% increase), 312.50 µg/mL (13% increase), 625.00 µg/mL (26% increase), 1250.00 µg/mL (21% increase) and 2500 µg/mL (31% increase).

ZnO exhibited low – moderate reductions in *P. aeruginosa* biofilm bacterial on plate wells at lower concentrations of 19.53 µg/mL (23% reduction), 39.06 µg/mL (17% reduction), 78.13 µg/mL (9% reduction) and 156.25 µg/mL (6% reduction) (Figure 5.24). There were low – high increases of *P. aeruginosa* biofilm cell counts observed at higher concentrations, which was noted to increase with concentration from 312.50 µg/mL (18% increase), 625.00 µg/mL (32% increase), 1250 µg/mL (35% increase), 2500 µg/mL (54% increase) and 5000 µg/mL (66% increase) (Figure 5.24). ZnO-PVP demonstrated mixed effects against *P. aeruginosa* biofilms on plate wells, with minor reductions at the lowest test concentration of 19.53 µg/mL (4% reduction) and at concentrations of 312.50 µg/mL (9% reduction), 625.00 µg/mL (7% reduction) and 1250.00 µg/mL (1% reduction) (Figure 5.24). There were low – moderate increases observed at lower concentrations of 39.06 µg/mL (3% increase), 78.13 µg/mL (6% increase), 156.25 µg/mL (15% increase), 2500 µg/mL (12% increase) and 5000 µg/mL (34% increase) (Figure 5.24).

ZnO exhibited very effective reductions of *S. aureus* biofilm on lid pegs bacteria which increased with concentration (Figure 5.24). Reductions were seen at all test concentrations

of 19.53 µg/mL (15% reduction), 39.06 µg/mL (29% reduction), 78.13 µg/mL (42% reduction), 156.25 µg/mL (64% reduction), 312.5 µg/mL (74% reduction), 625 µg/mL (79% reduction), 1250 µg/mL (86% reduction) 2500 µg/mL (91% reduction) and 5000 µg/mL (96% reduction). ZnO-PVP also exhibited effective reductions, but only at test concentrations of 312.5 µg/mL (49% reduction), 625 µg/mL (71% reduction), 1250 µg/mL (86% reduction), 2500 µg/mL (93% reduction) and 5000 µg/mL (94% reduction), while there was moderate – high increases in biofilm bacterial activity at lower concentration of 19.53 µg/mL (40% increase), 39.06 µg/mL (58% increase), 78.13 µg/mL (66% increase). There was no noteworthy effect at 156.25 µg/mL.

ZnO had varying effects against *S. aureus* biofilms on plate wells, with minor increases in activity observed at concentrations of 19.53 µg/mL (15% increase), 39.06 µg/mL (20% increase), 78.13 µg/mL (4% increase), 156.25 µg/mL (22% increase), 312.5 µg/mL (25% increase), 625 µg/mL (30% increase) and 1250 µg/mL (6% increase) and moderate – high reductions seen at concentrations of 2500 µg/mL (33% reduction), 5000 µg/mL (55% reduction) and 10000 µg/mL (67% reduction) (Figure 5.24).

5.4 Discussion

In this study, four chosen bioactives were assessed for their anti-biofilm abilities, by determining their individual effects against physical biofilm formations and also against the internal bacterial population of two major biofilm producing bacterial pathogens, *S. aureus* and *P. aeruginosa*. The test methods utilised were adapted and developed from previous studies, in an attempt to establish a reproducible and overarching assessment, that could be standardised and carried forward in future anti-biofilm studies.

5.4.1 Comparison of biofilm growth and development on lid pegs and plate well walls

The present study is, to best knowledge, the first biofilm study which offers comparisons between the use of lid pegs and microplate well walls as attachment and subsequent growth sites for bacterial biofilms. As there were no clear advantages or disadvantages remarked upon to the use of either material in previous studies, both were utilised in the present study in order to compare the two mediums and differentiate biofilm growth patterns. Both the lid pegs and plate well walls were pre-treated, inoculated, and incubated under identical

conditions. Initial preliminary studies of optimal growth patterns for both plate well walls and lid pegs were carried out in order to determine the optimal concentrations of blood plasma for use as surface coatings to promote bacterial attachment, as well as studies to determine the optimal attachment times. It was reported that a plasma concentration of 1% was the lowest concentration to provide the most consistent and adequate improvements to bacterial attachment on both surfaces, resulting in improved biofilm formations. Furthermore, a 1-hour attachment period was also chosen as the most satisfactory time, as longer attachment times did not yield greater results and as such, was deemed unnecessary.

It was determined through the use of CV staining and resazurin reductions, that there is a definite correlation between biofilm growth and the chosen growth surface, which is also dependent on the chosen bacterial strain. Final CV staining revealed *S. aureus* to produce much greater biofilm formations on plate well walls, across all test points and test plates (24 test plates), with differences of up to 188%. Resazurin reduction studies have also shown a prevailing preference towards plate well walls, with greater internal biofilm populations being noted in the majority of test plates (17/24 plates). Results from *P. aeruginosa* were quite varied and did not report a certain preference of growth surface. *P. aeruginosa* CV straining reported greater biofilm formations in 11/18 test plates, with growth differences of up to 68%. Conversely, resazurin reductions reported greater biofilm populations in those grown on peg lids (13/18 test plates).

5.4.2 Development of standardised biofilm testing and the Minimum Attachment Inhibition Concentration (MAIC)

The development of a standardised method for biofilm assessment has proven a difficult endeavour, primarily due to the nature of bacterial biofilm development which can vary and alter greatly. Presently, the methods and procedures developed and reported offer a number of key steps in order to produce consistent biofilm formations, with reportable and reproducible results. The inclusion of an attachment inhibition assessment was also a key step in the development of a future, standardised approach, as the prevention of bacterial attachment to surfaces should be treated as equally important in anti-biofilm studies as the inhibition and eradication of biofilm formations. While the use of CV staining and resazurin have been utilised in separate studies, the present study demonstrates the ability to successfully incorporate both methods of analysis into a single experiment, allowing for great

data yield which can report upon different aspects of biofilm behaviour. Furthermore, while previous resazurin studies used comparisons to plate counts, the present methods allow for a more accurate representation of actual biofilm bacterial counts, while also needing less materials and resources to finalise (Rosa et al. 2019, 2017; Pantanella et al. 2008).

A noted drawback in the use of resazurin reduction analysis is the differing reduction rates between bacterial species. It was noted that *S. aureus* converted resazurin at a much higher rate than *P. aeruginosa*, which restricts the establishment of a standardised analysis protocol. Readings for analysis were taken from *S. aureus* at the 2-hour time points, and at the 4-hour time points for *P. aeruginosa*. The timepoints for *S. aureus* chosen as beyond 2 hours, the reduced resazurin signal was noted to drop. This is presumably due to the samples reaching the maximal conversion point, after which the converted resazurin was breaking down faster than new conversions were occurring. This is also possible due to the fact of acidic by products from *S. aureus* metabolism, which is known to cause further breakdown of reduced resazurin (Rampersad 2012; Driessche et al. 2014; Sandberg et al. 2009). The timepoints for *P. aeruginosa* were chosen because, due to its slow conversion rate, it was necessary to allow sufficient time for a response to produce from all test wells, while also not extending the time to unnecessary periods and thus increasing workload and necessary resources. While these extra steps cause additional work, they can be alleviated by inclusion of an additional pre-step in order to determine the most appropriate time point from which to take measurements for each individual bacterial species. While this particular step was not performed in this particular study, through hourly measurements as standard, it was possible to identify the most suitable timepoint after the fact and use the results from those times. While this did cause longer run times overall and thus, greater use of resources, produced results were still satisfactory.

5.4.3 Antibiofilm capabilities of chosen bioactives

Through use of the methods and procedures described here, the total anti-biofilm capabilities of each individual bioactive, before and after polymer incorporation, were assessed against *S. aureus* and *P. aeruginosa*. The extended analysis included presently has given a greater insight into the activity of the chosen bioactives, and also into the bacterial and biofilm responses to each. Here, the bioactives will be discussed individually against *P. aeruginosa*

and *S. aureus* in terms of their attachment inhibition, biofilm inhibition and biofilm reduction. A overall, final summary of results is presented in Tables 5.1 and 5.2.

$AgNO_3$ versus *P. aeruginosa*

$AgNO_3$ reported highly effective attachment inhibition against *P. aeruginosa* at concentrations above 312.5 µg/mL. Resazurin analysis reported attachment inhibition of approximately 75% on lid pegs and plate well walls, while crystal violet analysis reported inhibition of 75% on plate well walls and 100% on lid pegs. Concentrations lower than 312.5 µg/mL reported reduced attachment on plate well walls, however slight increases in attachment (up to approximately 45%) were observed on lid pegs. $AgNO_3$-PVP exhibited differing results overall, with CV results showing highly effective inhibition of attachment on plate well walls while resazurin results indicate large increases in bacterial activity. These results indicate that $AgNO_3$-PVP pre-treatment caused reduced physical biofilm formations with a number concentration of internal bacterial numbers. Similar results were observed against *P. aeruginosa* on lid pegs, with slight – moderate reduction in physical biofilm formations, as per CV staining, with increased internal cellular response note by increased resazurin reductions.

Results also show highly effective inhibition of biofilm formations against *P. aeruginosa* on both lid pegs and plate well walls. Physical biofilm inhibition of up to 100% was noted at concentrations above 156.25 µg/mL, while lower concentrations reported no major effects against biofilm formations on plate wells and was even noted to cause increased biofilm formations on lid pegs (up to 50%). Other studies have reported *P. aeruginosa* biofilm inhibition at concentrations between 5 – 41.8 µg/mL (Pormohammad, Greening, and Turner 2022). Resazurin analysis also indicated similar inhibition at concentrations above 156.25 µg/mL, with reduced cell numbers of up to 80% in biofilms grown on lid pegs and well walls while also indicating increases at lower concentrations in biofilms on lid pegs. $AgNO_3$-PVP reported very comparable results from CV staining and resazurin reductions on both lid pegs and plate well walls.

$AgNO_3$ was not overly effective against *P. aeruginosa* biofilms grown on lid pegs, with CV staining indicating full reductions only at the highest test concentration 1250 µg/mL while other studies have reported much lower concentrations of 5 – 84 µg/mL causing complete reduction of *P. aeruginosa* biofilms (Pormohammad, Greening, and Turner 2022). Reductions

were seen to drop with the treatment concentration, with lower concentrations (39.06 – 156.25 µg/mL) observed to cause increases in biofilm formations. $AgNO_3$-PVP was, however, quite effective at eliminating *P. aeruginosa* biofilms on lid pegs, with reductions of approx. 90% at concentrations above 156.25 µg/mL. Resazurin analysis demonstrated a much different effect, with complete reductions of bacterial biofilm numbers resulting from treatments of $AgNO_3$ above 78.13 µg/mL. $AgNO_3$-PVP too was shown to have great effect against biofilm bacterial numbers at concentrations above 156.25 µg/mL. The increase in physical biofilm formations may have been a defensive reaction produced by the biofilms in response to the initial treatment by $AgNO_3$, which eventual had enough expose time to eliminate internal bacterial cells. Such an occurrence may indicate that while biofilms are able to identify the treatment, they fail completely at neutralising or removing the compound from its internal structure before it can have effect. Against *P. aeruginosa* biofilms grown on plate wells, $AgNO_3$ and $AgNO_3$-PVP demonstrated very effective reductions at concentrations above 78.13 µg/mL, as shown by both CV and resazurin analysis. At lower test concentrations, resazurin revealed a linear response to $AgNO_3$-PVP which saw bacterial numbers increasing at the lowest test concentration of 9.77 µg/mL. However, CV staining showed a plateau of 25% physical biofilm reductions at lower concentrations. This could indicate the mechanism of $AgNO_3$ can cause physical biofilm disruptions even at low level treatments. Such an occurrence could hold great benefit in co-treatment applications.

$AgNO_3$ versus *S. aureus*

$AgNO_3$ and $AgNO_3$-PVP did not hold effective inhibition against *S. aureus* attachment on lid pegs or plate well walls. There were reduced biofilm formations reported on lid pegs pre-treated with $AgNO_3$ at all concentrations, however internal biofilm populations were only reported to have reduced numbers at the higher test concentrations, which suggests positive effect against biofilm formations but only minor effects against the bacterial cells. $AgNO_3$-PVP caused similar reductions at lower concentrations but was noted to result in greater biofilm formations and higher concentrations and much greater biofilm populations on lid pegs. This increase of internal cell numbers is notably significant to the concentration of pre-treatment, as higher concentrations resulted in greater numbers, a contradictive observation to the effect of $AgNO_3$ alone which suggests a supportive influence of the polymer carrier upon cell health and replication within the biofilm. While $AgNO_3$ and $AgNO_3$-PVP pre-treatments results

in much larger biofilm formations on plate well walls, relative to treatment concentration, internal biofilm cell numbers were somewhat unaffected.

$AgNO_3$ exhibited notable inhibitory effect against *S. aureus* biofilm growth on lid pegs but showed limited effect against biofilm growth on plate well walls, with lower test concentrations even promoting biofilm growth. While this is not an ideal response, other studies have noted that silver requires extended exposure in order to exhibit full inhibitory effect (Namasivayam et al. 2012). While reductions of physical biofilm formations on lid pegs were noted at all test concentrations, internal biofilm populations were only affected at concentrations above 78.13 µg/mL. Similarly on plate well walls, while there were significant changes observed on physical biofilm formations, internal bacterial populations were only affected at concentrations above 156.25 µg/mL. While this observation holds insight into a greater effect of $AgNO_3$ versus bacterial cells rather than biofilm formations, it also shows an interesting relationship between the size of biofilm formations and their internal population.

$AgNO_3$-PVP also produced interesting results, with concentrations below 78.13 µg/mL causing huge increases of biofilm growth on lid pegs (up to 600%) while there was no reported change of internal bacterial numbers. While similar occurrence was observed with $AgNO_3$ on plate well walls to a lesser extent, the unchanged bacterial populations suggest a mechanism wherein the physical biofilm formations can gather or collect a greater extent of materials for use in growth. Furthermore, this mechanism seems to occur independently of bacterial numbers, where large constructs can house a nominal number of cells.

Biofilm reduction studies also support the impression that $AgNO_3$ has a much greater effect against internal bacterial cells than the physical biofilm layers. While CV staining reports effective reduction of up to 75% on both lid pegs and plate well walls, resazurin studies reported reductions in cell numbers of up to 100%. It should also be mentioned, that $AgNO_3$ reported the highest reductions of physical biofilms throughout this study, which suggests that while the treatment was unable to completely eradicate 100% of the biofilm, it stands to reason that there would be some remnants or surface materials that could still bind CV and produce a response. In such cases, it may be more appropriate to pay emphasis on resazurin results. There was an interesting occurrence noted, where lower treatment concentrations of $AgNO_3$-PVP caused an increase of internal population numbers in biofilms grown on lid pegs. Similar incident was noted in lower concentrations of $AgNO_3$ against biofilms grown on plate

well walls, however the CV staining of both growth surfaces reported reductions in biofilm formations at these points. These events might suggest a relationship between resources used for biofilm formation and cell reproduction, where a loss of biofilm structure may leave additional resources for cell replication.

Nisin versus *P. aeruginosa*

As mentioned in previous chapters, nisin's mechanism of action involves binding of the intramembrane bound molecule lipid-II, which is only possible against Gram positive bacteria which lack an outer membrane (Wiedemann et al. 2001). However, effects against Gram negative biofilm forming bacteria are not well documented, nor are effects against the physical biofilm formations. Results of the present study have shown nisin to hold a slight inhibitory effect upon *P. aeruginosa* bacterial attachment on both lid pegs and plate well walls. While the nisin-PVP held varying effects against attachment on lid pegs (with higher concentrations causing increased attachment) there was consistent inhibition on plate well walls. Such results suggest nisin holding some inhibitory effect upon cell attachment. However, while these observations hold some promise for initial reductions, resazurin analysis has reported different outcomes whereby there were slight to moderate increases in biofilm populations, particularly in plate wells pre-treated with nisin-PVP.

Against growing biofilms, nisin appeared to elicit greater physical formations as well as larger internal populations of *P. aeruginosa* on peg lid. This increase in growth was proportional to the concentration of nisin treatment and would indicate a form of defensive response from *P. aeruginosa*. Other studies have reported effective reductions of *P. aeruginosa* biofilms from treatment with nisin, however such studies used different strains of *P. aeruginosa* and also held longer exposure times (Ghapanvari et al. 2022) Physical formation on peg lids also increased in response to nisin-PVP, however internal populations were relatively unaffected. A similar increase in both physical biofilm and internal biofilm populations was also observed with *P. aeruginosa* biofilm growth on plate well walls, however the response was triggered by nisin-PVP treatments. It was also noted that while the increase in biofilm activity was generally higher at all test concentrations, the peak increase was not as high as that observed from nisin treatments against lid pegs. Unexpectedly, nisin did cause slight reduction in biofilm formations on plate well walls at lower concentrations, but this effect was not reflected by internal biofilm populations. Furthermore, similar to lid peg studies, a large

increase in biofilm formations was noted at the highest concentration of nisin, however not to the same extent.

Effects against established *P. aeruginosa* biofilm formations varied greatly for both nisin and nisin-PVP on lid pegs and plate well walls, with some test treatments causing slight reductions and other treatments causing slight – moderate increases. The resazurin analysis of biofilm populations gave more consistent results, with nisin and nisin-PVP causing increases of biofilm populations on both lid pegs and well walls at all concentrations. The largest increases were noted on lid pegs under treatment by nisin-PVP, which caused increases of up to ~95%.

Nisin versus *S. aureus*

Nisin demonstrated promising effects against *S. aureus* attachment on lid pegs, with moderate to high reductions in biofilm formations observed after pre-treatment with nisin, which increased with treatment concentrations. These reduced biofilm formations were also mirrored with reduced internal biofilm populations, revealing strong effect against biofilm forming *S. aureus*. Nisin-PVP did show some moderate reductions in biofilm formations, however it was noted to cause increases at the highest test concentration. Furthermore, resazurin analysis show little inhibitory effect upon internal populations, with highest concentration also causing increases. These results indicate a loss of activity from nisin following polymer incorporation, which also lead to increased biofilm formations at higher concentrations which may suggest that the polymer element may promote attachment. CV results from plate well wall analysis were very inconsistent, with no clear trend from either nisin or nisin-PVP. However there was a noted reduction in biofilm formation at the highest test concentration which matched the effects on lid pegs. There are clearer results from resazurin analysis which show no noteworthy impact upon internal biofilm populations following well wall surface pre-treatment with nisin-PVP. Nisin had a notable influence at the higher test range, with reductions of up to 75%, however lower concentrations did not hold much effect.

Both nisin and nisin-PVP demonstrated great interruption in biofilm development on peg lids but did not hold similar efficacy against biofilm growth on well walls which reported very inconsistent results. These effects against physical biofilm formations did not parallel those observed against the internal biofilm populations, however the reported internal population reductions were comparable between plate well walls and lid pegs. Previous studies have

reported that sub-MIC levels of nisin was seen to upregulate expression of genes associated with bacterial adhesion and polymer matrix production (Shivaee et al. 2021). While nisin reported moderate to high reductions at the higher test concentrations, nisin-PVP did not report any such results. This again indicates a change or loss of activity from nisin following extrusion.

Nisin appeared to have its highest effect against established biofilms, causing moderation reductions in biofilm formations and moderate to high reductions of internal populations. While the physical reductions were mostly consistent across the treatment range, reductions in cells numbers were higher proportional to treatment concentration. The greater effect of nisin against *S. aureus* viability within the biofilm has also been reported in other studies (Ceotto-Vigoder et al. 2016) There were, however, noted increases in biofilm formations at the highest concentration of nisin on lid pegs. Nisin-PVP held similar effects upon physical formations, however there were no reports of increased biofilm formations across the test range. While internal analysis reported increases in numbers of biofilm populations on lid pegs, there were noted reductions across the test range again biofilms on plate well walls. These observed effects of nisin-PVP do not adhere to previous occurrences of attachment or biofilm inhibitory studies. While the lowered effects of previous studies would suggest loss of effect due to polymer incorporation, the biofilm reduction study suggests otherwise. The reduced effect upon internal biofilm populations (in comparison to nisin) would suggest a hindered ability to infiltrate biofilm formations, however the present studies show that it held a lower effect as pre-treatment and co-treatment with developing biofilms in comparison to it being used as a direct treatment against already formed biofilms. The lower effects noted by attachment and biofilm inhibition studies may suggest the polymer component of nisin-PVP to aid biofilm development, more so that the effect that its nisin component holds to hinder development.

Chitosan versus *P. aeruginosa*

Chitosan held varied effects upon *P. aeruginosa* biofilms, depending upon the stage of treatment application and surface. Pre-treatment using chitosan and chitosan-PVP produced a positive reduction in resulting biofilm formations and internal populations on lid pegs and plate wells. While chitosan appears to have hindered initial bacterial attachment, its viscid properties likely also caused residual material to remain on the surfaces, causing further

action upon cells within biofilms upon development. This can be identified on peg lids, where resulting biofilm formations varies largely, the internal biofilm populations are consistently reduced. This increased biofilm formation is like due to chitosan and PVP being incorporated into the biofilm matrix, and thus attaching CV dye. There does appear to be a trend of activity loss against the biofilm bacteria as the concentration increases in both chitosan and chitosan-PVP. This is most evident in plate well walls studies as higher test concentrations of chitosan-PVP were observed to cause an increase biofilm formations and internal biofilm populations.

There was moderate biofilm inhibition observed on lid pegs and well walls at lower concentrations of chitosan, but was seen to promote attachment at higher concentrations, particularly on plate well walls where there were increases of up to 75%. Chitosan-PVP reported slight inhibition at the lowest and highest concentration on lid pegs only, with mid-range concentrations on lid pegs causing moderate to high increases (proportional to concentrations). Like chitosan, higher concentrations of chitosan-PVP were noted to cause increases in biofilm formations on plate well walls, however there was no noteworthy inhibition at other test concentrations. Due to the complex composition of the biofilm matrix, it may be possible for external polymer materials to be incorporated into the biofilm during development. There appears to be a point at which the antimicrobial effects of chitosan become insignificant, and the polymer instead begins to aid in biofilm formation on plate well walls. Chitosan-PVP was also noted to have greater effect than chitosan alone, suggesting a supporting role of the PVP polymer in biofilm development as well. Effects against bacterial populations on plate well wall biofilms appeared to mirror the effects seen against the physical biofilm, with higher treatment concentrations resulting in increased bacterial numbers, however, the reported increases are of a much greater magnitude. The fact that chitosan and chitosan-PVP affect both internal and external biofilm further support that idea that they aid in biofilm development, as increases to physical biofilm alone would suggest that the polymers were just attaching to the biofilm matrix rather than supporting their development. There were some comparisons noted from the lid peg studies, however, while it was reported that chitosan-PVP was promoting biofilm growth, it was chitosan pre-treatment that caused the greatest increase of biofilm population. Regardless, there is again a concentration point at which chitosan fails to inhibit biofilm and bacterial growth, and instead supports these developments. These observations do not reflect previous studies,

where chitosan coatings were reported to greatly reduced biofilm formations by a number of different bacterial species, including *P. aeruginosa* and *S. aureus* (Carlson et al. 2008)

Chitosan failed to cause reductions of *P. aeruginosa* biofilms on lid pegs, both against physical formations and to the internal populations, however there was moderate reductions seen against biofilms grown on plate wells at lower concentrations and highest. The reduced activity against lid peg biofilms suggest that these biofilms hold stronger resilience compared to those grown on plate well walls. Results gained from plate well walls show these physical biofilms to be more susceptible to chitosan treatment, except at the mid-upper treatment range. Resazurin analysis reveals interesting occurrence, where the internal biofilm population increases proportional to increasing treatment concentration. This occurrence has also been identified in biofilm inhibition studies and suggests a defence mechanism of the *P. aeruginosa* bacteria to chitosan, in which they reproduce rapidly. Chitosan-PVP held distinct effects upon the mature biofilms, with a clear reduction in both physical biofilm and internal population, which was seen to increase with treatment concentration. Results suggest that chitosan-PVP holds a unique mechanism to interact with developed biofilms and remove them. The loss of physical biofilm and bacterial population support this idea, along with the fact that chitosan alone could not produce similar results. Other studies analysing chitosan and chitosan polymer mixtures have also found that chitosan showed increased adhesion and biofilm inhibition when used in combination with other polymers, specifically PVA (Y. Wu et al. 2018).

Chitosan versus *S. aureus*

Pre-treatment of surfaces with chitosan and chitosan-PVP did not confer an attachment inhibitory effect upon *S. aureus* cells, but instead was seen to greatly promote it. Physical biofilms were observed to increase up to approximately 250% when exposed to chitosan, and up to approximately 800% with chitosan-PVP on lid pegs. This was seen to increase proportional to the treatment concentration, which suggest that the antimicrobial effect of chitosan was holding no effect upon bacterial attachment to lid pegs and was just acting as an attachment medium for the cells. This is further supported by the fact that chitosan-PVP was having even greater effect, as both chitosan and PVP are polymer compounds which may aid attachment. This thought is somewhat supported by resazurin analysis, which shows a large increase in internal populations due to chitosan-PVP pre-treatment. While not as large

as increases seen of the biofilm itself, this does support the hypothesis that the PVP is greatly aiding attachment, as no such increase was seen in populations of biofilm surfaces pre-treated with chitosan. Interestingly, there were moderate decreases of biofilm population across the test range for chitosan pre-treatment. This holds the notion that while the physical biofilm did benefit from pre-treatment with chitosan, the bioactive was still able to exhibit its antimicrobial abilities upon the developing internal bacteria.

These observations do however oppose results gained from plate well wall analysis. While there were clear increases in biofilm formations due to pre-treatments, these growths were most noted at the lower test range and observed to decrease as treatment concentration increases. There were also instances of slight inhibition noted at higher concentrations of chitosan which suggests that *S. aureus* biofilms that settled on surfaces similar to plate well walls, were somewhat more susceptible to chitosan activity at higher concentrations. This would however require greater test concentrations to investigate. The resazurin results do give somewhat more insight, as there were slight inhibitory effect upon internal populations, this does suggest that the changes were only due to lower concentrations of the polymers aiding in bacterial attachment. While similar studies have noted effect inhibition of biofilm formations, and even reductions of viable bacterial *S. aureus* cells following chitosan, these studies used alternative forms of chitosan (Felipe et al. 2019)

Treatments of chitosan and chitosan-PVP had hugely proliferating effects upon *S. aureus* biofilm development, causing massive increases in produced biofilms. These increases were mostly proportional to the treatment concentration but increases due to chitosan-PVP were much greater at lower concentrations. While there were great increases observed on plate well walls, the magnitude of the increases on lid pegs were much greater. Resazurin analysis reveals that while there were increases in biofilm formations on plate well walls, the internal populations were reduced slightly. This suggests that the response was primarily physical, whereby the treatment polymers were interacting and binding to the developing biofilms, causing the increased growths. Resazurin analysis of lid pegs presented an alternative phenomenon, wherein the biofilm population also increased in response to chitosan treatment. These increases matched with the largest increases in physical biofilm formations, indicating a correlation. It is quite possible that the treatment elicited a defence response from *S. aureus* biofilm bacteria, causing upregulated growth and replication. The fact this only

occurs on lid pegs suggests that the bacteria undergo a dramatic shift once they attached to such surfaces. The difference between bacteria which attach to lid pegs and well wall surfaces can only be speculated at this point, but the present results are indicating a definite divergence of the bacterial cells behaviours.

Treatments of developed biofilms also results in large increases in biofilm formations, on both lid pegs and plate well walls. There was an odd trend of the growth peaking in the mid treatment concentration range in both instances. This suggests that the increasing amount of polymer was adding to the formed biofilm and increasing its physical formation to a point, after which the amount of chitosan present began to influence the biofilm formations. While this did not lead to a reduction of the biofilm, internal population analysis did reveal that the populations were reduced, which was also seen to occur at higher concentrations indicating that the chitosan was exhibiting its antimicrobial effects, even though the physical biofilm formations were increasing. There were, however, increases in bacterial populations noted on lid pegs at lower concentrations of chitosan-PVP which relate to the major increases in biofilm formations. While the reduction in cell numbers caused by chitosan and chitosan-PVP treatment is beneficial, the huge increase is physical formations could pose greater issue.

ZnO versus *P. aeruginosa*

Pre-treatment with ZnO exhibited slight attachment inhibition of *P. aeruginosa* on lid pegs, which was noted to increase with treatment concentration. However this inhibitory effect was not observed against *P. aeruginosa* attachment on plate well walls. While there was slight inhibition at lower concentrations, higher concentrations were seen to increase attachment, as determined by greater biofilm formations. This observation supports the previous theory that *P. aeruginosa* has greater biofilm formations on plate wells compared to lid pegs, which hold more resilience towards to treatment. ZnO-PVP exhibited similar effects against bacterial attachment on lid pegs, however it was noted to cause increased attachment on lid pegs. This is a similar occurrence observed in several other attachment studies and suggests the PVP polymer component of treatments to aid in bacterial attachment.

While CV analysis has revealed reduced physical biofilm formations on lid pegs, resazurin analysis indicates a negative effect of ZnO and ZnO-PVP pre-treatments where biofilm

populations were reported to have metabolised resazurin much faster, suggesting greater bacterial numbers even though the physical biofilm itself was reduced. However, comparing both results may suggest another situation, where the remaining bacteria population has an altered metabolic rate in response to the external pressures caused by the treatments. However, such theory would require further studies to confirm. While analysis of plate wells shows decreased biofilm populations at lower concentration ranges, there was a large increase noted in the highest pre-treatment concentration of ZnO-PVP.

Both ZnO and ZnO-PVP treatment demonstrated quite effective inhibition of biofilm growth on peg lids, with ZnO-PVP showing much greater effect. These effects were not reflected in results of plate well analysis, which exhibited minor inhibition at lower concentrations, and then was shown to cause increased biofilm formations at higher concentrations. This again suggests *P. aeruginosa* biofilm growth to be more resilient on plate wells while also responding by upregulating physical growth. Previous studies analysing ZnO effects versus *P. aeruginosa* biofilms found it to hold very effective biofilm inhibition against those grow on plate well walls, however these studies produced their own ZnO-NPs which may hold much different effect that the ZnO used presently (Sangani, Moghaddam, and Forghanifard 2015). ZnO-PVP was seen to cause greater increases at mid-range treatments, however ZnO alone caused the highest increase at the max test concentration. This the ZnO-PVP results suggest the PVP polymer to aid in biofilm growth, the ZnO results suggests the increases to be a bacterial response to stress. Similar to results from attachment studies, the reduced biofilm formations on lid pegs were seen to have greater resazurin metabolism, suggesting either increase bacterial numbers or altered metabolic activity. Regardless of the true nature of this increased response, it appears that ZnO alone caused the greater effect, resulting in much greater response. ZnO-PVP appears as the more effect treatment in these regards, as it caused the greater reduction in biofilm formations and did not increase resazurin metabolism significantly. However, analysis of plate wells shows an increase in bacterial activity, which increased with treatment concentration, and it was also noted that ZnO held a much greater effect overall. Analysis overall suggests ZnO and ZnO-PVP to be quite ineffective against more robust *P. aeruginosa* biofilms, such as those grown on plate well walls.

Both ZnO and ZnO-PVP exhibited effective reductions of *P. aeruginosa* biofilms, however ZnO-PVP was more effective against biofilms on lid pegs and plate well walls. Unlike previous

studies, there was a greater effect noted against biofilm on plate wells. While there were notable reductions of biofilm formations at all concentrations, resazurin analysis reported increases in bacterial activity in response to both ZnO and ZnO-PVP on lid pegs, but only ZnO caused increased activity on plate well walls. Results indicate ZnO and ZnO-PVP to be more effective at reducing formed *P. aeruginosa* biofilms rather than inhibiting attachment and growth, moreover, it appears that ZnO-PVP to be most effective in this with regards to reduced biofilm formations and also unaltered bacterial activity.

ZnO versus *S. aureus*

Pre-treatment exposure with ZnO or ZnO-PVP did not exhibit favourable effects upon *S. aureus* attachment, with the majority of test concentrations causing increased attachment on both lid pegs and plate well walls. There is a recognisable trend on plate well walls where increasing the concentration of the pre-treatments caused increased attachment, however there was no such trend seen on lid pegs. Previous growth analysis has shown *S. aureus* biofilms to develop stronger and more consistently on plate well walls in comparison to lid pegs, which suggests that the pre-treatments were not adequate to prevent initial attachment on the plate well walls but still held effect enough causing the biofilm growth to respond, resulting in greater formations. This too can explain responses from lid pegs, where initial attachment and growth is normally weaker. There is a higher growth response in mid-range concentrations, which are similar to those seen on plate well walls, however at higher concentrations of ZnO, these are seen to return to null effects, with partial inhibition, suggesting there is an effect. However, there is still no obvious inhibition observed. Furthermore, ZnO-PVP was seen to cause much higher biofilm formations at higher concentrations, which suggests the polymer component to aid in attachment and biofilm development, an occurrence noted in other parts of this study. Resazurin analysis reveals little to no effect upon internal biofilm populations due to ZnO and ZnO-PVP pre-treatment, indicating that the growth responses to ZnO and ZnO-PVP is related to the physical biofilm only and not to the bacterial cell numbers. ZnO inability to affect bacterial cell populations may be due the bacteria's physical changes upon initiating biofilm development. ZnO main mechanism of action involves interacting with bacterial cell membranes, causing ruptures in the outer layers. A number of previous studies have noted a large shift in a bacteria's genetic and physical behaviour upon initiating biofilm development, with one such change being the

loss of a solid, membrane form (Melchior, Vaarkamp, and Fink-Gremmels 2006). This loss of a cellular membrane may disable ZnO from interacting with the actual bacterial cells.

Biofilm inhibition studies show similar behaviours observed from attachment inhibition studies. While lower concentrations of ZnO and ZnO-PVP had no major impact against biofilm growth on plate well walls, higher concentrations were seen to cause huge increases in growth. However, this increase was seen to peak at the mid-range of test concentration, and was not as great at higher concentrations, suggesting that even higher concentrations of ZnO and ZnO-PVP may even inhibit growth. Unfortunately, such concentrations were not attainable during this study and so such effects cannot be confirmed.

While ZnO was observed to cause some increases of *S. aureus* biofilms growing on lid pegs, ZnO-PVP held tremendous influence on biofilm growth. Biofilm formations were noted to increase up to 1500% in mid-range concentrations of ZnO-PVP, suggesting a major mechanism of influence upon physical growth caused by the inclusion of the PVP polymer which has also been noted in other results from the present study, although not to this magnitude. While physical biofilm growth was noted to vastly increase, resazurin analysis indicates that ZnO-PVP instead caused reductions in biofilm populations. This decrease was seen to follow ZnO-PVP treatment concentration, with the highest decrease at the highest concertation. Comparison of CV and resazurin results show no correlation between responses, suggesting that the antimicrobial effects of ZnO-PVP hold no influence upon physical biofilm growth but can effectively reduce internal cell numbers. In comparison to ZnO results, the inclusion of the PVP polymer appears to be vital for this effect to occur. While ZnO alone did reduce final cell numbers at higher concentrations, in mid to lower concentrations it was noted to increase final cell numbers. Analysis of internal biofilm populations grown on plate well walls show no major effect caused by ZnO or ZnO-PVP, reporting results similar to those seen in attachment inhibition studies.

As noted during the biofilm inhibition study, results have suggested that ZnO-PVP is unable to exhibit an inhibitory effect upon physical biofilm developments on lid pegs but is effective at reducing internal cell numbers. This observation is further supported by results of biofilm reduction studies, which report large increases in physical *S. aureus* biofilms (on both lid pegs and plate well walls) in response to ZnO-PVP treatments. Similarly to results gathered from the biofilm inhibition studies, lower concentrations of ZnO-PVP were noted to cause slight

increases in biofilm populations but shifts to reductions as concentrations increase. Furthermore, the observed responses of physical biofilm and internal population do not correlate to one another, again supporting the notion that ZnO-PVP cannot hinder or eradicate physical biofilm formations but is quite effective at reducing the internal population numbers.

In contrast to the previous results, ZnO reported successful reductions in physical biofilm formations on lid pegs. These reductions were observed equally across the concentration range, suggesting that the amount of ZnO needed to carry out this effect is irrelevant. These results are also reported in other studies assessing ZnO-NPs against *S. aureus* biofilms (Abdelghafar, Yousef, and Askoura 2022). However, study of the internal population shows different. While reduction of internal bacterial populations were noted at all concentrations, the magnitude of reduction was noted to increase with treatment concentration. Results also show more robust biofilm growth on plate well walls, as indicated by resilience of the physical biofilm to ZnO treatment. However, internal studies indicate a sensitivity of bacterial population to higher concentrations of ZnO. These noted reduction correlate with a slight reduction in physical biofilm formations which is noted at the highest concentrations of ZnO.

5.5 Conclusion

Biofilms and biofilm-mediated resistance are important and developing areas of study in the understanding of antimicrobial resistance, which may open a number of avenues for the successful treatment of biofilm mediated infections and other biofilm related incidents. During the present study, a number of methods have been adapted and modified in order to allow for high throughput, anti-biofilm screening analysis which may aid in the future study of biofilm forming bacteria. While there are several standardised protocols for biofilm analysis, the present methods have built upon these and added what are considered important enhancements for comprehensive understanding of biofilm and anti-biofilm behaviour. Results gained have supported the inclusion of these additional elements and offer a more comprehensive evaluation of the bacterial biofilms and the utilised antimicrobial compounds.

Findings have shown that each of the four bioactive compounds affect *P. aeruginosa* and *S. aureus* biofilm developments in different capacities, which can be further altered if utilized as part of a polymer compound. A summary of the current findings is presented in Tables 5.1 and 5.2, which gives a clearer visualisation of the following key points with regards each bioactive effect against each bacterial species, at each stage of biofilm development. Studies have also indicated a clear preference of *P. aeruginosa* and *S. aureus* biofilms to grow on plate well walls. Furthermore, treatment studies have shown that biofilm developments on well walls are more resistant to treatments.

$AgNO_3$ showed highly effective anti-biofilm capabilities against *P. aeruginosa* however, it was less effective as a pre-treatment in its polymer form. When used to treat *S. aureus*, it was quite ineffective as a pre-treatment. As a co-treatment, it was somewhat effective against physical formations when used as $AgNO_3$ but was seen to be highly effective against internal bacterial populations. As a treatment to fully formed biofilms, $AgNO_3$ was very effective, especially against internal populations. $AgNO_3$-PVP was, however, quite ineffective as a treatment.

Nisin and nisin-PVP were not effective against *P. aeruginosa* biofilms at any stage of development and were instead noted to cause increased biofilm activity. Nisin was very effective as a pre-treatment against *S. aureus* biofilms on lid pegs, but not against those on plate well walls. Nisin-PVP showed some promise as a pre-treatment on lid pegs, but otherwise was ineffective. As a cotreatment, nisin was quite effective against *S. aureus* biofilms forming on lid pegs but had little effect against biofilms on plate well walls. Nisin-PVP has some effect against physical formations on lid pegs but was very ineffective against well wall biofilms. As a treatment, nisin and nisin-PVP held varying degrees of efficacy against *S. aureus* biofilms formed on lid pegs and plate well walls, but with an overall net reduction at most concentrations. Furthermore, nisin was noted to be very effective at reducing internal population numbers of biofilms grown on both lid pegs and well walls.

Chitosan and chitosan-PVP pre-treatment was quite ineffective against reducing *P. aeruginosa* formations on lid pegs but was somewhat effective at causing reduced bacterial numbers. Chitosan and chitosan-PVP were somewhat effective against bacterial attachment on plate well walls, however higher chitosan-PVP has very negative effects. Overall, chitosan and chitosan-PVP were highly ineffective as pre-treatments for *S. aureus* attachment and

biofilm inhibition. Chitosan and chitosan-PVP were also highly ineffective as cotreatments for the inhibition of biofilm growth against *S. aureus* but also against *P. aeruginosa*. As treatments for established biofilms, chitosan and chitosan-PVP were also unsuitable against *S. aureus* and *P. aeruginosa*. While there were some positive results for physical or cell number reductions, the negative results greatly overshadowed these.

ZnO and ZnO-PVP were ineffective as pre-treatments against *S. aureus* and *P. aeruginosa* attachment and biofilm formation. As co-treatments, there was positive efficacy seen against *P. aeruginosa* biofilms on peg lids, however internal population analysis results was not desirable. In contrast, ZnO-PVP co-treatment appeared to reduce bacterial numbers on lid pegs, however the major increase to physical biofilms reduces this positive effect. As treatments, ZnO and ZnO-PVP were quite effect against physical *P. aeruginosa* biofilms on both peg lids and plate well walls; however, were noted to cause increases of internal populations. ZnO appeared to be very effective against *S. aureus* biofilms on lid pegs, while ZnO-PVP was highly ineffective against physical biofilms on the lid pegs, it was very effective at reducing cell numbers at higher concentrations. Against physical *S. aureus* biofilms on plate well walls, ZnO and ZnO-PVP were very ineffective; however, they both appeared to have great effect in reducing internal populations at higher concentrations.

In conclusion, the present results indicate varying strengths of each bioactive against both bacteria under different test conditions. While some treatments were effective against the external, physical biofilm formations, others were more effective against internal bacterial cell populations. Other results suggest that, while there was no major reduction or inhibition upon physical biofilm development or internal bacterial population numbers, slight alteration of treatments could otherwise result in vastly different outcomes. The possibility of these chosen bioactives to perform in combination with one another could result in achieving much more effective anti-biofilm treatments and even unlocking some treatments inability to affect the bacterial biofilms. As such, the four bioactives will be assessed in a series of combinational studies to determine their potential synergistic abilities from an antimicrobial and biofilm disruptive perspective.

5.6 Figures

5.6.1 Bacterial Attachment Inhibition

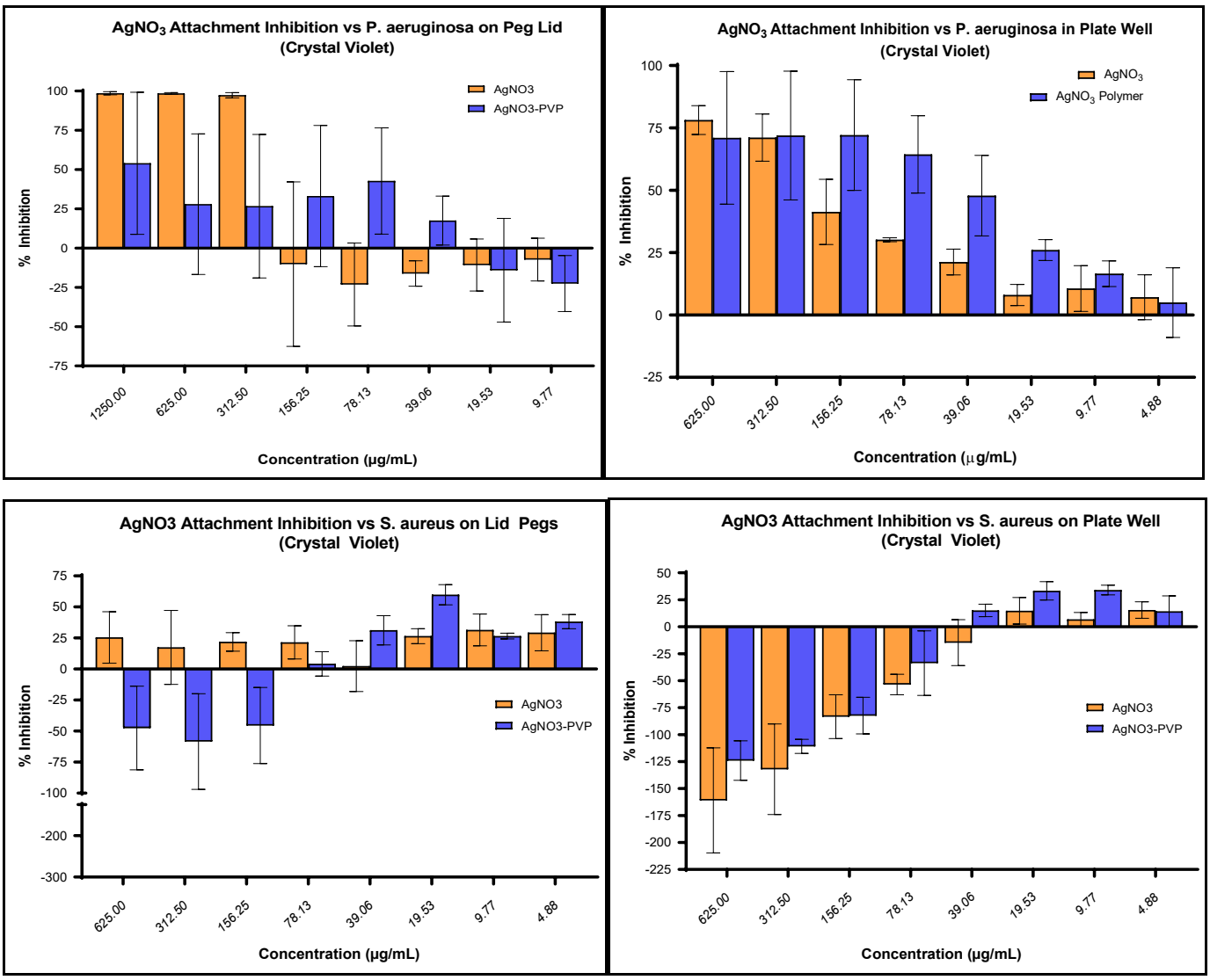

Figure 5.1 *Crystal Violet Evaluation of Silver Nitrate Bacterial Attachment Inhibition*
Bars represent mean % inhibition of bacterial attachment by silver nitrate (AgNO3) and silver nitrate following HME (AgNO3-PVP) across a range of concentrations (µg/mL) against S. aureus and P. aeruginosa biofilm forming bacteria. Biofilms were quantified by use of crystal violet staining, solubilisation and measurement of absorbance. Inhibition was determined by reduced physical biofilm growth in comparison to the untreated growth control (GC), following 24 hours incubation, at 37°C. Error bars represent SEM, N=3.

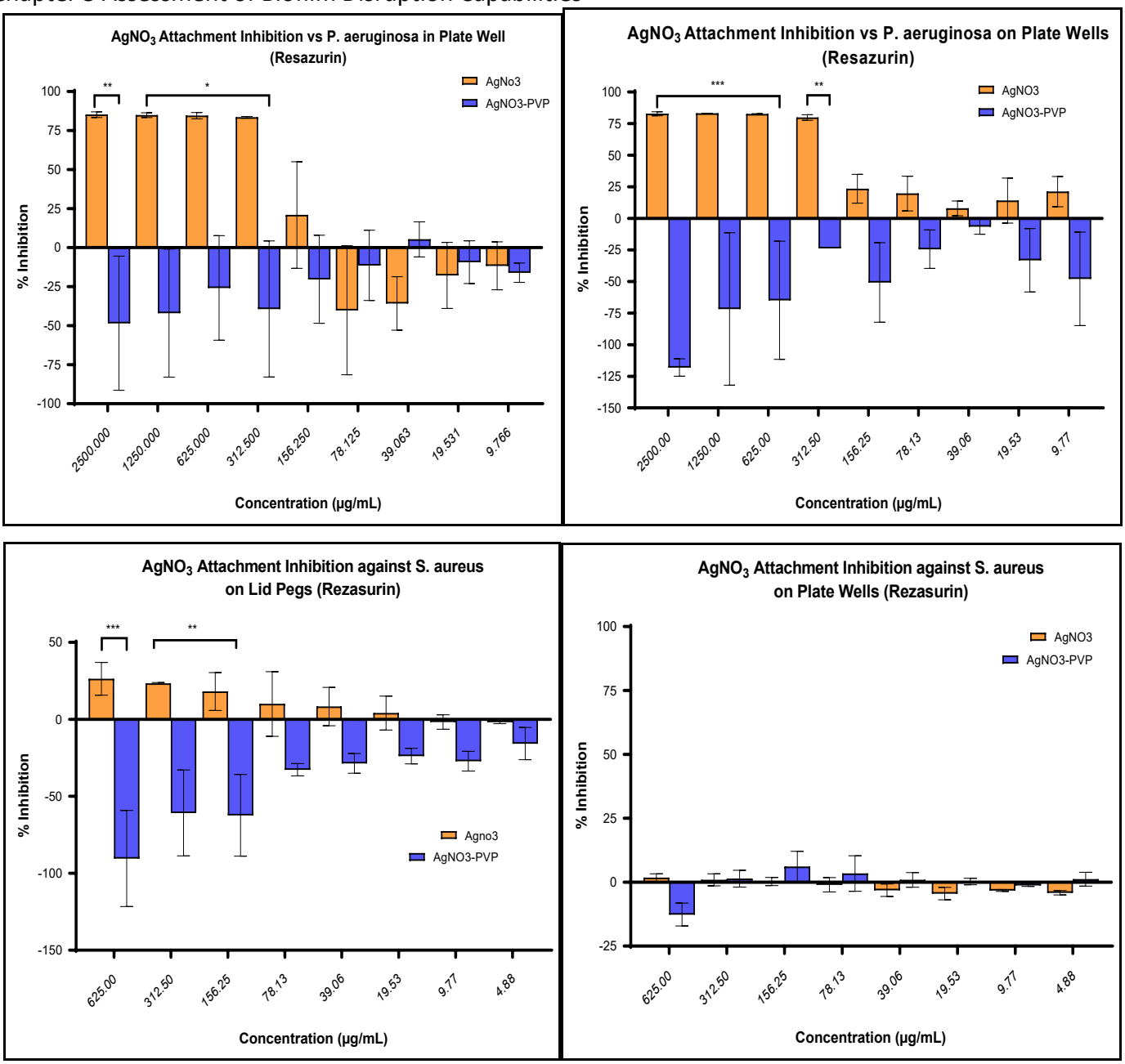

Figure 5.2 *Resazurin Evaluation of Silver Nitrate Attachment Inhibition*.
Bars represent mean % inhibition of bacterial attachment by silver nitrate (AgNO3) and silver nitrate following HME (AgNO3-PVP), across a range of concentrations (µg/mL) against S. aureus and P. aeruginosa biofilms. Attachment inhibition was determined by reduced bacterial populations in the final biofilm following 24 hours incubation, at 37°C. Biofilms were exposed to resazurin solution and converted resazurin was measured fluorescently (Excitation: 528/20, Emission: 590/35). Responses from treated biofilms were compared to response of untreated growth control (GC) biofilm to determine differences in cell numbers. Significant changes in values before and after polymer incorporation were determined by use of two-way ANOVA, with Sidak's multiple comparisons test, and expressed in terms of P value following the APA style (* $p<0.05$, ** $p<0.01$, *** $p<0.001$). Error bars represent SEM, N=3.

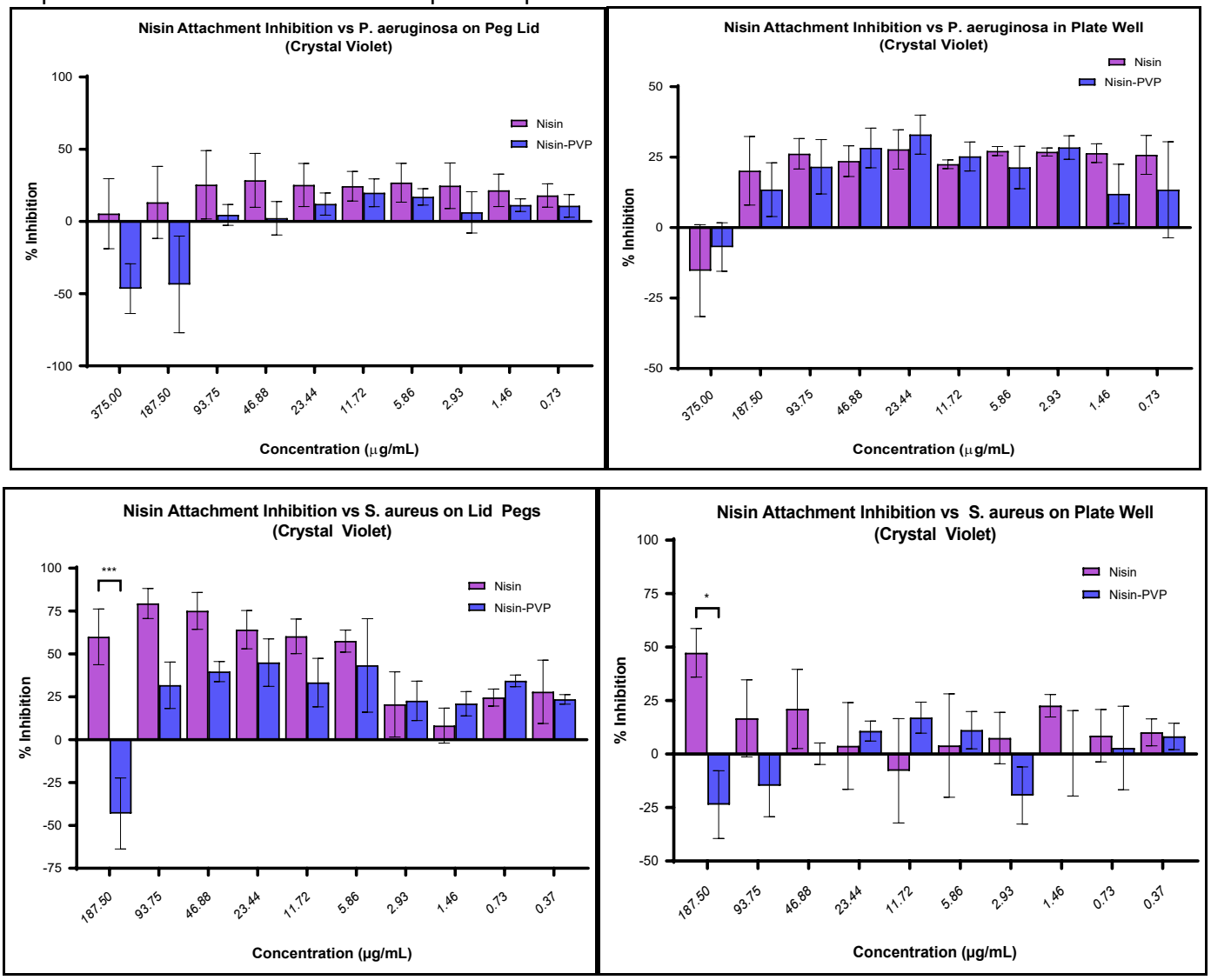

Figure 5.3 *Crystal Violet Evaluation of Nisin Bacterial Attachment Inhibition*.
Bars represent mean % inhibition of bacterial attachment by nisin and nisin following HME (nisin-PVP) across a range of concentrations (µg/mL) against *S. aureus* and *P. aeruginosa* biofilm forming bacteria. Biofilms were quantified by use of crystal violet staining, solubilisation, and measurement of absorbance. Inhibition was determined by reduced physical biofilm growth in comparison to the untreated growth control (GC), following 24 hours incubation, at 37°C. Significant changes in values before and after polymer incorporation were determined by use of two-way ANOVA, with Sidak's multiple comparisons test, and expressed in terms of P value following the APA style (* $p<0.05$, ** $p<0.01$, *** $p<0.001$). Error bars represent SEM, N=3.

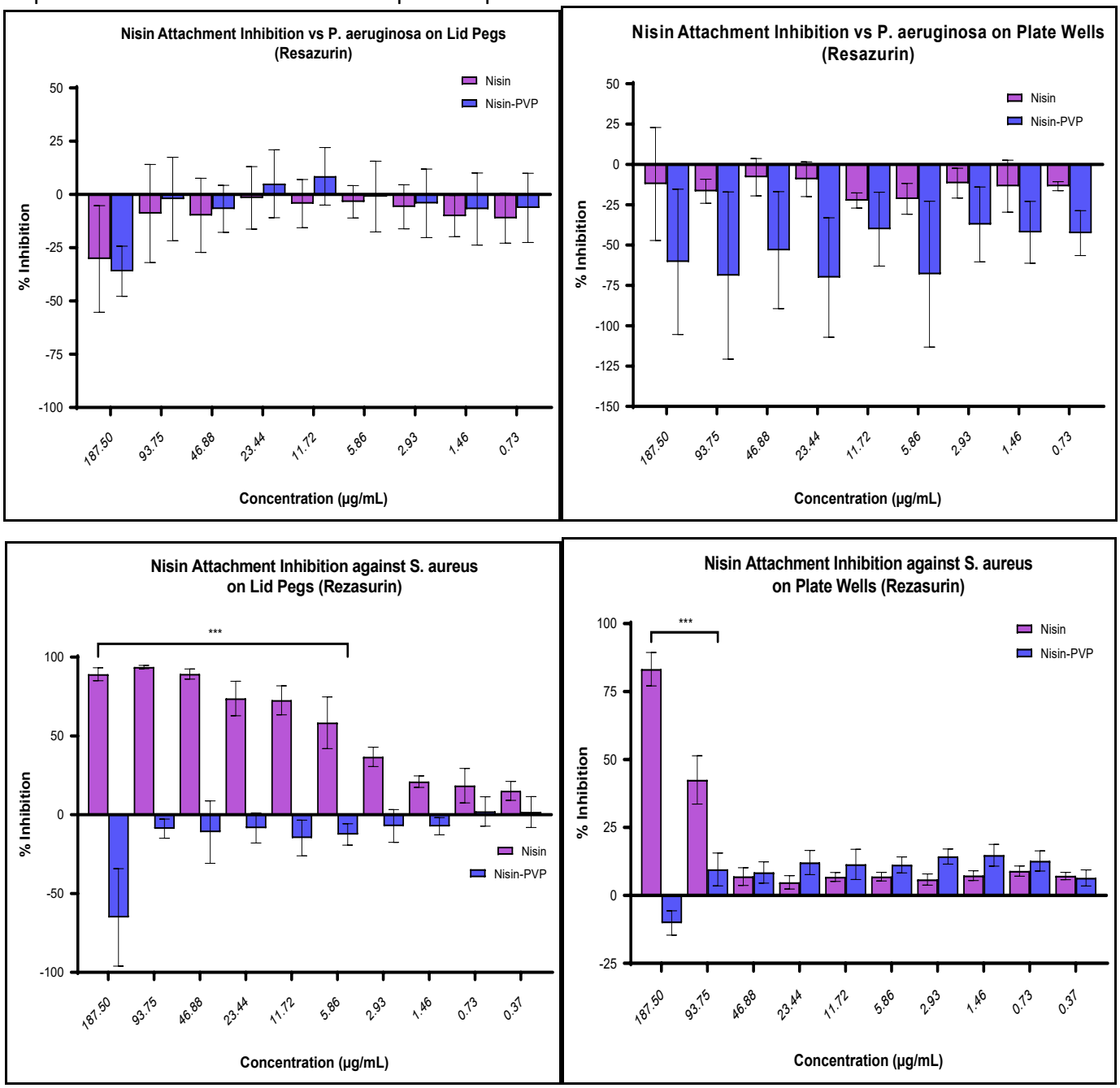

Figure 5.4 *Resazurin Evaluation of Nisin Attachment Inhibition*.
Bars represent mean % inhibition of bacterial attachment by nisin and nisin following HME (nisin-PVP), across a range of concentrations (µg/mL) against S. aureus and P. aeruginosa biofilms. Attachment inhibition was determined by reduced bacterial populations in the final biofilm following 24 hours incubation, at 37°C. Biofilms were exposed to resazurin solution and converted resazurin was measured fluorescently (Excitation: 528/20, Emission: 590/35). Responses from treated biofilms were compared to response of untreated growth control (GC) biofilm to determine differences in cell numbers. Significant changes in values before and after polymer incorporation were determined by use of two-way ANOVA, with Sidak's multiple comparisons test, and expressed in terms of P value following the APA style (* $p<0.05$, ** $p<0.01$, *** $p<0.001$). Error bars represent SEM, N=3.

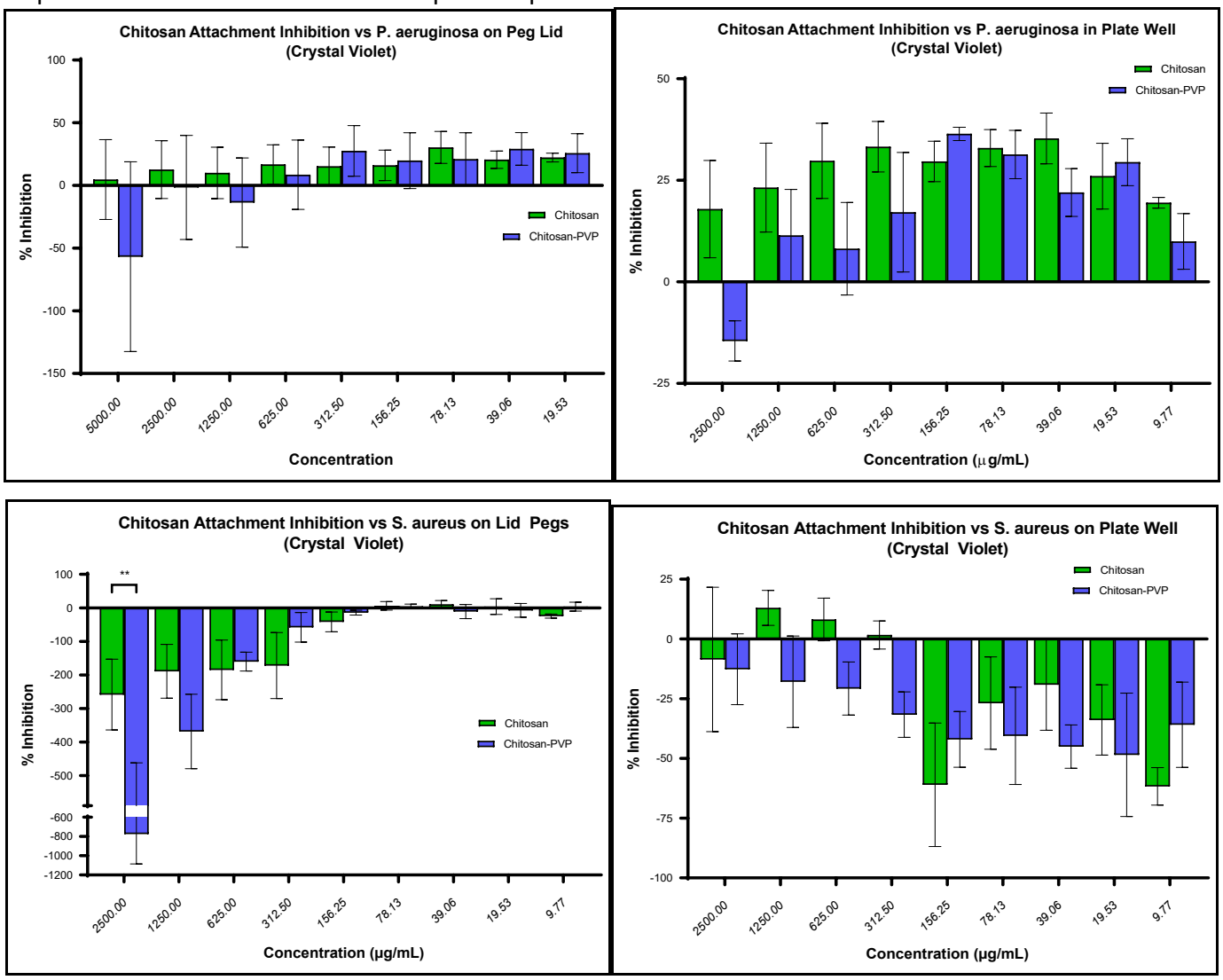

Figure 5.5 *Crystal Violet Evaluation of Chitosan Bacterial Attachment Inhibition*.
Bars represent mean % inhibition of bacterial attachment by chitosan and nisin following HME (chitosan-PVP) across a range of concentrations (µg/mL) against *S. aureus* and *P. aeruginosa* biofilm forming bacteria. Biofilms were quantified by use of crystal violet staining, solubilisation, and measurement of absorbance. Inhibition was determined by reduced physical biofilm growth in comparison to the untreated growth control (GC), following 24 hours incubation, at 37°C. Significant changes in values before and after polymer incorporation were determined by use of two-way ANOVA, with Sidak's multiple comparisons test, and expressed in terms of P value following the APA style (* $p<0.05$, ** $p<0.01$, *** $p<0.001$). Error bars represent SEM, N=3.

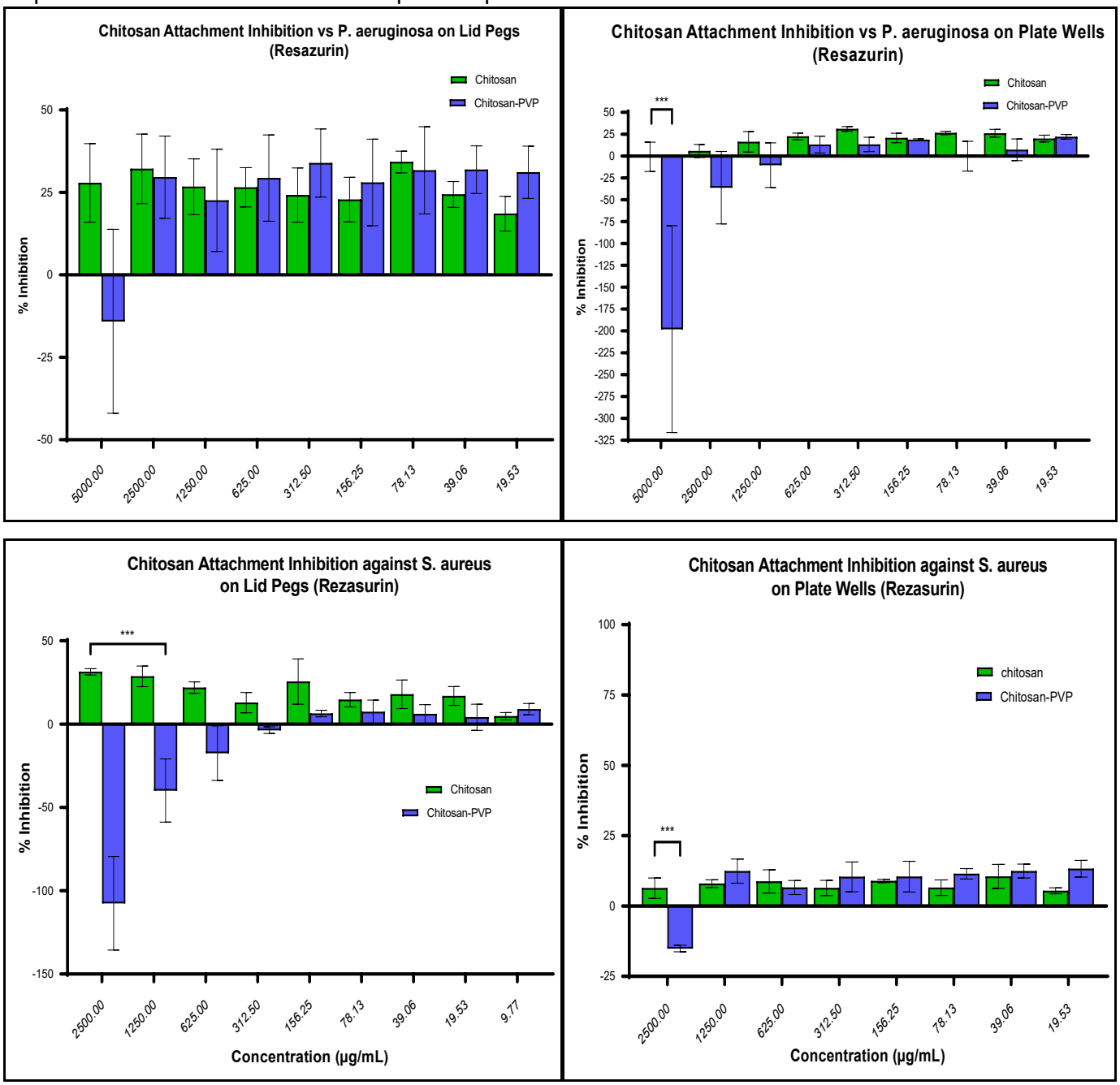

Figure 5.6 *Resazurin Evaluation of Chitosan Attachment Inhibition*.
Bars represent mean % inhibition of bacterial attachment by chitosan and chitosan following HME (chitosan-PVP), across a range of concentrations (µg/mL) against S. aureus and P. aeruginosa biofilms. Attachment inhibition was determined by reduced bacterial populations in the final biofilm following 24 hours incubation, at 37°C. Biofilms were exposed to resazurin solution and converted resazurin was measured fluorescently (Excitation: 528/20, Emission: 590/35). Responses from treated biofilms were compared to response of untreated growth control (GC) biofilm to determine differences in cell numbers. Significant changes in values before and after polymer incorporation were determined by use of two-way ANOVA, with Sidak's multiple comparisons test, and expressed in terms of P value following the APA style (* $p<0.05$, ** $p<0.01$, *** $p<0.001$). Error bars represent SEM, N=3.

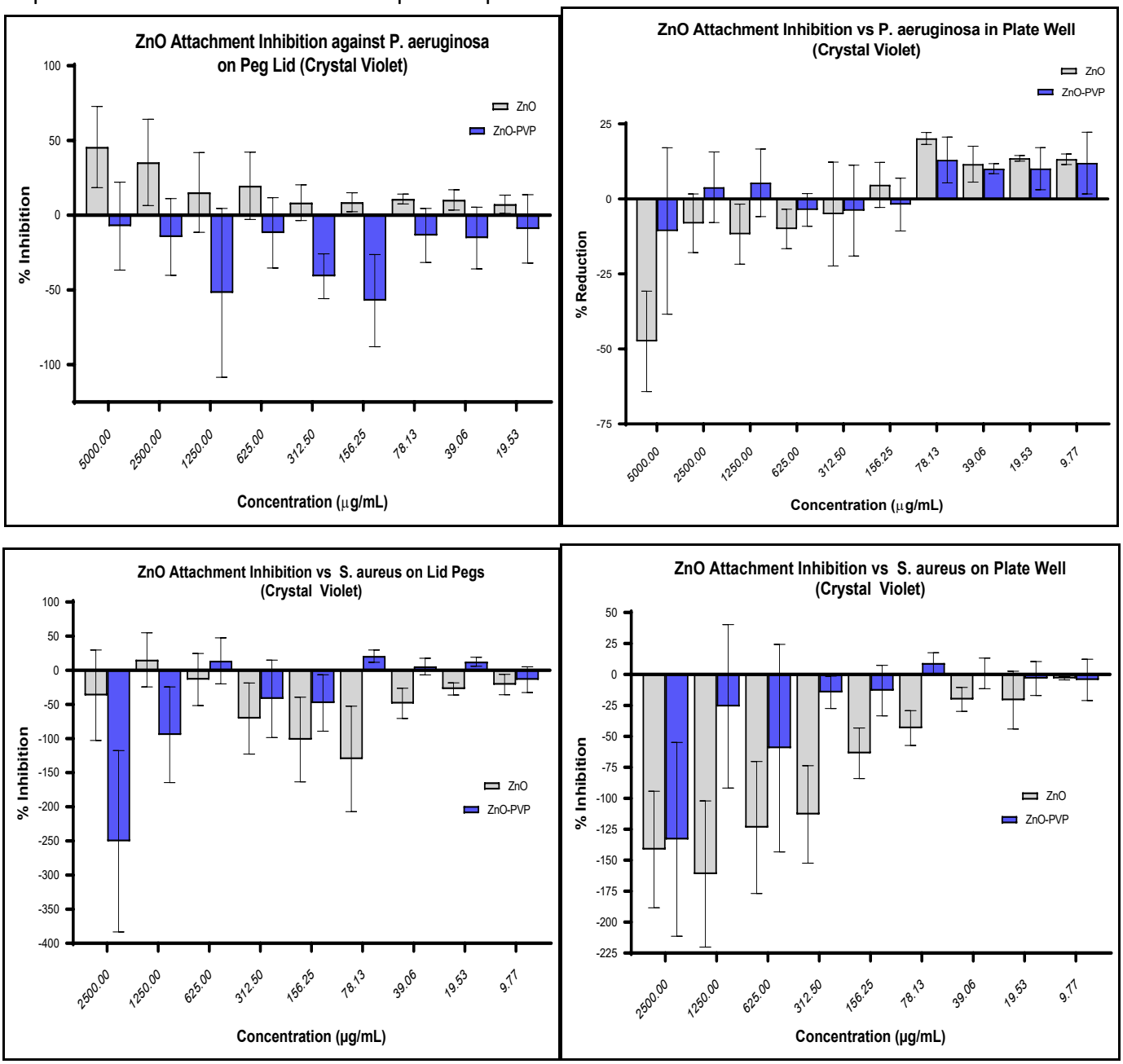

Figure 5.7 *Crystal Violet Evaluation of Zinc Oxide Bacterial Attachment Inhibition*.
Bars represent mean % inhibition of bacterial attachment by zinc oxide (ZnO) and zinc oxide following HME (ZnO-PVP) across a range of concentrations (µg/mL) against S. aureus and P. aeruginosa biofilm forming bacteria. Biofilms were quantified by use of crystal violet staining, solubilisation, and measurement of absorbance. Inhibition was determined by reduced physical biofilm growth in comparison to the untreated growth control (GC), following 24 hours incubation, at 37°C. Significant changes in values before and after polymer incorporation were determined by use of two-way ANOVA, with Sidak's multiple comparisons test, and expressed in terms of P value following the APA style (* $p<0.05$, ** $p<0.01$, *** $p<0.001$). Error bars represent SEM, N=3.

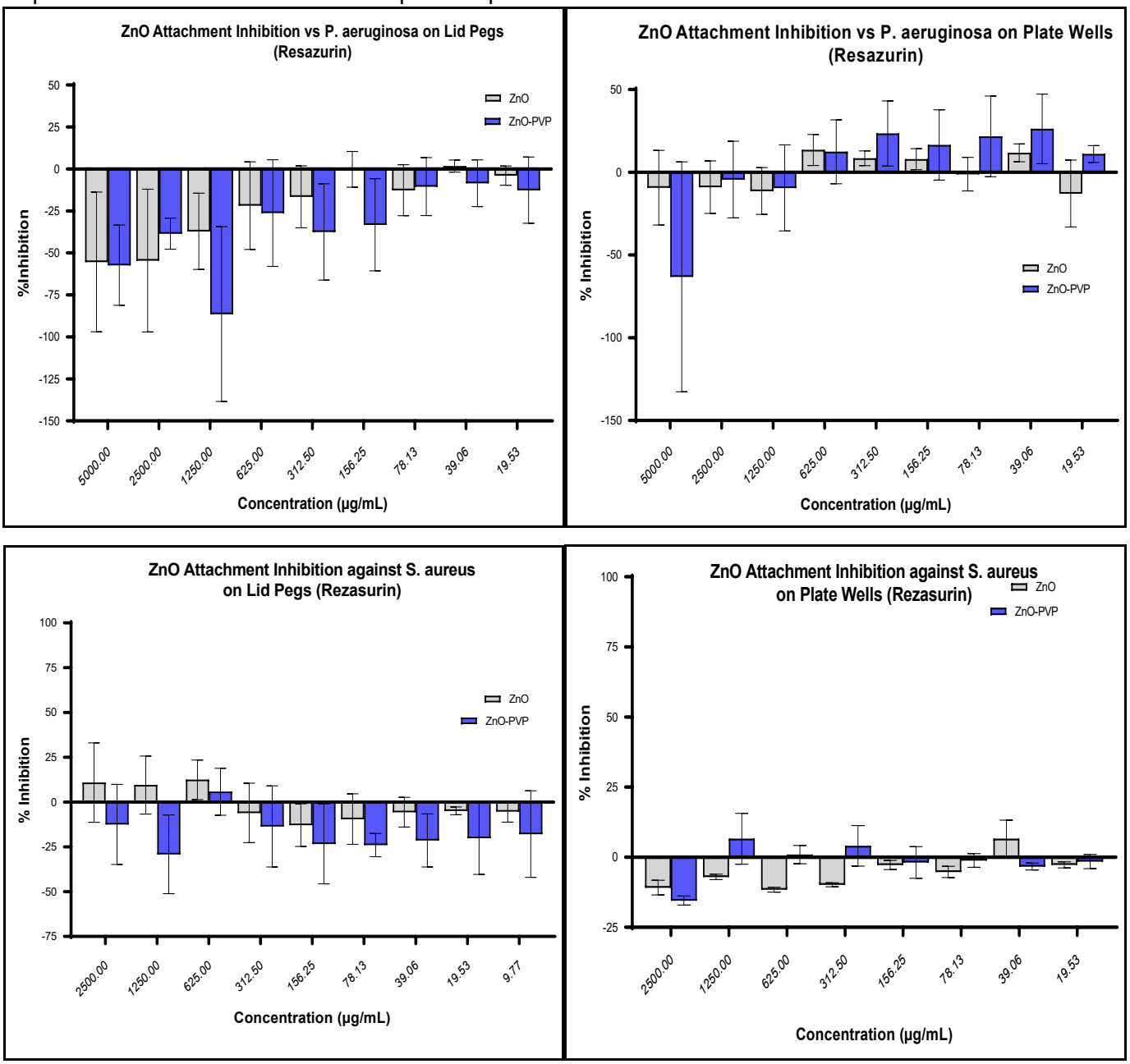

Figure 5.8 *Resazurin Evaluation of Zinc Oxide Attachment Inhibition*.
Bars represent mean % inhibition of bacterial attachment by zinc oxide (ZnO) and zinc oxide following HME (ZnO-PVP), across a range of concentrations (µg/mL) against S. aureus and P. aeruginosa biofilms. Attachment inhibition was determined by reduced bacterial populations in the final biofilm following 24 hours incubation, at 37°C. Biofilms were exposed to resazurin solution and converted resazurin was measured fluorescently (Excitation: 528/20, Emission: 590/35). Responses from treated biofilms were compared to response of untreated growth control (GC) biofilm to determine differences in cell numbers. Significant changes in values before and after polymer incorporation were determined by use of two-way ANOVA, with Sidak's multiple comparisons test, and expressed in terms of P value following the APA style (* $p<0.05$, ** $p<0.01$, *** $p<0.001$). Error bars represent SEM, N=3.

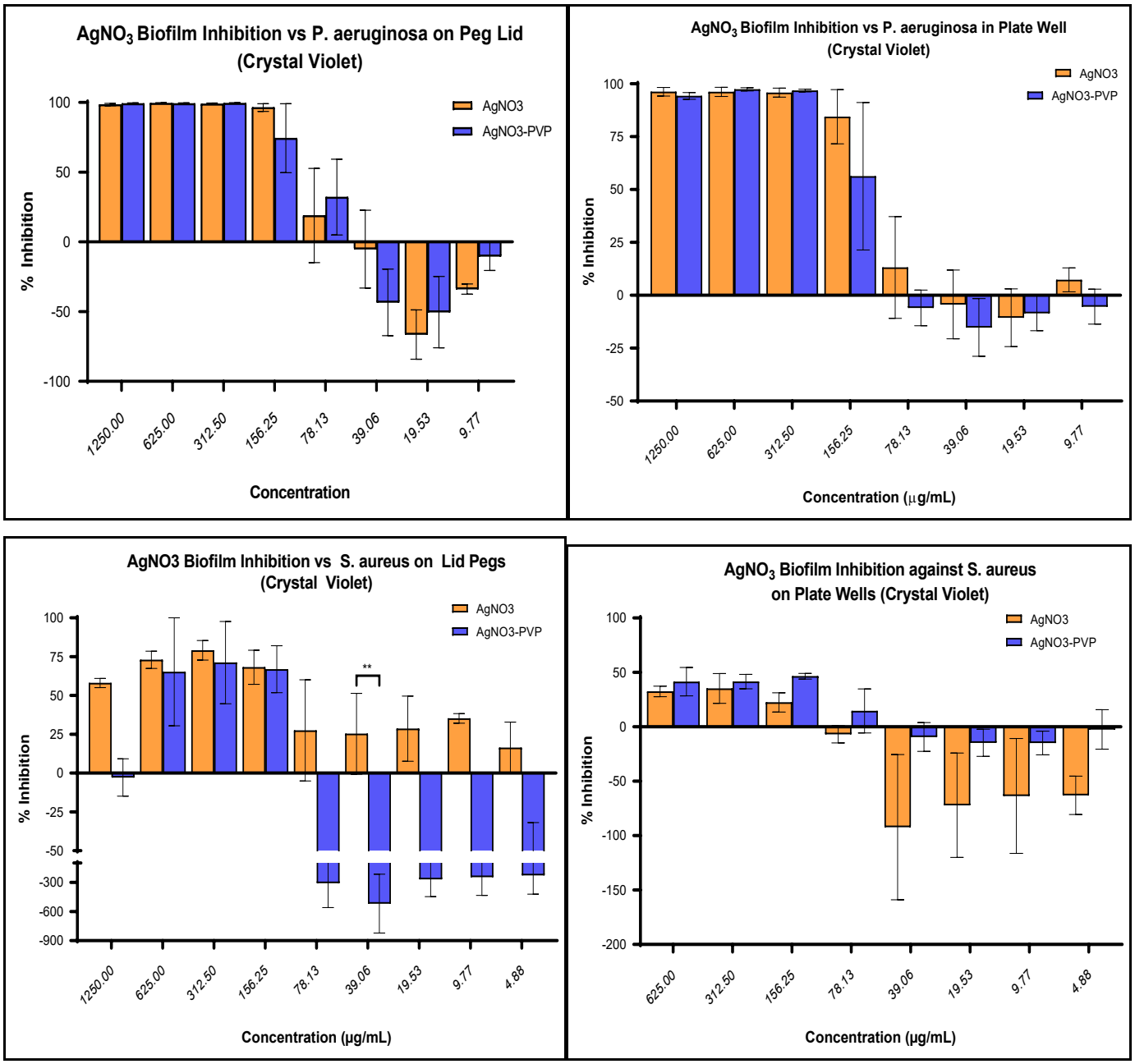

Figure 5.9 *Crystal Violet Evaluation of Silver Nitrate Biofilm Growth Inhibition*.
Bars represent mean % inhibition of biofilm growth by silver nitrate (AgNO3) and silver nitrate following HME (AgNO3-PVP) across a range of concentrations (µg/mL) against S. aureus and P. aeruginosa biofilm forming bacteria. Biofilms were quantified by use of crystal violet staining, solubilisation, and measurement of absorbance. Inhibition was determined by reduced physical biofilm growth in comparison to the untreated growth control (GC), following 24 hours incubation, at 37°C. Significant changes in values before and after polymer incorporation were determined by use of two-way ANOVA, with Sidak's multiple comparisons test, and expressed in terms of P value following the APA style (* $p<0.05$, ** $p<0.01$, *** $p<0.001$). Error bars represent SEM, N=3.

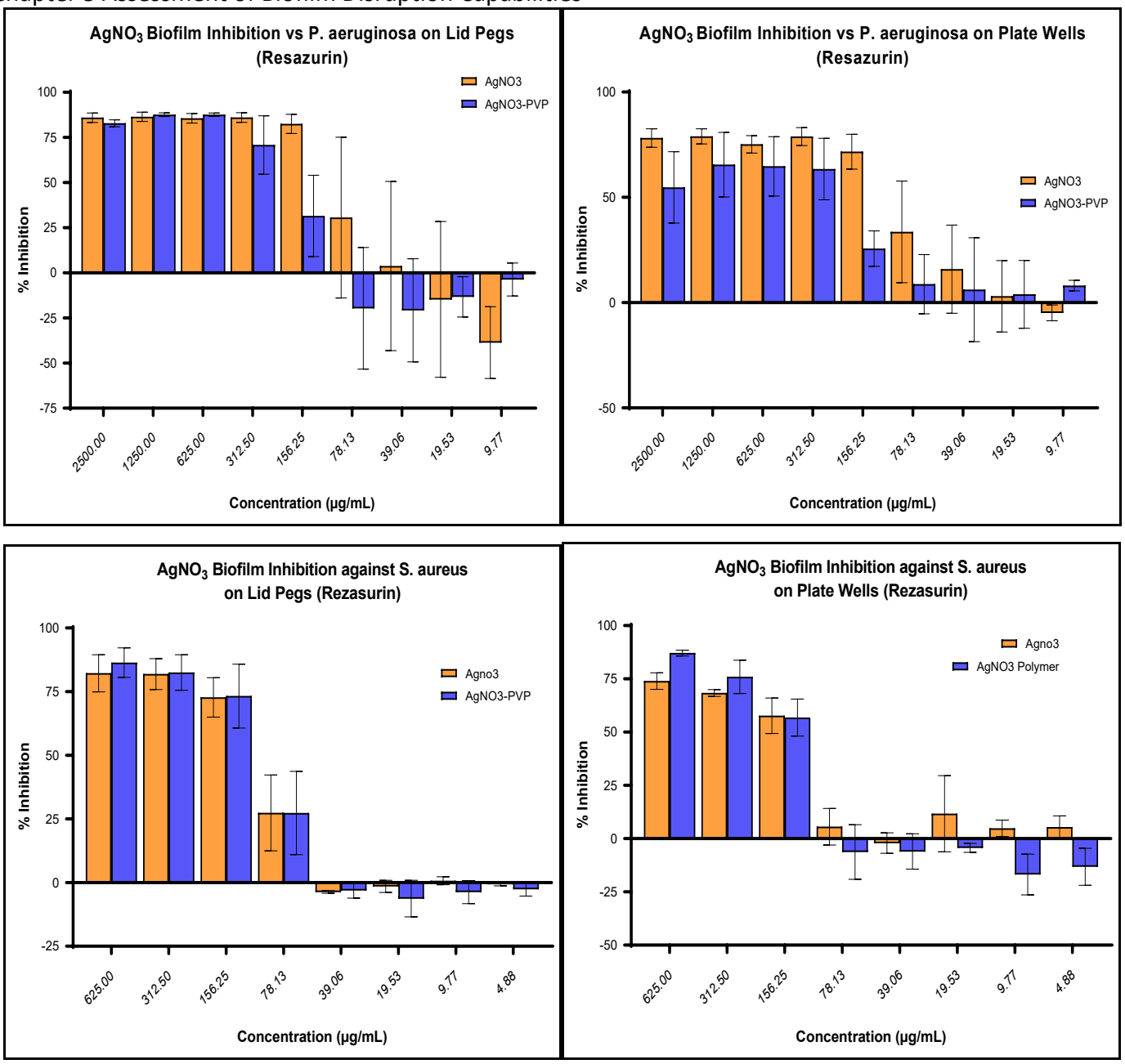

Figure 5.10 *Resazurin Evaluation of Silver Nitrate Biofilm Inhibition*.
Bars represent mean % inhibition of biofilm development by silver nitrate (AgNO3) and silver nitrate following HME (AgNO3-PVP), across a range of concentrations (µg/mL) against S. aureus and P. aeruginosa biofilms. Biofilm growth inhibition was determined by reduced bacterial populations in the final biofilm following 24 hours incubation, at 37°C. Biofilms were exposed to resazurin solution and converted resazurin was measured fluorescently (Excitation: 528/20, Emission: 590/35). Responses from treated biofilms were compared to response of untreated growth control (GC) biofilm to determine differences in cell numbers. Significant changes in values before and after polymer incorporation were determined by use of two-way ANOVA, with Sidak's multiple comparisons test, and expressed in terms of P value following the APA style (* $p<0.05$, ** $p<0.01$, *** $p<0.001$). Error bars represent SEM, N=3.

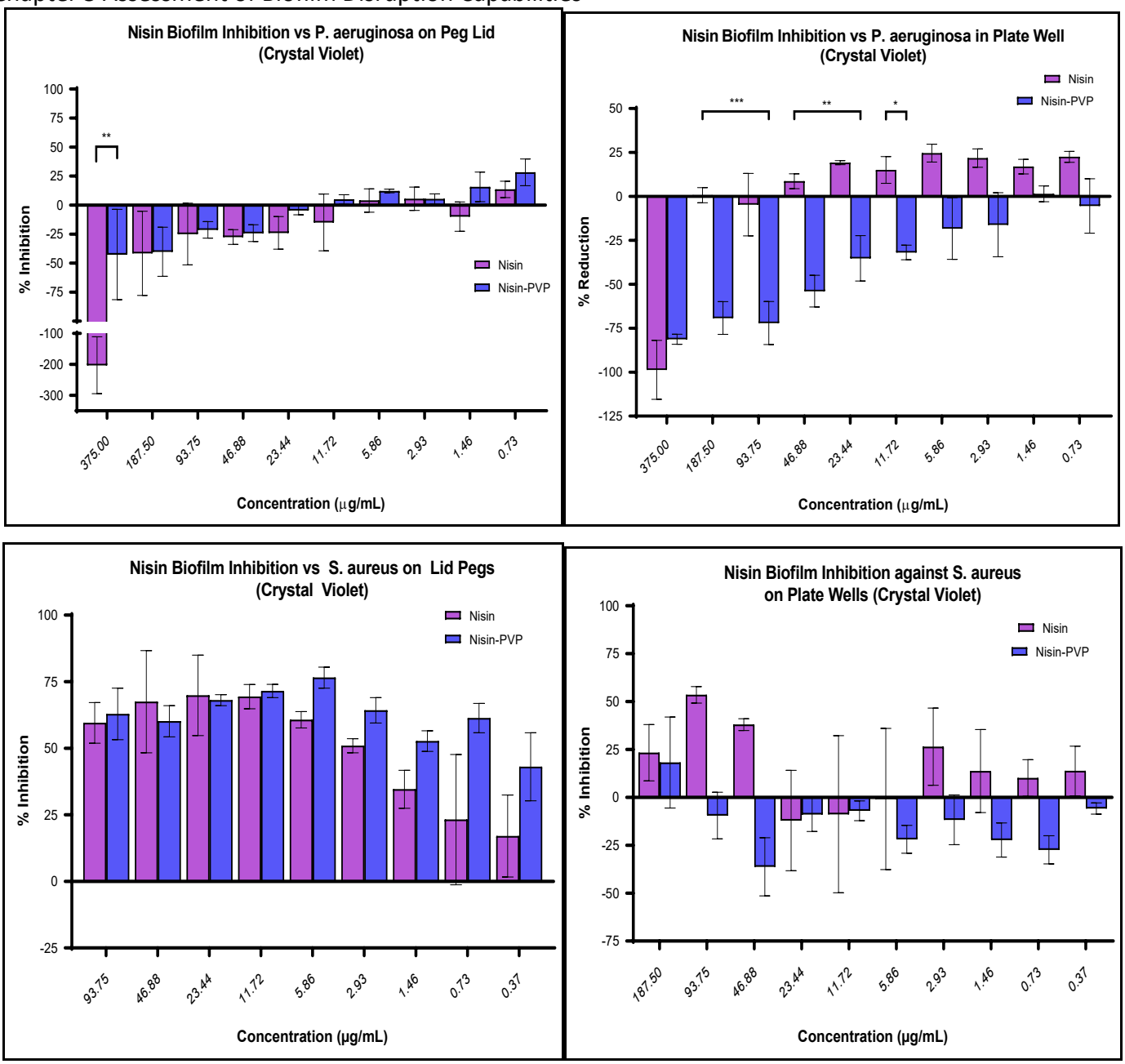

Figure 5.11 *Crystal Violet Evaluation of Nisin Biofilm Growth Inhibition*.
Bars represent mean % inhibition of biofilm growth by nisin and nisin following HME (nisin-PVP) across a range of concentrations (µg/mL) against S. aureus and P. aeruginosa biofilm forming bacteria. Biofilms were quantified by use of crystal violet staining, solubilisation, and measurement of absorbance. Inhibition was determined by reduced physical biofilm growth in comparison to the untreated growth control (GC), following 24 hours incubation, at 37°C. Significant changes in values before and after polymer incorporation were determined by use of two-way ANOVA, with Sidak's multiple comparisons test, and expressed in terms of P value following the APA style (* $p<0.05$, ** $p<0.01$, *** $p<0.001$). Error bars represent SEM, N=3.

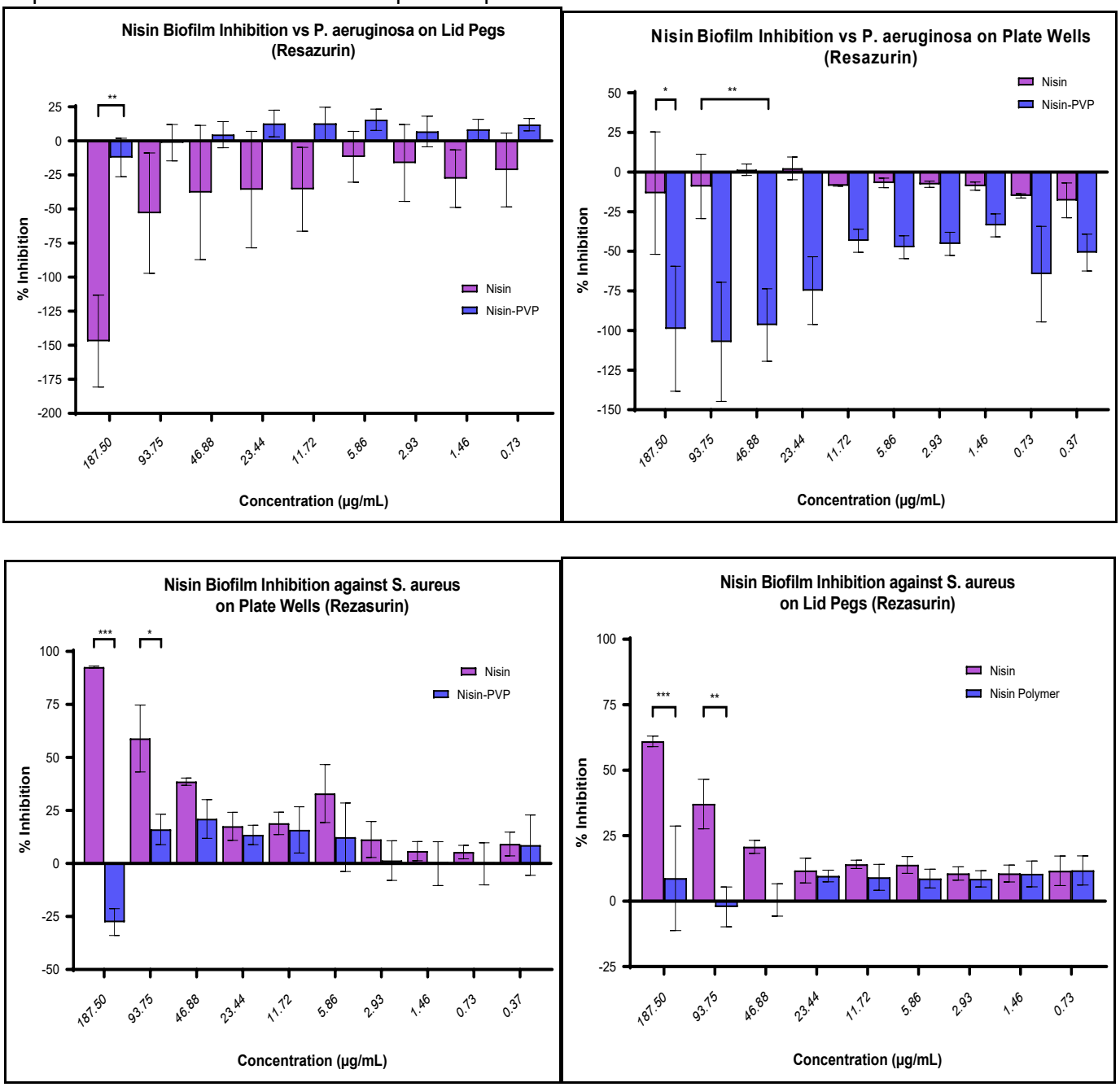

Figure 5.12 *Resazurin Evaluation of Nisin Biofilm Inhibition*.
Bars represent mean % inhibition of biofilm development by nisin and nisin following HME (Nisin-PVP), across a range of concentrations (µg/mL) against S. aureus and P. aeruginosa biofilms. Biofilm growth inhibition was determined by reduced bacterial populations in the final biofilm following 24 hours incubation, at 37°C. Biofilms were exposed to resazurin solution and converted resazurin was measured fluorescently (Excitation: 528/20, Emission: 590/35). Responses from treated biofilms were compared to response of untreated growth control (GC) biofilm to determine differences in cell numbers. Significant changes in values before and after polymer incorporation were determined by use of two-way ANOVA, with Sidak's multiple comparisons test, and expressed in terms of P value following the APA style (* $p<0.05$, ** $p<0.01$, *** $p<0.001$). Error bars represent SEM, N=3.

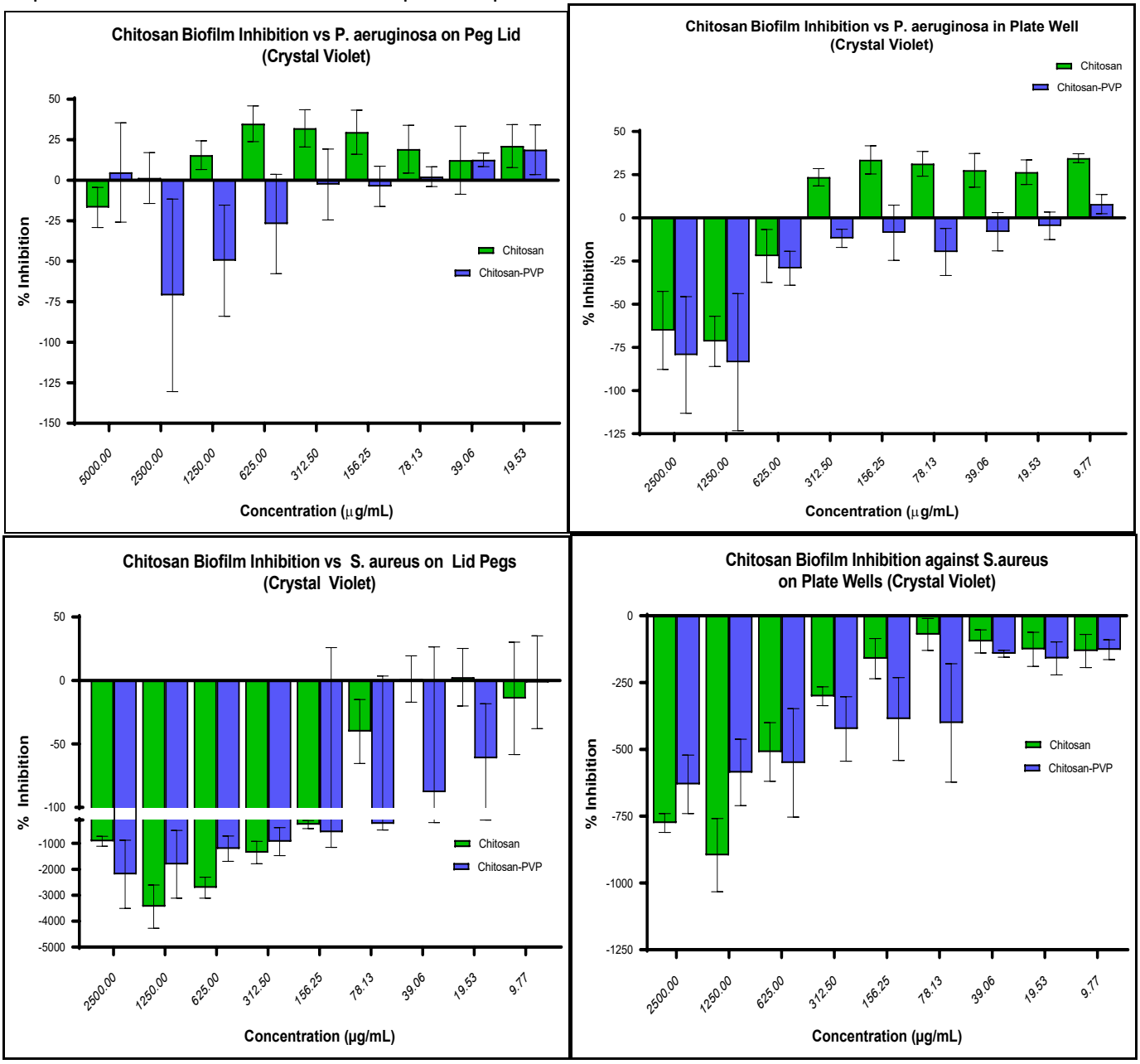

Figure 5.13 *Crystal Violet Evaluation of Chitosan Biofilm Growth Inhibition*.
Bars represent mean % inhibition of biofilm growth by chitosan and chitosan following HME (Chitosan-PVP) across a range of concentrations (µg/mL) against S. aureus and P. aeruginosa biofilm forming bacteria. Biofilms were quantified by use of crystal violet staining, solubilisation, and measurement of absorbance. Inhibition was determined by reduced physical biofilm growth in comparison to the untreated growth control (GC), following 24 hours incubation, at 37°C. Significant changes in values before and after polymer incorporation were determined by use of two-way ANOVA, with Sidak's multiple comparisons test, and expressed in terms of P value following the APA style (* $p<0.05$, ** $p<0.01$, *** $p<0.001$). Error bars represent SEM, N=3.

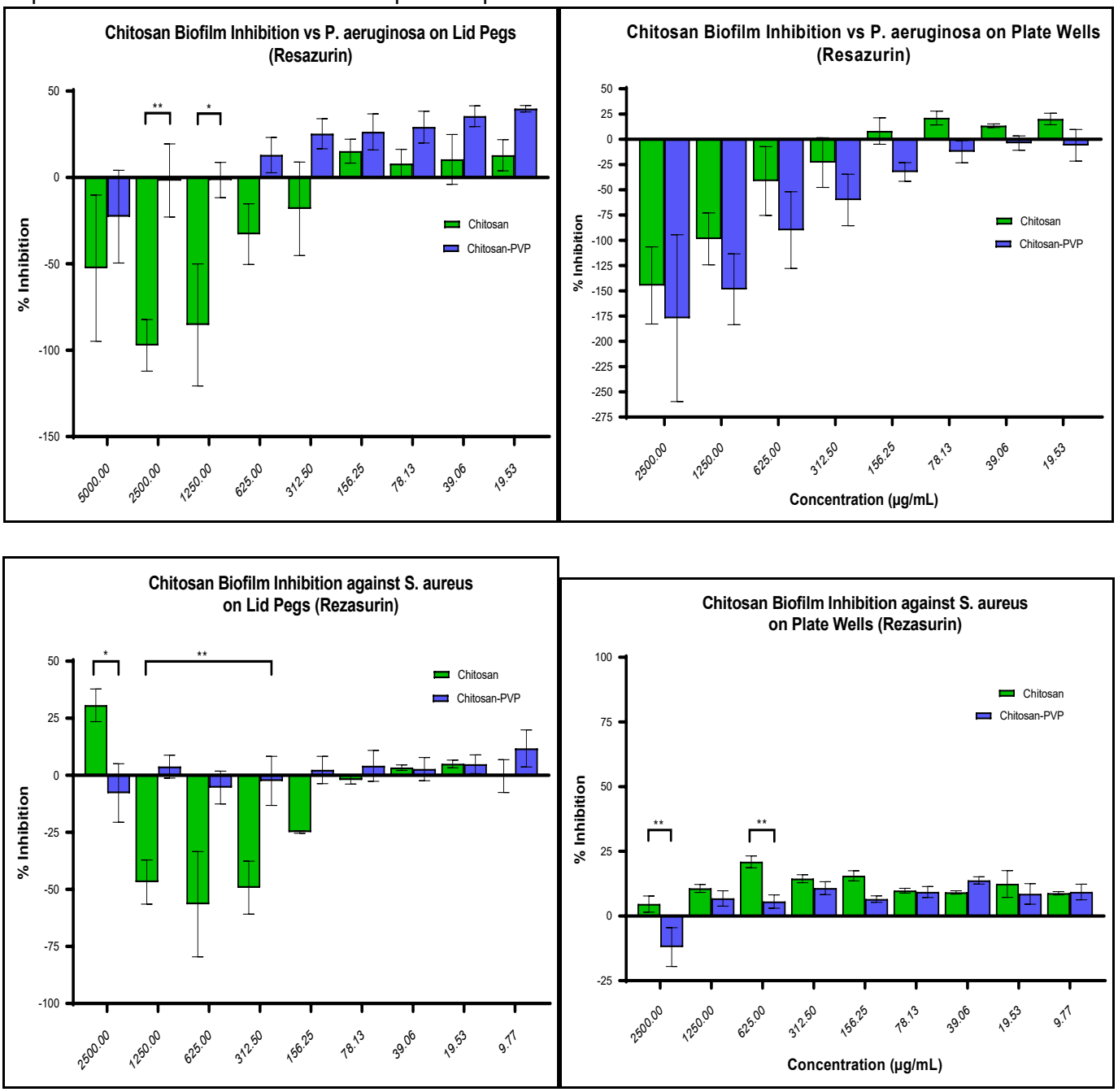

Figure 5.14 Resazurin Evaluation of Chitosan Biofilm Inhibition.
Bars represent mean % inhibition of biofilm development by chitosan and chitosan following HME (Chitosan-PVP), across a range of concentrations (µg/mL) against S. aureus and P. aeruginosa biofilms. Biofilm growth inhibition was determined by reduced bacterial populations in the final biofilm following 24 hours incubation, at 37°C. Biofilms were exposed to resazurin solution and converted resazurin was measured fluorescently (Excitation: 528/20, Emission: 590/35). Responses from treated biofilms were compared to response of untreated growth control (GC) biofilm to determine differences in cell numbers. Significant changes in values before and after polymer incorporation were determined by use of two-way ANOVA, with Sidak's multiple comparisons test, and expressed in terms of P value following the APA style (* $p<0.05$, ** $p<0.01$, *** $p<0.001$). Error bars represent SEM, N=3.

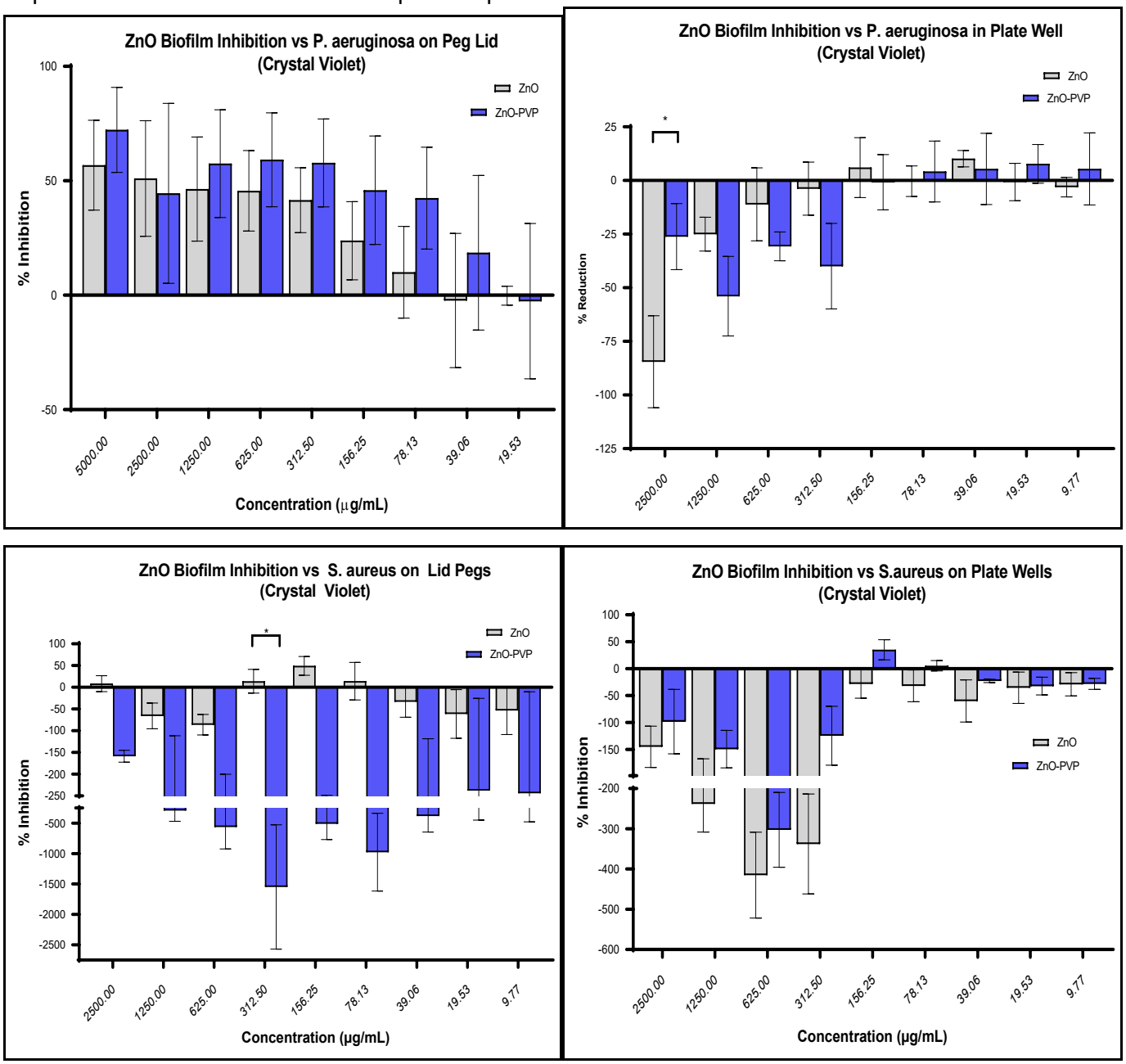

Figure 5.15 *Crystal Violet Evaluation of Zinc Oxide Biofilm Growth Inhibition*.
Bars represent mean % inhibition of biofilm growth by zinc oxide (ZnO) and zinc oxide following HME (ZnO-PVP) across a range of concentrations (µg/mL) against S. aureus and P. aeruginosa biofilm forming bacteria. Biofilms were quantified by use of crystal violet staining, solubilisation, and measurement of absorbance. Inhibition was determined by reduced physical biofilm growth in comparison to the untreated growth control (GC), following 24 hours incubation, at 37°C. Significant changes in values before and after polymer incorporation were determined by use of two-way ANOVA, with Sidak's multiple comparisons test, and expressed in terms of P value following the APA style (* $p<0.05$, ** $p<0.01$, *** $p<0.001$). Error bars represent SEM, N=3.

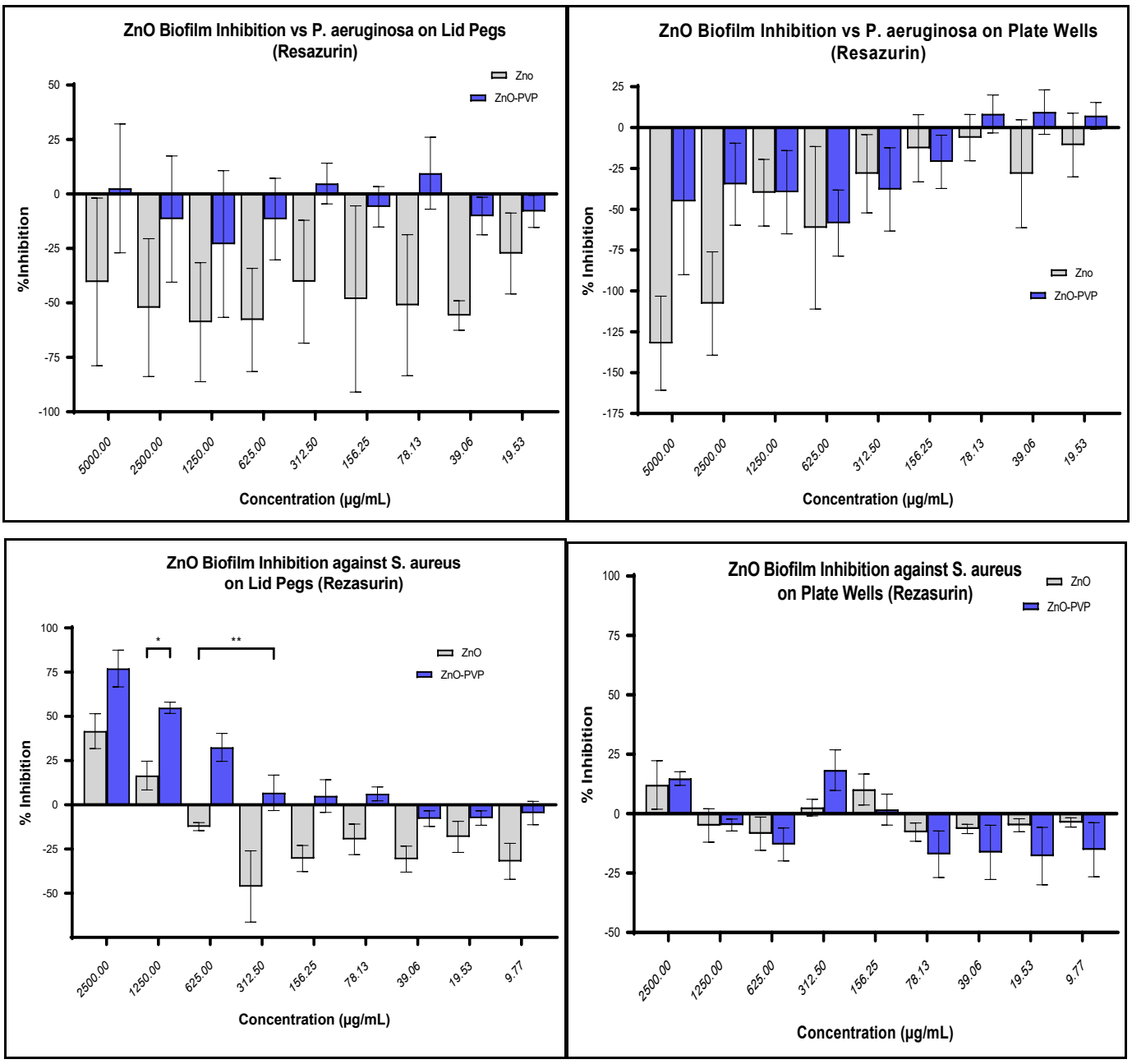

Figure 5.16 *Resazurin Evaluation of Zinc Oxide Biofilm Inhibition*.
Bars represent mean % inhibition of biofilm development by zinc oxide (ZnO) and zinc oxide following HME (ZnO-PVP), across a range of concentrations (µg/mL) against S. aureus and P. aeruginosa biofilms. Biofilm growth inhibition was determined by reduced bacterial populations in the final biofilm following 24 hours incubation, at 37°C. Biofilms were exposed to resazurin solution and converted resazurin was measured fluorescently (Excitation: 528/20, Emission: 590/35). Responses from treated biofilms were compared to response of untreated growth control (GC) biofilm to determine differences in cell numbers. Significant changes in values before and after polymer incorporation were determined by use of two-way ANOVA, with Sidak's multiple comparisons test, and expressed in terms of P value following the APA style (* $p<0.05$, ** $p<0.01$, *** $p<0.001$). Error bars represent SEM, N=3.

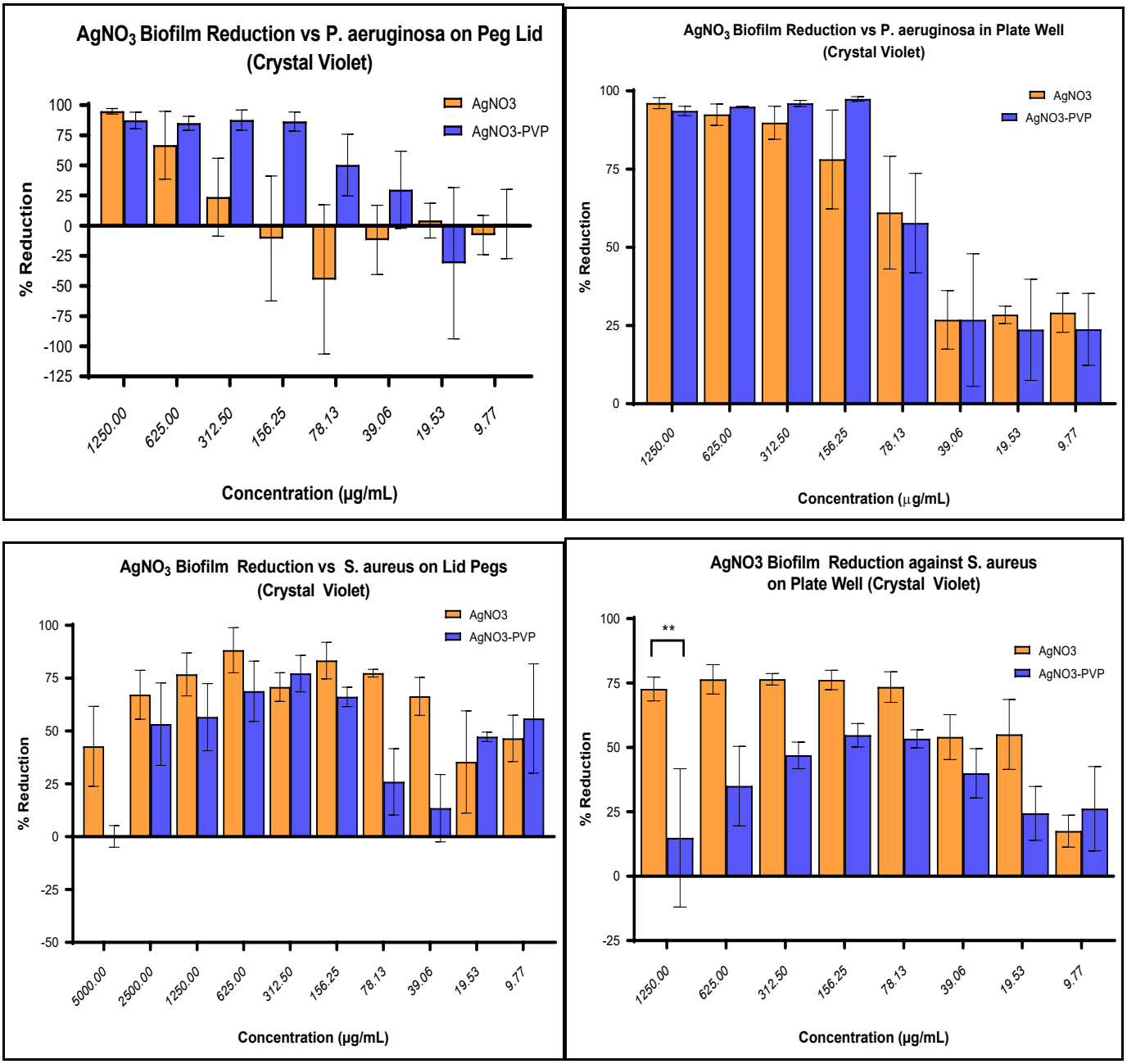

Figure 5.17 *Crystal Violet Evaluation of Silver Nitrate Biofilm Reduction*.
Bars represent mean % reduction of biofilm formations by silver nitrate (AgNO3) and silver nitrate following HME (AgNO3-PVP), across a range of concentrations (µg/mL) against *S. aureus* and *P. aeruginosa* biofilms. Physical biofilms were quantified by use of crystal violet staining, solubilisation, and measurement of absorbance (595nm). Reduction was determined by reduced crystal violet response following treatment in comparison to the untreated growth control (GC) biofilms following 24 hours incubation, at 37°C. Significant changes in values before and after polymer incorporation were determined by use of two-way ANOVA, with Sidak's multiple comparisons test, and expressed in terms of P value following the APA style (* $p<0.05$, ** $p<0.01$, *** $p<0.001$). Error bars represent SEM, N=3.

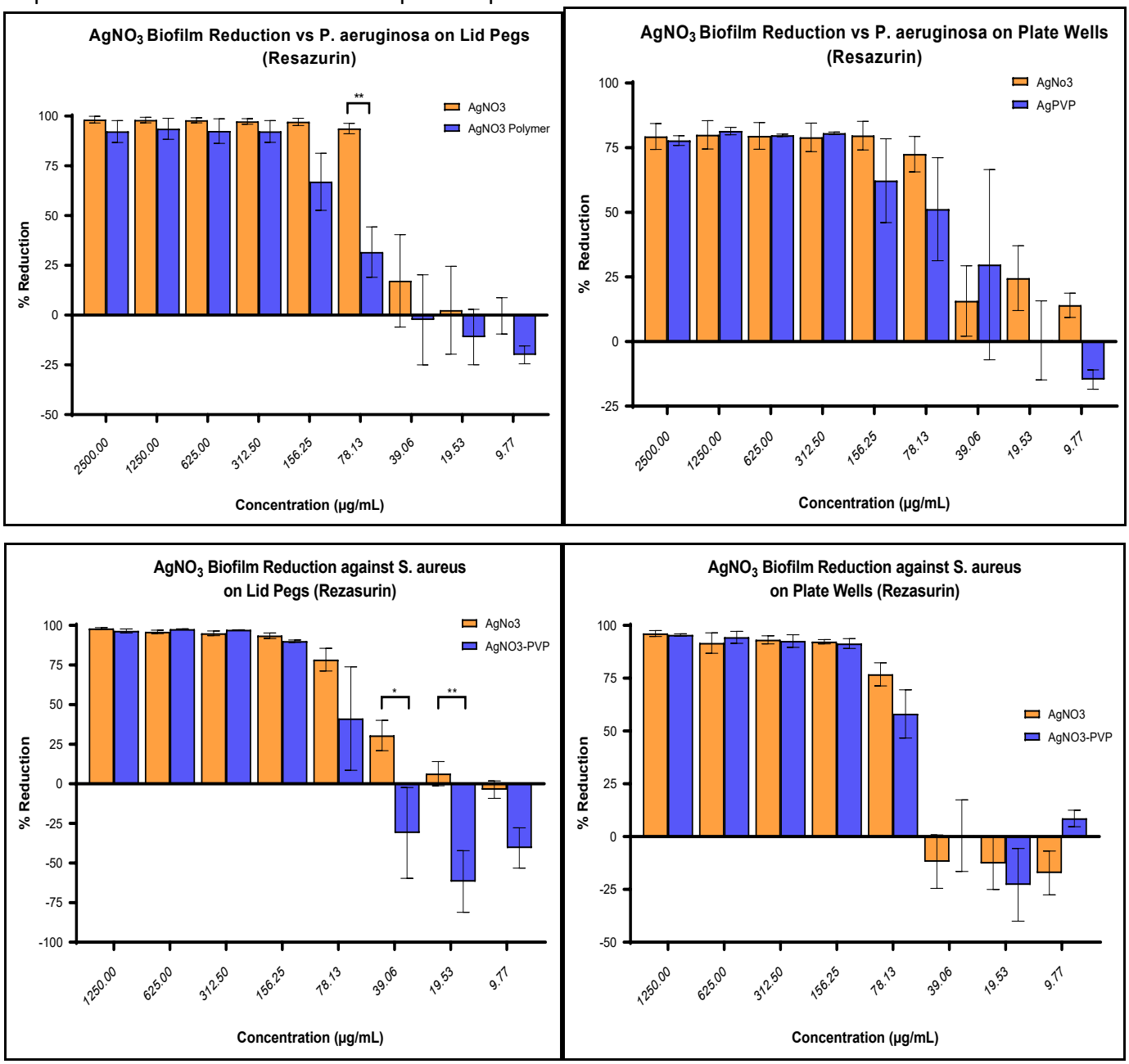

Figure 5.18 *Resazurin Evaluation of Silver Nitrate Biofilm Reduction*.
Bars represent mean % reduction of developed biofilms by silver nitrate (AgNO3) and silver nitrate following HME (AgNO3-PVP), across a range of concentrations (µg/mL) against S. aureus and P. aeruginosa biofilms. Biofilm reduction was determined by reduced bacterial populations in the biofilm following 24 hours incubation (37°C) with treatment exposure. Biofilms were subsequently exposed to resazurin solution and converted resazurin was measured fluorescently (Excitation: 528/20, Emission: 590/35). Responses from treated biofilms were compared to response of untreated growth control (GC) biofilm to determine differences in cell numbers. Significant changes in values before and after polymer incorporation were determined by use of two-way ANOVA, with Sidak's multiple comparisons test, and expressed in terms of P value following the APA style (* $p<0.05$, ** $p<0.01$, *** $p<0.001$). Error bars represent SEM, N=3.

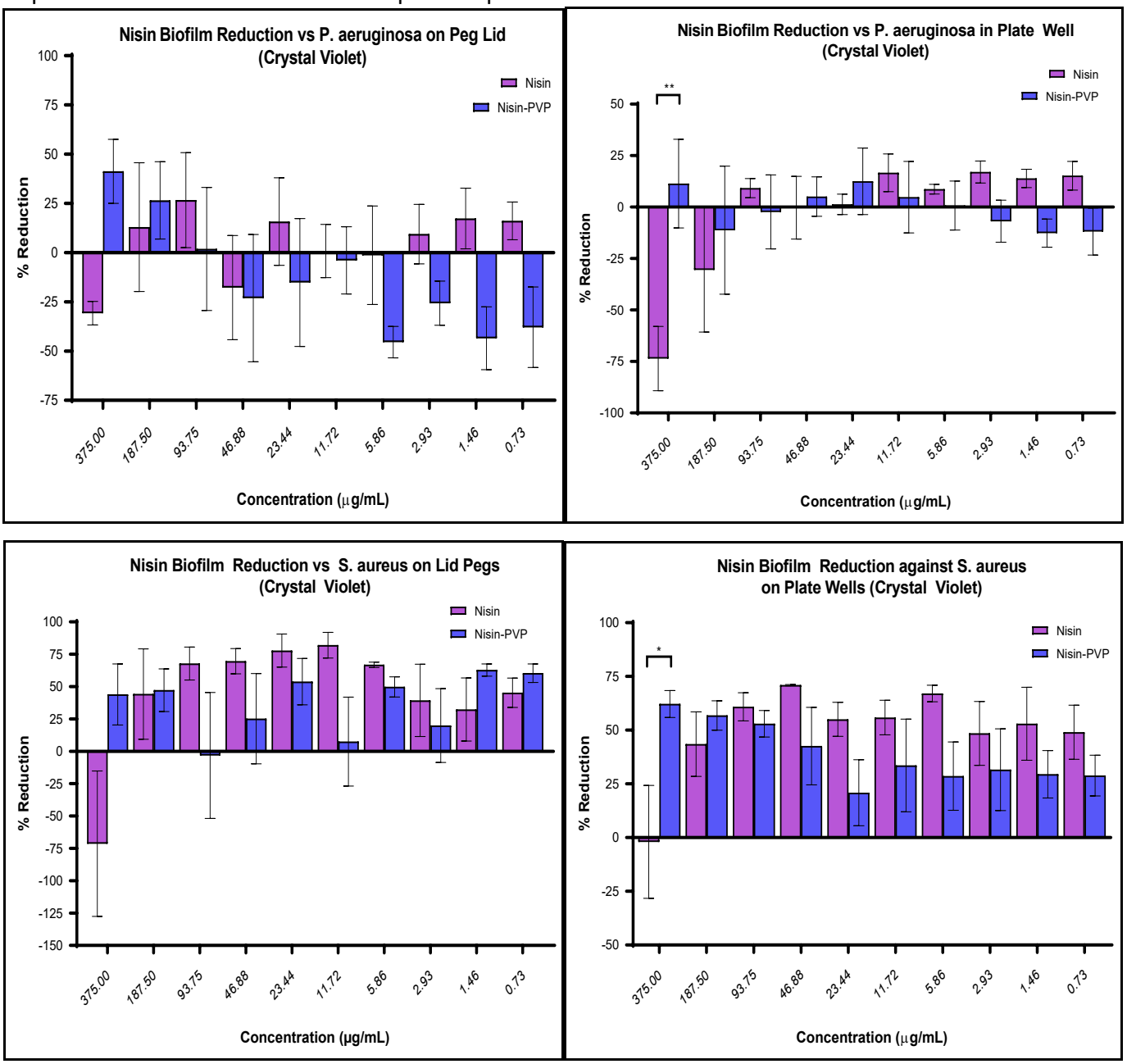

Figure 5.19 *Crystal Violet Evaluation of Nisin Biofilm Reduction*.
Bars represent mean % reduction of biofilm formations by nisin and nisin following HME (nisin-PVP), across a range of concentrations (µg/mL) against S. aureus and P. aeruginosa biofilms. Physical biofilms were quantified by use of crystal violet staining, solubilisation, and measurement of absorbance (595nm). Reduction was determined by reduced crystal violet response following treatment in comparison to the untreated growth control (GC) biofilms following 24 hours incubation, at 37°C. Significant changes in values before and after polymer incorporation were determined by use of two-way ANOVA, with Sidak's multiple comparisons test, and expressed in terms of P value following the APA style (* $p<0.05$, ** $p<0.01$, *** $p<0.001$). Error bars represent SEM, N=3.

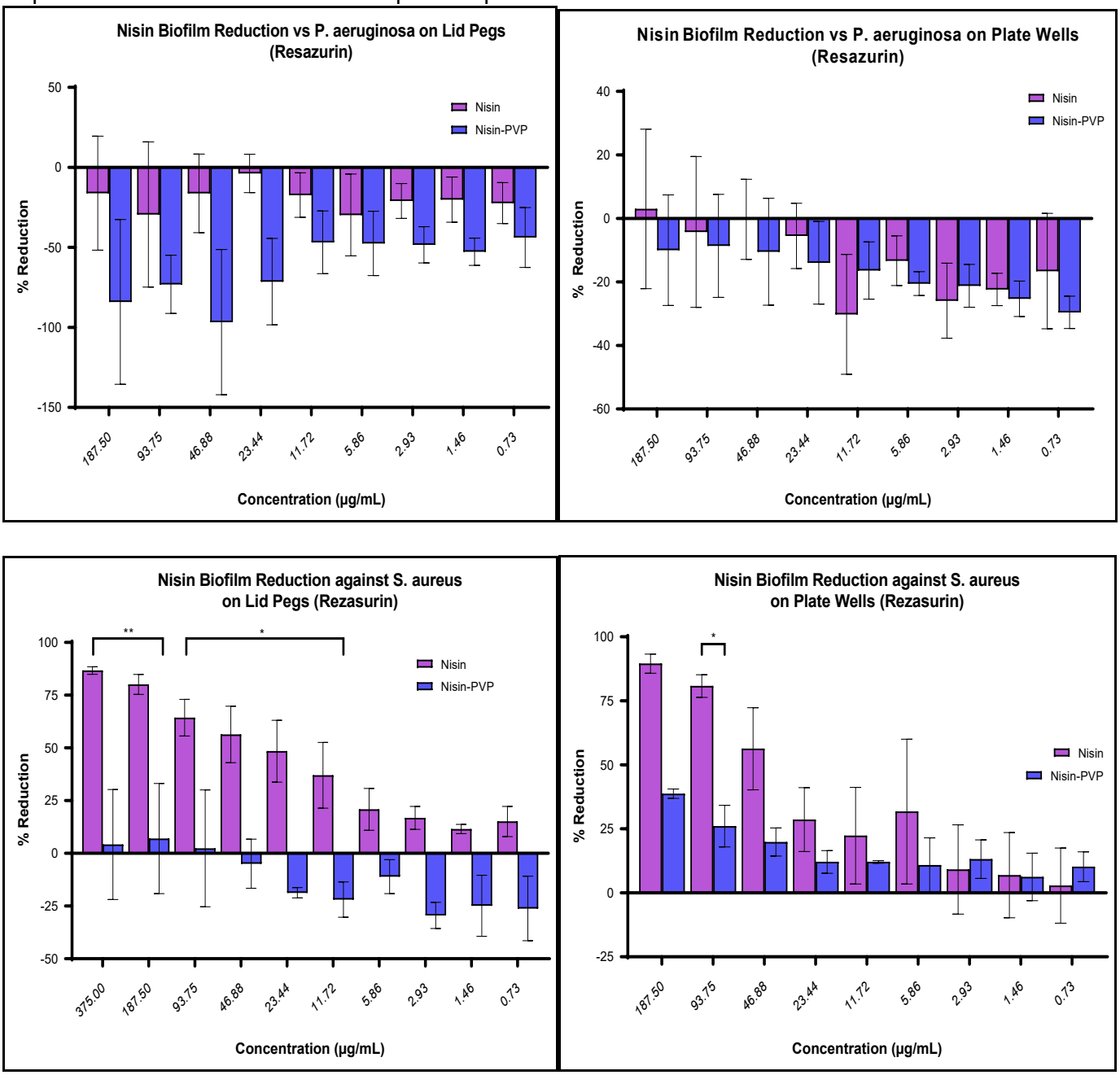

Figure 5.20 *Resazurin Evaluation of Nisin Biofilm Reduction*.
Bars represent mean % reduction of developed biofilms by nisin and nisin following HME (Nisin-PVP), across a range of concentrations (µg/mL) against S. aureus and P. aeruginosa biofilms. Biofilm reduction was determined by reduced bacterial populations in the biofilm following 24 hours incubation (37°C) with treatment exposure. Biofilms were subsequently exposed to resazurin solution and converted resazurin was measured fluorescently (Excitation: 528/20, Emission: 590/35). Responses from treated biofilms were compared to response of untreated growth control (GC) biofilm to determine differences in cell numbers. Significant changes in values before and after polymer incorporation were determined by use of two-way ANOVA, with Sidak's multiple comparisons test, and expressed in terms of P value following the APA style (* $p<0.05$, ** $p<0.01$, *** $p<0.001$). Error bars represent SEM, N=3.

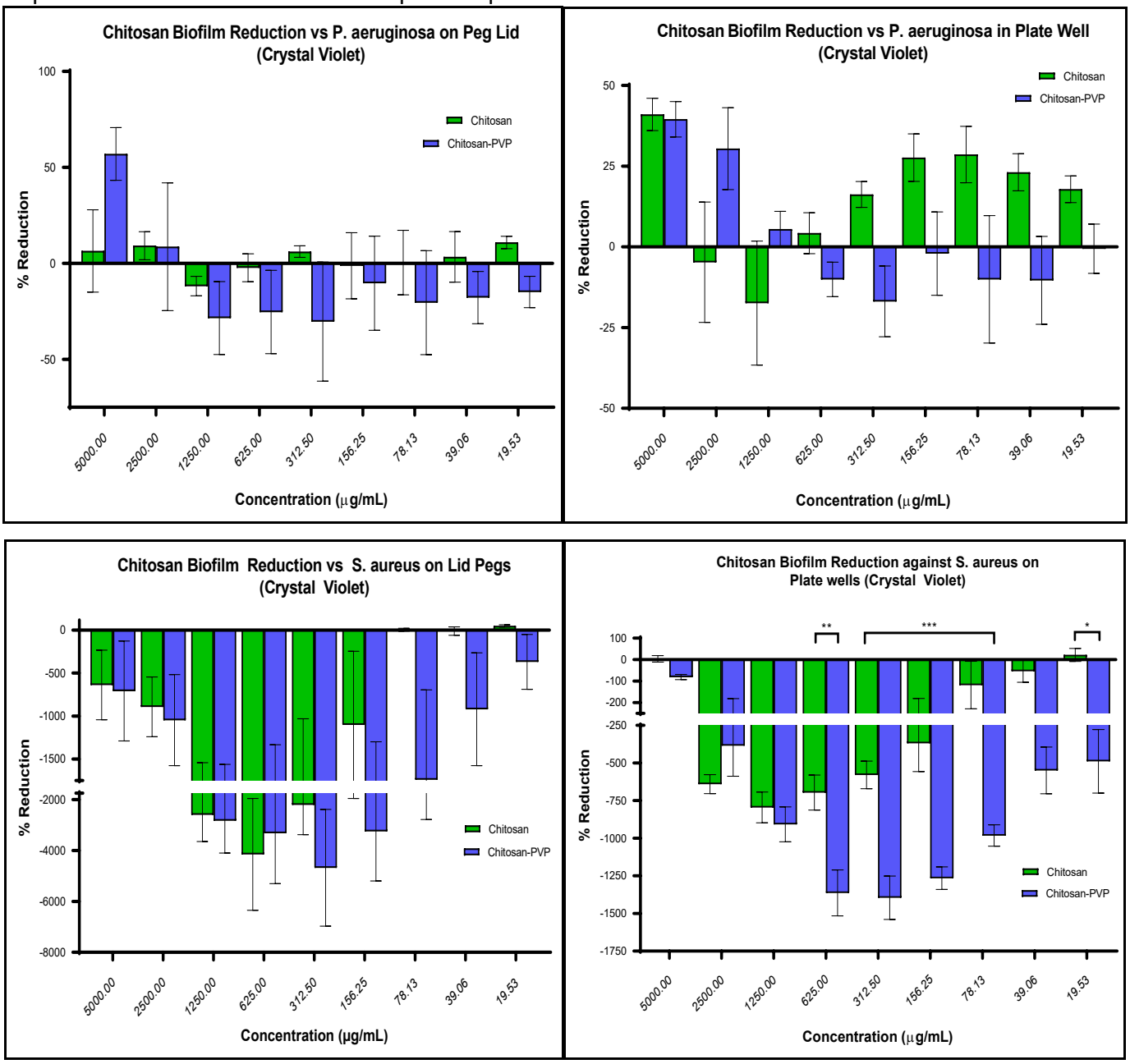

Figure 5.21 *Crystal Violet Evaluation of Chitosan Biofilm Reduction*.
Bars represent mean % reduction of biofilm formations by chitosan and chitosan following HME (chitosan-PVP), across a range of concentrations (µg/mL) against S. aureus and P. aeruginosa biofilms. Physical biofilms were quantified by use of crystal violet staining, solubilisation, and measurement of absorbance (595nm). Reduction was determined by reduced crystal violet response following treatment in comparison to the untreated growth control (GC) biofilms following 24 hours incubation, at 37°C. Significant changes in values before and after polymer incorporation were determined by use of two-way ANOVA, with Sidak's multiple comparisons test, and expressed in terms of P value following the APA style (* $p<0.05$, ** $p<0.01$, *** $p<0.001$). Error bars represent SEM, N=3.

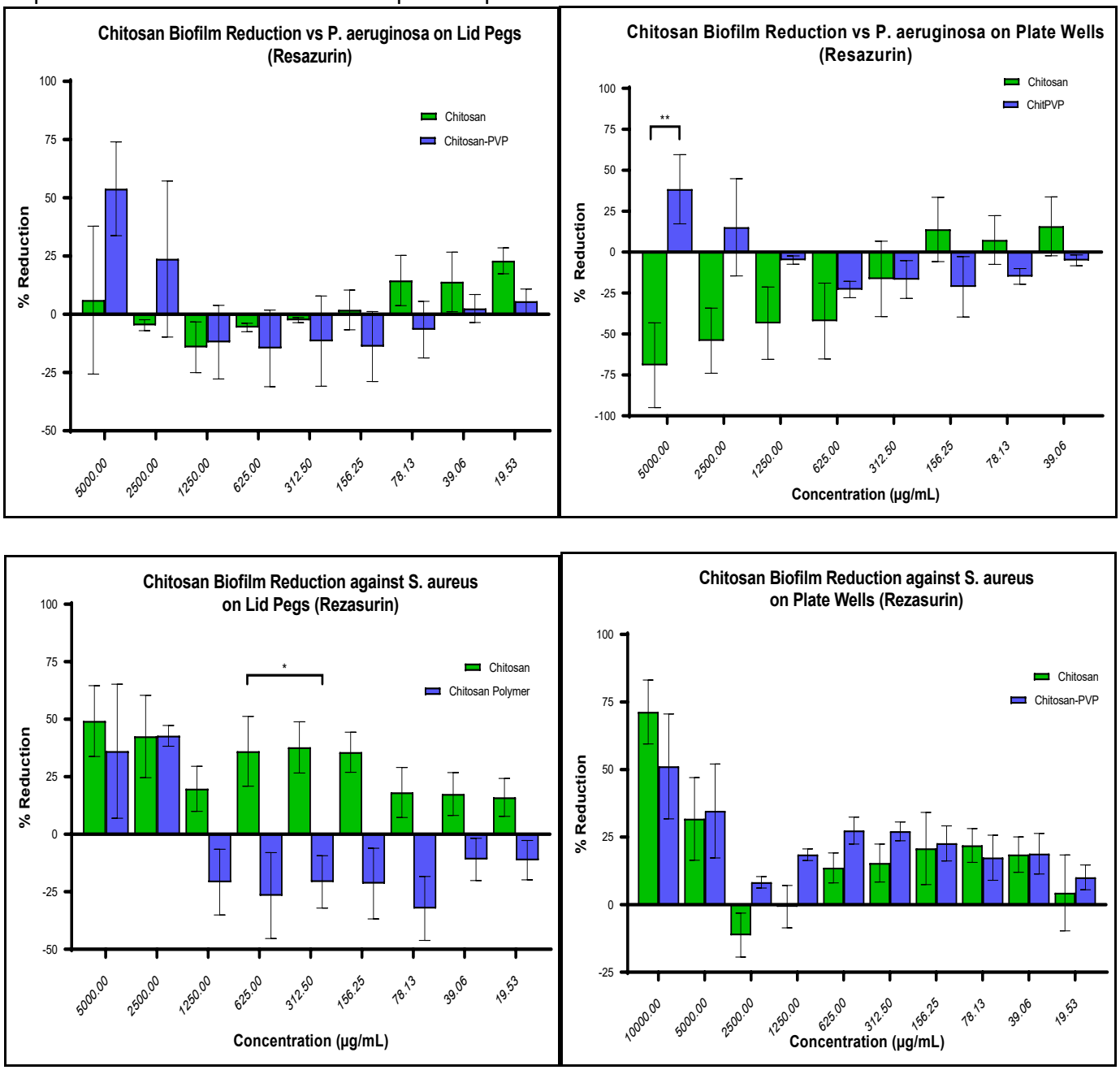

Figure 5.22 *Resazurin Evaluation of Chitosan Biofilm Reduction*.
Bars represent mean % reduction of developed biofilms by chitosan and chitosan following HME (Chitosan-PVP), across a range of concentrations (µg/mL) against S. aureus and P. aeruginosa biofilms. Biofilm reduction was determined by reduced bacterial populations in the biofilm following 24 hours incubation (37°C) with treatment exposure. Biofilms were subsequently exposed to resazurin solution and converted resazurin was measured fluorescently (Excitation: 528/20, Emission: 590/35). Responses from treated biofilms were compared to response of untreated growth control (GC) biofilm to determine differences in cell numbers. Significant changes in values before and after polymer incorporation were determined by use of two-way ANOVA, with Sidak's multiple comparisons test, and expressed in terms of P value following the APA style (* $p<0.05$, ** $p<0.01$, *** $p<0.001$). Error bars represent SEM, N=3.

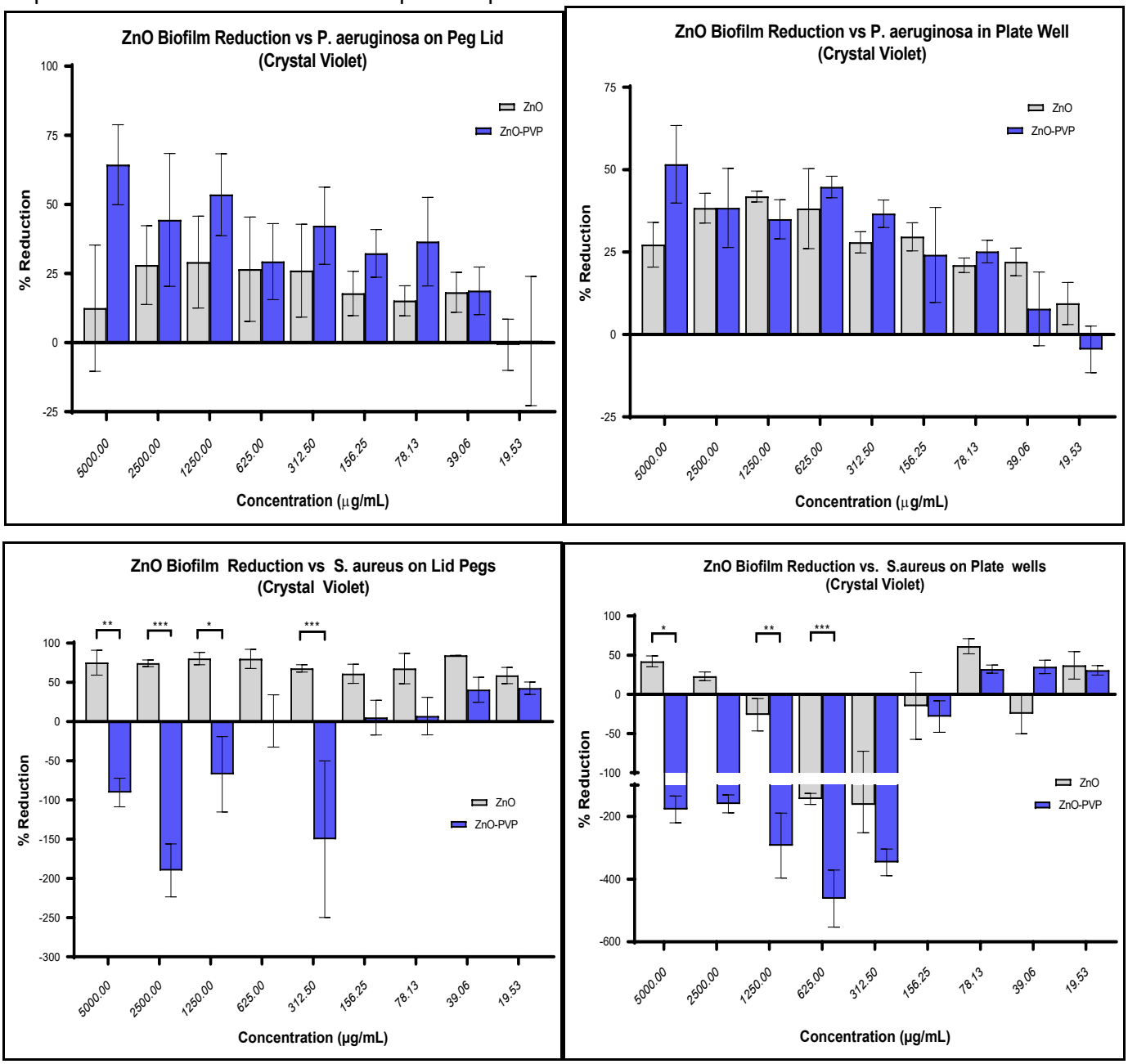

Figure 5.23 *Crystal Violet Evaluation of Zinc Oxide Biofilm Reduction*.
Bars represent mean % reduction of biofilm formations by zinc oxide (ZnO) and zinc oxide following HME (ZnO-PVP), across a range of concentrations (µg/mL) against S. aureus and P. aeruginosa biofilms. Physical biofilms were quantified by use of crystal violet staining, solubilisation, and measurement of absorbance (595nm). Reduction was determined by reduced crystal violet response following treatment in comparison to the untreated growth control (GC) biofilms following 24 hours incubation, at 37°C. Significant changes in values before and after polymer incorporation were determined by use of two-way ANOVA, with Sidak's multiple comparisons test, and expressed in terms of P value following the APA style (* $p<0.05$, ** $p<0.01$, *** $p<0.001$). Error bars represent SEM, N=3.

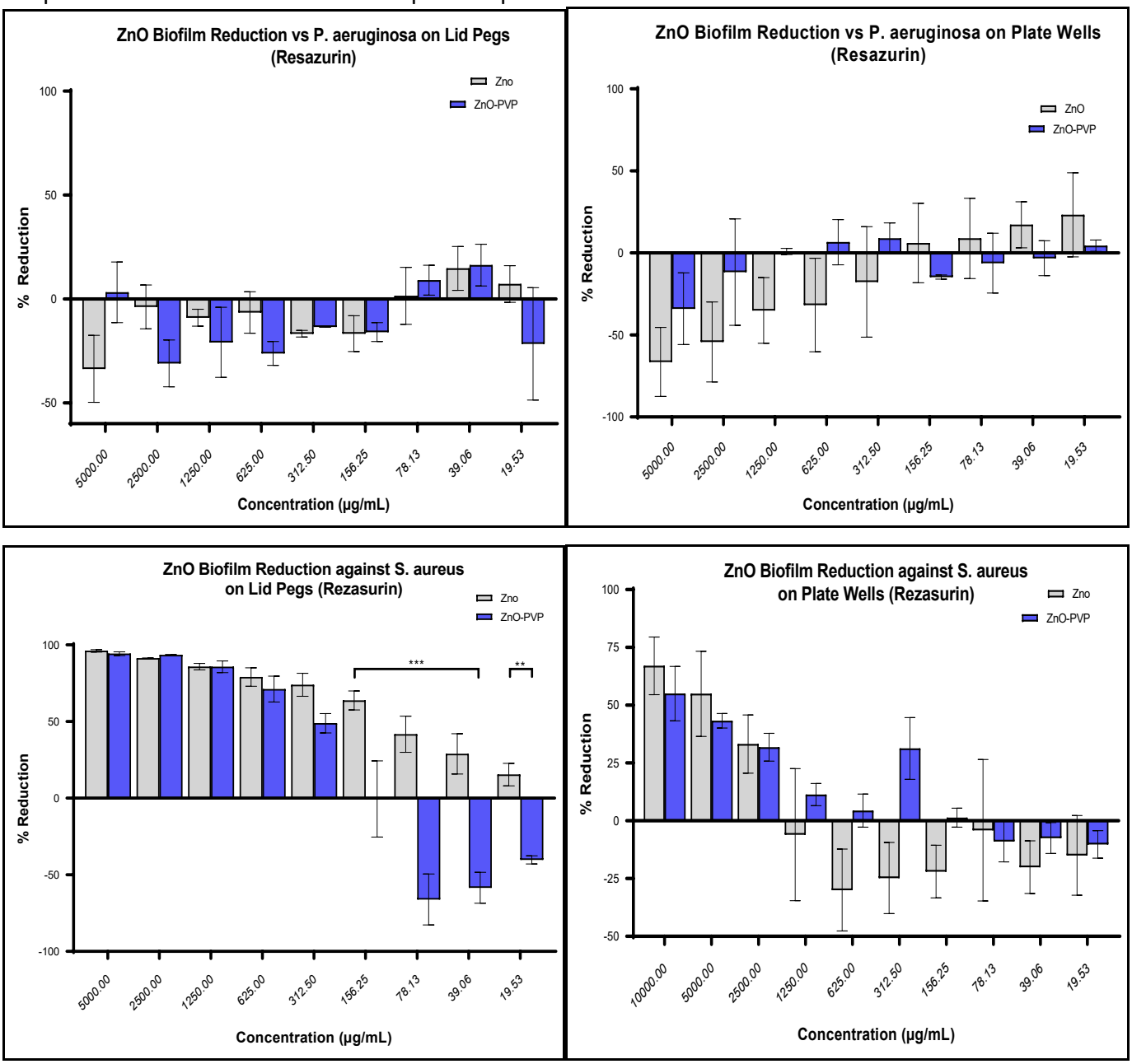

Figure 5.24 *Resazurin Evaluation of Zinc Oxide Biofilm Reduction*.
Bars represent mean % reduction of developed biofilms by zinc oxide (ZnO) and zinc oxide following HME (ZnO-PVP), across a range of concentrations (µg/mL) against S. aureus and P. aeruginosa biofilms. Biofilm reduction was determined by reduced bacterial populations in the biofilm following 24 hours incubation (37°C) with treatment exposure. Biofilms were subsequently exposed to resazurin solution and converted resazurin was measured fluorescently (Excitation: 528/20, Emission: 590/35). Responses from treated biofilms were compared to response of untreated growth control (GC) biofilm to determine differences in cell numbers. Significant changes in values before and after polymer incorporation were determined by use of two-way ANOVA, with Sidak's multiple comparisons test, and expressed in terms of P value following the APA style (* $p<0.05$, ** $p<0.01$, *** $p<0.001$). Error bars represent SEM, N=3.

5.7 Tables

Table 5.1 Summary of Physical Biofilm Disruptive Capabilities. Table summarises the effects of silver nitrate ($AgNO_3$), nisin, chitosan and ZnO before and after incorporation with the PVPVA64 polymer against *P. aeruginosa* and *S. aureus* physical biofilm development as determined by crystal violet analysis. Effects are averaged based on their effects against biofilm development at bacterial attachment, biofilm growth inhibition or formed biofilm reduction on both peg lids and plate well walls. Effects are scaled from +++ (High inhibition/reduction) to --- (High promotion/increase), with o marking an averaged "no effect".

	Physical Biofilm Disruptive Effects					
	Attachment Inhibition		**Biofilm Inhibition**		**Biofilm Reduction**	
	P. aeruginosa	*S. aureus*	*P. aeruginosa*	*S. aureus*	*P. aeruginosa*	*S. aureus*
$AgNO_3$	+++	--	+++	+	++	++
$AgNO_3$-PVP	++	--	+++	---	+++	+
Nisin	+	+	--	++	o	+
Nisin-PVP	o	+	---	++	-	+
Chitosan	o	--	o	---	+	---
Chitosan-PVP	o	---	--	---	-	---
ZnO	+	---	o	--	+	+
ZnO-PVP	--	---	+	---	++	---

Table 5.2 Summary of Internal Biofilm Population Disruptive Capabilities. Table summarises the effects of silver nitrate ($AgNO_3$), nisin, chitosan and ZnO before and after incorporation with the PVPVA64 polymer against *P. aeruginosa* and *S. aureus* internal biofilm populations as determined by resazurin analysis. Reported results are averaged based on their effects against final internal biofilm populations from treatment at bacterial attachment, biofilm growth inhibition or against formed biofilms on both peg lids and plate well walls. Effects are scaled from +++ (High inhibition/reduction) to --- (High promotion/increase), with o marking an averaged "no effect".

	Internal Bacterial Population Disruptive Effects					
	Attachment Inhibition		**Biofilm Inhibition**		**Biofilm Reduction**	
	P. aeruginosa	*S. aureus*	*P. aeruginosa*	*S. aureus*	*P. aeruginosa*	*S. aureus*
$AgNO_3$	+++	o	+++	++	+++	+++
$AgNO_3$-PVP	--	--	++	++	+++	+++
Nisin	o	++	--	++	-	++
Nisin-PVP	-	o	---	o	--	o
Chitosan	+	+	---	-	-	+
Chitosan-PVP	---	--	--	o	o	o
ZnO	--	o	---	-	-	++
ZnO-PVP	--	-	-	+	-	++

Chapter 6 Synergy Assessment of Bioactives

6.1 Introduction

While there are vast number of antimicrobial compounds in use today, many have specific modes of action and thus have a narrow effective spectrum in terms of the bacterial species which they can target (Acuña, Morero, and Bellomio 2011). A common method used across a number of various research areas is the use of two or more treatments in combination to treat a single target (Torres et al. 2018; Fisher et al. 2015; Palou et al. 2016; Bollenbach 2015). Resulting effects from combination therapy can be described as synergistic, additive, or antagonistic (Bollenbach 2015; Yadav et al. 2015; Torres et al. 2018). Synergy describes a total effect greater than the sum of the individual effects. An additive effect describes that the combined drugs exhibit a total effect equal to the sum of the individual effects, no lesser nor greater. An antagonistic effect describes combinations where the total effect is lessened compared to the sum of the individual effects (Tang, Wennerberg, and Aittokallio 2015). Combination therapies that result in an overall synergistic effect can allow for much greater impact from treatments that would normally hold less or perhaps no effect alone. While co-treatment therapies have been widely used in the treatment of diseases such as cancer, there is a rising interest in the synergistic abilities of previously established antimicrobial compounds (Duss et al. 2019; Torres et al. 2018; Tomasinsig et al. 2010). Antimicrobial synergy holds great promise for a number of reasons. While a bacterial species may hold or even develop resistance against a single treatment, co-treatment with an alternative compound which carries an alternative mode of action, could alleviate this issue. Additionally, certain groups of bacteria hold intrinsic metabolic or physical characteristics which can prevent certain classes of antimicrobials from exhibiting their effect. Co-treatment with a compound that can disrupt these characteristics would allow the primary treatment to carry out its effect unimpeded. Gram-negative bacteria are an example of one such group, having an additional, outer membrane with can act to prevent compounds from reaching their target ligands. Following this example, nisin is a poly-cyclic lantibiotic which targets the inner-membrane bound lipid II molecule. Due to the presence of an outer membrane, nisin is prevented from reaching its target rendering it ineffective (L. He et al. 2016; Ruhr and Sahl 1985). However, in theory it would be possible to enable nisin by combining it in treatment

with an additional compound that targets the outer membrane. By removing the outer membrane or compromising its integrity, nisin would be allowed to freely interact with its lipid-II target. While this interaction can be clearly deemed synergistic, it is not enough on its own to observe a positive end result from the combination. In order to determine synergistic abilities of two or more compounds, it is necessary to assess an array of various concentrations in different combinations. It is not important to determine the highest effect of combined treatments, the concept is to instead determine combinations that express a higher effect in comparison to that of the individual drugs at the same concentrations. The aim is to more so discern the ratio of each drug required to enable each other's mechanism of action, thus giving the most efficient synergy.

There are a number of models and indexes used to evaluate interactions between combined treatments. One of the more commonly seen indexes in the study of antimicrobial combinations is the fractional inhibitory concentration (FIC) index. The FIC index analyses the MIC of individual treatments in combination and compares it to that of the MIC of treatments alone. The FIC index uses the following equation:

$$FIC_I = \left(\frac{MIC_{A-B}}{MIC_A}\right) + \left(\frac{MIC_{B-A}}{MIC_B}\right)$$

Where MIC_A and MIC_B represent the MIC values of two agents to be analysed. A FIC_I value close to 1 indicates an *additive* effect, >1 indicates *synergistic* and <1 indicates *antagonistic*.

The FIC model, however, holds a number of drawbacks. This basic format does not determine synergy/antagonism, but only gives a simple trend overview. As previously mentioned, it is not enough to show increased effect, as this does not indicate the treatments are having an effect upon each other. Furthermore, the formula only uses MIC values, which not only restricts its use to bacterial and fungal studies, but it also limits the amount of information that can be gained from such studies, requiring all treatments to have an MIC value. Also, by using concentrations as an input, this demands the treatments be in a similar concentration range/format. Despite these drawbacks, the FIC models are still used for studies involving microorganisms (Kim et al. 2017; Fatsis-Kavalopoulos et al. 2020).

With the aim of analysing drug interactions and their combined effect, the FIC is not suitable. However, there is a great number of alternative models developed through pharmaceutical

studies which hold greater means for analysing drug interactions and have valuable potential in antimicrobial research. The majority of drug synergy analysis models in use today fall under one of two major principles, the Dose Equivalence Principle (DEP), introduced by Loewe in 1926, or the Multiplicative Survival Principle (MSP) introduced by Bliss in 1939 (Tang, Wennerberg, and Aittokallio 2015). There have been numerous models developed from these initial Loewe and Bliss models, however there is no universal standard for the determination of synergy. In 1992, a committee in Saariselkä, Finland gathered to find a consensus between models allowing a framework for the comparison and interpretation of drug combination studies. However, they were unable to conclude on a suitable framework, and only agreed on a compromise for studies to report on how their synergy scores were determined (Tang, Wennerberg, and Aittokallio 2015). Recent years have seen the development of additional models, such as the Zero Interaction Potency (ZIP) model, built off the Bliss model with the intent of establishing a standard model that also overcomes drawbacks seen in existing models (Yadav et al. 2015). Another model from Vanderbilt University, called the Multidimensional Synergy of Combinations (MuSyC) model, is the most recent endeavour at developing a universal standard for drug synergy analysis (D. Wooten et al. 2019). The MuSyC model, based on the Law of Mass Action, combine the DEP and MSP principles, attempting to unify both avenues of thought on synergy models.

In addition to these recent models, there have been a number of tools developed to aid in analysing combinational interactions, allowing for mass data input/output, while also generating graphs. Some such tools are available as downloadable programs. *Combenefit* is one such program developed at the University of Cambridge (Di Veroli et al. 2016). *Combenefit* was designed for analysis of cancer therapeutics and performs using three models: Loewe, Bliss and Highest Single Agent (HSA) models. CompuSyn is another program, developed in 2005 under Dr. Chou *et al.* which uses the median-effect principle of mass-action law and the combination index (CI) theorem (Chou and Martin 2007). Other tools, such as *SynergyFinder*, are online based applications for determining synergy (Ianevski et al. 2017; Ianevski, Giri, and Aittokallio 2020). *SynergyFinder* was developed by the group who designed the ZIP model; however it also allows for analysis by Bliss, Loewe and HSA. Finally, there are a number of packages available for use in R and Python coding language environments. The *SynergyFinder* app was developed using the R coding language, and its R package is still

available. The Vanderbilt University research group, while developing their MuSyC model, also compiled an extensive Python library for synergy analysis. The library, simply called *synergy*, includes many different synergy frameworks such as Zimmer, BRAID, Bliss, Loewe, HSA, CI, ZIP, Schindler, as well as their own MuSyC model (D. J. Wooten et al. 2021).

While most drug combination studies focus on two-drug interactions, there is increasing interest in developing higher-order studies involving three or more drug combinations. Recent developments in synergy tools has greatly enabled such studies. From the previously mentioned tools, the *synergy* python package is the most capable for multi-drug analysis. *SynergyFinder* does have the capacity for three-drug, but only *synergy* can analyse up to four drugs. In conjunction with the tools utilised, only certain synergy models are able to support multi-drug synergy analysis. In the *synergy* library, for example, only Bliss, Loewe, HSA, CI, MuSyC and Schindler are supported for three or more drug combinations.

As evident from previous studies, analysis of drug interactions holds many benefits in the development of new treatments (Huang et al. 2019; Cokol-Cakmak et al. 2020; Lewis 2010). High through-put analysis also allows for rapid, large-scale determination of effective and ineffective combinations, which can allow treatments to be removed while in-process towards a final product. As findings reported in Chapter 4 have established the individual antibacterial capabilities of $AgNO_3$, nisin, chitosan and ZnO, determination of their combined effects would be the appropriate follow up study. This is an important step towards fulfilling the project's specific aim and hypothesis, as the bioactives are to be incorporated into the polymer, it is crucial that they do not hinder each other's activity. Furthermore, if the bioactives are found to hold synergistic interactions, this would be thoroughly beneficial in the development of a broad-spectrum antibiotic alternative. Previously, $AgNO_3$ was shown to be the most effective bacterial growth inhibitor versus all tested species. Nisin was shown to have very efficient inhibitory effects against test Gram-positive bacterial species, with no effect versus Gram positive. Both compounds differ majorly in their modes of action, with $AgNO_3$ permeating bacterial membranes through reactive silver ions (Ag^{2+}), while nisin has specific binding affinity towards the lipid-II molecules bound in the inner bacterial membrane. Nisin's inability to affect Gram-negative bacteria lie with its inability to breach its outer membrane and interact with the lipid-II ligand. By combining both $AgNO_3$ and nisin, it is hypothesised that the reactive Ag^{2+} ions of $AgNO_3$ with breach the Gram-negative outer

bacterial membrane, allowing nisin to reach its target ligand(Pandian et al. 2010; Prabhu and Poulose 2012; Gut, Blanke, and Van Der Donk 2011; Van Heusden, De Kruijff, and Breukink 2002). Similar hypothesises can be made with ZnO and nisin, as ZnO held efficacy versus Gram-negative and Gram-positive, and also has a similar mode of action wherein it destabilises membranes through release of Zn^{2+} ions and reactive oxygen species (ROS) (Pasquet, Chevalier, Couval, et al. 2014; Espitia et al. 2012; Pasquet, Chevalier, Pelletier, et al. 2014; Fiedot-Toboła et al. 2018). Chitosan also held noteworthy effect versus all test strains but holds an alternate mechanism in which it targets the bacterial cell wall (Qin et al. 2006; Kunjachan and Jose 2010). The varying mechanisms hold great significance combination studies and will allow us to observe if effects do indeed unlock one another's drawbacks ($AgNO_3$-nisin, ZnO-Nisin), stack upon one another ($AgNO_3$-ZnO) or complement one another (Chitosan-Nisin, Chitosan-$AgNO_3$, Chitosan-ZnO). Studies will initially be carried out using two-drug combinations, followed by three-drug and finally four-drug. In theory, a four-drug combination would be sufficient, but for the purpose of analysing all interactions and with the fact that these particular methods for synergy determination have not been properly utilised in microbial studies previously, they will be carried out in their entirety at each combinational level. Due to the intended higher order combinations, results from these studies will be analysed by use of the *synergy* Python package, using the bliss model for two, three and four-drug combinations. The bliss model was chosen for its simplicity, it's well-established use, and ability to analyse higher order combinations. Studies will be carried out using *E. coli*, *S. aureus* and *S. epidermidis* as test bacterial species, which represent the commonly encountered bacterial pathogens related to mastitis as well as numerous other biofilm-mediated infections and diseases. Furthermore, *E. coli* and *S. aureus* are also commonly used representatives of Gram-negative and Gram-positive bacteria respectively.

6.2 Aims and Hypothesis

The aim of this study is a to assess the interactions between four chosen antimicrobial bioactives versus *E. coli*, *S. aureus* and *S. epidermidis*. The individual antimicrobial properties have already been assessed (Chapter 4) and they will now be evaluated together in combinations of two, three and four.

The hypothesis of the study states that the four bioactive compounds, $AgNO_3$, nisin, chitosan and ZnO will hold a synergistic, antimicrobial effect while in combination, enabling them to inhibit both Gram-positive and also Gram-negative species.

6.3 Results

6.3.1 Bliss Synergy Scores

Due to the number of combinations analysed during this study, only the three highest scoring interactions of each combination and their average will be reported and discussed upon. Three-drug and four-drug combinations with any zero concentration treatments will also be excluded, as these are not three or four-drug combinations (i.e. they would technically be two and three-drug combinations. Synergy scores represent the magnitude of the combination interactions, where a higher score indicates greater synergy, scores close to 0 indicate an additive effect while negative scores represent antagonism. Results are presented in Table 6.1 – 6.5. Tables show the drug combination, concentration of each individual drug (µg/mL), the % growth inhibition exhibited from the combination and the calculated bliss synergy score. The two-drug combination results are divided into separate tables by their target bacteria, *E. coli* (Table 6.1), *S. aureus* (Table 6.2) and *S. epidermidis* (Table 6.3). Two-drug combination results are also presented in terms of a heat map which gives a visual representation of the entire combination of treatments (Figure 6.1 – 6.6) and also as X/Y plots showing top three combinations against each bacterial species (Figure 6.7, A-F). Three-drug combination results are presented in Table 6.4 and Figure 6.8, A-D. Four-drug combinations are presented in Table 6.5 and Figure 6.9.

- **Two-drug Combinations**

$AgNO_3$ – Chitosan

$AgNO_3$ and Chitosan reported good synergistic interactions against each bacterial strain. The combination reported the highest average synergy score against *E. coli* (average 0.4) and *S. aureus* (average 0.32). While the average concentration of chitosan was similar to that of the MIC versus *E. coli*, $AgNO_3$ was reported in lower concentrations. The most effective combination versus *S. aureus* reported concentrations that were 1/2 the MIC, with an inhibition of approximately 69%. Results versus *S. epidermidis* reported good synergy overall, with much lower concentrations of each treatment exhibiting more effective inhibition, with

the second reported combination exhibiting 99% inhibition, with 1/3 the MIC of $AgNO_3$ and less than 1/2 the MIC of chitosan being used.

Nisin – $AgNO_3$

Nisin and $AgNO_3$ demonstrated a number of highly synergistic combinations (average 0.32 versus *E. coli*, average 0.24 versus *S. aureus*), while also reporting the highest two-drug score from this study (average 0.68 versus *S. epidermidis*). While the highest scoring combinations versus *E. coli* did not report inhibition exceeding 70%, there was moderate synergy observed with concentrations of 8.49 µg/mL $AgNO_3$ and 1.56 – 6.25 µg/mL nisin, which show promise compared single treatments in which $AgNO_3$ reported a MIC of 20.83 µg/mL, and nisin exhibited no effect. The third highest scoring combination versus *S. aureus* reported 99% inhibition, with less than 1/4 MIC of $AgNO_3$ and 1/10 MIC of nisin. The three highest scoring combinations versus *S. epidermidis* indicate a concentration of 10 µg/mL $AgNO_3$ to be most effective in enabling nisin, which was reported in relatively low concentrations, while still having notable effect upon bacterial growth.

$AgNO_3$ – ZnO

$AgNO_3$ and ZnO reported moderate synergy against *E. coli* (average 0.22) and *S. aureus* (average 0.26), and relatively high synergy versus *S. epidermidis* (average 0.44). The highest reporting *E. coli* combination exhibited 98.5% growth inhibition with a $AgNO_3$ concentration 1/4MIC, and ZnO concentration 1/2.5MIC, demonstrating a noticeable increase of efficacy in both treatments. *S. aureus* results reported lower concentrations of both $AgNO_3$ and ZnO exhibiting greater effect when combined. One reported combination exhibited 95.5% growth inhibition using 1/1.8MIC $AgNO_3$ and 1/2.5MIC ZnO. $AgNO_3$ and ZnO demonstrated the second highest scoring average of all two-drug combinations (average 0.44) versus *S. epidermidis*. Reported combinations exhibited effective growth inhibition at much lower concentrations, even reaching 95.4% growth inhibition with 1/1.6MIC $AgNO_3$ and 1/3.33MIC ZnO.

Nisin – Chitosan

Nisin and chitosan reported mixed results in combination. The highest scoring combinations were seen versus *S. aureus* (average 0.24); however the highest inhibition of these combinations reached only 50% with no major reduction seen in the concentrations of nisin or chitosan. Results versus *E. coli* show that greater concentrations of chitosan were needed

to enable nisin, however these concentrations exceeded the MIC of chitosan, making the combination ineffective. Results versus *S. epidermidis* demonstrated no major interactions, nearing a synergy score of 0 in all combinations. Only one combination reported effective synergy, exhibiting 87.3% inhibition with a score of 0.11, however the concentration of nisin used in this combination exceeded that of its MIC when tested alone.

Chitosan – ZnO

Chitosan and ZnO reported very few synergistic interactions versus *E. coli* (average 0.11), *S. aureus* (average 0.09) and *S. epidermidis* (average 0.27). Analysis of interactions versus *E. coli* show a high concentration of chitosan was required for synergy to be identified, however the amount of chitosan was 2xMIC and the synergy score relatively low. While synergy was seen versus *S. aureus* at quite low concentrations of the two highest scoring combinations, the exhibited growth inhibition was not noteworthy (3.1%, 2.6% respectively). Combinations versus *S. epidermidis* reported moderate synergy at quite low concentrations of each, however the inhibition did not exceed 31%.

Nisin – ZnO

Nisin and ZnO reported low synergy versus *E. coli* (average 0.08), *S. aureus* (average 0.06) and *S. epidermidis* (average 0.14). The highest scoring combination versus *E. coli* (0.09) did not yield noteworthy inhibition, while the next highest combinations reported concentrations of ZnO that exceed the MIC in order to enable nisin. Highest scoring combinations versus *S. aureus* reported low concentrations of each treatment, however they held no noteworthy growth inhibitory effect (3.7 – 14%). Combinations versus *S. epidermidis* exhibited moderate inhibitory effects, however the concentrations of ZnO exceeded that of the average MIC, and concentrations of nisin were not much lower that the previously reported MIC average.

- **Three-drug Combinations**

Chitosan – $AgNO_3$ – Nisin

Chitosan, $AgNO_3$ and nisin reported moderate to high synergy in growth inhibition versus *E. coli* (average 0.38), *S. aureus* (average 0.56), and *S. epidermidis* (average 0.43). While the higher scoring combinations versus *E. coli* included high concentrations of chitosan (80 – 160 µg/mL), reported concentrations of $AgNO_3$ were low (2 – 4 µg/mL) # with 99% inhibition.

Concentrations of nisin were rather high, relative to the other test species (3.91 – 7.81 µg/mL). The highest scoring combination versus *S. aureus* reported relatively low concentrations of each compound (78.13 µg/mL chitosan, 8 µg/mL $AgNO_3$, 10.63 µg/mL nisin), while expressing 99% inhibition. The second highest scoring combination showed similar concentrations and inhibition, however used twice the amount of $AgNO_3$ (16 µg/mL), which was still less than the previously reported MIC. The third highest scoring combination reported lower chitosan (39.06 µg/mL) but did not fully inhibit *S. aureus* growth (71.45%). These combinations versus *S. aureus* reported the second highest average score of all three-drug test combinations. Combinations versus *S. epidermidis* reported near full inhibition (92 – 96%) with good synergy and low concentrations of chitosan (39.06 – 78.13 µg/mL) and nisin (0.63 – 1.25 µg/mL) however concentrations of $AgNO_3$ were nearing the MIC (8 – 16 µg/mL).

Chitosan – $AgNO_3$ – ZnO

Chitosan, $AgNO_3$ and ZnO held moderately low synergy versus *E. coli* (average 0.14), *S. aureus* (average 0.28) and *S. epidermidis* (average 0.35), with combinations versus *E. coli* scoring the lowest of all three-drug combinations. *E. coli* were quite low, each of the reported combinations exhibited full inhibition (97.15 – 100%) with low concentrations of chitosan (40 – 80 µg/mL), $AgNO_3$ (0.5 – 4 µg/mL) and ZnO (20 µg/mL). The highest scores versus *S. aureus* reported consistently low concentrations of ZnO (62.5 µg/mL), with low concentrations of chitosan (39.06 – 78.13 µg/mL) and $AgNO_3$ (8 – 16 µg/mL) while growth inhibition high (97.55 – 98.32%). Combinations versus *S. epidermidis* reported good growth inhibition (87.95 – 98.4%), with relatively low concentrations of chitosan (20 – 40 µg/mL), $AgNO_3$ (2 – 4 µg/mL) and ZnO (10 µg/mL).

Nisin – $AgNO_3$ – ZnO

Nisin, $AgNO_3$ and ZnO reported strong synergy versus *E. coli* (average 0.36), *S. aureus* (average 0.38) and *S. epidermidis* (average 0.53). Results versus *E. coli* show that very high concentrations of nisin (31.25 µg/mL) were yielding high synergy with low concentrations of $AgNO_3$ (0.5 – 1 µg/mL) and ZnO (31.25 – 62.5 µg/mL), however growth inhibition did not exceed 77%. Combinations versus *S. aureus* reported moderate synergy with low concentrations of nisin (0.63 – 1.25 µg/mL), moderate concentrations of $AgNO_3$ (4 – 16 µg/mL) and moderate concentrations of ZnO (39.06 µg/mL). Combinations versus *S. epidermidis* reported the third highest average score synergy, with low concentrations of nisin (1.25 – 2.5

μg/mL), $AgNO_3$ (2 – 4 μg/mL) and ZnO (5 μg/mL), however these combinations exhibited low to moderate growth inhibition (33.6 – 72.3%).

Nisin – Chitosan – ZnO

Nisin, chitosan and ZnO reported low inhibition synergy versus *E. coli* (average 0.23) and *S. epidermidis* (average 0.21), however combinations versus *S. aureus* reported the highest synergy score across all three-drug combinations (average 0.83). Concentrations of the reported combinations versus *E. coli* indicate poor synergy between treatments, as there are high concentrations of chitosan (9.77 – 312.5 μg/mL) and ZnO (31.25 – 125 μg/mL) utilised. Combinations using the lower concentrations of each exhibited very low inhibition(26.6%).

The highest scoring combination (0.93) versus *S. aureus* reported low concentrations of nisin (3.91 μg/mL), chitosan (39.06 μg/mL) and ZnO (62.5 μg/mL), with high inhibition (98.7%). The second highest scoring combination (0.84) also reported low concentrations of nisin (0.977 μg/mL), chitosan (156.25 μg/mL) and ZnO (62.5 μg/mL), with high inhibition (99.4%). While the third highest scoring combination reported low concentrations of nisin (0.977 μg/mL), chitosan (78.13 μg/mL) and ZnO (62.5 μg/mL), the reported growth inhibition was moderate (71.5%). While results versus *S. epidermidis* reported low concentrations of nisin (0.98 – 1.95 μg/mL), chitosan (39.06 μg/mL) and ZnO (31.25 μg/mL), along with high growth inhibition (99%), there was little synergy observed as denoted by the two highest scores. The third highest scoring combination reported very high concentration of chitosan (625 μg/mL).

- **Four-drug Combination**

$AgNO_3$ – Nisin – Chitosan – ZnO

Chitosan, nisin, $AgNO_3$ and ZnO exhibited moderately high synergy in combination versus *E. coli* (average 0.36) and very high synergy versus *S. aureus* (average 0.91) and *S. epidermidis* (average 1.11). While the average synergy score versus *E. coli* is lower than that versus the other two test species, results indicate positive contributions from each treatment with low concentrations of chitosan (80 μg/mL), nisin (1.95 – 31.25 μg/mL), $AgNO_3$ (8 μg/mL) and ZnO (10 – 40 μg/mL), with effective inhibition (69 – 98.9%). The highest scoring combination, exhibiting 98.9% inhibition, reported a very high concentration of nisin (31.25 μg/mL), indicating nisin had a strong influence in the combination.

Reported synergy scores versus *S. aureus* are quite high, with top scoring combinations exhibiting effective inhibition (97.5 – 99.5%), with low concentrations of chitosan (19.53 – 78.13 µg/mL), nisin (0.39 – 1.56 µg/mL) and $AgNO_3$ (4 µg/mL) with moderate concentrations of ZnO (62.50 µg/mL).

Combinations versus *S. epidermidis* have reported the highest synergy scores within the present study, with low concentrations chitosan (20 – 80 µg/mL), nisin (1.25 µg/mL), $AgNO_3$ (8 µg/mL) and ZnO (10 – 40 µg/mL). While the top combination reported a very high synergy score (1.3), the reported inhibition deviated greatly (stdev 69.18) with an average of 24.96%. The second highest (1.13) and third highest (0.9) scoring combinations exhibited stable inhibition (98.7 – 99.1%) with similarly low concentrations of each treatment.

6.4 Discussion

With the rise of antimicrobial resistance (AMR) and the need for new forms of treatment, use of already well-established treatments in combination has been an area of extensive interest and study. As previously mentioned, different antimicrobial treatments vary greatly in their mechanisms of action, which opens up the possibility for their combined use against AMR species, enabling one another to carry out their effect. In order for such combinations to be utilised, they must first be assessed to determine their compatibility. As it is difficult to predict their combined activity *in vivo*, *in vitro* assessment is needed to ascertain potential activity.

6.4.1 Inhibition & Synergy

In this study, the combinatory compatibility of four chosen bioactives was successfully established and the magnitude of their interactions with one another. The checkboard assay was utilised for screening the inhibitory effect of bioactive combinations against each test bacterial strain. The checkerboard assay is a well-established method for screening drug combinations in various areas of clinical research (Mataraci and Dosler 2012; Torres et al. 2018; Cokol-Cakmak et al. 2020; Meletiadis et al. 2010; Fatsis-Kavalopoulos et al. 2020). While the majority of studies have focused on two-drug combinations, here it has been adapted to allow for three and four-drug combinations, the latter of which, to best knowledge, has never previously been performed outside of predictive models. While the adapted models follow a core arrangement akin to the classic checkerboard layout, the final checkerboard grid sizes were significantly reduced. This reduction was necessary in order to allow a full combination

screening, while remaining within a manageable, high throughput setting. While the resulting 6x6 and 4x4 checkerboards were not as extensive as that of an 8x8, careful considerations of treatment concentrations allowed for intuitive screening of major combinations. The percentage inhibitory effect of each combination was calculated, and this data was analysed in order to determine the combination synergy score. In order to accurately and consistently process the large volume of data produced, the python package *synergy* was utilised for analysis. *Combenefit* and *SynergyFinder* were trialled during the earlier stages of this study however the *synergy* package was chosen during the final stages. This decision came with the packages ability to analyse higher-order combinations (three-drug and four-drug). While *SynergyFinder* was also capable of three-drug combination analysis, the results were inconsistent, and the lack of four-drug compatibility left it unsuitable for the full study. While *synergy* included numerous synergy models, the Bliss model was used due to its compatibility for higher-order combinations and its consistent outputs. The more recently developed MuSyC model was also trialled, and while it did give simple and descriptive results for two-drug analysis, it was unsatisfactory for higher-order combinations, denoting its unsuitability.

Through the use of the *synergy* python package and the bliss model, the synergy score of each test combination was successfully determined. The results of this study have presented interesting interactions between the bioactives, many of which were predictable but others of which were unanticipated. Nisin, a lantibiotic which targets the inner membrane bound, lipid II molecule is hindered by the outer membrane found in Gram negative bacteria which prevents nisin from carrying out its mechanism of action. It was hypothesised that combining nisin with a compound capable of penetrating the outer membrane, such as $AgNO_3$ or ZnO, would enable nisin, with such an interaction being marked as synergetic.

6.4.2 Two-Drug Combinations

Results of two-drug combinations studies carried out here against the Gram-negative bacteria *E. coli* has yielded varying results. Combinations of nisin-$AgNO_3$ exhibited moderate-high synergy (average 0.32), showing a consistent concentration of $AgNO_3$ (8.49 µg/mL) to be the most accommodating for varying concentrations of nisin. While the inhibition ranged between 64 – 68% for this combination, it shows that nisin was able to have an effect upon a previously unaffected target. In contrast, ZnO was not found to enable nisin, but rather it appeared that nisin was antagonising ZnO as the concentrations of ZnO in the most synergistic

combinations was higher than that of its previously determined MIC. Combinations of nisin-chitosan also exhibited undesired results, with higher concentrations of chitosan being utilised to observe an inhibitory effect. While such results are unfavourable, they still present a promising observation that nisin is having an effect upon a Gram-negative bacteria. Combinations of $AgNO_3$-chitosan exhibited a strong synergistic interaction, with effects evident at lower concentrations of $AgNO_3$, which would indicate chitosan's ability to enable it. Chitosan has also shown to enable ZnO, which also exhibited lower concentrations; however, these combinations were scored quite low which also holds with the fact that the concentration of chitosan was quite high.

Two-drug combinations used to inhibit *S. aureus* and *S. epidermidis* growth presented some moderate to strong synergistic combinations, however there was a pattern that ZnO was not combining effectively with nisin or chitosan. $AgNO_3$ demonstrates itself to be the most effect bioactive, enabling all other bioactives that it is combined with, reporting lower concentrations with higher inhibition responses. The highest overall scoring two-drug combination involved nising-$AgNO_3$ versus *S. epidermidis*. Chitosan also demonstrates notable synergy with most bioactives, but only combined well with ZnO against *S. epidermidis* where much lower concentrations of both gave a greater response, however the inhibition response was weak.

6.4.3 Three-Drug Combinations against Gram-negative

Increasing the combination number can further alter the treatments exhibited effect, as is evident from three-drug combinations. Combinations including nisin were shown to demonstrate high synergy versus *E. coli* with near full inhibition. Following the two-drug analysis, it was predictable that chitosan-$AgNO_3$-nisin would synergise well, presnting the highest scoring combination versus *E. coli*. Furthermore, the relatively high concentrations of nisin in this combination show that it was having an active effect upon *E. coli*, as it can be presumed to be heavily involved (i.e. a concentration close to 0 would indicate little to no input). A more unpredicatable result was seen with combinations involving ZnO, as two-drug combinations demonstrated ZnO to be a poor component in combination, three-drug combinations have shown otherwise. Nisin-ZnO was the lowest scoring combination versus *E. coli*, however with the inclusion of $AgNO_3$ or chitosan, these combinations were the second and third highest scoring three-drug combinations against *E. coli* repsectively. Most

interesting of the nisin-$AgNO_3$-ZnO combination is how little $AgNO_3$ was reported in the higher scoring combinations, while relatively high concentrations of nisin were reported. This again indicates nisins active role in the combination, whereas $AgNO_3$ is at too low of a concentration to have an inhibitory effect. This could also demonstrate $AgNO_3$ ability to enable the mechanism of nisin. While chitosan-$AgNO_3$-ZnO reported low scoring combinations, the results seemed promising with low concentrations of all three bioactives and nearly full inhibition. This again does not follow what was observed in two-drug combinations of the same bioactives.

6.4.4 Three-Drug Combinations against Gram-positive

Three-drug combinations versus *S. aureus* and *S. epidermidis* offered intersting comparatives. The chitosan-$AgNO_3$-nisin combination scored highly versus both bacterial strains, however concentrations of $AgNO_3$ were quite high with low concentrations of nisin. Scores from combinations involving ZnO proved to also be quite unpredictable versus Gram-positive bacteria. Combinations of nisin-Zno and chitosan-ZnO against *S. aureus* scored quite poorly, however nisin-chitosan-ZnO reported the highest score of all three-drug combinations. In contrast however, this combination reported the second lowest score against *S. epidermidis*. While the individual concentrations were quite low, the reported synergy scores were also quite low. An interesting observation of this combination, is that it was also predictable from the two-drug combinations of nisin-chitosan, nisin-ZnO and chitosan-ZnO, which produced synergy scores averaging very closely to that of the nisin-chitosan-ZnO synergy score. Concentrations versus *S. aureus* indicate that ZnO was enabling the effects of chitosan and $AgNO_3$ however concentrations versus *S. epidermidis* do not indicate any single bioactive to be enabling another, displaying an even distribution of activity between the three bioactives.

Nisin-$AgNO_3$-ZnO demonstrated strong synergy versus both Gram-positive bacteria. While the reported synergy was particularly high against *S. epidermidis*, the reported inhibitory effects were quite low. Two-drug reports show nisin-ZnO to interact very poorly, which implies that influences from $AgNO_3$ were causing the three-drug combination to interact more favourably, which is also predictable considering the synergy scores of nisin-$AgNO_3$ and $AgNO_3$-ZnO.

6.4.5 Four-Drug Combinations

Four-drug combinations reported a marked increase in efficacy of all four bioactives in comparison to their individual capabilities against each bacterial strain. The combination of chitosan-nisin-$AgNO_3$-ZnO against *E. coli* exhibited some predictable results, with synergy scores comparable to scores from two-drug and three-drug combinations. While concentrations of each bioactive in the highest scoring combinations were lower than their individual MICs, concentrations of chitosan and $AgNO_3$ were still quite moderate. Furthermore, only the highest scoring combination reported complete inhibition while also using a high concentration of nisin, which was quite expected due to nisin's inability to target Gram-negative species.

The reported four-drug synergy scores against *S. aureus* and *S. epidermidis* were very high in comparison to other scores determined during this study. Concentrations versus *S. aureus* were notably lower than their individual MICs with strong inhibitory effects. While *S. epidermidis* reported the highest synergy score of this study, its highest scoring combination reported low inhibition. When compared to the other two reported combinations, a slight increase of either chitosan or ZnO was sufficient in pushing the effects to complete inhibition, while still remaining well below their individual MICs.

6.5 Conclusion

While it would stand to reason that combining two or more already well known and effective treatments would produce a greater gross effect than that of each individual treatment, previous studies of drug combinations have shown this to not be the case, as has the results presented here (Yadav et al. 2015; Torres et al. 2018; Chen et al. 2015). Drug antagonism is a well-documented occurrence in pharmaceuticals, and while there are a number of models under development for its prediction, in many cases it is difficult to determine which treatments may interact negatively without pre-clinical or clinical studies. Though it is important to find compatible combinations of drugs, another key goal should be focused on finding combinations in which the individual drugs are more effective within a combination than they are on their own. Determining synergy scores is an efficient method for screening many combinations of treatments and deduce the most effective. It is evident from results presented here that treatment interactions cannot be accurately predicted and that they can

differ greatly between bacterial strains. Furthermore, increasing combination number has also been shown to have unpredictable effect, wherein two-drug combinations cannot predict the effect of three-drug combinations of the same components, and likewise two and three-drug combinations cannot predict the effect of four-drugs. Findings show that previously used models for predicting drug combinations cannot be wholly trusted, as there are aberrant results that go against such models.

The four chosen bioactives, $AgNO_3$, ZnO, nisin and chitosan, have successfully been characterised in terms of their combinational interactions. From this data, we can accurately develop materials which contain the most effective concentrations of each compound, limiting the amount needed to inhibit bacterial growth while also holding broad-spectrum effect, which is presented in Table 6.6. While it is important that the appropriate amount of each compound be utilised to inhibit microbial growth, it is also crucial that the concentrations used have no effect upon treated tissue and cells. It is vitally important in terms of the overall project aim, that the bioactives hold no toxicological effect upon mammalian cells. Furthermore, if the compounds were to elicit an inflammatory response, this could cause greater harm to the treated animal, particularly due to the fact that mastitis also causes inflammation (Argaw 2016; Contreras and Rodríguez 2011; Deb et al. 2013). In order to address these concerns, a toxicological assessment of the bioactives will be carried out to determine their effects upon bovine mammary epithelial cells. Additionally, an immune response assay will also be conducted in order to determine the inflammatory response of these cells to each bioactive.

6.6 Tables

Table 6.1 Three highest Bliss scoring two-drug combinations against *E. coli*,showing individual concentrations (Conc 1, Conc 2), % inhibition of bacterial growth, synergy score and average synergy score.

	Drug 1-Drug 2	Concentration 1 (µg/mL)	Concentration 2 (µg/mL)	% Growth Inhibition	Bliss Synergy Score	Average Synergy
E. coli	$AgNO_3$-Chitosan	7.81	156.25	75.49	0.49	0.40
		15.63	156.25	85.56	0.40	
		7.81	312.50	97.31	0.31	
	Nisin-$AgNO_3$	6.25	8.49	67.40	0.34	0.32
		3.13	8.49	68.26	0.33	
		1.56	8.49	64.05	0.29	
	$AgNO_3$-ZnO	5.00	125.00	98.46	0.24	0.23
		5.00	62.50	77.63	0.23	
		5.00	31.25	66.38	0.21	
	Nisin-Chitosan	0.39	312.50	97.73	0.11	0.10
		0.20	312.50	97.12	0.10	
		0.78	312.50	96.40	0.10	
	Chitosan-ZnO	312.50	31.25	98.78	0.14	0.11
		312.50	15.63	93.97	0.10	
		312.50	62.50	98.79	0.09	
	Nisin-ZnO	31.25	62.50	47.39	0.09	0.08
		15.63	500.00	100.00	0.07	
		31.25	500.00	100.00	0.07	

Table 6.2 Three highest Bliss scoring two-drug combinations against *S. aureus*, showing individual concentrations (Conc 1, Conc 2), % inhibition of bacterial growth, synergy score and average synergy score.

	Drug 1-Drug 2	Concentration 1 (µg/mL)	Concentration 2 (µg/mL)	% Growth Inhibition	Synergy Score	Average Synergy
S. aureus	$AgNO_3$-Chitosan	15.63	156.25	69.00	0.39	0.31
		7.81	156.25	62.75	0.35	
		15.63	78.13	36.23	0.20	
	Nisin-$AgNO_3$	1.56	4.25	77.46	0.27	0.24
		0.78	4.25	58.17	0.24	
		0.78	8.49	98.98	0.20	
	$AgNO_3$-ZnO	10.00	125.00	82.23	0.41	0.26
		20.00	62.50	95.47	0.20	
		5.00	125.00	60.83	0.17	
	Nisin-Chitosan	3.91	156.25	50.04	0.31	0.25
		1.95	78.13	18.98	0.22	
		3.91	78.13	27.05	0.21	
	Chitosan-ZnO	78.13	7.81	3.05	0.11	0.09
		78.13	15.63	2.60	0.10	
		156.25	125.00	73.85	0.06	
	Nisin-ZnO	0.24	31.25	14.02	0.06	0.06
		1.95	15.63	3.69	0.06	
		0.98	15.63	6.10	0.05	

Table 6.3. Three highest Bliss scores of each two-drug combination versus *S. epidermidis*, showing individual concentrations (Conc 1, Conc 2), % Inhibition of bacterial growth, synergy score and average of synergy score.

	Drug 1-Drug 2	Concentration 1 (µg/mL)	Concentration 2 (µg/mL)	% Growth Inhibition	Synergy Score	Average Synergy
S. epidermidis	$AgNO_3$-Chitosan	2.50	4.88	29.61	0.31	0.25
		10.00	78.13	99.08	0.22	
		2.50	19.53	56.96	0.21	
	Nisin-$AgNO_3$	1.95	10.00	78.07	0.69	0.68
		0.49	10.00	40.90	0.68	
		0.24	10.00	39.81	0.66	
	$AgNO_3$-ZnO	5.00	62.50	88.24	0.50	0.44
		10.00	62.50	95.40	0.44	
		5.00	31.25	69.25	0.38	
	Nisin-Chitosan	7.81	156.25	87.28	0.11	0.04
		1.95	156.25	71.93	0.01	
		15.63	0.00	97.82	0.00	
	Chitosan-ZnO	4.88	15.63	22.15	0.29	0.27
		9.77	15.63	31.35	0.28	
		4.88	31.25	26.47	0.24	
	Nisin-ZnO	1.95	125.00	83.63	0.16	0.14
		3.91	125.00	91.79	0.15	
		0.24	31.25	17.39	0.10	

Table 6.4. Three highest Bliss Synergy Scores of each three-drug combination versus *E. coli*, *S. aureus* and *S. epidermidis*, showing individual drug concentrations (Conc 1, Conc 2, Conc 3), % inhibition of bacterial growth, combination synergy score and average score.

	Drug 1-Drug 2-Drug 3	Conc 1 (µg/mL)	Conc 2 (µg/mL)	Conc 3 (µg/mL)	% Inhibition	Synergy Score	Average Synergy
E. coli	Chitosan-AgNO3-Nisin	80.00	4.00	3.91	99.13	0.40	0.38
		160.00	2.00	3.91	98.66	0.37	
		80.00	4.00	7.81	98.92	0.36	
	Chitosan-AgNO3-ZnO	40.00	4.00	20.00	100.00	0.15	0.14
		40.00	4.00	20.00	99.55	0.14	
		80.00	0.50	20.00	97.15	0.13	
	Nisin-AgNO3-ZnO	31.25	1.00	31.25	77.38	0.48	0.36
		31.25	1.00	62.50	74.84	0.31	
		31.25	0.50	62.50	58.62	0.29	
	Nisin-Chitosan-ZnO	3.91	312.50	125.00	100.00	0.21	0.20
		0.98	9.77	31.25	26.64	0.19	
		3.91	312.50	62.50	97.72	0.19	
S. aureus	Chitosan-AgNO3-Nisin	78.13	8.00	0.63	99.26	0.64	0.56
		78.13	16.00	0.63	99.32	0.59	
		39.06	8.00	0.63	76.57	0.46	
	Chitosan-AgNO3-ZnO	39.06	4.00	62.50	98.24	0.29	0.28
		39.06	8.00	62.50	98.32	0.29	
		78.13	8.00	62.50	97.55	0.27	
	Nisin-AgNO3-ZnO	0.31	8.00	39.06	98.32	0.40	0.38
		0.63	8.00	39.06	98.39	0.40	
		1.25	8.00	39.06	100.00	0.35	
	Nisin-Chitosan-ZnO	3.91	39.06	62.50	98.66	0.93	0.83
		0.98	156.25	62.50	99.39	0.84	
		0.98	78.13	62.50	71.45	0.71	
S. epidermidis	Chitosan-AgNO3-Nisin	39.06	16.00	0.63	95.12	0.51	0.43
		78.13	16.00	0.63	96.15	0.43	
		39.06	8.00	1.25	92.17	0.35	
	Chitosan-AgNO3-ZnO	40.00	2.00	10.00	95.99	0.36	0.35
		20.00	4.00	10.00	87.95	0.35	
		40.00	4.00	10.00	98.40	0.32	
	Nisin-AgNO3-ZnO	1.25	2.00	5.00	33.58	0.63	0.53
		1.25	4.00	5.00	46.64	0.52	
		2.50	4.00	5.00	72.31	0.45	
	Nisin-Chitosan-ZnO	0.98	39.06	31.25	99.36	0.22	0.17
		1.95	39.06	31.25	99.42	0.21	
		1.95	625.00	31.25	99.22	0.08	

Table 6.5 Three highest Bliss Synergy Scores and the average of each four-drug combination versus *E. coli*, *S. aureus* and *S. epidermidis*, showing individual concentrations (Conc 1, Conc 2, Conc 3, Conc 4), % Inhibition of bacterial growth, synergy score and average synergy score of the three.

	Drug 1-Drug 2-Drug 3-Drug 4	Conc 1 (µg/mL)	Conc 2 (µg/mL)	Conc 3 (µg/mL)	Conc 4 (µg/mL)	% Inhibition	Synergy Score	Average Synergy
E. coli	Chitosan-Nisin-AgNO3-ZnO	80.00	31.25	8.00	40.00	98.90	0.44	0.36
		80.00	1.95	8.00	40.00	76.61	0.34	
		80.00	1.95	8.00	10.00	69.13	0.30	
S. aureus	Chitosan-Nisin-AgNO3-ZnO	78.13	0.39	4.00	62.50	98.15	1.04	0.91
		19.53	0.39	4.00	62.50	85.02	0.85	
		78.13	1.56	4.00	62.50	98.52	0.85	
S. epidermidis	Chitosan-Nisin-AgNO3-ZnO	20.00	1.25	8.00	10.00	24.96	1.30	1.11
		20.00	1.25	8.00	40.00	99.12	1.13	
		80.00	1.25	8.00	10.00	98.77	0.90	

Table 6.6 Most effective concentrations of the four bioactive compounds in combination against *E. coli*, *S. aureus* and *S. epidermidis*. These concentrations were established by evaluating the highest scoring combinations against each bacterial species and determining the lowest concentrations of each that would cause complete inhibition of all three bacterial species.

Bioactive	Most effective concentration (µg/mL)
Chitosan	80
Nisin	2
$AgNO_3$	8
ZnO	60

6.7 Figures

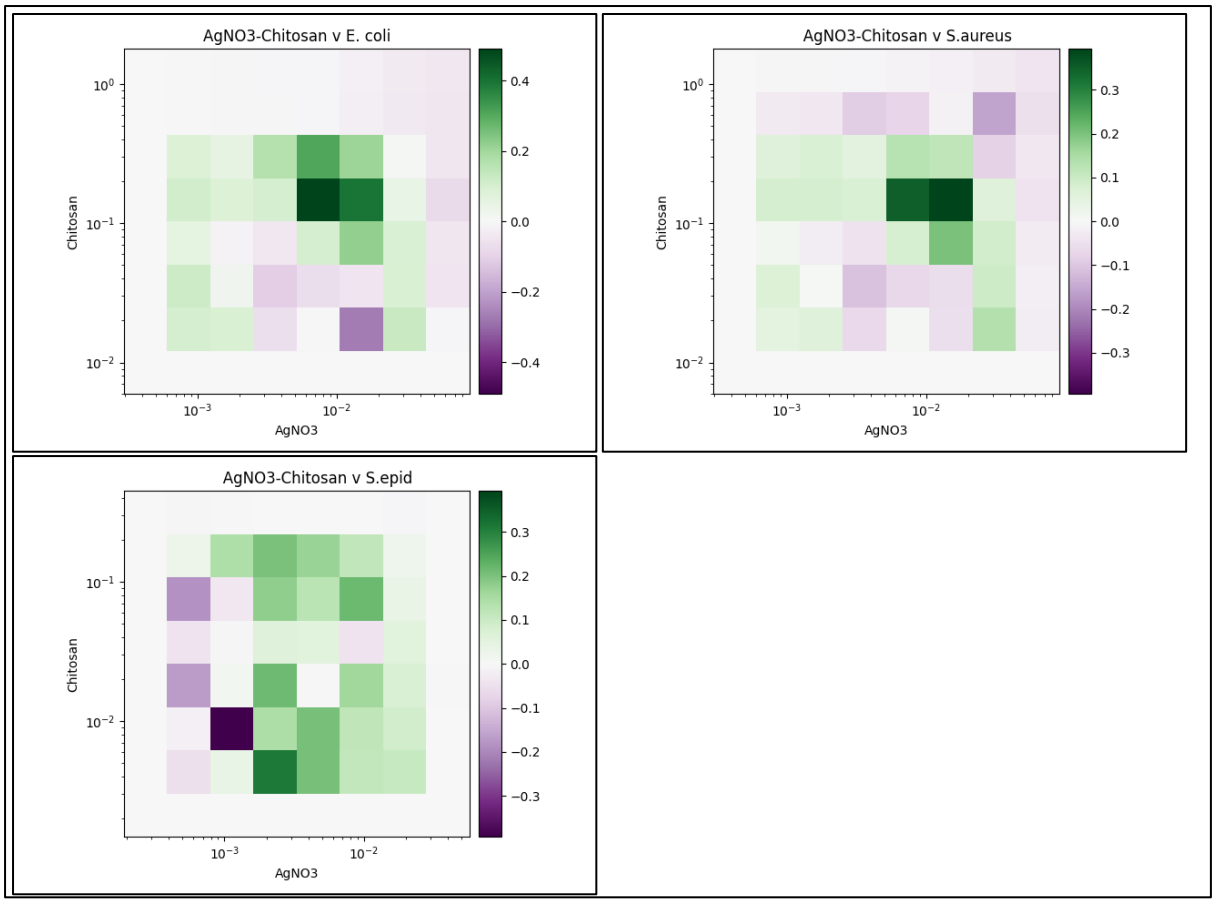

Figure 6.1 AgNO3-Chitosan Synergy Heat Map.
Graphs show heat map of synergy between silver nitrate ($AgNO_3$) and Chitosan in inhibiting *E. coli*, *S. aureus* and *S. epidermidis* growth as determined by broth microdilution and absorbance readings. Inhibition results were analysed with the *synergy* python package using the bliss synergy model. The *synergy* python package produced the heatmap graphs of each combination results, giving visual presentations of combinations of high (green) synergy or high (purple) antagonism. N=3.

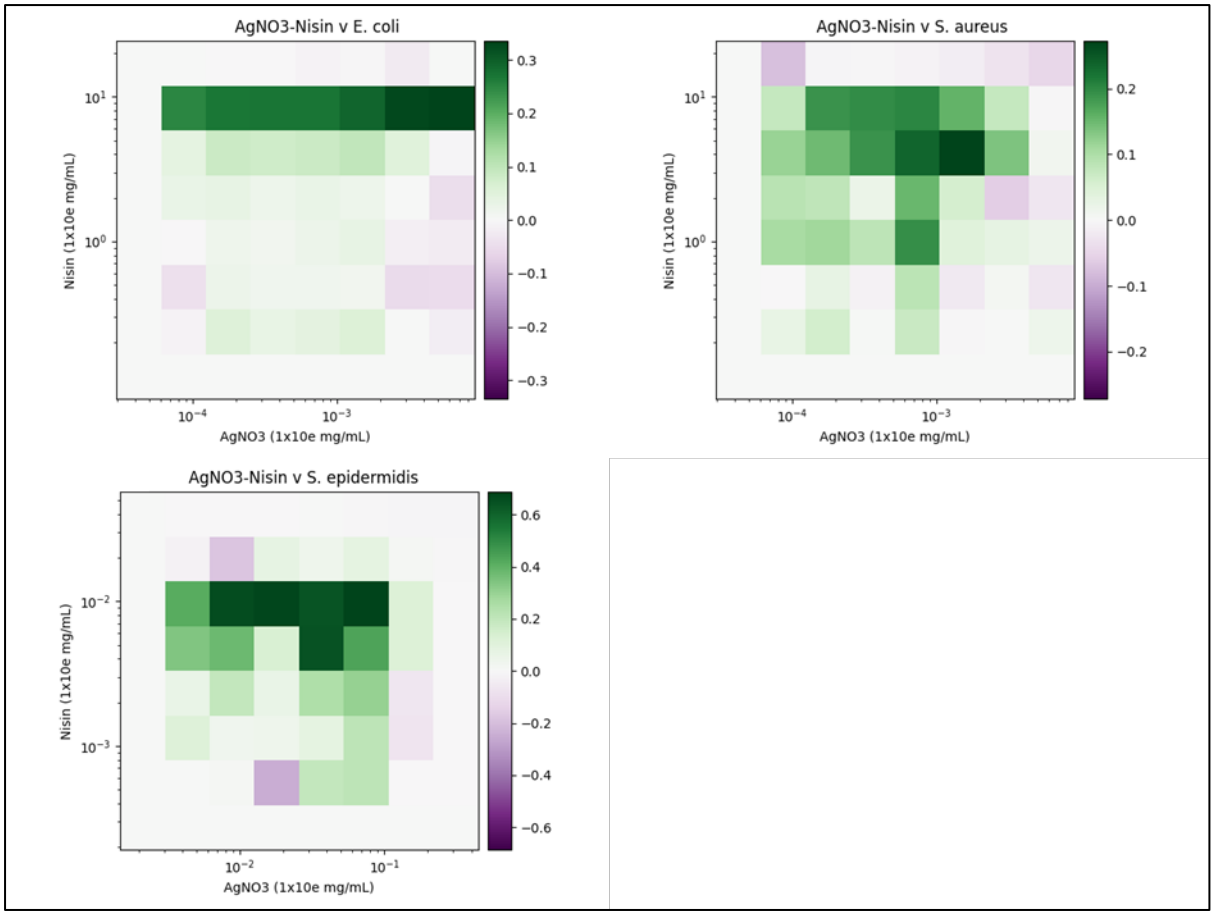

Figure 6.2 AgNO3-Nisin Synergy Heat Map.
Graphs show heat map of synergy between silver nitrate ($AgNO_3$) and Nisin in inhibiting *E. coli*, *S. aureus* and *S. epidermidis* growth as determined by broth microdilution and absorbance readings. Inhibition results were analysed with the *synergy* python package using the bliss synergy model. The *synergy* python package produced the heatmap graphs of each combination results, giving visual presentations of combinations of high (green) synergy or high (purple) antagonism. N=3.

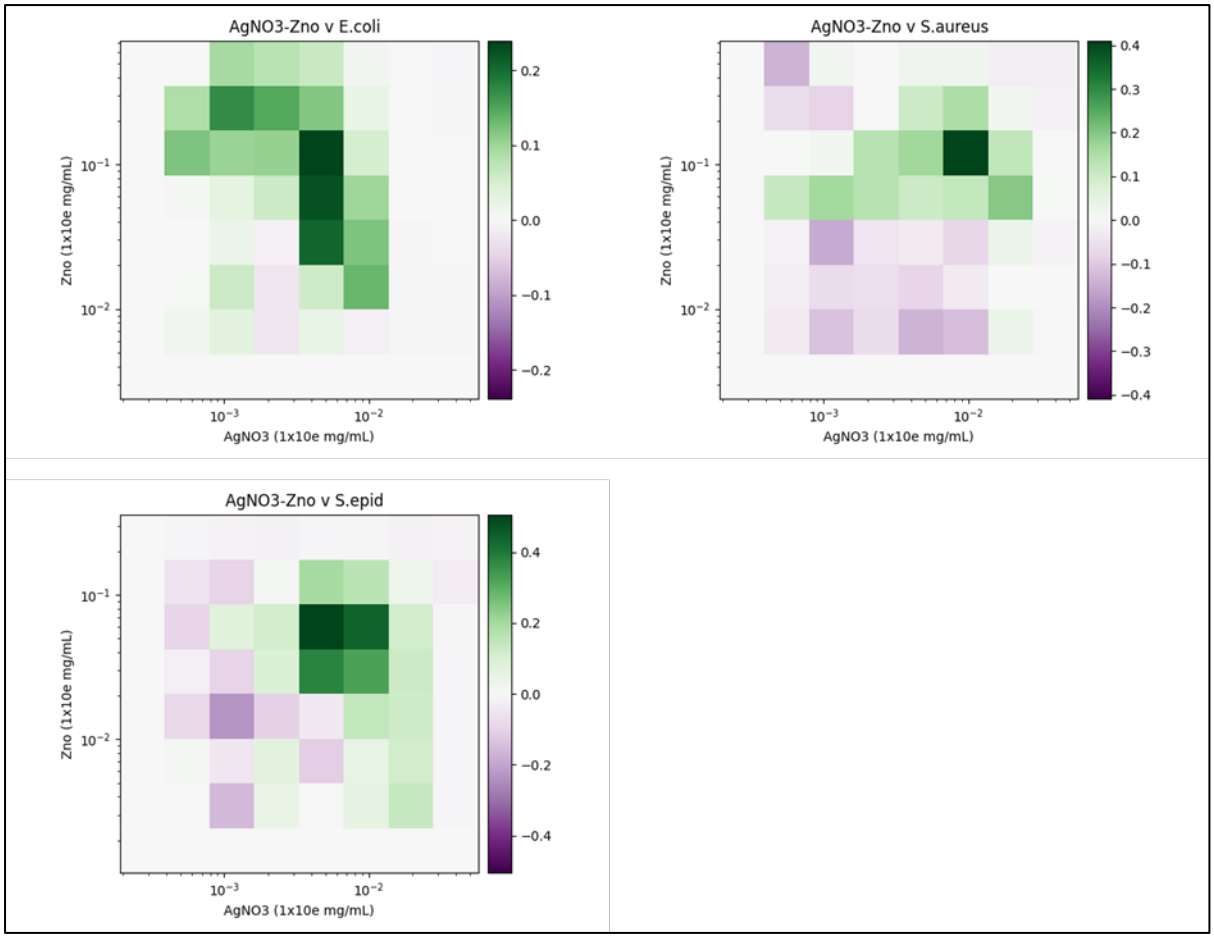

Figure 6.3 AgNO3-ZnO Synergy Heat Map.
Graphs show heat map of synergy between silver nitrate ($AgNO_3$) and zinc oxide (ZnO) in inhibiting *E. coli*, *S. aureus* and *S. epidermidis* growth as determined by broth microdilution and absorbance readings. Inhibition results were analysed with the *synergy* python package using the bliss synergy model. The *synergy* python package produced the heatmap graphs of each combination results, giving visual presentations of combinations of high (green) synergy or high (purple) antagonism. N=3.

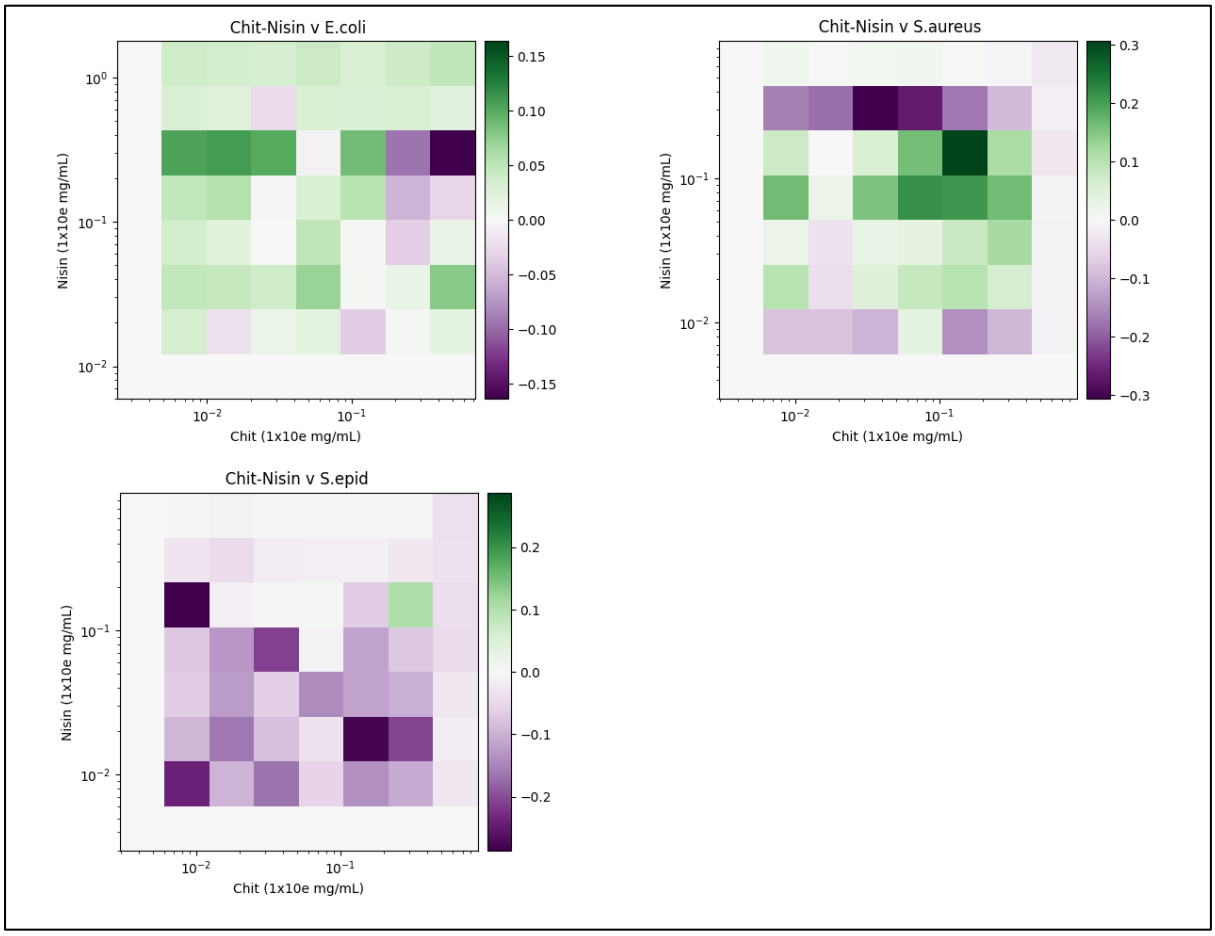

Figure 6.4 Chitosan-Nisin Synergy Heat Map.
Graphs show heat map of synergy between Chitosan and Nisin in inhibiting *E. coli*, *S. aureus* and *S. epidermidis* growth as determined by broth microdilution and absorbance readings. Inhibition results were analysed with the *synergy* python package using the bliss synergy model. The *synergy* python package produced the heatmap graphs of each combination results, giving visual presentations of combinations of high (green) synergy or high (purple) antagonism. N=3.

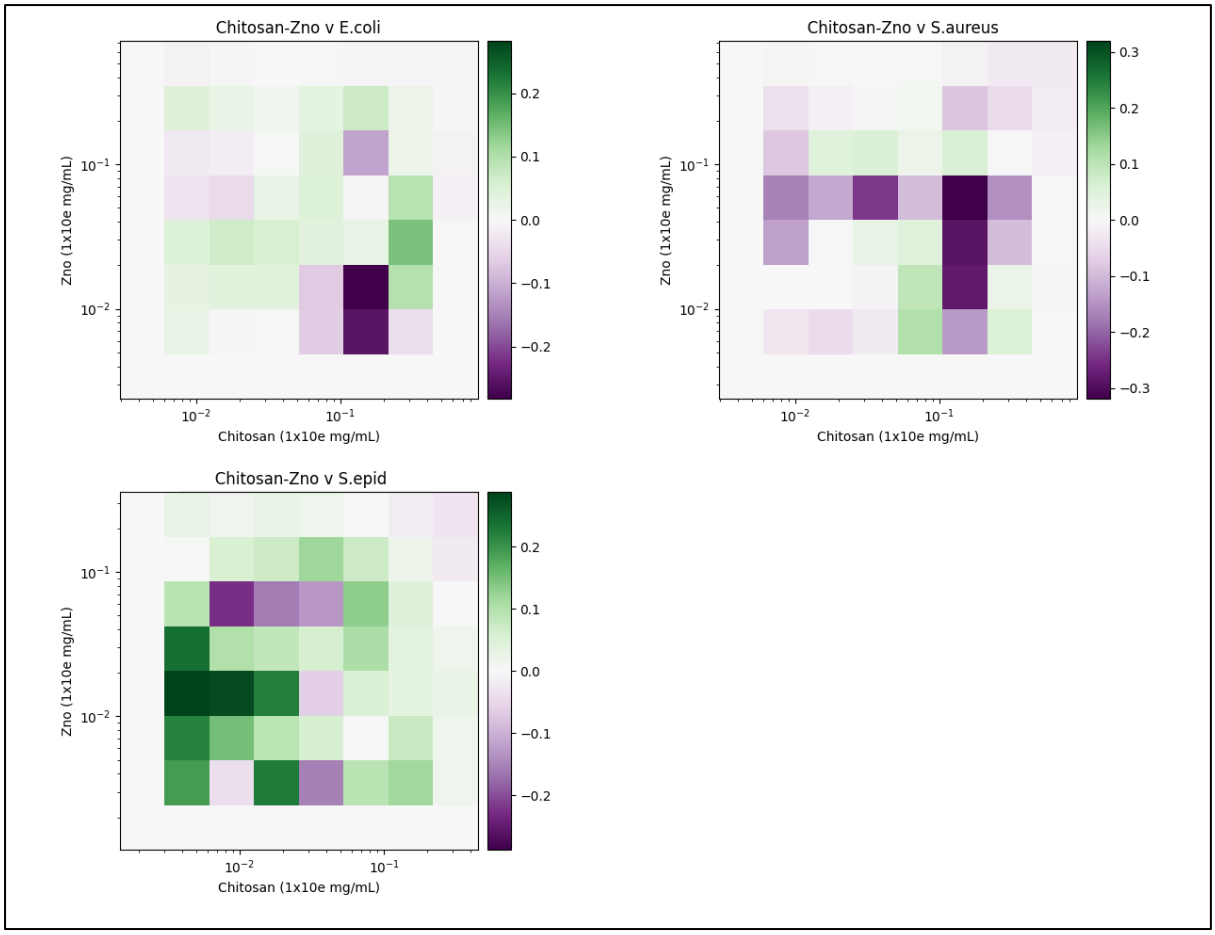

Figure 6.5 Chitosan-ZnO Synergy Heat Map.
Graphs show heat map of synergy between Chitosan and zinc oxide (ZnO) in inhibiting *E. coli*, *S. aureus* and *S. epidermidis* growth as determined by broth microdilution and absorbance readings. Inhibition results were analysed with the *synergy* python package using the bliss synergy model. The *synergy* python package produced the heatmap graphs of each combination results, giving visual presentations of combinations of high (green) synergy or high (purple) antagonism. N=3.

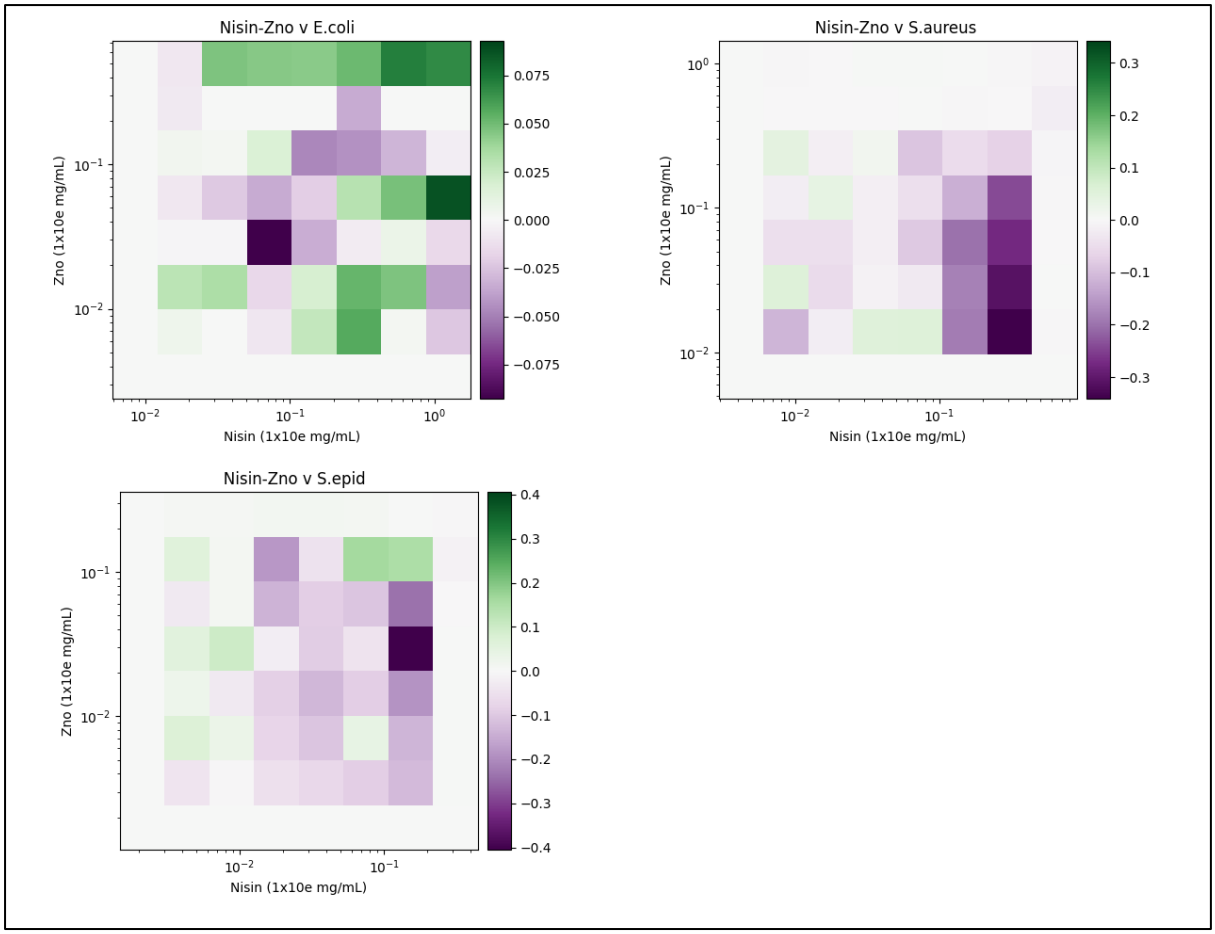

Figure 6.6 Nisin-ZnO Synergy Heat Map.
Graphs show heat map of synergy between Nisin and zinc oxide (ZnO) in inhibiting *E. coli*, *S. aureus* and *S. epidermidis* growth as determined by broth microdilution and absorbance readings. Inhibition results were analysed with the synergy python package using the bliss synergy model. The synergy python package produced the heatmap graphs of each combination results, giving visual presentations of combinations of high (green) synergy or high (purple) antagonism. N=3.

A

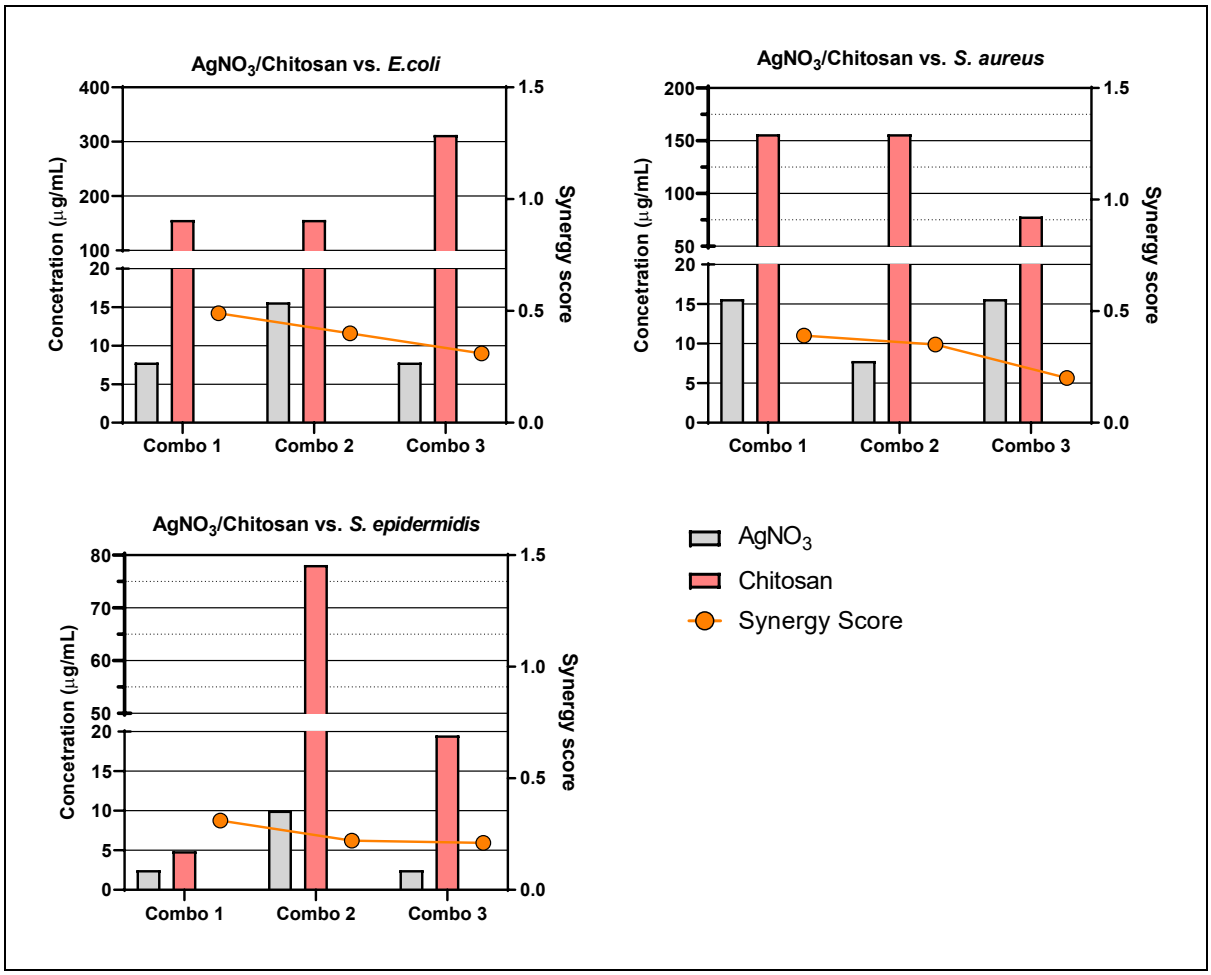
AgNO3/Chitosan vs. E.coli
Concetration (µg/mL)
Synergy score
Combo 1
Combo 2
Combo 3
AgNO3/Chitosan vs. S. aureus
AgNO3/Chitosan vs. S. epidermidis
AgNO3
Chitosan
Synergy Score

B

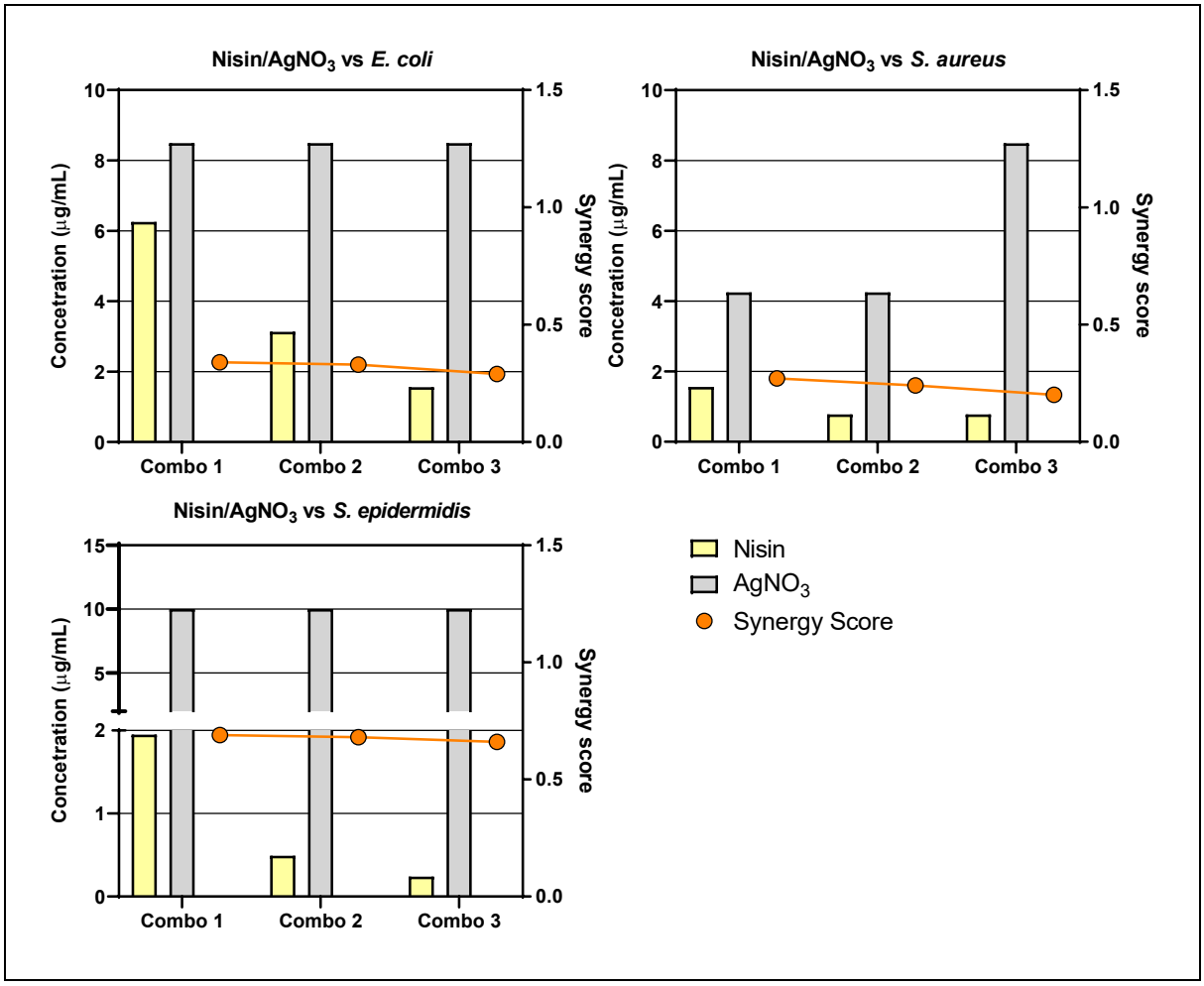
Nisin/AgNO3 vs E. coli
Nisin/AgNO3 vs S. aureus
Nisin/AgNO3 vs S. epidermidis
Concetration (µg/mL)
Synergy score
Combo 1
Combo 2
Combo 3
Nisin
AgNO3
Synergy Score

C

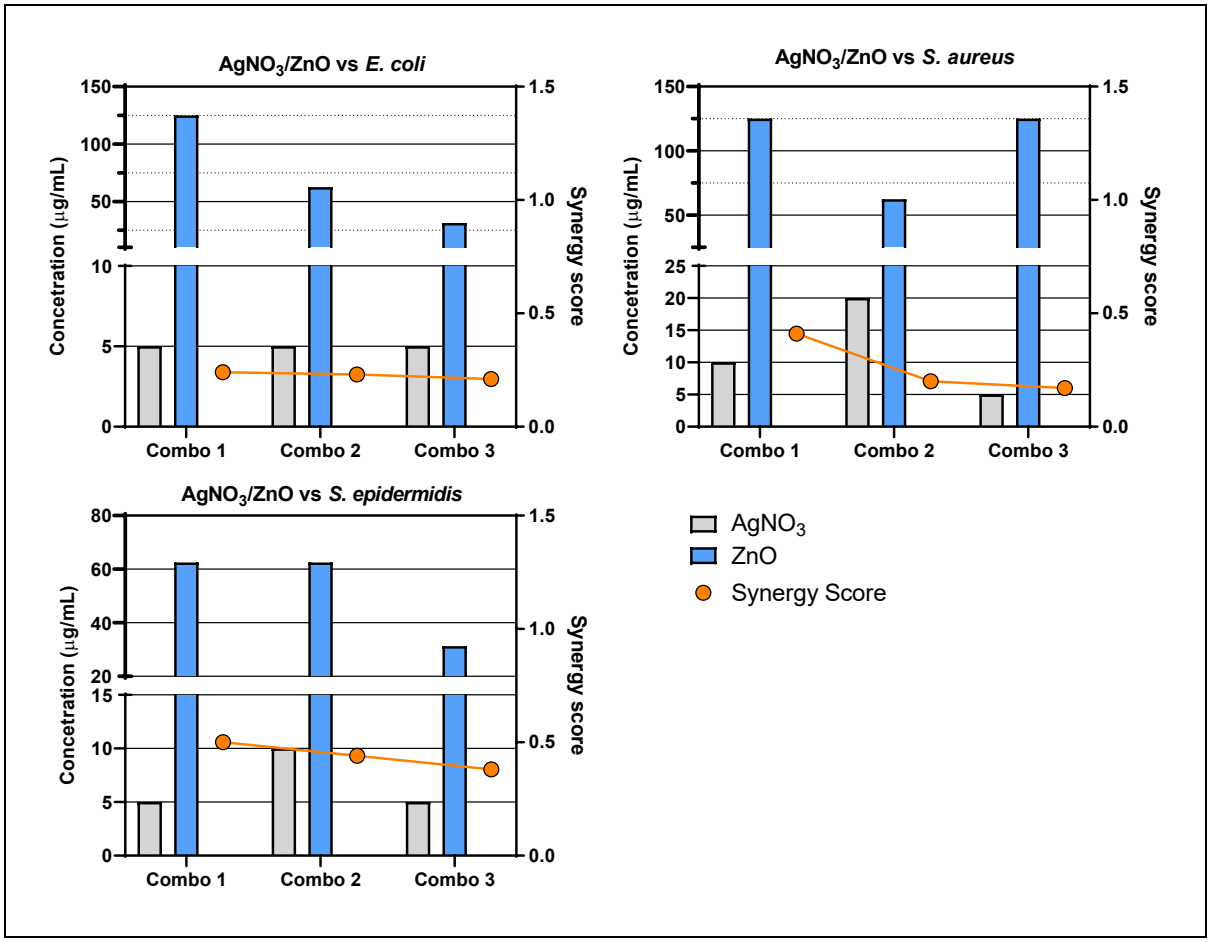
AgNO3/ZnO vs E. coli
AgNO3/ZnO vs S. aureus
AgNO3/ZnO vs S. epidermidis
Concetration (µg/mL)
Synergy score
Combo 1
Combo 2
Combo 3
AgNO3
ZnO
Synergy Score

D

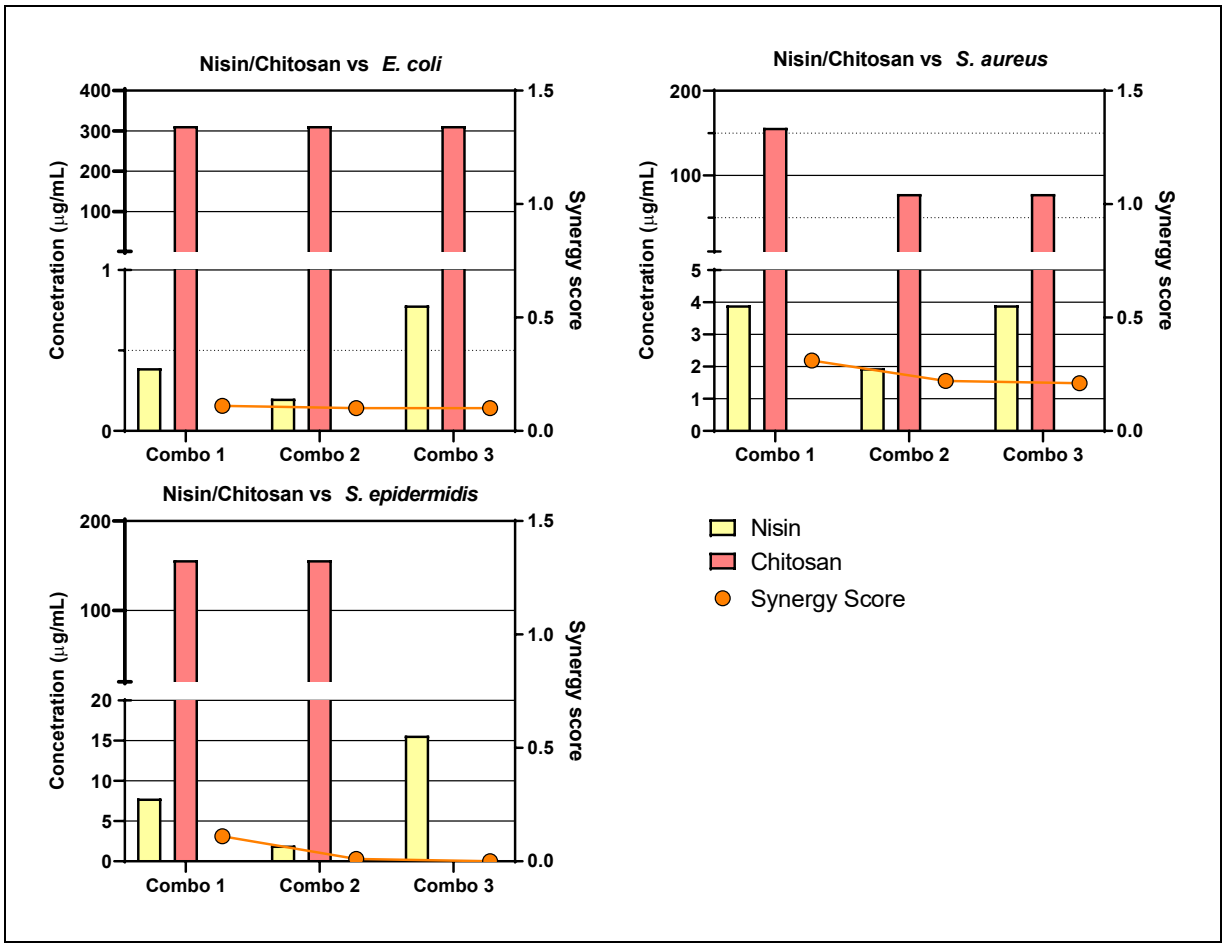
Nisin/Chitosan vs E. coli
Concetration (µg/mL)
Synergy score
400
300
200
100
1
0
1.5
1.0
0.5
0.0
Combo 1
Combo 2
Combo 3
Nisin/Chitosan vs S. aureus
200
100
5
4
3
2
1
0
Nisin/Chitosan vs S. epidermidis
20
15
10
5
Nisin
Chitosan
Synergy Score

E

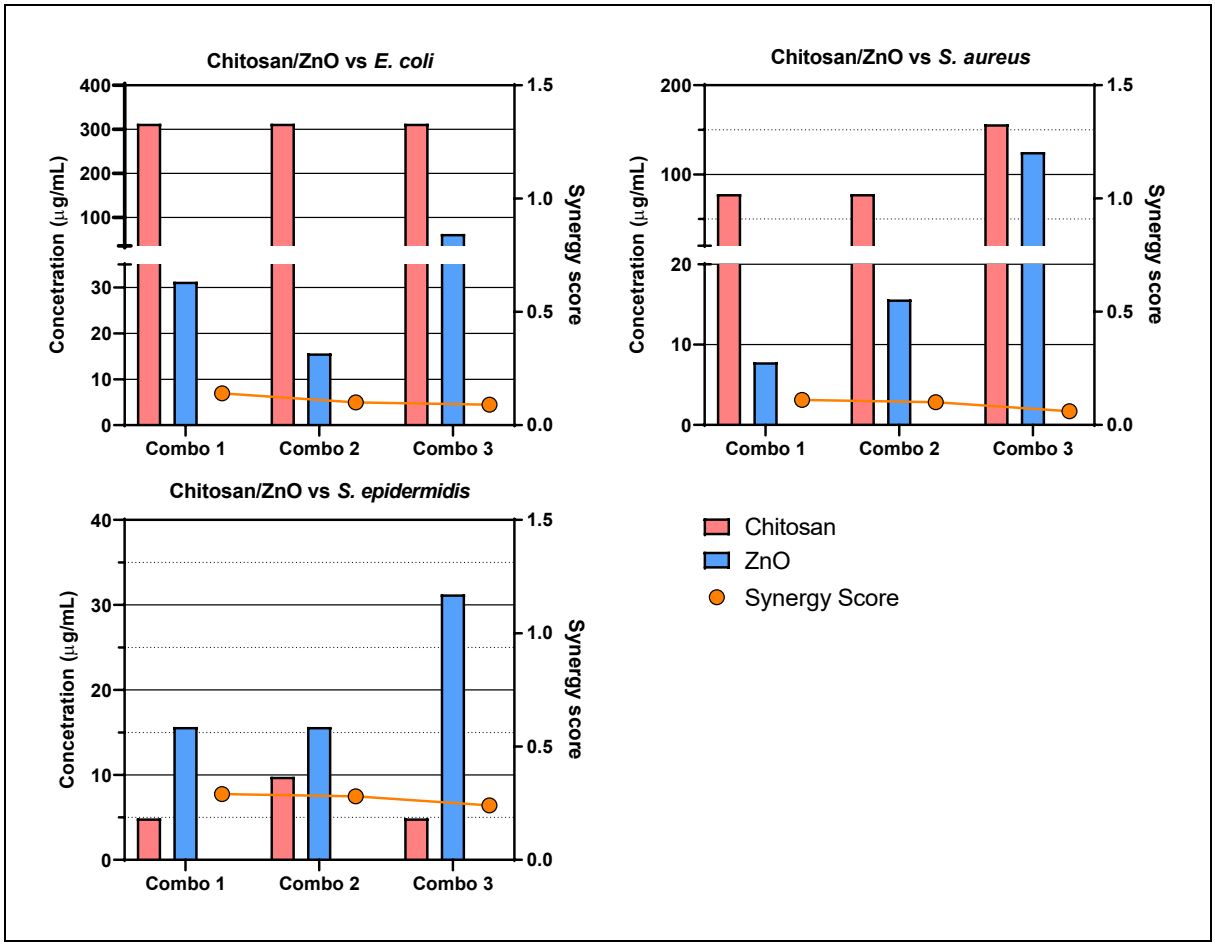
Chitosan/ZnO vs E. coli
Concetration (µg/mL)
Synergy score
400
300
200
100
30
20
10
0
1.5
1.0
0.5
0.0
Combo 1
Combo 2
Combo 3
Chitosan/ZnO vs S. aureus
Concetration (µg/mL)
Synergy score
200
100
20
10
0
1.5
1.0
0.5
0.0
Combo 1
Combo 2
Combo 3
Chitosan/ZnO vs S. epidermidis
Concetration (µg/mL)
Synergy score
40
30
20
10
0
1.5
1.0
0.5
0.0
Combo 1
Combo 2
Combo 3
Chitosan
ZnO
Synergy Score

F

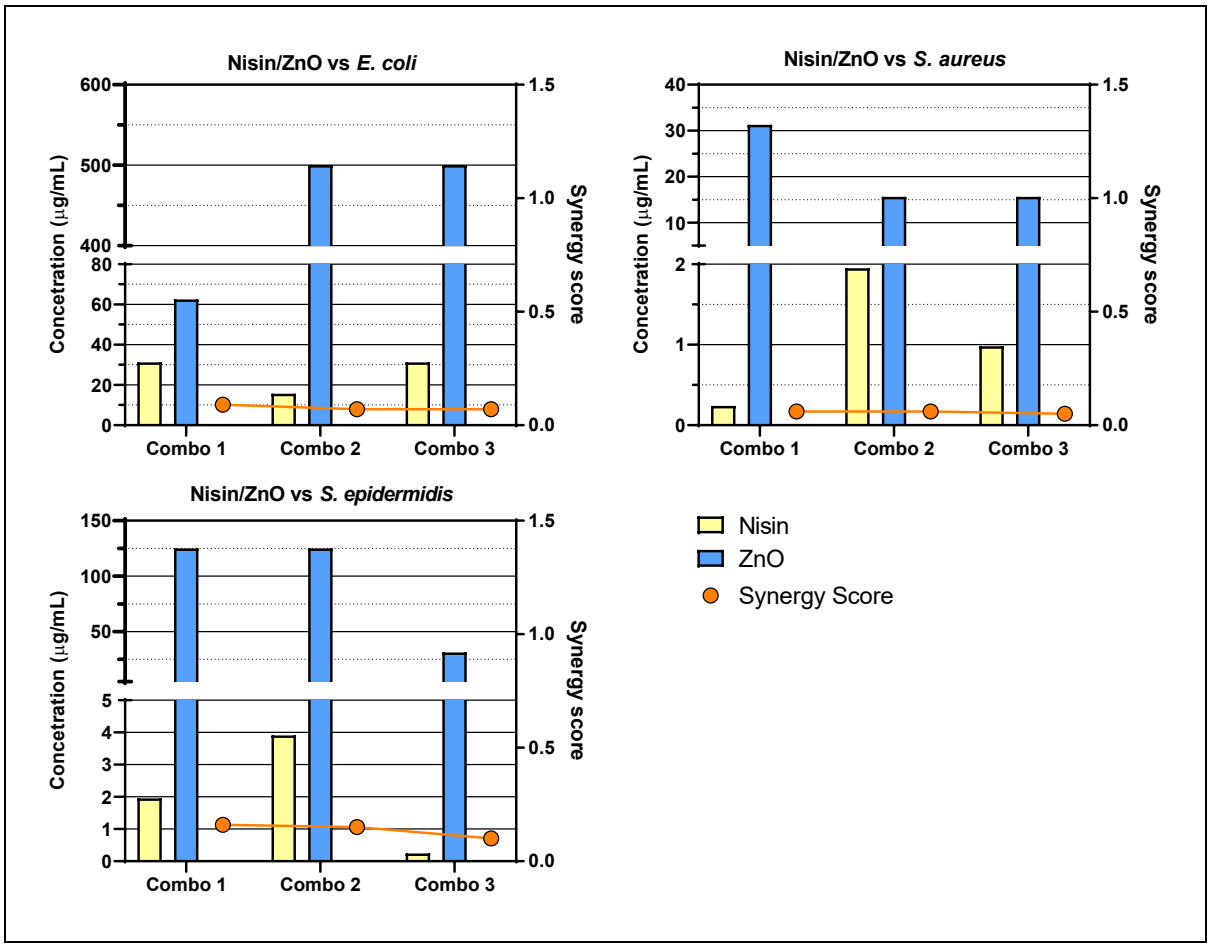

Figure 6.7 Synergy score results of top three two-drug combinations: Bar graphs presenting the concentrations of each drug and their respective synergy scores from the top three two-drug combinations (**A** – **F**) against *E. coli*, *S. aureus* and *S. epidermidis*. (**A**) $AgNO_3$/Chitosan, (**B**) Nisin/$AgNO_3$, (**C**) $AgNO_3$/ZnO, (**D**) Nisin/Chitosan, (**E**) Chitosan/ZnO and (**F**) Nisin/ZnO. Bars show drug concentrations as indicated on the left y-axis and the line/symbols show each combination (combo) synergy score as indicated on the right y-axis.

A

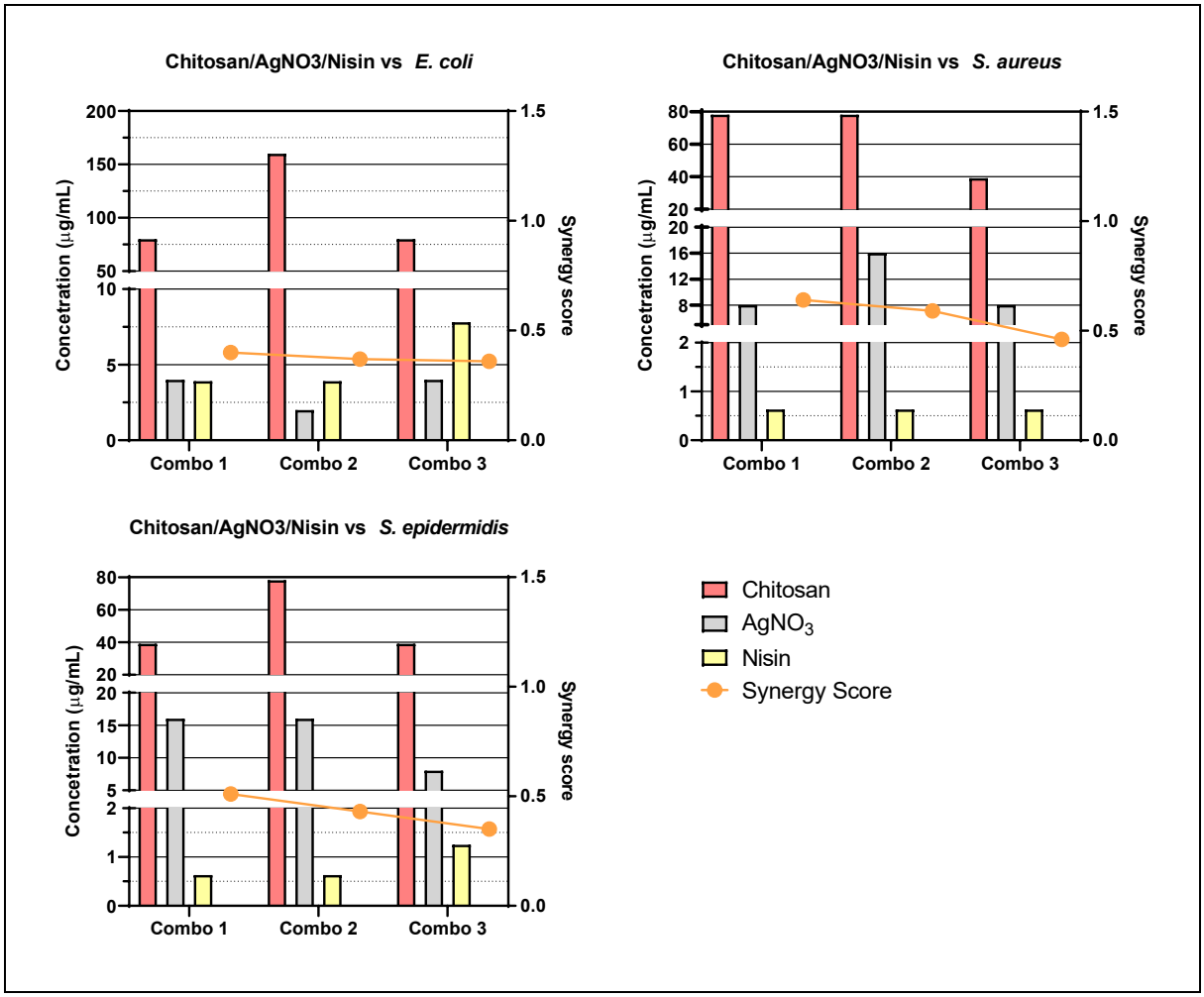
Chitosan/AgNO3/Nisin vs E. coli
Concetration (µg/mL)
Synergy score
200
150
100
50
10
5
0
1.5
1.0
0.5
0.0
Combo 1
Combo 2
Combo 3
Chitosan/AgNO3/Nisin vs S. aureus
80
60
40
20
16
12
8
2
1
Chitosan/AgNO3/Nisin vs S. epidermidis
15
Chitosan
AgNO3
Nisin
Synergy Score

B

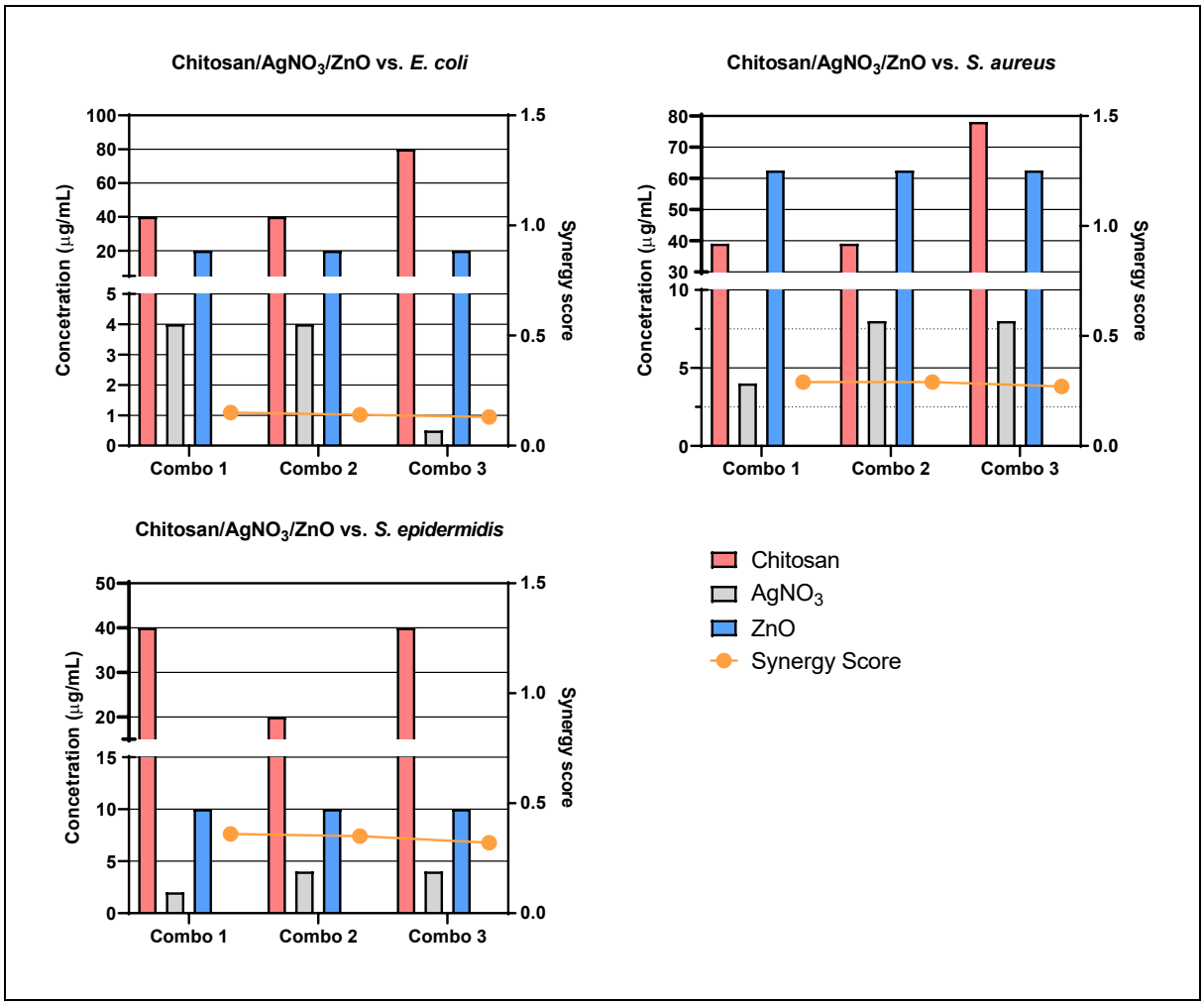
Chitosan/AgNO3/ZnO vs. E. coli
Concetration (µg/mL)
Synergy score
Combo 1
Combo 2
Combo 3
Chitosan/AgNO3/ZnO vs. S. aureus
Chitosan/AgNO3/ZnO vs. S. epidermidis
Chitosan
AgNO3
ZnO
Synergy Score

C

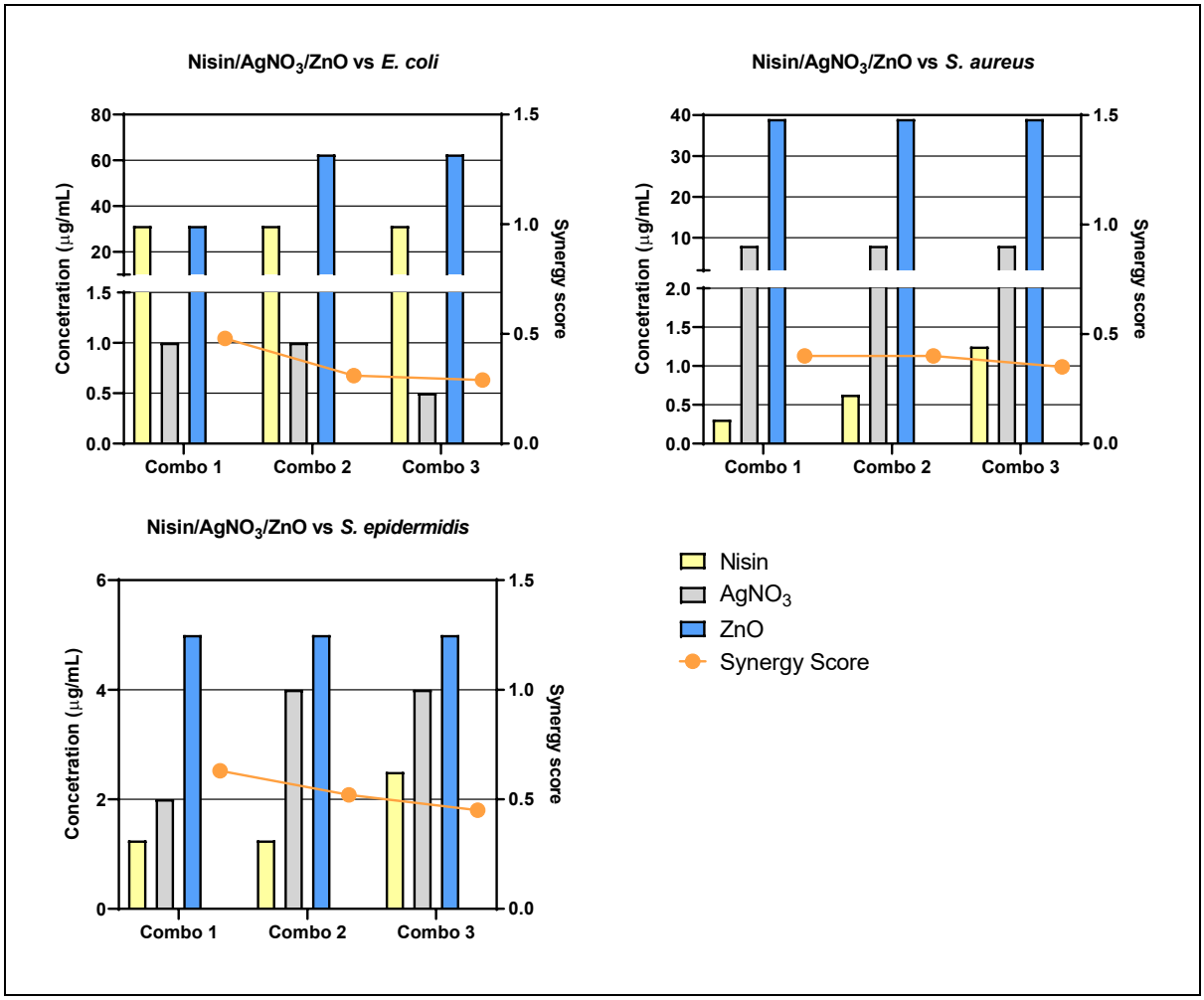
Nisin/AgNO3/ZnO vs E. coli
Concetration (µg/mL)
Synergy score
Combo 1
Combo 2
Combo 3
Nisin/AgNO3/ZnO vs S. aureus
Concetration (µg/mL)
Synergy score
Combo 1
Combo 2
Combo 3
Nisin/AgNO3/ZnO vs S. epidermidis
Concetration (µg/mL)
Synergy score
Combo 1
Combo 2
Combo 3
Nisin
AgNO3
ZnO
Synergy Score

D

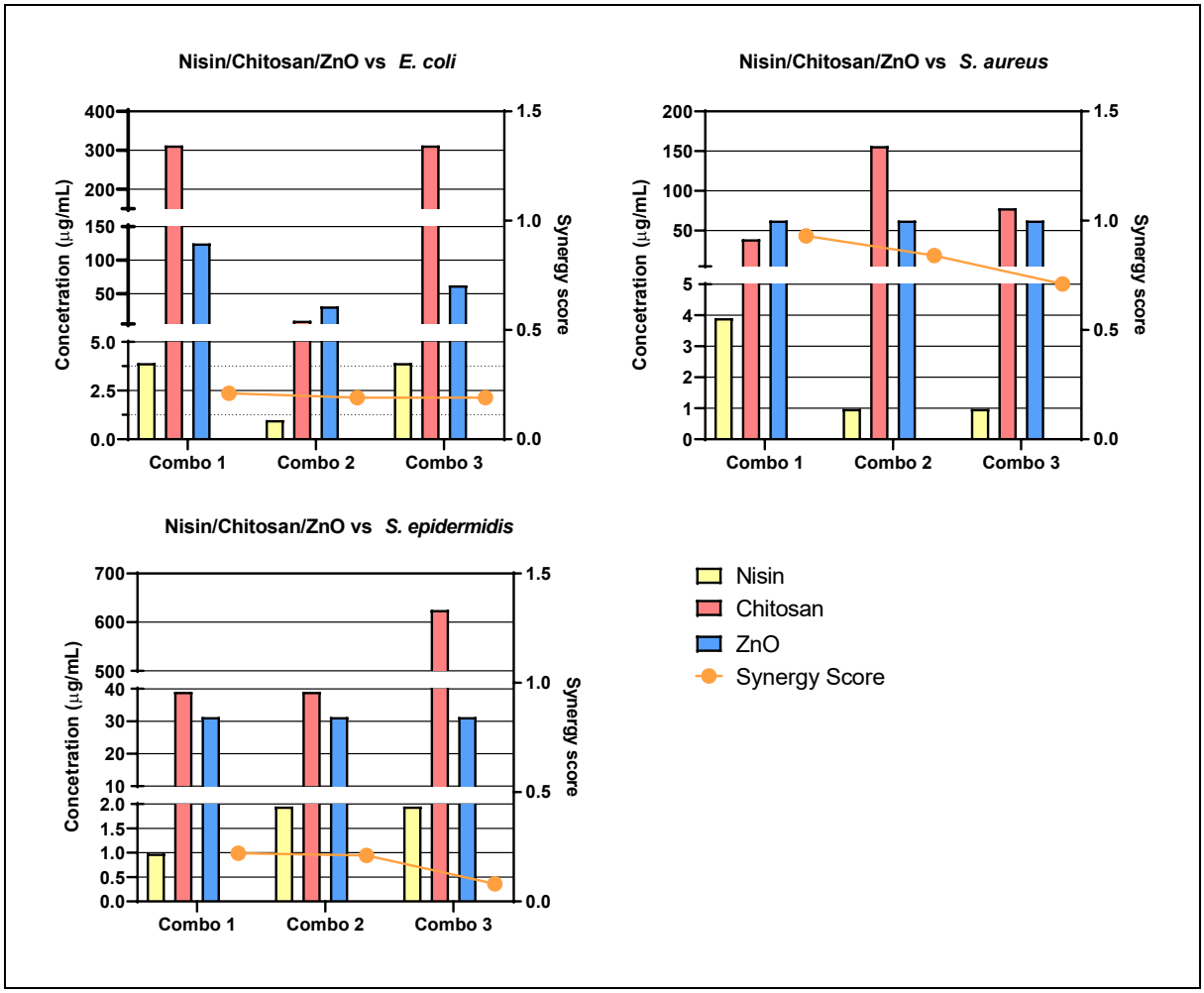

Figure 6.8 Synergy score results of top three three-drug combinations: Bar graphs presenting the concentrations of each drug and their respective synergy scores from the top three three-drug combinations (**A** – **D**) against *E. coli*, *S. aureus* and *S. epidermidis*. (**A**) Chitosan/$AgNO_3$/Nisin, (**B**) Chitosan/$AgNO_3$/ZnO, (**C**) Nisin/$AgNO_3$/ZnO and (**D**) Nisin/Chitosan/ZnO. Bars show drug concentrations as indicated on the left y-axis and the line/symbols show each combination (combo) synergy score as indicated on the right y-axis.

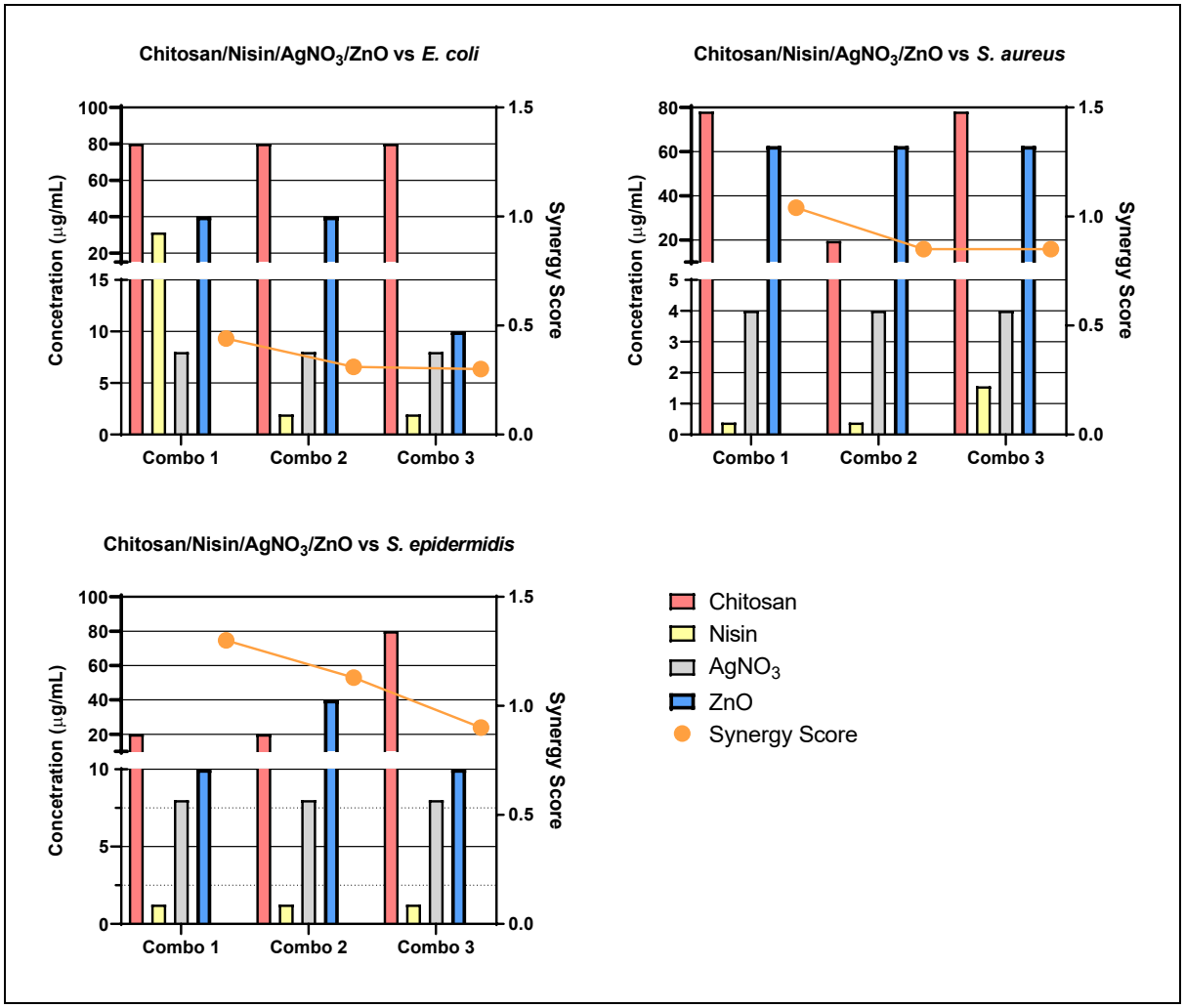

Figure 6.9 Synergy score results of top three four-drug combinations: Bar graphs presenting the concentrations of each drug and their respective synergy scores from the top three four-drug combinations (Chitosan/Nisin/$AgNO_3$/ZnO) against *E. coli*, *S. aureus* and *S. epidermidis*. Bars show drug concentrations as indicated on the left y-axis and the line/symbols show each combination (combo) synergy score as indicated on the right y-axis.

Chapter 7 Cytotoxicological and Inflammatory Response Assessment of Bioactives

7.1 Introduction

The pressing interest in discovering new antimicrobial compounds is considerable given the global AMR crisis. However, the inclusion of appropriate bioactives into medicinal treatments requires extensive study and safety screening to ensure they hold no negative effects upon treated individuals. Such studies can be divided into two stages: pre-clinical (toxicological) and clinical. Preclinical studies involve the collection of preliminary data involving a compounds characteristics and effects. Such data includes pharmacokinetics, efficacy versus the designed target and cytotoxicity. Initial preliminary studies are most commonly carried out using cell culture specimens (*in vitro*) to simulate conditions similar to real-world infection without the need to use animals or other in vivo infectivity models. . While it is difficult to completely simulate all variabilities and conditions, *in vitro* studies are indispensable for understanding efficacy of pharmaceutical investigations. For pre-clinical studies involving antimicrobials, with a future prospect of being used in the treatment of bacterial infections, it is not only important to assess their efficacy versus microbial pathogens, but also their effects against animal cells and tissue. The primary effects that are determined from such studies are cytotoxicity (i.e. the degree to which a substance can cause damage to a cell) and inflammatory response (i.e. the degree to which a substance can affect an cellular immune response) (LI, ZHOU, and XU 2015). In order to perform an accurately representative study, it is important to choose appropriate cell lines to use during the experimental phase. For example, studies which aim to development oncological treatment of cervical cancer should utilise a cervical cancer cell line such as CaSki cells (Abidin et al. 2020). Cytotoxicological assays follow standard measurements of cytotoxicity, including distorted cellular morphology, altered metabolic activity and general loss of cell viability (LI, ZHOU, and XU 2015). One of the most commonly used means of determining cellular viability is through the use of metabolic assays which utilise tetrazolium salts such as MTT or WST (Stockert et al. 2012). These salts can vary in their approach but are common in their mechanisms. The salts are metabolised by cells, producing formazan products which have a strong colour which can be quantified by

dissolving in a suitable solvent and measuring their absorbance. Cells unable to carry out such metabolic activities are generally considered to be un-viable. Standard protocols and guidelines have been published throughout the years to aid researchers in unifying methods and definitions, in order to unify safe international assessment, such as those for biomedical devices which defines cytotoxicity as a compound which induces ≥ 70% cell death (International Organization for Standardization 2018).

As previously mentioned, during the experimental design of an *in vitro* assay, it is essential to select cell lines appropriate for the study. Inflammation can be studied through a number of methods, with the most commonly used involving quantification of cellular immune response messengers, known as cytokines (Zheng et al. 2016). Cytokines are the medium by which a cell can activate the local host immune response upon receiving certain stimuli, such as stresses or detection of secreted signalling proteins (Zheng et al. 2016; Lahouassa et al. 2007). Measurement of the immune response by cytokine analysis can fall into two major paths, quantification of produced cytokines or quantification of gene activation related to cytokine production (Favre, Bordmann, and Rudin 1997). The primary means of cytokine quantification utilised in many modern research facilities is the enzyme-linked immunosorbent assay (ELISA). The basis of an ELISA involves preparing or using microtiter plate coated with antibodies targeted towards a specific antigen (in the case of immune response assays, a particular cytokine). There are a number of different ELISA designs such as direct, indirect, competitive or sandwich, which vary upon their detection method but all involve use of enzymes which react to a substrate, producing a quantifiable colour change relative to the amount of bound antigen (Alhajj and Farhana 2023).

The principal means of determining gene activation involves the use of polymerase chain reaction (PCR) assays. PCR has been a hugely important technique used for many years and has seen a many numbers of developments over this time. The principle of PCR involves the use of polymerase, a naturally occurring intracellular enzyme which assembles nucleic acids strands based a template. In its most basic form, PCR involves denaturing a nucleic acid, such as DNA, to produce two individual single-stranded DNA (ssDNA) sequences. Primers, which are short nucleic acids, are designed specifically to bind both sides of a genetic sequence of interest. Primers are introduced and bind their designated sites and set a template for polymerase to bind. Polymerase is then introduced which binds this site and reassembles the

DNA, producing two DNA strands identical to the original DNA strand, with the target gene sequence. Conditions can be tailored and manipulated to induce this cycle many times, causing exponential amplification of the target gene sequence. Some of the previously mentioned developments includes modifying the polymerase enzyme, which will then integrate a specific fluorescent reporter molecule into newly formed nucleic acid sequences. This allows quantification of the PCR products and is known as quantitative-PCR (qPCR).

In the following study, four chosen bioactives compounds, silver nitrate ($AgNO_3$), chitosan, zinc oxide (ZnO) and nisin shall be assessed for their cytotoxicity against a mammalian cell line relevant to the onset of bovine mastitis. The chosen cell line, bovine mammary epithelial (BME) cells, represent the specific area within the mammary gland where chronic mastitis infections are known to occur. The BME cells will be treated with varying concentrations of each bioactive, and analysis of cellular viability will then be used to determine their cytotoxic against the cell line. Furthermore, the bioactives will also be assessed in order to determine their effect upon BME cell lines immune response. While it is important to determine a compounds effect upon a host immune response, mastitis in itself is an inflammatory disease, which can elicit significant inflammation, which is known to be the primary cause of tissue damage in individuals (Günther et al. 2016; Zheng et al. 2016; Contreras and Rodríguez 2011; Gomes, Saavedra, and Henriques 2016). As such, it will be important that the bioactives do not cause further inflammation, and it may even be beneficial in treatment if they are found to cause an anti-inflammatory response. In order to ascertain this, cells will be pre-treated with lipopolysaccharide (LPS), a bacterial compound which is known to stimulate a full immune response in the majority of mammalian cell lines (Gilbert et al. 2013; Tomasinsig et al. 2010). Following pre-treatment, cells will be co-treated with an individual bioactive and LPS. Cells will be harvested and used for reverse-transcriptase-quantitative PCR (RT-qPCR). This form of PCR involves using reverse-transcriptase (RT) to produce DNA from messenger-RNA (mRNA) allowing quantification of this mRNA which is directly related to the amount of a target compound being produced withing the cell. For the purposes of this study, the cytokines chosen to be quantified are TNFα, IL-1β, IL-6 and IL-8, which are commonly targeted cytokines in a number of immune response assays (Gilbert et al. 2013; Zheng et al. 2016). In-order to quantify whether the cytokine production is up-regulated or down-regulated, they

will be compared to a common housekeeping gene, β-actin. β-actin production should remain consistent in all cells, regardless of treatment and so acts as a baseline.

7.2 Aims and Hypothesis

The aim of this study is to perform a toxicological assay of silver nitrate ($AgNO_3$), chitosan, zinc oxide (ZnO) and nisin against BME cells. BME cells were chosen to represent the internal tissue of bovine mammary gland as this is the primary area of mastitis infection and therefore, treatment exposure. Cells will be grown in culture and exposed to varying concentrations of each bioactive to assess their effects. Cells will also be processed for use in RT-qPCR in order to determine their inflammatory response to each bioactive. The bioactive solutions will be prepared as per bacterial assays (see Chapter 4.6).

It is hypothesised that both $AgNO_3$ and ZnO, being composed of heavier inorganic materials, will hold an adverse effect upon the cells. Although, considering the low MIC of $AgNO_3$ (see Chapter 4.2.2) it is possible that it will not exhibit a significant effect in a range that may still hold it effective against bacterial species. Nisin, being solely a bacterial targeting peptide, will have little to no effect. Similarly, due chitosan's relatively safe nature it will also have little effect. However, since both nisin and chitosan are prepared at lower pH, the acidic properties of the solution will mostly have negative effect on cell viability and immune response.

7.3 Results

7.3.1 Cytotoxicity Assessment

- **Silver Nitrate**

BME cells were treated with silver nitrate ($AgNO_3$) at a concentration range of 1.95 – 1000 µg/mL for 18 hours. The treatment system also included wells treated with the $AgNO_3$ - treatment vehicle (Tv) consisting of 28% (v/v) Poly(ethylene glycol), average molecular weight 400 (PEG-400) and 26% (w/v) d-sorbitol. The $AgNO_3$ treated wells exhibited 100% cell death (CD) (+/- 5%) at concentrations from 1000 – 31.3 µg/mL and ~50% cell death at 15.6 µg/mL (see Figure 7.1). $AgNO_3$ concentrations below this figure did not induce death, but in contrast, promoted a marginal increase in viability when compared to that of the untreated cells (UT). As seen in Figure 7.1, the $AgNO_3$-Tv induced CD at higher concentrations with approximately 100% CD at concentrations relative to 1000 µg/mL $AgNO_3$, but this reduced in a linear fashion

with concentration. In comparison to $AgNO_3$, the $AgNO_3$-Tv exhibited a lesser toxic effect. The highest test concentration of $AgNO_3$ determined to be non-cytotoxic is 7.81 µg/mL.

- **Chitosan**

BME cells were treated with chitosan at a concentration range of 9.77 – 5000 µg/mL for 18 hours. The treatment system also included wells treated with the chitosan-Tv consisting of 1% acetic acid (AcOH), pH 5.5. Both chitosan and the chitosan-Tv exhibited complete CD at the highest concentrations (5000 µg/mL chitosan). However, as seen in Figure 7.2, at 2500 µg/mL, chitosan exhibited significant changes in viability, resulting in ~ 30% cell viability compared to the chitosan-Tv treated cells which exhibited ~90% viability ($p < 0.001$). There were no noteworthy reductions in cell viability seen at any other treatment concentration; thus the highest non-cytotoxic test concentration was determined to be 1250 µg/mL chitosan (International Organization for Standardization 2018).

- **Zinc Oxide**

BME cells were treated with zinc oxide (ZnO) at a concentration range of 4 – 2048 µg/mL for 18 hours. There was no Tv included in this assay as the ZnO was suspended in BME growth media (BMEM) and as such would have no impact on results. As seen in Figure 7.3, ZnO treatment showed negative effects upon the BME cell viability, causing significant cell death at test concentrations of 32 – 2048 µg/mL ($P < 0.01$). Treatment at concentrations of 4 – 16 µg/mL was seen to have a lesser effect upon cell viability (99 – 87% viability). The highest non-toxic ZnO treatment was determined to be 16 µg/mL.

- **Nisin**

BME cells were treated with nisin at a concentration range of 0.244 – 125 µg/mL for 18 hours. A nisin-Tv was also included, consisting of dH_2O (400 mM NaCl, pH 3.25). As seen in Figure 7.4, both nisin and the nisin-Tv induced notable CD at the highest concentrations (125 µg/mL), with ~20% and ~40% cell viability respectively. These values were significantly different ($P < 0.001$) suggesting nisin was producing a major effect itself. As evident from Figure 7.4, nisin has slight effect upon cell viability at all test concentrations between 3.9 – 62.5 µg/mL (approximately 10 – 12% CD), whereas the nisin-Tv ceases to hold any noteworthy effect from 31.3 µg/mL. The highest non-cytotoxic test concentration of nisin was determined to be 62.5 µg/mL.

7.3.2 Cell Immune Response Assay

Results are presented in Figures 7.11 – 7.14 as bar graphs showing mean cytokine expression relative to β-actin expression, with 1 hour pre-treatment of LPS followed by 24-hour exposure of BME cells with LPS alone or in co-treatment with one of the other stated treatments. Untreated (UT) cells were not exposed to any compounds. Mean relative cytokine expression greater than that of LPS alone indicates an increased inflammatory response whereas expression lower than that of LPS indicates a reduction of inflammation, which suggests an anti-inflammatory effect.

- **TNFα**

Mean TNFα expression is represented by bars in Figure 7.11. Results indicate reduced cytokine expression in BME cells following exposure with each bioactive and PVP. The greatest reduction seen with $AgNO_3$ exposure, causing a 2.47-fold reduction in TNFα expression relative to LPS alone. ZnO also caused strong reduction, reporting a 2.04-fold decrease in TNFα expression. Chitosan, nisin and PVP also held moderate effects with 1.41-fold, 1.75-fold and 1.64-fold reductions respectively.

- **IL-1β**

Mean IL-1β expression is presented as bars in Figure 7.12. Results show treatment with $AgNO_3$ and ZnO to cause reduced IL-1β expression up to 2.50-fold and 1.98-fold respectively relative to LPS alone. Chitosan and nisin was also noted to cause reduction of cytokine expression, but to much lower intensity with 1.23-fold and 1.13-fold reductions respectively. PVP held very little effect upon IL-1β expression.

- **IL-6**

Mean relative IL-6 expression following treatment is presented in Figure 7.13. Results show reduced IL-6 expression from 24-hour exposure with $AgNO_3$ (1.37-fold) and nisin (1.59-fold), while chitosan, PVP and ZnO were seen to cause 1.11-fold, 1.49-fold and 1.13-fold increases of expression respectively, relative to LPS alone.

- **IL-8**

Mean relative IL-8 expression is presented in figure 7.14. $AgNO_3$ treatment was noted to cause reduced IL-8 expression, with a 1.22-fold reduction in expression relative to LPS alone. There

was no mean change in expression following exposure with nisin. Chitosan, ZnO and PVP exposure was seen to cause minor increases in expression, with 1.16-fold, 1.20-fold and 1.09-fold increases respectively.

7.4 Discussion

Silver nitrate ($AgNO_3$) exhibited severe toxicity towards BME in a range of 31.3 – 1000 µg/m L, while inducing ~50% CD at a concentration of 15.6 µg/mL. The $AgNO_3$ -Tv also exhibited toxicity, but from comparison of calculated cell viabilities, it did not have an overly substantial effect as part of the $AgNO_3$ treatment. The highest non-cytotoxic test concentration was found to be 7.81 µg/mL, which is lower than the mean MIC values determined previously (See Figure 7.5 for comparisons). The observed toxicity of $AgNO_3$ was somewhat expected due its composition and effects, however it was expected to be less severe towards mammalian cells than bacterial cell. While $AgNO_3$ did exhibit somewhat cytotoxic effects, its influence upon cellular inflammatory response were much more favourable. When cells were exposed to co-treatments of $AgNO_3$ and LPS, it was found that the inclusion of $AgNO_3$ caused a notable reduction the expression of TNFα, IL-1β, IL-6 and IL-8, all of which are pro-inflammatory cytokines. Similar reductions in cytokine production have been noted in other cell lines (S. H. Shin et al. 2007). The ability to reduce inflammation would be quite beneficial in the treatment of infections and inflammatory diseases such as mastitis, where the high inflammatory response can cause sever tissue damage to the host (Zheng et al. 2016; Garcia 2004).

Nisin and chitosan exhibited the lowest toxic effects towards BME cells, in terms of their effect on cell viability. While chitosan was exhibiting noticeable toxic effects in a range of 2500 – 5000 µg/mL, concentrations below this did not induce any noteworthy effect. However, while nisin only appeared to cause cell death at the highest concentration (125 µg/mL), it still exhibited a slight toxic effect at all test concentrations. This noted occurrence could be due to the presence of macromolecules in the treatment solution, as seen in Figure 7.9. The small black molecules, which may be by-products from the commercial nisin powder, are only visible in image A and B, which are cells treated with nisin (125 µg/mL) at time-points 0 and 18 respectively. These molecules may have disrupted the cell viability through steric effects, which could explain the minor effect across all concentrations.

Immune response studies show chitosan to have varying effects upon cytokine expression, with IL-1β and IL-6 expression remaining relatively similar to LPS only treated cells, while IL-8 expression was seen to increase and TNFα expression was noted to decrease. Similar reductions were noted in other studies, however the IL-6 expression reduction was much more notable (Yoon et al. 2007). Other studies have also show that the effect of chitosan upon cytokine production, particularly TNFα, can vary depending on the grade of chitosan used (Davydova et al. 2016). Such variance in effects cannot conclude whether chitosan is pro or anti-inflammatory, as all test cytokines are heavily involved in the inflammatory response cascade. Similar effects were noted from nisin, which was seen to cause reduced expression of TNFα and IL-6. Mean expressions of IL-1β and IL-8 were slightly less or similar to that of LPS alone. As there were no notable increases in expression, it could be established that nisin is somewhat anti-inflammatory, as supported by other similar studies (Jia et al. 2019; Małaczewska and Kaczorek-Łukowska 2021).

Zinc oxide (ZnO) exhibited very severe toxicity towards BME cells, from a concentration range of 32 2048 μg/mL. Unlike the toxicity range exhibited by $AgNO_3$, ZnO toxicity does not fall within a satisfactory range in comparison to its mean MIC value versus the bacterial strains (Figure 7.5). As can be observed in Figure 7.10, ZnO formed a heavy precipitate on top of the cell layer. This precipitate is the most likely cause for the reported cell viability at the concentration range of 1024 – 2048umg/mL as it's actual presence would interfere with absorbance readings of the MTT assay, and the linear decline in absorbance would also reinforce this assumption. Furthermore, as per images shown in Figure 7.10, the envelopment of the cells with the ZnO compound would cause the cells great stress which would cause decline in viability. Immune response results indicate ZnO to have favourable effect in reducing expression of TNFα and IL-1β, however it was also noted to cause increases in IL-6 and IL-8 expression, however it is worth noting that the decreases in expression are much greater than the increases. Other similar studies have noted a decrease in TNFα expression from ZnO exposure to cells, but they have also noted decreases in IL-6 expression, which may be due to the cell type or even the form of ZnO used (Hu et al. 2013). Other studies have also suggested that the ZnO form can greatly alter the effects upon cytokine expression, particularly the ZnO-NP size .

7.5 Conclusion

Of the four bioactives assessed during this study, $AgNO_3$, chitosan and nisin showed promising results in terms of their toxicity status towards BME cells. While $AgNO_3$ did exhibit toxicity at a concentration lower than the mean MIC, previous combinational studies have shown that it can have a significant effect in aiding the antimicrobial abilities of the other, less toxic bioactives, especially nisin (See Figure 7.5). Furthermore, its ability to reduce expression of all four test cytokines give its greater value as a potential therapeutic for inflammatory diseases.

Both chitosan and nisin showed very promising potential due to their low cytotoxic effects, especially in comparison with to their mean MIC values. Furthermore, they were noted to both reduce TNFα and IL-1β expression. The previous synergy studies have also clearly indicated their suitability for combinational together, and also with the other bioactives.

While the results of ZnO show severe loss of cell viability, this could be challenged due to the nature of the chosen cell viability assess. Images taken of cells show a heavy later of precipitate which could easily interfere with the successful implementation of the MTT assay. It could also be hypothecated that if a solid carrier for ZnO was utilised, it could stop such accumulation and prevent such mammalian cell death, while still leaving ZnO available to interact with bacterial cells.

In conclusion, final findings show the four bioactives to vary greatly in the effects exhibited upon BME cells, however in conjunction with results of previous studies, there is a clearer idea of how they can be implemented and incorporated into a treatment successfully and safely.

7.6 Figures

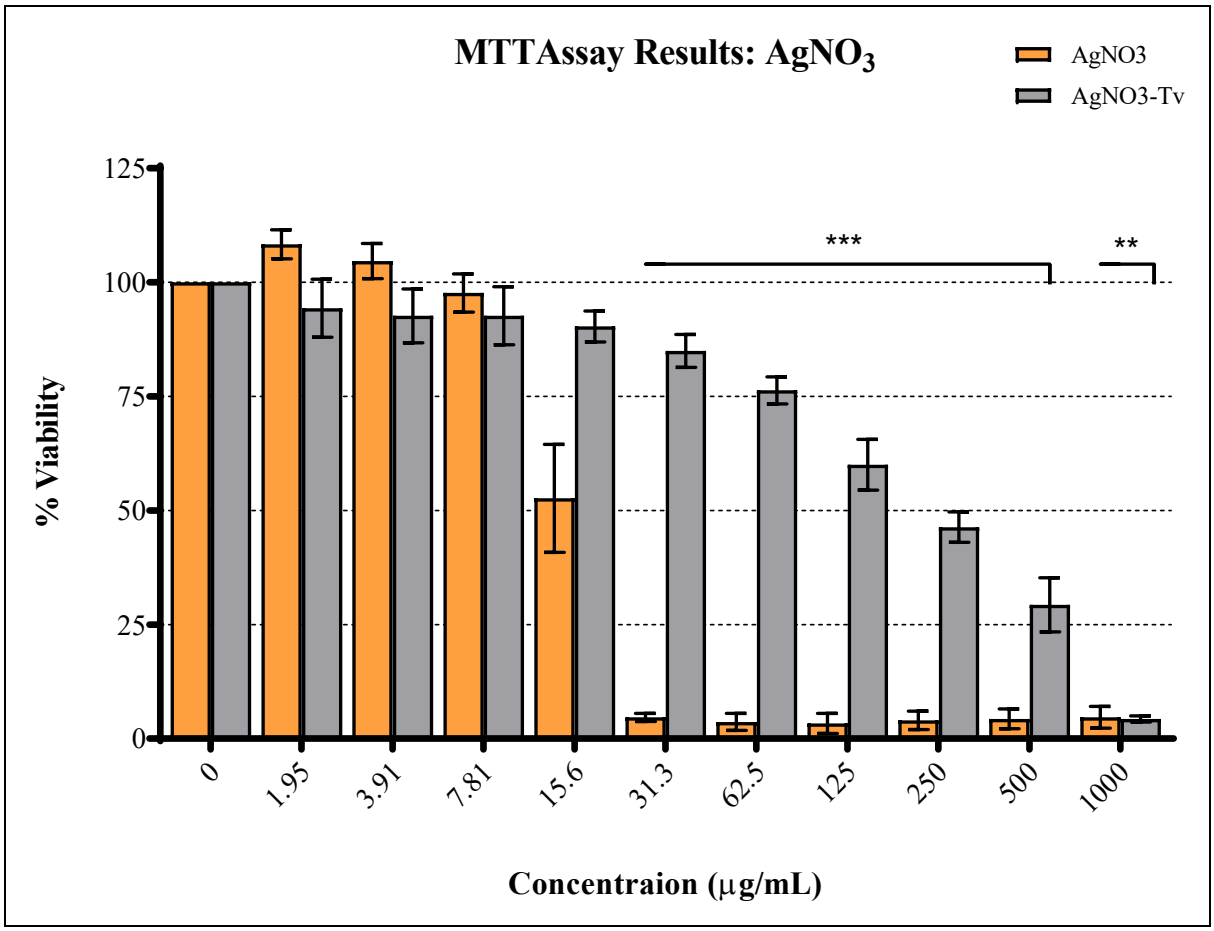

Figure 7.1 MTT Results of Silver Nitrate and Bovine Mammary Epithelial Cells.
Bars represent the mean viability of bovine mammary epithelial (BME) cells following 18-hour treatment with silver nitrate ($AgNO_3$) at a range of concentrations (µg/mL). The silver nitrate treatment vehicle ($AgNO_3$-Tv) was also included. Cell viability determined by use of MTT assay. Error bars represent standard error of the mean (SEM). Significance between effects of $AgNO_3$ and $AgNO_3$-Tv was determined by use of two-way ANOVA with Sidak's multiple comparisons test and expressed in terms of a P value following the APA style. P = 0.002 (**), P < 0.001 (***). N = 3

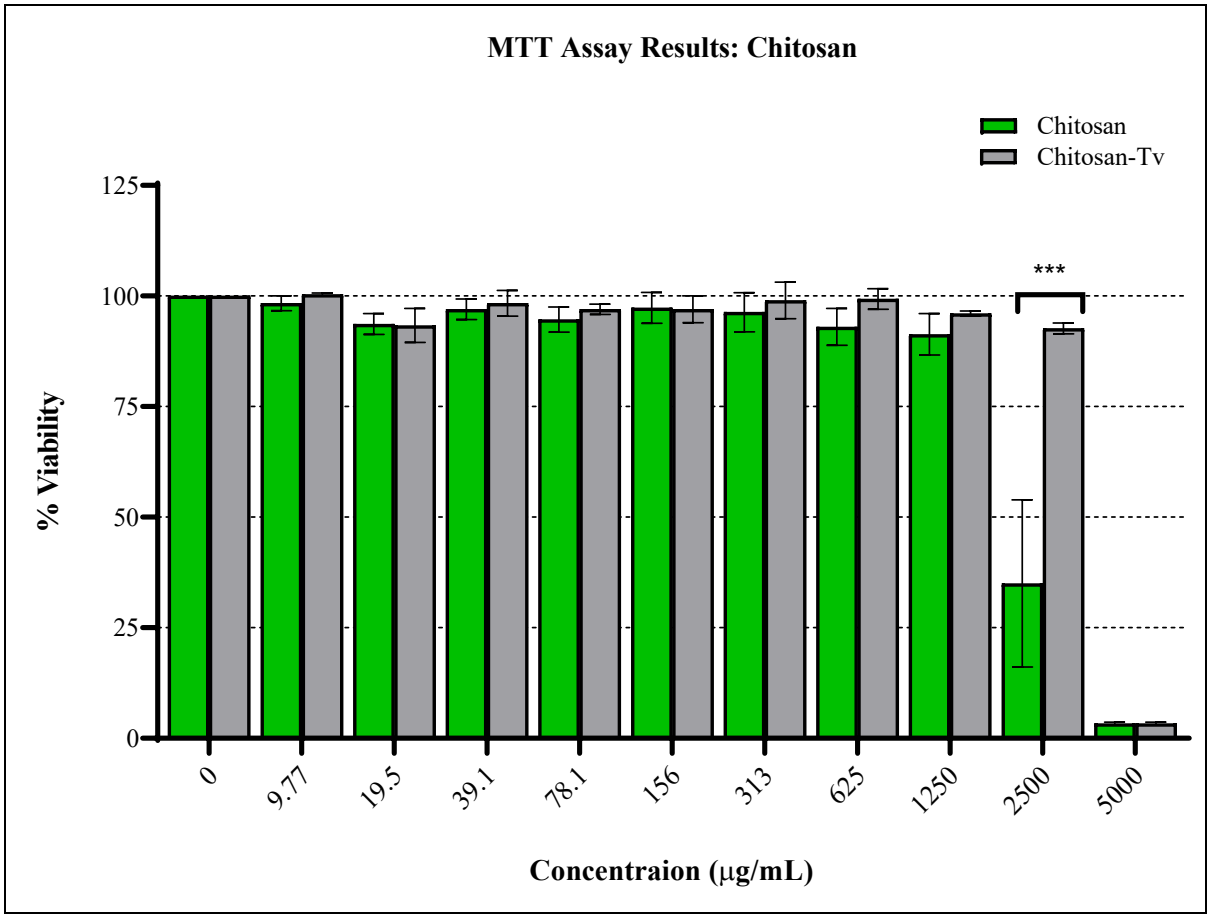

Figure 7.2 Dose Response curve of Chitosan and Bovine Mammary Epithelial Cells.
Bars represent the mean viability of bovine mammary epithelial (BME) cells following 18-hour treatment with chitosan at a range of concentrations (μg/mL). The chitosan treatment vehicle (chitosan-Tv) was also included. Cell viability determined by use of MTT assay. Error bars represent standard error of the mean (SEM). Significance between effects of chitosan and chitosan-Tv was determined by use of two-way ANOVA with Sidak's multiple comparisons test and expressed in terms of a P value following the APA style. $P < 0.001$ (***). N = 3

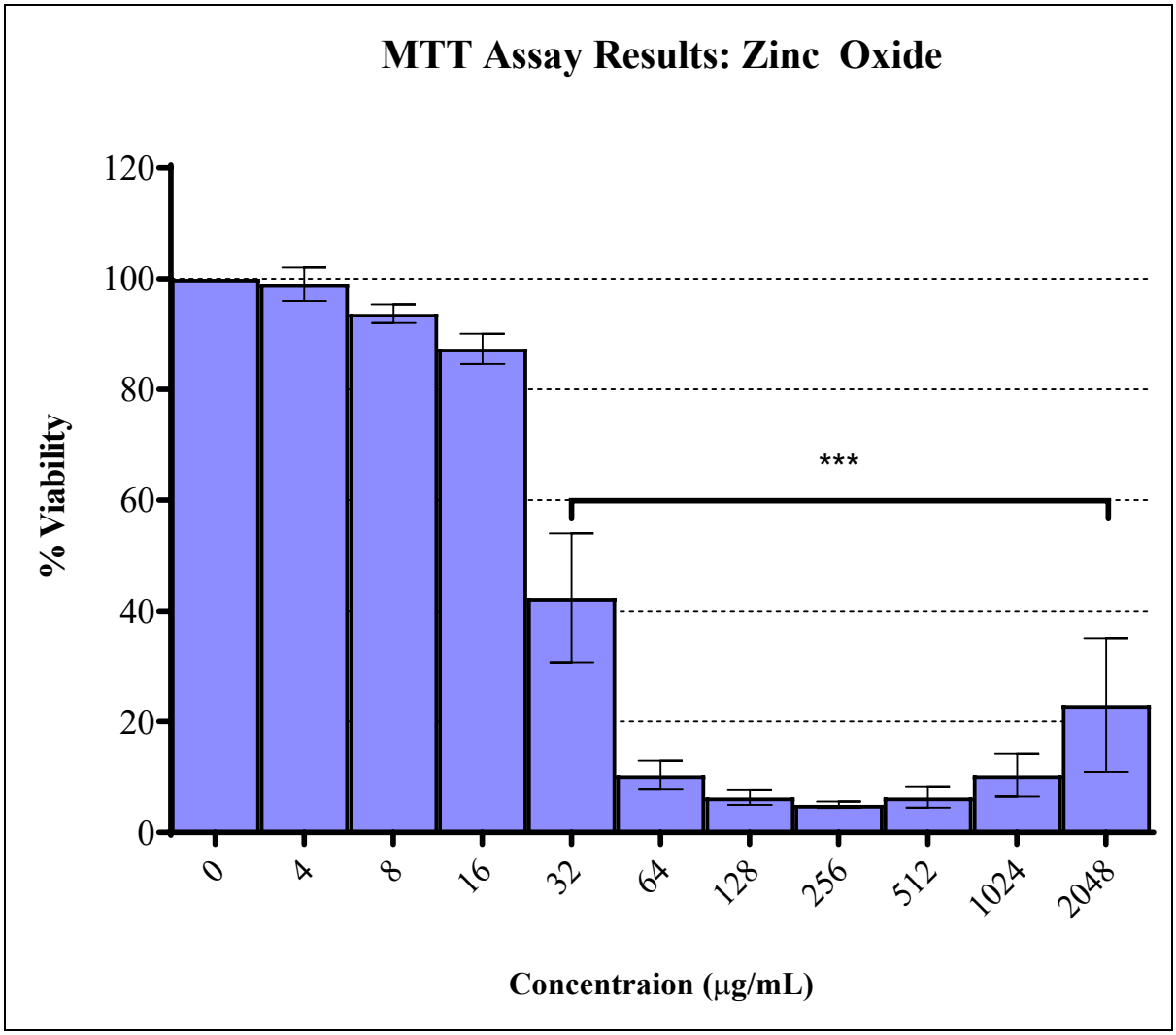

Figure 7.3 MTT Results of Zinc Oxide vs. Bovine Mammary Epithelial Cells.
Bars represent the mean viability of bovine mammary epithelial (BME) cells following 18-hour treatment with zinc oxide (ZnO) at a range of concentrations (µg/mL). Cell viability determined by use of MTT assay. Error bars represent standard error of the mean (SEM). Significance was determined by a two-way ANOVA with Sidak's multiple comparisons test which was used to compare % viability of treated and untreated (i.e., 100% viability) to show significant effects of treatment. $P < 0.001$ (***). N = 3

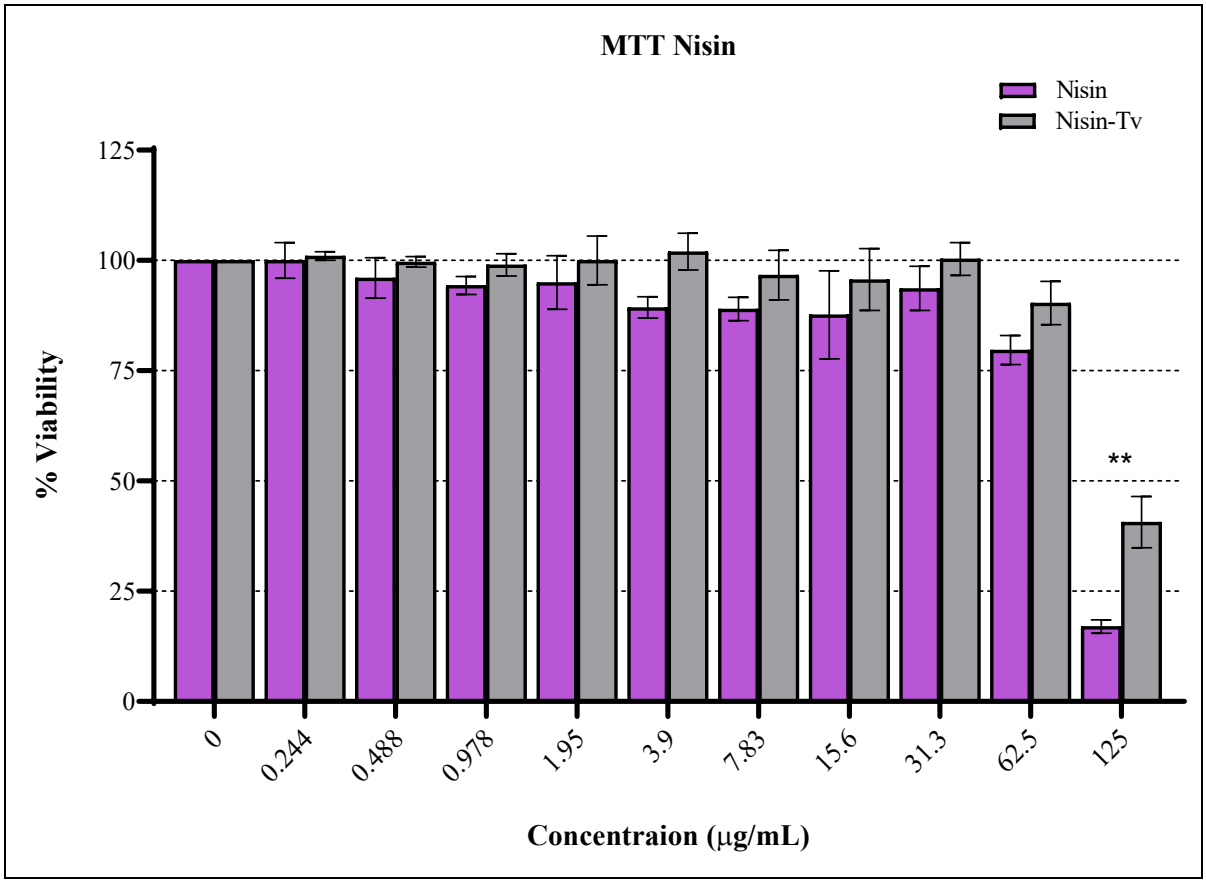

Figure 7.4 MTT Results of Nisin vs. Bovine Mammary Epithelial Cells.
Bars represent the mean viability of bovine mammary epithelial (BME) cells following 18-hour treatment with nisin at a range of concentrations (μg/mL). The nisin treatment vehicle (nisin-Tv) was also included. Cell viability determined by use of MTT assay. Error bars represent standard error of the mean (SEM). Significance between effects of nisin and nisin-Tv was determined by use of two-way ANOVA with Sidak's multiple comparisons test and expressed in terms of a P value following the APA style. P = 0.002 (**). N = 3

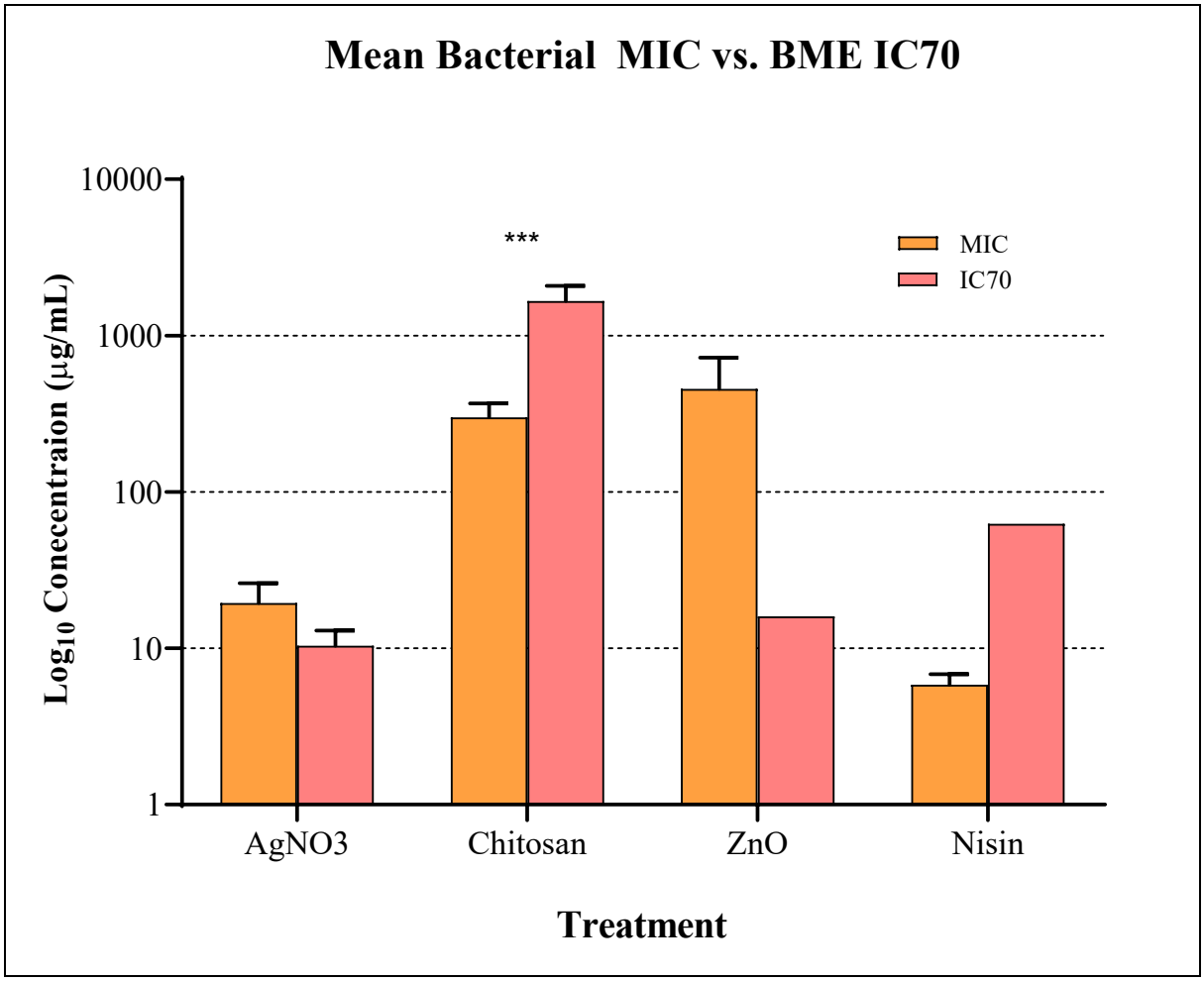

Figure 7.5 Mean Bacterial Minimum Inhibitory Concentrations vs. BME IC70
Bars represent the mean bacterial minimum inhibitory concentrations (MIC) and the mean bovine mammary epithelial cell (BME) cytotoxic concentration (IC70) of silver nitrate (AgNO3), chitosan, zinc oxide (ZnO) and nisin. P<0.001 ***

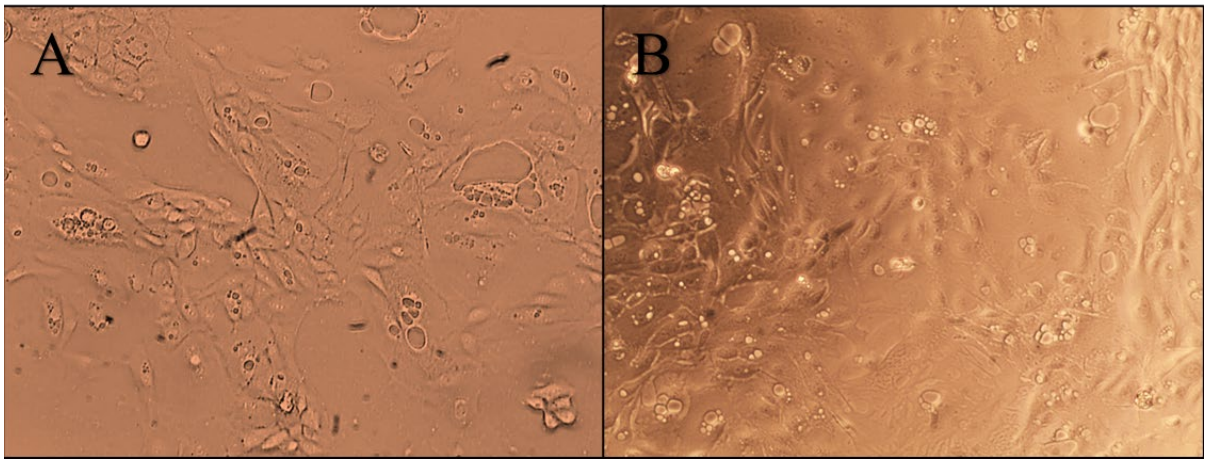

Figure 7.6 Images of Untreated Bovine Mammary Epithelial Cells.
Images showing untreated (UT) bovine mammary epithelial cells. **A:** UT (t = 0), **B:** UT (t = 18) M = 100X.

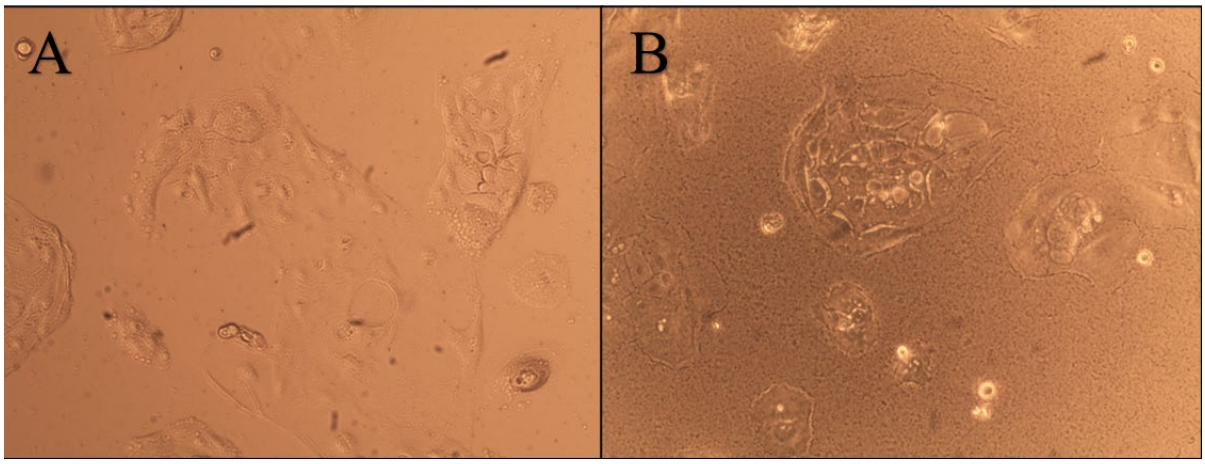

Figure 7.7 Images of AgNO3 Silver Nitrate Treated Bovine Mammary Epithelial Cells.
Images showing bovine mammary epithelial cells following treatment with silver nitrate ($AgNO_3$). **A:** $AgNO_3$ [1000 µg/mL] (t = 0), **B:** $AgNO_3$ [1000 µg/mL] (t = 18). M = 100X.

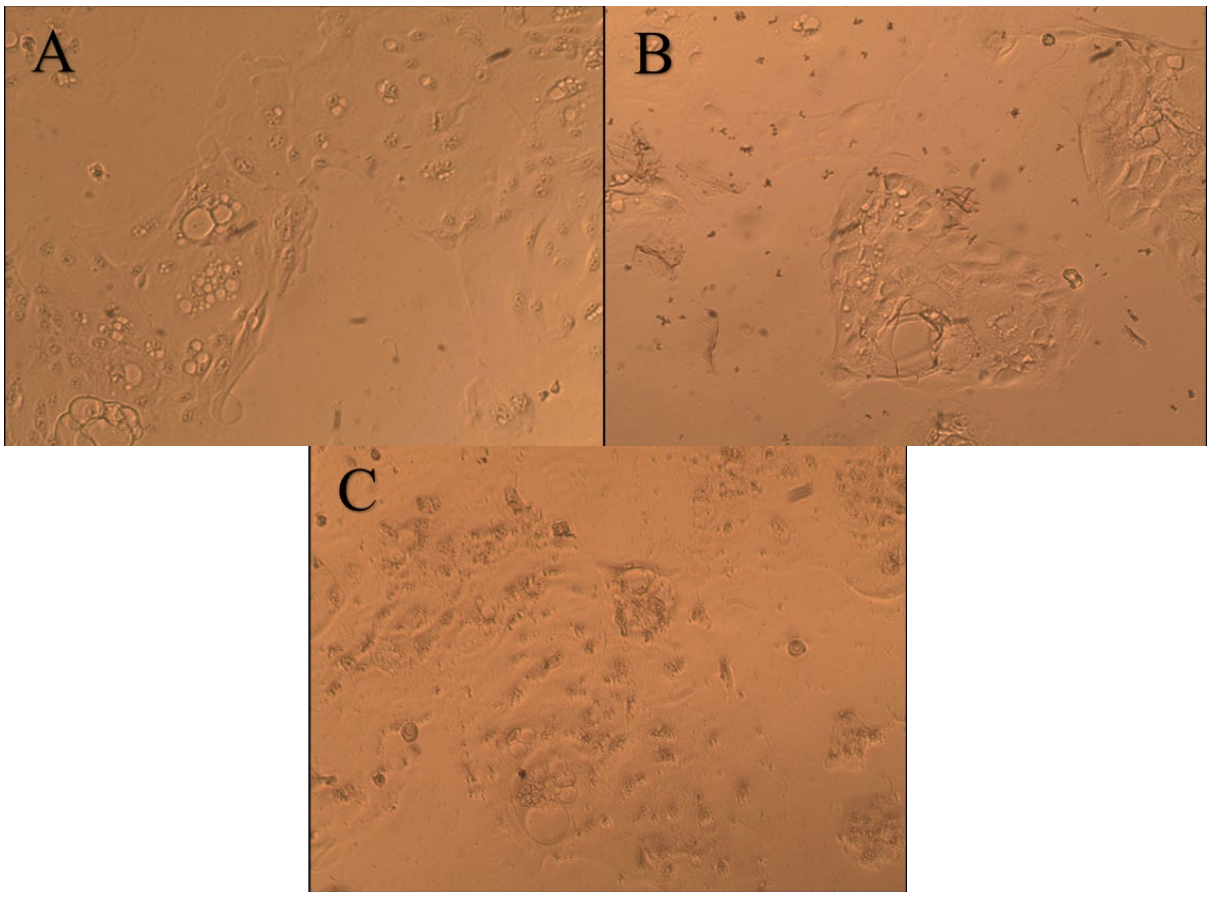

Figure 7.8 Images of Chitosan Treated Bovine Mammary Epithelial Cells.
Images showing bovine mammary epithelial cells following treatment with chitosan. **A:** Chitosan [5000 µg/mL] (t = 0), **B:** Chitosan [5000 µg/mL] (t = 18) **C:** Chitosan-Tv [equivalent 5000 µg/mL] (t = 18). M = 100X.

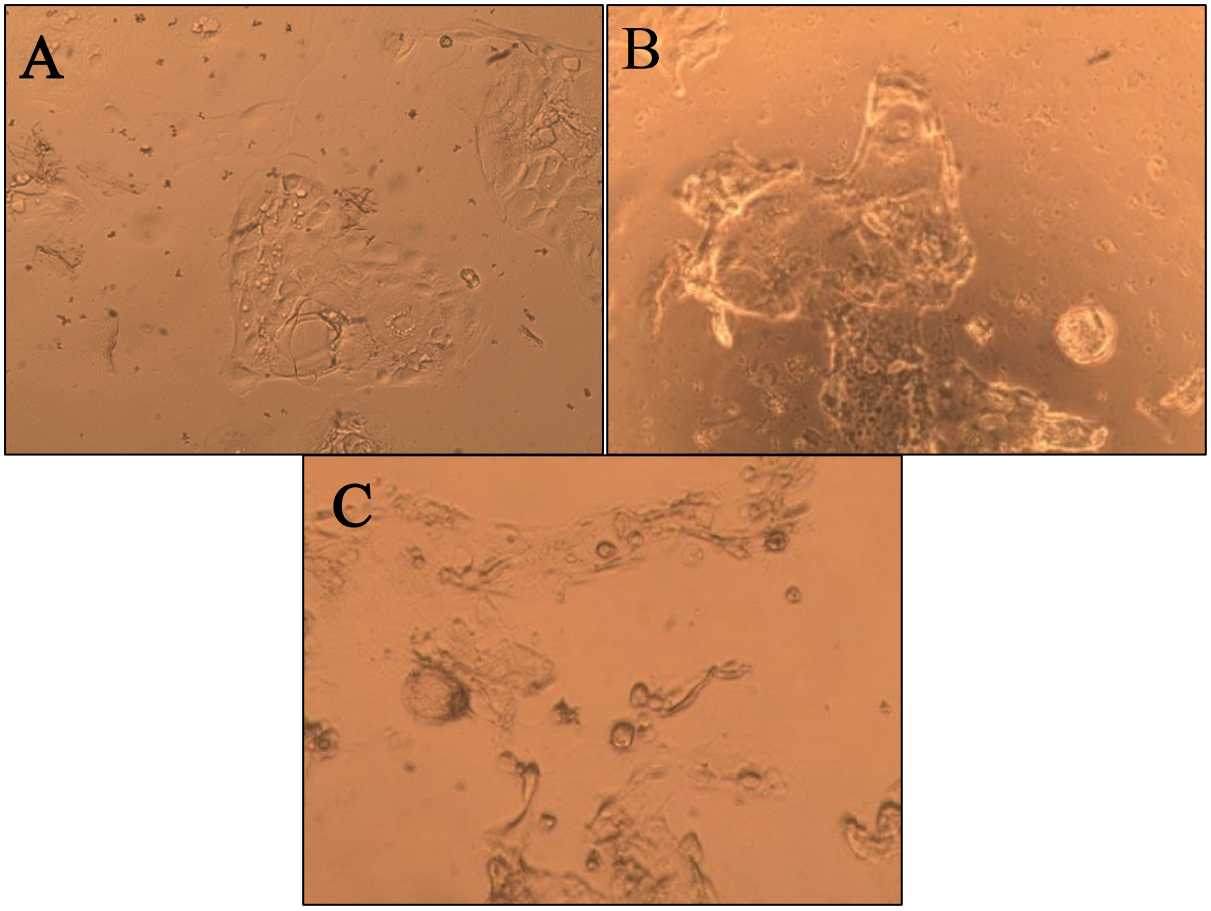

Figure 7.9 Nisin Treated Bovine Mammary Epithelial Cells.
Images showing bovine mammary epithelial cells following 18-hour treatment with nisin. A: Nisin [125 µg/mL] (t = 0), B: Nisin [125 µg/mL] (t = 18), C: Nisin Treatment Vehicle [equivalent 125 µg/mL Nisin] (t = 18). M = 100X.

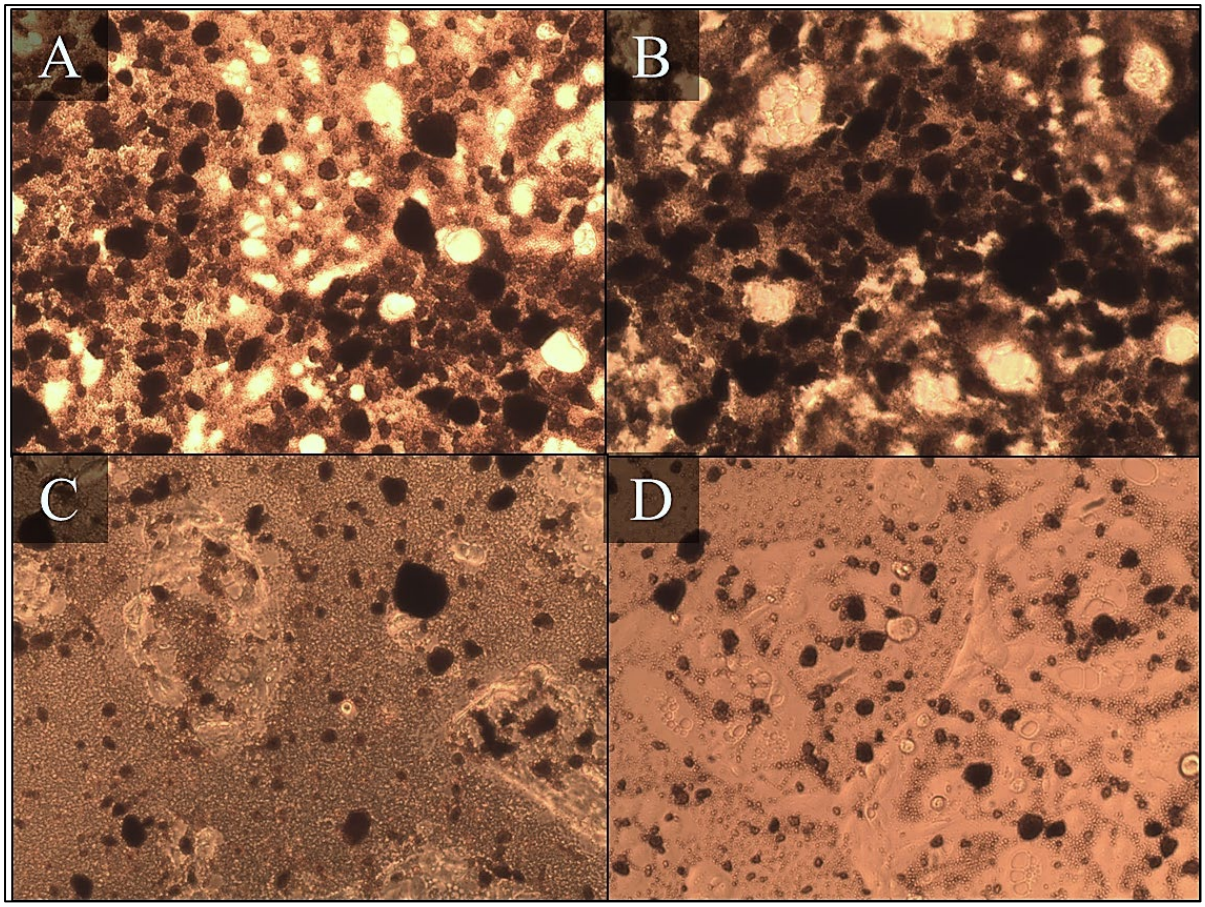

Figure 7.10 Images of Zinc Oxide Treated Bovine Mammary Epithelial Cells.
Images showing bovine mammary epithelial cells following treatment with zinc oxide (ZnO). **A:** ZnO [2048 µg/mL] (t = 0), **B:** ZnO [2048 µg/mL] (t = 18), **C:** ZnO [1024 µg/mL] (t = 0), **D:** ZnO [1024 µg/mL] (t = 18). M = 100X.

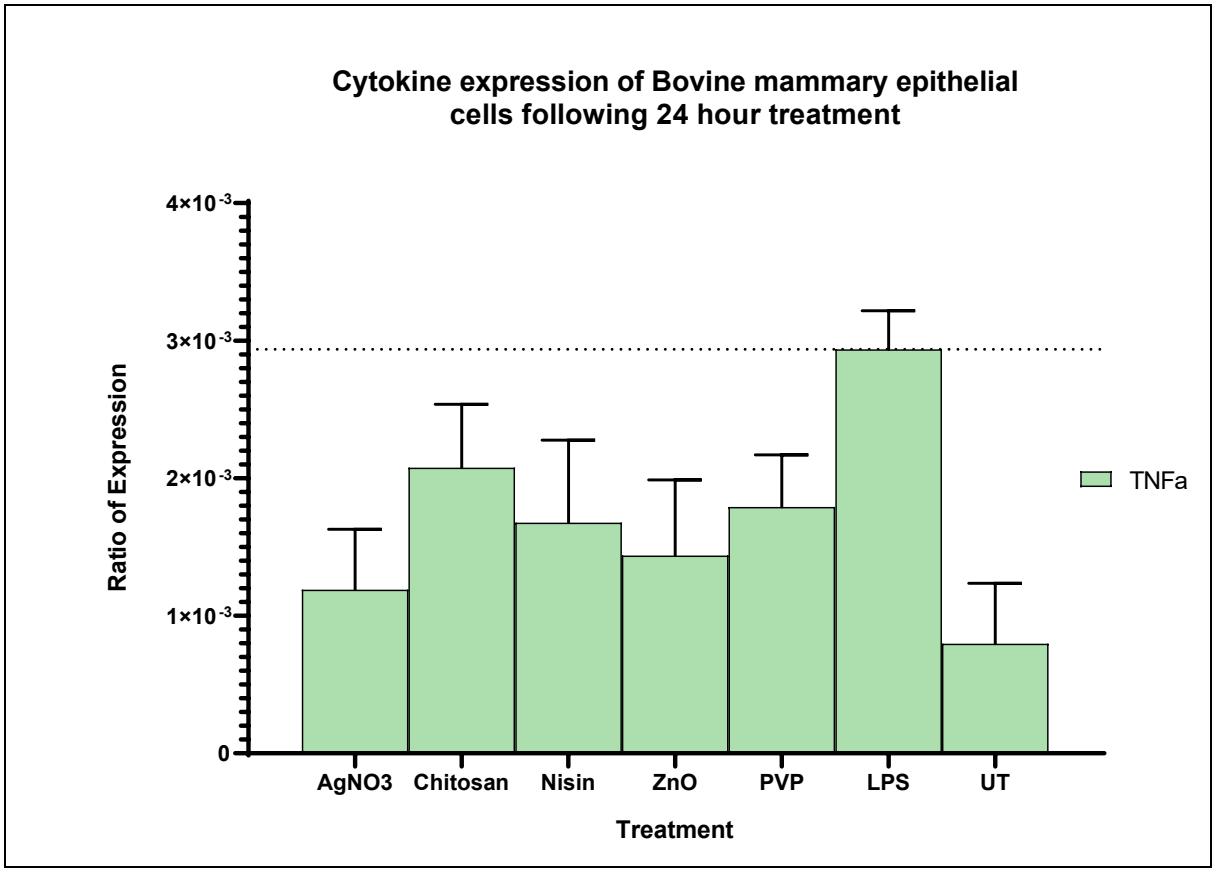

Figure 7.11 Relative ratio of TNFα expression in Bovine Mammary Epithelial Cells. Bars represent mean TNFα ratio of expression relative to housekeeping β-actin gene expression following 1 hour pre-treatment with LPS and 24-hour treatment of LPS alone, or in combination with either $AgNO_3$, chitosan, Nisin, PVP or ZnO. Untreated cells (UT) also shown. Two sets of Bovine mammary epithelial cells were treated in replicates of 2. Following RNA extraction/isolation and cDNA synthesis, cytokine expression was determined by use of qRT-PCR. Line intercept at mean result for LPS.

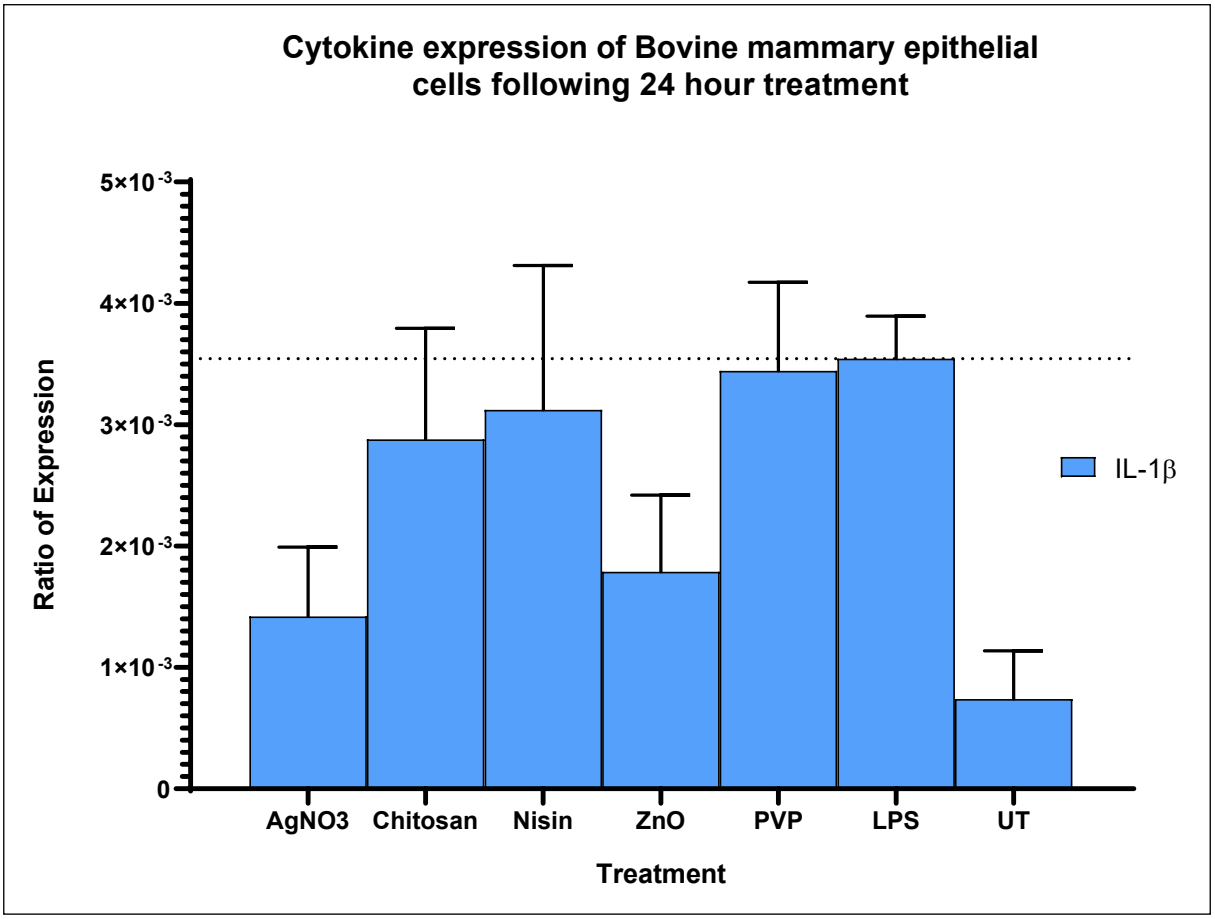

Figure 7.12 Relative ratio of IL-1β expression in Bovine Mammary Epithelial Cells. Bars represent mean IL-1β ratio of expression relative to housekeeping β-actin gene expression following 1 hour pre-treatment with LPS and 24-hour treatment of LPS alone, or in combination with either $AgNO_3$, chitosan, Nisin, PVP or ZnO. Untreated cells (UT) also shown. Two sets of Bovine mammary epithelial cells were treated in replicates of 2. Following RNA extraction/isolation and cDNA synthesis, cytokine expression was determined by use of qRT-PCR. Line intercept at mean result for LPS.

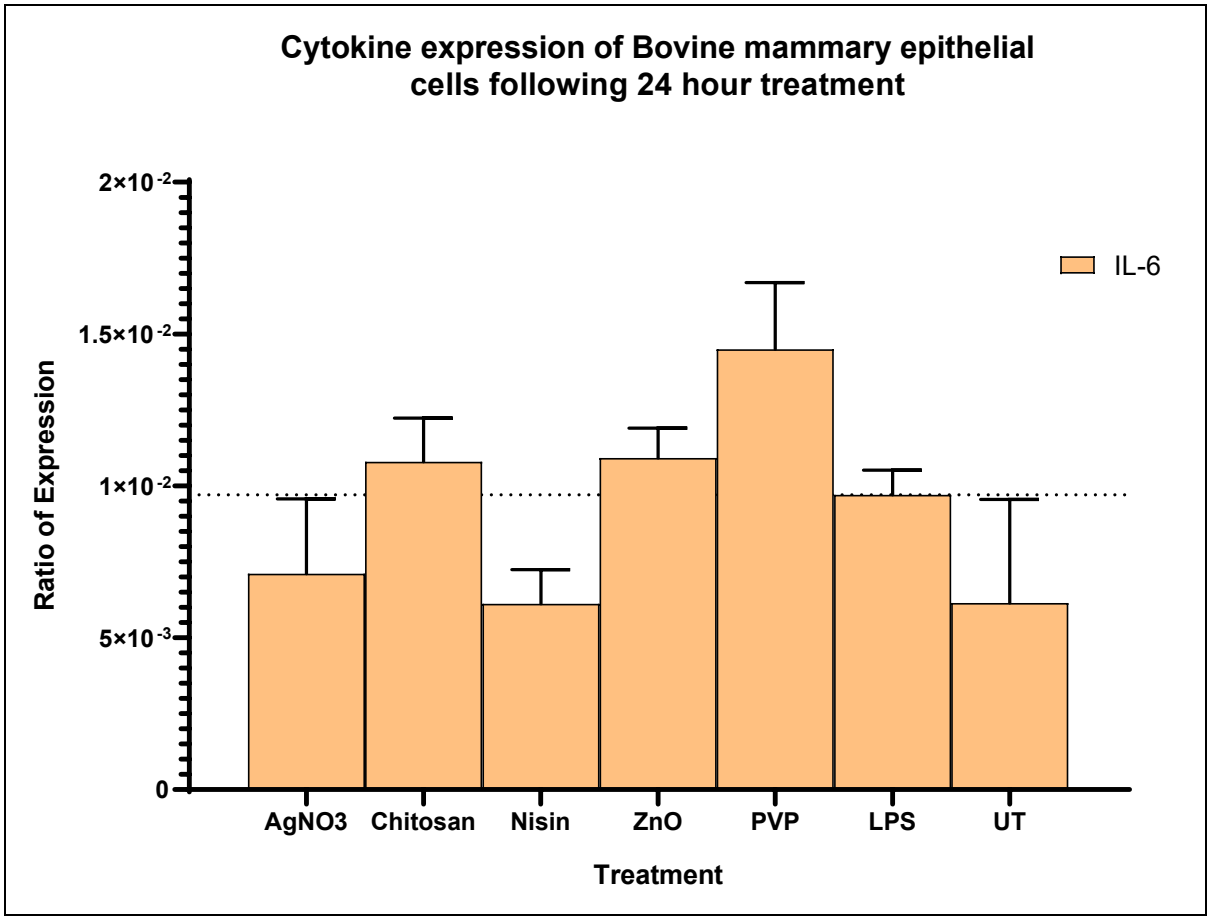

Figure 7.13 Relative ratio of IL-6 expression in Bovine Mammary Epithelial Cells. Bars represent mean IL-6 ratio of expression relative to housekeeping β-actin gene expression following 1 hour pre-treatment with LPS and 24-hour treatment of LPS alone, or in combination with either $AgNO_3$, chitosan, Nisin, PVP or ZnO. Untreated cells (UT) also shown. Two sets of Bovine mammary epithelial cells were treated in replicates of 2. Following RNA extraction/isolation and cDNA synthesis, cytokine expression was determined by use of qRT-PCR. Line intercept at mean result for LPS.

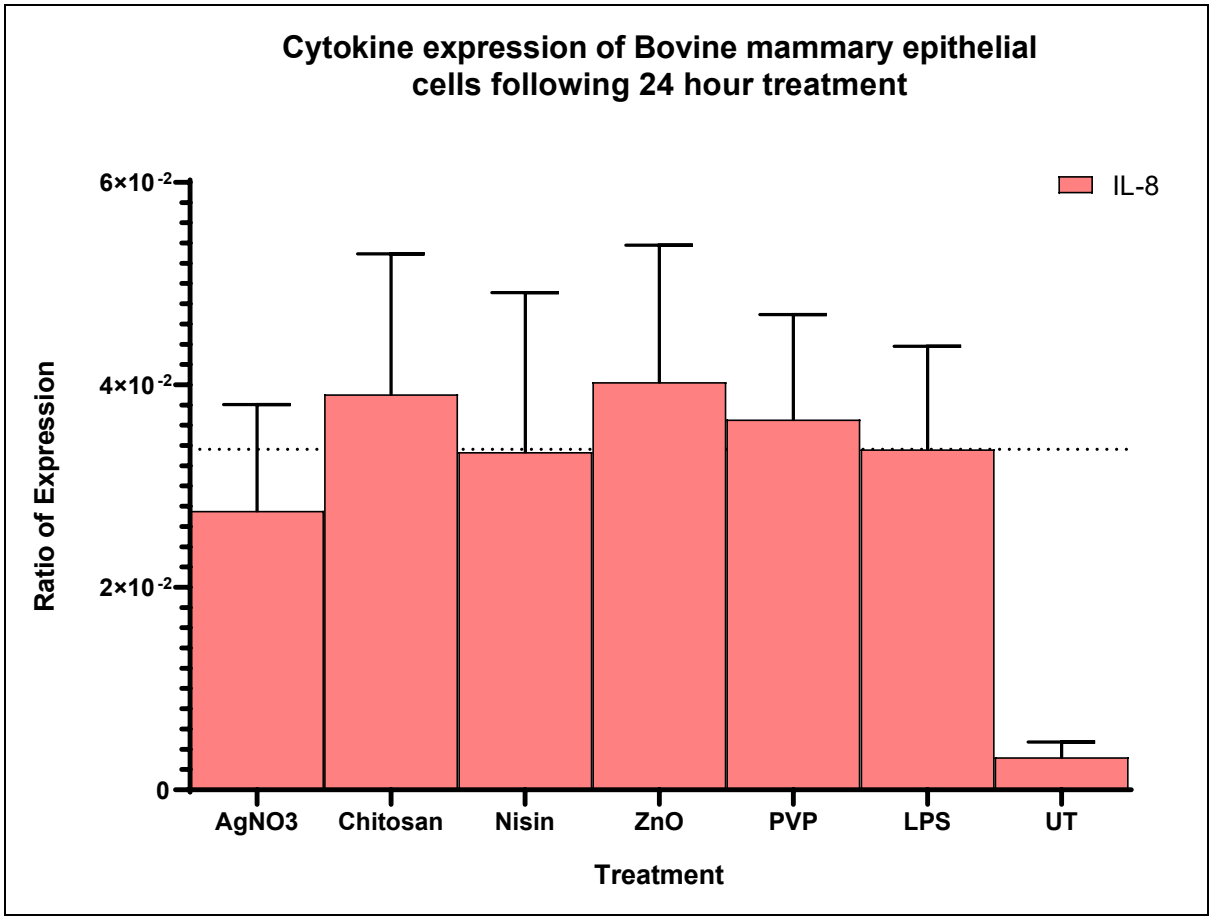

Figure 7.14 Relative ratio of IL-8 expression in Bovine Mammary Epithelial Cells. Bars represent mean sIL-8 ratio of expression relative to housekeeping β-actin gene expression following 1 hour pre-treatment with LPS and 24-hour treatment of LPS alone, or in combination with either $AgNO_3$, chitosan, Nisin, PVP or ZnO. Untreated cells (UT) also shown. Two sets of Bovine mammary epithelial cells were treated in replicates of 2. Following RNA extraction/isolation and cDNA synthesis, cytokine expression was determined by use of qRT-PCR. Line intercept at mean result for LPS.

Chapter 8 Conclusion and Implications for Future Research

The pressing need to find new appropriate antimicrobial compounds as safe alternatives to antibiotics has triggered intensive research, particularly in the cross-cutting areas of novel compound characterization, *in vitro* screening methods and drug (bioactive) delivery vehicles. This present novel study has contributed to addressing these needs by developing appropriate methods that support effective testing and screening of candidate bioactive compounds including assessing antimicrobial and antibiofilm performance, polymer incorporation suitability, and cytotoxic and inflammatory effects. The latter relates to important biocompatibility efficacy.

The chosen bioactive compounds, silver nitrate ($AgNO_3$), chitosan, zinc oxide (ZnO) and nisin were selected as their chemical structures support heat stability that has been well described in the literature. This is important for appropriate incorporation into carrier polymers for bioactive delivery and will also inform effectiveness of smart coatings for preventing future biofilm development on medical devices for veterinary and potentially human applications. These four bioactive exhibited encouraging results in terms of their microbial inhibitory effects against the various microbial pathogens selected for the project, including for the future addressing of complex mastitis infections in dairy cattle. The ability to incorporate these thermotolerant compounds into a polymer matrix opens many possibilities in terms of their delivery method and how a final product can be designed for ease of production, access, and use. The test polymer, PVP-VA64, also demonstrated great suitability towards a final polymer treatment for bovine mastitis. Its low melting temperature ensured low effect upon incorporated compounds. As well as this, its' hard brittle extruded form allowed the product to be easily ground into a water-soluble powder.

The extensive biofilm studies have shown very in-depth capabilities of the bioactives against Gram-negative and Gram-positive bacterial species. As biofilms represent a major cause of antibiotic resistance, any ability of an alternative antibiotic treatment to disrupt formation of biofilms holds huge economic and societal importance. Antibiotics alone are very ineffective in tackling biofilm-mediated infections, as biofilms by complex design diminish or negate the

effects of front-line antibiotics. While individual bioactives developed for this novel project showed promise at different stages of biofilm development, their use in combination could prove to have vastly greater effect, such as demonstrated by combinational antimicrobial growth studies. This too can hold importance with regard to the bioactives cytotoxicity, wherein combinational studies have shown that very small amounts of each in combination can produce desirable outcomes. Moreover, use of smaller amounts of bioactives via a combinational approach could by-pass the cytotoxic effects reported in this present project. Thus, these GRAS grade bioactives characterized in this novel project were shown to reduce many of key indicators of inflammation *in vitro* highlighting their biocompatibility potential supporting more intensive studies during a future *in vivo* infection model phase.

Mastitis remains a major hinderance in the dairy industry worldwide, and antibiotics remain the main treatment method. Intramammary infusions is the principal means that farmers use in order to treat bovine mastitis. This approach involves dissolving a powder containing antibiotic mixtures (supplied in large containers) into a liquid solution, which can then be injected directly into the teat of an infected mammary gland. A multi-compound polymer, developed to hold the most effective concentrations of each bioactive (as determined by the combination studies) ground into a fine powder, would provide a simple substitute for this well-established method. With such a small alteration of the procedure, there would be no need for additional training or knowledge, allowing a streamline introduction to farms globally. This simple change could eliminate a huge proportion of antibiotic exposure to our food chain as well as the amount of antibiotics released into the natural environment.

Implications for future work

Technical domain

- While the current project has answered many of the initial questions regarding the bioactives and their suitability as antibiotic alternatives for the use in treating mastitis, there does remain a select few before implementation. Future studies will be required to determine the effects of the bioactives in combination *in vitro* against the bovine mammary epithelial cells, as well as potentially further *in vivo* trials.

- The bioactives must also be assessed for their antimicrobial and antibiofilm capabilities when incorporated into the polymer matrix together, as combinational studies of bioactives outside of the polymer have indicated that they do hold altered efficacy and even possibly altered mechanisms in microbial growth reduction. Results of post-HME analysis of individual bioactives also indicate some alterations of their abilities. With these considerations, it would be prudent to further assess the combined bioactives once they are incorporated into a polymer matrix.
- The combination of bioactives showing greatest efficacy will require broader applications for antimicrobial including potential for anti-fungal therapies where the WHO declared many fungal pathogens as priority for new innovations and solutions
- Future studies on the stability and functionality of these polymer-based bioactives post sterilization modalities (including Sterility Assurance Level) for smart coatings on medical devices that can be used to address complex infection scenarios, including for small animals

Policy Domain

- Dissemination findings including additional social media (LinkedIn) outputs in terms of creating a greater awareness of the potential of this HME polymer-bioactive approach to inform top-down policies to address AMR crisis including many of the UN SDGs.
- Presentations to Health Service Executive through linked Department of Nursing and Health Science for regional impact and awareness
- Adopt a Quadruple Helix approach (combining academia-industry-society and healthcare) at the interface for testing solutions for end-user engagement and acceptance
- Publish in appropriate policy journals
- Adopt a OneHealth Approach that embraces interface between health and the environment to inform policies and decision-making for new innovations.

Societal Domain

- Create a greater awareness of the emergence of AMR and the need for effective solutions such as potentially this HME-polymer delivery option to inform and enable

behavioural change including reduction on the use of antibiotics through Citizen Science

- Greater outreach to schools such as what is delivered in TUS under the Science Foundation Ireland Cell Explorers Programme
- Greater network and communication between veterinary and healthcare on challenges presented by AMR with dialogue with communities to promote change.
- Consider new digital technological to inform rapid dissemination and communication

Environmental Domain

- Highlight the benefit of novel food grade bioactives as alternative to antibiotics where resistance to latter therapeutics is evident in the environment (such as antibiotic resistance genes found in aquatic settings)
- Consider circularity of new products such as biobased bioactives from a life cycle assessment perspective and environmental footprint

Chapter 9 Publications

9.1 Peer Reviewed and Published

Development of a low-temperature extrusion process for production of GRAS bioactive-polymer loaded compounds for targeting antimicrobial-resistant (AMR) bacteria.

Masterson, K., Meade, E., Garvey, M., Lynch, M., Major, I., & Rowan, N. J. (2021). *Science of The Total Environment*, *800*, 149545.
https://doi.org/https://doi.org/10.1016/j.scitotenv.2021.149545

9.2 Submitted for Peer Review

Synergy Assessment of Four Antimicrobial Bioactive Compounds for the Combinational Treatment of Bacterial Pathogens

Kevin Masterson, Ian Major, Mark Lynch, Neil Rowan

Biomedicines 2023, 11(8), 2216;

https://doi.org/10.3390/biomedicines11082216

9.3 Currently On-going

Assessment of antibiofilm capabilities of polymer loaded compounds for the treatment of antimicrobial resistant, biofilm forming bacteria.

Bibliography

Abdelghafar, Aliaa, Nehal Yousef, and Momen Askoura. 2022. “Zinc Oxide Nanoparticles Reduce Biofilm Formation, Synergize Antibiotics Action and Attenuate Staphylococcus Aureus Virulence in Host; an Important Message to Clinicians.” *BMC Microbiology* 22 (1): 1–17. https://doi.org/10.1186/s12866-022-02658-z.

Abidin, Ismin Zainol, Emanuele Rezoagli, Bianca Simonassi-Paiva, Gustavo Waltzer Fehrenbach, Kevin Masterson, Robert Pogue, Zhi Cao, Neil Rowan, Emma J. Murphy, and Ian Major. 2020. “A Bilayer Vaginal Tablet for the Localized Delivery of Disulfiram and 5-Fluorouracil to the Cervix.” *Pharmaceutics* 12 (12): 1185. https://doi.org/10.3390/pharmaceutics12121185.

Abts, André, Antonino Mavaro, Jan Stindt, Patrick J. Bakkes, Sabine Metzger, Arnold J.M. Driessen, Sander H.J. Smits, and Lutz Schmitt. 2011. “Easy and Rapid Purification of Highly Active Nisin.” *International Journal of Peptides* 2011. https://doi.org/10.1155/2011/175145.

Acuña, Leonardo, Roberto Dionisio Morero, and Augusto Bellomio. 2011. “Development of Wide-Spectrum Hybrid Bacteriocins for Food Biopreservation.” *Food and Bioprocess Technology* 4 (6): 1029–49. https://doi.org/10.1007/s11947-010-0465-7.

AHDB Dairy. 2018. “Mastitis in Dairy Cows.” 2018. https://dairy.ahdb.org.uk/technical-information/animal-health-welfare/mastitis/#.W_QsNDj7TRY.

Ahmed, Mohamed O., and Keith E. Baptiste. 2018. “Vancomycin-Resistant Enterococci: A Review of Antimicrobial Resistance Mechanisms and Perspectives of Human and Animal Health.” *Microbial Drug Resistance* 24 (5): 590–606. https://doi.org/10.1089/mdr.2017.0147.

Akram, Aasma, Muhammad Irfan, Walaa A. Abualsunun, Deena M. Bukhary, and Mohammed Alissa. 2022. “How to Improve Solubility and Dissolution of Irbesartan by Fabricating Ternary Solid Dispersions: Optimization and In-Vitro Characterization.” *Pharmaceutics* 14 (11). https://doi.org/10.3390/pharmaceutics14112264.

Alany, Raid G., Sushila Bhattarai, Sandhya Pranatharthiharan, and Padma V. Devarajan. 2013.

"Intramammary Delivery Technologies for Cattle Mastitis Treatment." In *Long Acting Animal Health Drug Products: Fundamentals and Applications*, edited by Michael J. Rathbone and Arlene McDowell, 295–327. Advances in Delivery Science and Technology. Boston, MA: Springer US. https://doi.org/10.1007/978-1-4614-4439-8_13.

Alekish, Myassar, Zuhair Bani Ismail, Borhan Albiss, and Sara Nawasrah. 2018. "In Vitro Antibacterial Effects of Zinc Oxide Nanoparticles on Multiple Drug-Resistant Strains of Staphylococcus Aureus and Escherichia Coli: An Alternative Approach for Antibacterial Therapy of Mastitis in Sheep." *Veterinary World* 11 (10): 1428–32. https://doi.org/10.14202/vetworld.2018.1428-1432.

Alhajj, Mandy, and Aisha Farhana. 2023. "Enzyme Linked Immunosorbent Assay." In . Treasure Island (FL).

Aliasghari, Azam, Mohammad Rabbani Khorasgani, Sedigheh Vaezifar, Fateh Rahimi, Habibollah Younesi, and Maryam Khoroushi. 2016. "Evaluation of Antibacterial Efficiency of Chitosan and Chitosan Nanoparticles on Cariogenic Streptococci: An in Vitro Study." *Iranian Journal of Microbiology* 8 (2): 93–100.

AlKhatib, Zainab, Marcel Lagedroste, Iris Fey, Diana Kleinschrodt, André Abts, and Sander H J Smits. 2014. "Lantibiotic Immunity: Inhibition of Nisin Mediated Pore Formation by NisI." *PLoS ONE* 9 (7). https://doi.org/10.1371/journal.pone.0102246.

Aminov, Rustam I. 2010. "A Brief History of the Antibiotic Era: Lessons Learned and Challenges for the Future." *Frontiers in Microbiology* 1 (DEC): 1–7. https://doi.org/10.3389/fmicb.2010.00134.

Anju Manuja, Raguvaran R. 2015. "Zinc Oxide Nanoparticles: Opportunities and Challenges in Veterinary Sciences." *Immunome Research* 11 (2). https://doi.org/10.4172/1745-7580.1000095.

Archana, D., Brijesh K. Singh, Joydeep Dutta, and P. K. Dutta. 2015. "Chitosan-PVP-Nano Silver Oxide Wound Dressing: In Vitro and in Vivo Evaluation." *International Journal of Biological Macromolecules* 73 (1): 49–57. https://doi.org/10.1016/j.ijbiomac.2014.10.055.

Argaw, Amare. 2016. "Review on Epidemiology of Clinical and Subclinical Mastitis on Dairy

Cows" 52: 56–65. www.iiste.org.

Asli, Abdelhamid, Eric Brouillette, Céline Ster, Mariana Gabriela Ghinet, Ryszard Brzezinski, Pierre Lacasse, Mario Jacques, and François Malouin. 2017. "Antibiofilm and Antibacterial Effects of Specific Chitosan Molecules on Staphylococcus Aureus Isolates Associated with Bovine Mastitis." *PLoS ONE*. https://doi.org/10.1371/journal.pone.0176988.

Atiyeh, Bishara S., Michel Costagliola, Shady N. Hayek, and Saad A. Dibo. 2007. "Effect of Silver on Burn Wound Infection Control and Healing: Review of the Literature." *Burns* 33 (2): 139–48. https://doi.org/10.1016/j.burns.2006.06.010.

Azeredo, Joana, Nuno F. Azevedo, Romain Briandet, Nuno Cerca, Tom Coenye, Ana Rita Costa, Mickaël Desvaux, et al. 2017. "Critical Review on Biofilm Methods." *Critical Reviews in Microbiology* 43 (3): 313–51. https://doi.org/10.1080/1040841X.2016.1208146.

Balazs, D. J., K. Triandafillu, P. Wood, Y. Chevolot, C. Van Delden, H. Harms, C. Hollenstein, and H. J. Mathieu. 2004. "Inhibition of Bacterial Adhesion on PVC Endotracheal Tubes by RF-Oxygen Glow Discharge, Sodium Hydroxide and Silver Nitrate Treatments." *Biomaterials* 25 (11): 2139–51. https://doi.org/10.1016/j.biomaterials.2003.08.053.

Barlow, John. 2011. "Mastitis Therapy and Antimicrobial Susceptibility: A Multispecies Review with a Focus on Antibiotic Treatment of Mastitis in Dairy Cattle." *Journal of Mammary Gland Biology and Neoplasia* 16 (4): 383–407. https://doi.org/10.1007/s10911-011-9235-z.

Barrett, Damien J., Anne M Healy, Finola C Leonard, and Michael L Doherty. 2005. "Prevalence of Pathogens Causing Subclinical Mastitis in 15 Dairy Herds in the Republic of Ireland." *Irish Veterinary Journal* 58 (6): 333. https://doi.org/10.1186/2046-0481-58-6-333.

Bastarrachea, Luis, Dana Wong, Maxine Roman, Zhuangsheng Lin, and Julie Goddard. 2015. "Active Packaging Coatings." *Coatings* 5 (4): 771–91. https://doi.org/10.3390/coatings5040771.

Beer, Dirk de, Paul Stoodley, Frank Roe, and Zbigniew Lewandowski. 1994. "Effects of Biofilm Structures on Oxygen Distribution and Mass Transport." *Biotechnology and Bioengineering*. https://doi.org/10.1002/bit.260431118.

Berry, D. P., and W. J. Meaney. 2005. “Cow Factors Affecting the Risk of Clinical Mastitis.” *Irish Journal of Agricultural and Food Research* 44 (2): 147–56.

Beyth, Nurit, Yael Houri-haddad, Avi Domb, Wahid Khan, and Ronen Hazan. 2015. “Alternative Antimicrobial Approach : Nano-Antimicrobial Materials” 2015. https://doi.org/10.1155/2015/246012.

Bjarnsholt, Thomas, Morten Maria Alhede, Morten Maria Alhede, Steffen R. Eickhardt-Sørensen, Claus Moser, Michael Kühl, Peter Østrup Jensen, and Niels Høiby. 2013. “The in Vivo Biofilm.” *Trends in Microbiology*. https://doi.org/10.1016/j.tim.2013.06.002.

Björk, Sandra. 2013. “Clinical and Subclinical Mastitis in Dairy Cattle in Kampala, Uganda,” 49.

Boekema, Bouke. 2018. “How to Prevent Silver Nitrate (AgNO3) Precipitating in Growth Broth?, ResearchGate.” https://www.researchgate.net/post/How_to_prevent_Silver_Nitrate_AgNO3_precipitating_in_growth_broth.

Bogni, Cristina Inés, Liliana Monica Odierno, Claudia Gabriela Raspanti, José Angel Giraudo, Alejandro Larriestra, Elina Beatriz Reinoso, Mirta C Lasagno, et al. 2011. “War against Mastitis: Current Concepts on Controlling Bovine Mastitis Pathogens.” *Science against Microbial Pathogens: Communicating Current Research and Technological Advances*, no. January 2015: 483–94.

Bollenbach, Tobias. 2015. “Antimicrobial Interactions: Mechanisms and Implications for Drug Discovery and Resistance Evolution.” *Current Opinion in Microbiology* 27: 1–9. https://doi.org/10.1016/j.mib.2015.05.008.

Bouchard, Emile, Jean-philippe Roy, and Denis Du Tremblay. 2014. “Mastitis and Milk Culture,” no. July.

Bradley, A. J. 2002. “Bovine Mastitis: An Evolving Disease.” *Veterinary Journal* 164 (2): 116–28. https://doi.org/10.1053/tvjl.2002.0724.

Bradley, Andrew J., and Martin J. Green. 2004. “The Importance of the Nonlactating Period in the Epidemiology of Intramammary Infection and Strategies for Prevention.” *Veterinary Clinics of North America - Food Animal Practice* 20 (3 SPEC. ISS.): 547–68.

https://doi.org/10.1016/j.cvfa.2004.06.010.

Brewster, Jeffrey D. 2003. “A Simple Micro-Growth Assay for Enumerating Bacteria.” *Journal of Microbiological Methods*. https://doi.org/10.1016/S0167-7012(02)00226-9.

Breyne, Koen, Ryan W. Honaker, Zachary Hobbs, Manuela Richter, Maciej Zaczek, Taylor Spangler, Jonas Steenbrugge, et al. 2017. “Efficacy and Safety of a Bovine-Associated Staphylococcus Aureus Phage Cocktail in a Murine Model of Mastitis.” *Frontiers in Microbiology* 8 (NOV): 1–11. https://doi.org/10.3389/fmicb.2017.02348.

Brötz, Heike, Michaele Josten, Imke Wiedemann, Ursula Schneider, Friedrich Götz, Gabriele Bierbaum, and Hans Georg Sahl. 1998. “Role of Lipid-Bound Peptidoglycan Precursors in the Formation of Pores by Nisin, Epidermin and Other Lantibiotics.” *Molecular Microbiology* 30 (2): 317–27. https://doi.org/10.1046/j.1365-2958.1998.01065.x.

Bueno, Juan. 2011. “Anti-Biofilm Drug Susceptibility Testing Methods: Looking for New Strategies against Resistance Mechanism.” *Journal of Microbial & Biochemical Technology* s3. https://doi.org/10.4172/1948-5948.S3-004.

Burvenich, C, J Detilleux, M J Paape, and A M Massart-Leën. 2000. “Physiological and Genetic Factors That Influence the Cows Resistance to Mastitis, Especially during Early Lactation.” In :, 9–20.

Cardozo, Viviane F., Cesar A.C. Lancheros, Adélia M. Narciso, Elaine C.S. Valereto, Renata K.T. Kobayashi, Amedea B. Seabra, and Gerson Nakazato. 2014. “Evaluation of Antibacterial Activity of Nitric Oxide-Releasing Polymeric Particles against Staphylococcus Aureus and Escherichia Coli from Bovine Mastitis.” *International Journal of Pharmaceutics*. https://doi.org/10.1016/j.ijpharm.2014.06.051.

Carlson, Ross P, Reed Taffs, William M Davison, and Philip S Stewart. 2008. “Anti-Biofilm Properties of Chitosan-Coated Surfaces.” *Journal of Biomaterials Science, Polymer Edition* 19 (8): 1035–46. https://doi.org/10.1163/156856208784909372.

Ceotto-Vigoder, H., S. L.S. Marques, I. N.S. Santos, M. D.B. Alves, E. S. Barrias, A. Potter, D. S. Alviano, and M. C.F. Bastos. 2016. “Nisin and Lysostaphin Activity against Preformed Biofilm of Staphylococcus Aureus Involved in Bovine Mastitis.” *Journal of Applied Microbiology* 121 (1): 101–14. https://doi.org/10.1111/jam.13136.

Ceri, H., M. Olson, D. Morck, D. Storey, R. Read, A. Buret, and B. Olson. 2001. “The MBEC Assay System: Multiple Equivalent Biofilms for Antibiotic and Biocide Susceptibility Testing.” *Methods in Enzymology* 337 (1996): 377–85. https://doi.org/10.1016/S0076-6879(01)37026-X.

Cha, D. S., K. Cooksey, M. S. Chinnan, and H. J. Park. 2003. “Release of Nisin from Various Heat-Pressed and Cast Films.” *LWT - Food Science and Technology* 36 (2): 209–13. https://doi.org/10.1016/S0023-6438(02)00209-8.

Chen, Di, Xi Liu, Yiping Yang, Hongjun Yang, and Peng Lu. 2015. “Systematic Synergy Modeling: Understanding Drug Synergy from a Systems Biology Perspective.” *BMC Systems Biology* 9 (1). https://doi.org/10.1186/s12918-015-0202-y.

Chou, Ting-Chao, and Nick Martin. 2007. “The Mass-Action Law-Based New Computer Software, CompuSyn, for Automated Simulation of Synergism and Antagonism in Drug Combination Studies.” *Cancer Research* 67 (9_Supplement): 637.

Chutipongtanate, Somchai, and Visith Thongboonkerd. 2010. “Systematic Comparisons of Artificial Urine Formulas for in Vitro Cellular Study.” *Analytical Biochemistry* 402 (1): 110–12. https://doi.org/10.1016/j.ab.2010.03.031.

Clark, Nathaniel J., David Boyle, Benjamin P. Eynon, and Richard D. Handy. 2019. “Dietary Exposure to Silver Nitrate Compared to Two Forms of Silver Nanoparticles in Rainbow Trout: Bioaccumulation Potential with Minimal Physiological Effects.” *Environmental Science: Nano* 6 (5): 1393–1405. https://doi.org/10.1039/c9en00261h.

Cleveland, Jennifer, Thomas J. Montville, Ingolf F. Nes, and Michael L. Chikindas. 2001. “Bacteriocins: Safe, Natural Antimicrobials for Food Preservation.” *International Journal of Food Microbiology* 71 (1): 1–20. https://doi.org/10.1016/S0168-1605(01)00560-8.

Coenye, T., D. Goeres, F. Van Bambeke, and T. Bjarnsholt. 2018. “Should Standardized Susceptibility Testing for Microbial Biofilms Be Introduced in Clinical Practice?” *Clinical Microbiology and Infection* 24 (6): 570–72. https://doi.org/10.1016/j.cmi.2018.01.003.

Cokol-Cakmak, Melike, Selim Cetiner, Nurdan Erdem, Feray Bakan, and Murat Cokolid. 2020. “Guided Screen for Synergistic Three-Drug Combinations.” *PLoS ONE* 15 (7 July): 1–12. https://doi.org/10.1371/journal.pone.0235929.

Colomer-Winter, Cristina, José Lemos, and Ana Flores-Mireles. 2019. “Biofilm Assays on Fibrinogen-Coated Silicone Catheters and 96-Well Polystyrene Plates.” *BIO-PROTOCOL* 9 (6): 100–106. https://doi.org/10.21769/BioProtoc.3196.

Community, Economic. 1984. “Official Journal of the European Communities.” *Analytical Proceedings* 21 (6): 196. https://doi.org/10.1039/AP9842100196.

Constable, Peter D., Kenneth W. Hinchcliff, Stanley H. Done, and Walter Grunberg. 2017. *A Textbook of the Diseases of Cattle, Horses, Sheep, Pigs and Goats*. *Veterinary Medicine*. https://doi.org/10.1111/j.1541-0420.2008.01010.x.

Constable, Peter D., Kenneth W. Hinchcliff, Stanley H. Done, and Walter Grünberg. 2017. *20 – Diseases of the Mammary Gland*. *Veterinary Medicine*. https://doi.org/10.1158/1078-0432.ccr-09-0506.

Contreras, G. Andres, and Juan Miguel Rodríguez. 2011. “Mastitis: Comparative Etiology and Epidemiology.” *Journal of Mammary Gland Biology and Neoplasia* 16 (4): 339–56. https://doi.org/10.1007/s10911-011-9234-0.

Cortes, Cristiano, Search Search, and Dry Period. 2018. “Mammary Gland : Physiology and Anatomy.” 2018. http://www.groupe-esa.com/ladmec/bricks_modules/brick01/co/_web_brick01.html.

Costerton, J. William. 2005. “Biofilm Theory Can Guide the Treatment of Device-Related Orthopaedic Infections.” *Clinical Orthopaedics and Related Research* 437 (437): 7–11. https://doi.org/10.1097/00003086-200508000-00003.

Cruz, Cristina D, Shreya Shah, and Päivi Tammela. 2018. “Defining Conditions for Biofilm Inhibition and Eradication Assays for Gram-Positive Clinical Reference Strains,” 1–9.

Cutter, C. N., J. L. Willett, and GRSiragusa. 2001. “Improved Antimicrobial Activity of Nisin-Incorporated Polymer Films by Formulation Change and Addition of Food Grade Chelator.” *Letters in Applied Microbiology* 33 (4): 325–28. https://doi.org/10.1046/j.1472-765X.2001.01005.x.

Davydova, V. N., A. A. Kalitnik, P. A. Markov, A. V. Volod’ko, S. V. Popov, and I. M. Ermak. 2016. “Cytokine-Inducing and Anti-Inflammatory Activity of Chitosan and Its Low-Molecular

Derivative." *Applied Biochemistry and Microbiology* 52 (5): 476–82. https://doi.org/10.1134/S0003683816050070.

Deb, Rajib, Amit Kumar, Sandip Chakraborty, Amit Kumar Verma, Ruchi Tiwari, Kuldeep Dhama, Umesh Singh, and Sushil Kumar. 2013. "Trends in Diagnosis and Control of Bovine Mastitis: A Review." *Pakistan Journal of Biological Sciences : PJBS*. https://doi.org/10.3923/pjbs.2013.1653.1661.

Delves-Broughton, J. 1996. "Applications of the Bacteriocin, Nisin." *Antonie van Leeuwenhoek, International Journal of General and Molecular Microbiology* 69 (2): 193–202. https://doi.org/10.1007/BF00399424.

Department of Agriculture Food and the Marine. 2015. "Local Roots Global Reach: Food Wise 2025. A 10-Year Vision for the Irish Agri-Food Industry," 1–108. https://www.agriculture.gov.ie/media/migration/foodindustrydevelopmenttrademarkets/agri-foodandtheeconomy/foodwise2025/report/FoodWise2025.pdf.

Ding, Zhuang, Lili Wang, Yangyang Xing, Yanna Zhao, Zhengping Wang, and Jun Han. 2019. "Enhanced Oral Bioavailability of Celecoxib Nanocrystalline Solid Dispersion Based on Wet Media Milling Technique: Formulation, Optimization and in Vitro/In Vivo Evaluation." *Pharmaceutics* 11 (7). https://doi.org/10.3390/pharmaceutics11070328.

Dingwell, Randy T., Ken E. Leslie, Ynte H. Schukken, Jan M. Sargeant, and Leo L. Timms. 2003. "Evaluation of the California Mastitis Test to Detect an Intramammary Infection with a Major Pathogen in Early Lactation Dairy Cows." *Canadian Veterinary Journal* 44 (5): 413–16. https://doi.org/2003-044.

Dohoo, I R, and A H Meek. 1982. "Somatic Cell Counts in Bovine Milk." *Can. Vet. J.* https://doi.org/1982-003.

Donnellan, Trevor, Thia Hennessy, and Fiona Thorne. 2015. "The End of the Quota Era: A History of the Dairy Sector and Its Future Prospects," 104.

Driessche, Freija Van Den, Petra Rigole, Gilles Brackman, and Tom Coenye. 2014. "Optimization of Resazurin-Based Viability Staining for Quanti Fi Cation of Microbial Bio Fi Lms" 98: 31–34. https://doi.org/10.1016/j.mimet.2013.12.011.

Duss, François Régis, Cristina Garcia De La Mària, Antony Croxatto, Stefano Giulieri, Frédéric Lamoth, Oriol Manuel, and José M. Miró. 2019. “Successful Treatment with Daptomycin and Ceftaroline of MDR Staphylococcus Aureus Native Valve Endocarditis: A Case Report.” *Journal of Antimicrobial Chemotherapy* 74 (9): 2626–30. https://doi.org/10.1093/jac/dkz253.

Economou, Vangelis, and Panagiota Gousia. 2015. “Agriculture and Food Animals as a Source of Antimicrobial-Resistant Bacteria.” *Infection and Drug Resistance* 8: 49–61. https://doi.org/10.2147/IDR.S55778.

Espitia, Paula Judith Perez, Nilda de Fátima Ferreira Soares, Jane Sélia dos Reis Coimbra, Nélio José de Andrade, Renato Souza Cruz, and Eber Antonio Alves Medeiros. 2012. “Zinc Oxide Nanoparticles: Synthesis, Antimicrobial Activity and Food Packaging Applications.” *Food and Bioprocess Technology* 5 (5): 1447–64. https://doi.org/10.1007/s11947-012-0797-6.

European Committe on Antimicrobial Susceptibility Testing (EUCAST). 2021. “Antimicrobial Susceptibility Testing EUCAST Disk Diffusion Method Version 9.0 January.” *European Society of Clinical Microbiology and Infectious Deseases* 0 (January): 1–21. https://www.eucast.org/fileadmin/src/media/PDFs/EUCAST_files/Disk_test_documents/2022_manuals/Manual_v_10.0_EUCAST_Disk_Test_2022.pdf.

Fang, Z., Wusgal, H. Cheng, and L. Liang. 2017. *Natural Biodegradable Medical Polymers: Therapeutic Peptides and Proteins*. *Science and Principles of Biodegradable and Bioresorbable Medical Polymers: Materials and Properties*. Elsevier Ltd. https://doi.org/10.1016/B978-0-08-100372-5.00011-8.

Fatsis-Kavalopoulos, Nikos, Roderich Roemhild, Po Cheng Tang, Johan Kreuger, and Dan I. Andersson. 2020. “CombiANT: Antibiotic Interaction Testing Made Easy.” *PLoS Biology* 18 (9): 1–22. https://doi.org/10.1371/journal.pbio.3000856.

Favre, Nicolas, Gérard Bordmann, and Werner Rudin. 1997. “Comparison of Cytokine Measurements Using ELISA, ELISPOT and Semi-Quantitative RT-PCR.” *Journal of Immunological Methods* 204 (1): 57–66. https://doi.org/10.1016/S0022-1759(97)00033-1.

Felipe, Verónica, María Laura Breser, Luciana Paola Bohl, Elizabete Rodrigues da Silva, Carolina Andrea Morgante, Silvia Graciela Correa, and Carina Porporatto. 2019. "Chitosan Disrupts Biofilm Formation and Promotes Biofilm Eradication in Staphylococcus Species Isolated from Bovine Mastitis." *International Journal of Biological Macromolecules* 126: 60–67. https://doi.org/10.1016/j.ijbiomac.2018.12.159.

Fenton, Mark, Ruth Keary, Olivia McAuliffe, R. Paul Ross, Jim O'Mahony, and Aidan Coffey. 2013. "Bacteriophage-Derived Peptidase <math Id="M1"> <mrow> <msub> <mrow> <mtext>CHAP</Mtext> </Mrow> <mrow> <mtext>K</Mtext> </Mrow> </Msub> </Mrow> </Math> Eliminates and Prevents Staphylococcal Biofilms." *International Journal of Microbiology* 2013: 1–8. https://doi.org/10.1155/2013/625341.

Fiedot-Toboła, Marta, Magdalena Ciesielska, Irena Maliszewska, Olga Rac-Rumijowska, Patrycja Suchorska-Woźniak, Helena Teterycz, and Marek Bryjak. 2018. "Deposition of Zinc Oxide on Different Polymer Textiles and Their Antibacterial Properties." *Materials* 11 (5): 1–16. https://doi.org/10.3390/ma11050707.

Fisher, Leanne E., Andrew L. Hook, Waheed Ashraf, Anfal Yousef, David A. Barrett, David J. Scurr, Xinyong Chen, et al. 2015. "Biomaterial Modification of Urinary Catheters with Antimicrobials to Give Long-Term Broadspectrum Antibiofilm Activity." *Journal of Controlled Release* 202: 57–64. https://doi.org/10.1016/j.jconrel.2015.01.037.

Fleischer, P., M. Metzner, M. Beyerbach, M. Hoedemaker, and W. Klee. 2001. "The Relationship Between Milk Yield and the Incidence of Some Diseases in Dairy Cows." *Journal of Dairy Science*. https://doi.org/10.3168/jds.S0022-0302(01)74646-2.

Frøsig, Merethe Mørch. 2017. "Analysis of Manual Cell Counting versus Automated Cell Counting." https://chemometec.com/manual-cell-counting/.

Gao, Sherry Shiqian, Irene Shuping Zhao, Steve Duffin, Duangporn Duangthip, Edward Chin Man Lo, and Chun Hung Chu. 2018. "Revitalising Silver Nitrate for Caries Management." *International Journal of Environmental Research and Public Health* 15 (1). https://doi.org/10.3390/ijerph15010080.

Garcia, Alvaro. 2004. "Contagious vs. Environmental Mastitis." *Dairy Science* ExEx 4028 (January).

Garvey, Mary, Damien Curran, and Michéal Savage. 2017. “Efficacy Testing of Teat Dip Solutions Used as Disinfectants for the Dairy Industry: Antimicrobial Properties.” *International Journal of Dairy Technology* 70 (2): 179–87. https://doi.org/10.1111/1471-0307.12344.

Geary, U., N. Lopez-Villalobos, N. Begley, F. McCoy, B. O’Brien, L. O’Grady, and L. Shalloo. 2012. “Estimating the Effect of Mastitis on the Profitability of Irish Dairy Farms.” *Journal of Dairy Science* 95 (7): 3662–73. https://doi.org/10.3168/jds.2011-4863.

George, Lisle W., Thomas J. Divers, Norm Ducharme, and Frank L. Welcome. 2008. “Diseases of the Teats and Udder.” In *Rebhun’s Diseases of Dairy Cattle*. https://doi.org/10.1016/B978-141603137-6.50011-9.

Ghapanvari, Parnia, Mohammad Taheri, Farid Aziz Jalilian, Sanaz Dehbashi, Aram Asareh Zadegan Dezfuli, and Mohammad Reza Arabestani. 2022. “The Effect of Nisin on the Biofilm Production, Antimicrobial Susceptibility and Biofilm Formation of Staphylococcus Aureus and Pseudomonas Aeruginosa.” *European Journal of Medical Research* 27 (1): 4–11. https://doi.org/10.1186/s40001-022-00804-x.

Gharsallaoui, Adem, Catherine Joly, Nadia Oulahal, and Pascal Degraeve. 2016. “Nisin as a Food Preservative: Part 2: Antimicrobial Polymer Materials Containing Nisin.” *Critical Reviews in Food Science and Nutrition* 56 (8): 1275–89. https://doi.org/10.1080/10408398.2013.763766.

Gilbert, Florence B., Patricia Cunha, Kirsty Jensen, Elizabeth J. Glass, Gilles Foucras, Christèle Robert-Granié, Rachel Rupp, and Pascal Rainard. 2013. “Differential Response of Bovine Mammary Epithelial Cells to Staphylococcus Aureus or Escherichia Coli Agonists of the Innate Immune System.” *Veterinary Research* 44 (1). https://doi.org/10.1186/1297-9716-44-40.

Gill, J. J., J. C. Pacan, M. E. Carson, K. E. Leslie, M. W. Griffiths, and P. M. Sabour. 2006. “Efficacy and Pharmacokinetics of Bacteriophage Therapy in Treatment of Subclinical Staphylococcus Aureus Mastitis in Lactating Dairy Cattle.” *Antimicrobial Agents and Chemotherapy* 50 (9): 2912–18. https://doi.org/10.1128/AAC.01630-05.

Gill, Ravinderpal, Wayne H. Howard, Kenneth E. Leslie, and Kerry Lissemore. 1990.

"Economics of Mastitis Control." *Journal of Dairy Science* 73 (11): 3340–48. https://doi.org/10.3168/jds.S0022-0302(90)79029-7.

Gomes, Fernanda, and Mariana Henriques. 2016a. "Bovine Mastitis: Current Concepts and Future Control Approaches." *Current Microbiology* 1 (1): 377–82. https://doi.org/10.1007/s00284-015-0958-8.

———. 2016b. "Control of Bovine Mastitis: Old and Recent Therapeutic Approaches." *Current Microbiology* 72 (4): 377–82. https://doi.org/10.1007/s00284-015-0958-8.

Gomes, Fernanda, Maria José Saavedra, and Mariana Henriques. 2016. "Bovine Mastitis Disease/Pathogenicity: Evidence of the Potential Role of Microbial Biofilms." *Pathogens and Disease* 74 (3): 1–7. https://doi.org/10.1093/femspd/ftw006.

Green, M.J., A.J. Bradley, G.F. Medley, and W.J. Browne. 2007. "Cow, Farm, and Management Factors During the Dry Period That Determine the Rate of Clinical Mastitis After Calving." *Journal of Dairy Science* 90 (8): 3764–76. https://doi.org/10.3168/jds.2007-0107.

Gröhn, Y. T., and P. J. Rajala-Schultz. 2000. "Epidemiology of Reproductive Performance in Dairy Cows." In *Animal Reproduction Science*. https://doi.org/10.1016/S0378-4320(00)00085-3.

Gruet, P., P. Maincent, X. Berthelot, and V. Kaltsatos. 2001. "Bovine Mastitis and Intramammary Drug Delivery: Review and Perspectives." *Advanced Drug Delivery Reviews* 50 (3): 245–59. https://doi.org/10.1016/S0169-409X(01)00160-0.

Günther, Juliane, Anna Czabanska, Isabel Bauer, James A. Leigh, Otto Holst, and Hans Martin Seyfert. 2016. "Streptococcus Uberis Strains Isolated from the Bovine Mammary Gland Evade Immune Recognition by Mammary Epithelial Cells, but Not of Macrophages." *Veterinary Research* 47 (1): 1–14. https://doi.org/10.1186/s13567-015-0287-8.

Gut, Ian M., Steven R. Blanke, and Wilfred A. Van Der Donk. 2011. "Mechanism of Inhibition of Bacillus Anthracis Spore Outgrowth by the Lantibiotic Nisin." *ACS Chemical Biology* 6 (7): 744–52. https://doi.org/10.1021/cb1004178.

Hall, Clayton W., and Thien Fah Mah. 2017. "Molecular Mechanisms of Biofilm-Based Antibiotic Resistance and Tolerance in Pathogenic Bacteria." *FEMS Microbiology Reviews*

41 (3): 276–301. https://doi.org/10.1093/femsre/fux010.

Hamdine, Mélina, Marie Claude Heuzey, and André Bégin. 2005. “Effect of Organic and Inorganic Acids on Concentrated Chitosan Solutions and Gels.” *International Journal of Biological Macromolecules* 37 (3): 134–42. https://doi.org/10.1016/j.ijbiomac.2005.09.009.

Han, Daewoo, Shalli Sherman, Shaun Filocamo, and Andrew J. Steckl. 2017. “Long-Term Antimicrobial Effect of Nisin Released from Electrospun Triaxial Fiber Membranes.” *Acta Biomaterialia* 53: 242–49. https://doi.org/10.1016/j.actbio.2017.02.029.

Hanušová, Kristýna, Monika Šťastná, Lenka Votavová, Kamila Klaudisová, Jaroslav Dobiáš, Michal Voldřich, and Miroslav Marek. 2010. “Polymer Films Releasing Nisin and/or Natamycin from Polyvinyldichloride Lacquer Coating: Nisin and Natamycin Migration, Efficiency in Cheese Packaging.” *Journal of Food Engineering* 99 (4): 491–96. https://doi.org/10.1016/j.jfoodeng.2010.01.034.

Harrison, Joe J., Raymond J. Turner, and Howard Ceri. 2005. “High-Throughput Metal Susceptibility Testing of Microbial Biofilms.” *BMC Microbiology* 5: 1–11. https://doi.org/10.1186/1471-2180-5-53.

Harrison, Joe J, Carol A Stremick, Raymond J Turner, Nick D Allan, Merle E Olson, and Howard Ceri. 2010. “Microtiter Susceptibility Testing of Microbes Growing on Peg Lids : A Miniaturized Biofilm Model for High-Throughput Screening.” *Nature Protocols* 5 (7): 1236–54. https://doi.org/10.1038/nprot.2010.71.

Hasper, Hester E., Naomi E. Kramer, James L. Smith, J. D. Hillman, Cherian Zachariah, Oscar P. Kuipers, Ben De Kruijff, and Eefjan Breukink. 2006. “An Alternative Bactericidal Mechanism of Action for Lantibiotic Peptides That Target Lipid II.” *Science* 313 (5793): 1636–37. https://doi.org/10.1126/science.1129818.

Hassan, Atef, Noha H Oraby, Aliaa A E Mohamed, and Hamlaoui Mahmoud. 2014. “The Possibility of Using Zinc Oxide Nanoparticles in Controlling Some Fungal and Bacterial Strains Isolated From Buffaloes.” *Egyptian J.of Applied Science* 29 (March): 58–83.

Hassan, Mohamed A., Ahmed M. Omer, Eman Abbas, Walid M.A. Baset, and Tamer M. Tamer. 2018. “Preparation, Physicochemical Characterization and Antimicrobial Activities of

Novel Two Phenolic Chitosan Schiff Base Derivatives." *Scientific Reports* 8 (1): 1–14. https://doi.org/10.1038/s41598-018-29650-w.

He, Haibing, Rui Yang, and Xing Tang. 2010. "In Vitro and in Vivo Evaluation of Fenofibrate Solid Dispersion Prepared by Hot-Melt Extrusion." *Drug Development and Industrial Pharmacy* 36 (6): 681–87. https://doi.org/10.3109/03639040903449720.

He, Li, Likou Zou, Qianru Yang, Jinghua Xia, Kang Zhou, Yuanting Zhu, Xinfeng Han, Biao Pu, Bin Hu, and Wenwen Deng. 2016. "Antimicrobial Activities of Nisin , Tea Polyphenols , and Chitosan and Their Combinations in Chilled Mutton" 81 (6): 1466–71. https://doi.org/10.1111/1750-3841.13312.

Heusden, Hester Emilie Van, Ben De Kruijff, and Eefjan Breukink. 2002. "Lipid II Induces a Transmembrane Orientation of the Pore-Forming Peptide Lantibiotic Nisin." *Biochemistry* 41 (40): 12171–78. https://doi.org/10.1021/bi026090x.

Hillerton, Eric, and James Booth. 2018. "The Five-Point Mastitis Control Plan-A Revisory Tutorial!" *National Mastitis Council Annual Meeting*, no. February: 3–19.

Høiby, Niels, Thomas Bjarnsholt, Michael Givskov, Søren Molin, and Oana Ciofu. 2010. "Antibiotic Resistance of Bacterial Biofilms." *International Journal of Antimicrobial Agents* 35 (4): 322–32. https://doi.org/10.1016/j.ijantimicag.2009.12.011.

Høiby, Niels, Thomas Bjarnsholt, Michael Givskov, Soren Søren Molin, Oana Ciofu, Niels Hoiby, Thomas Bjarnsholt, et al. 2010. "Antibiotic Resistance of Bacterial Biofilms." *International Journal of Antimicrobial Agents* 35 (4): 322–32. https://doi.org/10.1016/j.ijantimicag.2009.12.011.

Hu, Caihong, Juan Song, Yali Li, Zhaoshuang Luan, and Kang Zhu. 2013. "Diosmectite-Zinc Oxide Composite Improves Intestinal Barrier Function, Modulates Expression of pro-Inflammatory Cytokines and Tight Junction Protein in Early Weaned Pigs." *British Journal of Nutrition* 110 (4): 681–88. https://doi.org/10.1017/S0007114512005508.

Huang, Ruo Yue, Linlin Pei, Quanjin Liu, Shiqi Chen, Haibo Dou, Gang Shu, Zhi Xiang Yuan, et al. 2019. "Isobologram Analysis: A Comprehensive Review of Methodology and Current Research." *Frontiers in Pharmacology* 10 (OCT): 1–12. https://doi.org/10.3389/fphar.2019.01222.

Huijps, Kirsten, Theo J.G.M. Lam, and Henk Hogeveen. 2008. “Costs of Mastitis: Facts and Perception.” *Journal of Dairy Research*. https://doi.org/10.1017/S0022029907002932.

Ianevski, Aleksandr, Anil K. Giri, and Tero Aittokallio. 2020. “SynergyFinder 2.0: Visual Analytics of Multi-Drug Combination Synergies.” *Nucleic Acids Research*. https://doi.org/10.1093/nar/gkaa216.

Ianevski, Aleksandr, Liye He, Tero Aittokallio, and Jing Tang. 2017. “SynergyFinder: A Web Application for Analyzing Drug Combination Dose-Response Matrix Data.” *Bioinformatics* 33 (15): 2413–15. https://doi.org/10.1093/bioinformatics/btx162.

Imran, Muhammad, Amira Klouj, Anne-marie Revol-junelles, and Stéphane Desobry. 2014. “Controlled Release of Nisin from HPMC , Sodium Caseinate , Poly-Lactic Acid and Chitosan for Active Packaging Applications.” *JOURNAL OF FOOD ENGINEERING* 143: 178–85. https://doi.org/10.1016/j.jfoodeng.2014.06.040.

Ingvartsen, K. L., R. J. Dewhurst, and N. C. Friggens. 2003. “On the Relationship between Lactational Performance and Health: Is It Yield or Metabolic Imbalance That Cause Production Diseases in Dairy Cattle? A Position Paper.” In *Livestock Production Science*. https://doi.org/10.1016/S0301-6226(03)00110-6.

Innovotech. 2015. “MBEC™ Assay For High-Throughput Antimicrobial Susceptibility Testing of Biofilms.” *Innovotech*, 1–21. http://www.innovotech.ca/documents/MBEC-Procedural-Manual-v1.1.pdf.

Interagency Coordination Group on Antimicrobial Resistance. 2019. “No Time to Wait: Securing the Future from Drug-Resistant Infections Report to the Secretary-General of the United Nations.” *World Health Organisation*. https://www.who.int/antimicrobial-resistance/interagency-coordination-group/IACG_final_report_EN.pdf?ua=1.

International Organization for Standardization. 2018. “ISO 10993-1:2018 - Biological Evaluation of Medical Devices -- Part 1: Evaluation and Testing within a Risk Management Process.” *International Organization for Standardization* 2018: 41. https://www.iso.org/standard/68936.html.

Islam, MA, MZ Islam, MS Rahman, and MT Islam. 2011. “Prevalence of Mastitis in Dairy Cows in Selected Areas of Bangladesh.” *Bangladesh Journal of Veterinary Medicine* 9 (1): 73–

78. https://doi.org/http://dx.doi.org/10.3329/bjvm.v9i1.11216.

Jacques, Mario. 2013. “Bacterial Biofilms: Why Should We Care?” Animal Health Research Reviews. April 19, 2013. http://www.cresa.cat/blogs/sociedad/en/espanol-biofilms-bacterianos-por-que-deberia-importarnos/.

Jamal, Muhsin, Wisal Ahmad, Saadia Andleeb, Fazal Jalil, Muhammad Imran, Muhammad Asif Nawaz, Tahir Hussain, Muhammad Ali, Muhammad Rafiq, and Muhammad Atif Kamil. 2018. “Bacterial Biofilm and Associated Infections.” *Journal of the Chinese Medical Association* 81 (1): 7–11. https://doi.org/10.1016/j.jcma.2017.07.012.

Jamali, Hossein, Herman W. Barkema, Mario Jacques, Eve-Marie Lavallée-Bourget, François Malouin, Vineet Saini, Henrik Stryhn, and Simon Dufour. 2018. “Invited Review: Incidence, Risk Factors, and Effects of Clinical Mastitis Recurrence in Dairy Cows.” *Journal of Dairy Science*, 1–18. https://doi.org/10.3168/jds.2017-13730.

Javorová, J, D Falta, M Velecká, M Večeřa, J Andrýsek, and G Chládek. 2013. “COMPARISON OF LACTOSE , CALCIUM , CHLORIDE CONTENT AND SOMATIC CELL COUNT IN BULK MILK SAMPLES FROM HOLSTEIN AND CZECH FLECKVIEH BREED,” 207–11.

Jia, Zhifeng, Meiling He, Chunjie Wang, Aorigele Chen, Xin Zhang, Jin Xu, He Fu, and Bo Liu. 2019. “Nisin Reduces Uterine Inflammation in Rats by Modulating Concentrations of Pro- and Anti-Inflammatory Cytokines.” *American Journal of Reproductive Immunology* 81 (5): 1–11. https://doi.org/10.1111/aji.13096.

Jin, T., and H. Zhang. 2008. “Biodegradable Polylactic Acid Polymer with Nisin for Use in Antimicrobial Food Packaging.” *Journal of Food Science* 73 (3). https://doi.org/10.1111/j.1750-3841.2008.00681.x.

Jin, Tony, Linshu Liu, Howard Zhang, and Kevin Hicks. 2009. “Antimicrobial Activity of Nisin Incorporated in Pectin and Polylactic Acid Composite Films against Listeria Monocytogenes.” *International Journal of Food Science and Technology* 44 (2): 322–29. https://doi.org/10.1111/j.1365-2621.2008.01719.x.

Jolivet-Gougeon, Anne, and Martine Bonnaure-Mallet. 2014. “Biofilms as a Mechanism of Bacterial Resistance.” *Drug Discovery Today: Technologies* 11 (1): 49–56. https://doi.org/10.1016/j.ddtec.2014.02.003.

Jones, G.M., R.E. Pearson, G.A. Clabaugh, and C.W. Heald. 1984. “Relationships Between Somatic Cell Counts and Milk Production.” *Journal of Dairy Science*. https://doi.org/10.3168/jds.S0022-0302(84)81510-6.

Jones, G M, and T L Bailey. 2009. “Understanding the Basics of Mastitis.” *Virginia Cooperative Extension* 404 (233): 1–5. https://doi.org/10.1108/02621711111098406.

Jozala, Angela Faustino, Letícia Celia, and De Lencastre Novaes. 2015. “Nisin Concepts, Compounds and the Alternatives of Antibacterials Amphiphilic.” http://dx.doi.org/10.5772/60932.

Jung, Günther. 1991. “Lantibiotics—Ribosomally Synthesized Biologically Active Polypeptides Containing Sulfide Bridges and α,B-Didehydroamino Acids.” *Angewandte Chemie International Edition in English* 30 (9): 1051–68. https://doi.org/10.1002/anie.199110513.

Kaftanoglu, Osman. 2015. “{ATCC} {Bacterial} {Culture} {Guide}.” *Scribd*. http://www.scribd.com/doc/118917227/ATCC-Bacterial-Culture-Guide.

Kamphuis, C., R. Sherlock, J. Jago, G. Mein, and H. Hogeveen. 2008. “Automatic Detection of Clinical Mastitis Is Improved by In-Line Monitoring of Somatic Cell Count.” *Journal of Dairy Science* 91 (12): 4560–70. https://doi.org/10.3168/jds.2008-1160.

Kaşikçi, Güven, Ömer Çetin, Enver Bariş Bingöl, and Mehmet Can Gündüz. 2012. “Relations between Electrical Conductivity, Somatic Cell Count, California Mastitis Test and Some Quality Parameters in the Diagnosis of Subclinical Mastitis in Dairy Cows.” *Turkish Journal of Veterinary and Animal Sciences* 36 (1): 49–55. https://doi.org/10.3906/vet-1103-4.

Kawada-Matsuo, Miki, Atsuko Watanabe, Kaoru Arii, Yuichi Oogai, Kazuyuki Noguchi, Shouichi Miyawaki, Tetsuya Hayashi, and Hitoshi Komatsuzawa. 2019. “An Alternative Nisin A Resistance Mechanism Affects Virulence in Staphylococcus Aureus.” *Applied and Environmental Microbiology*. https://doi.org/10.1101/716191.

Kim, Ji Hoon, Daeung Yu, Sung Hwan Eom, Song Hee Kim, Junghwan Oh, Won Kyo Jung, and Young Mog Kim. 2017. “Synergistic Antibacterial Effects of Chitosan-Caffeic Acid Conjugate against Antibiotic-Resistant Acne-Related Bacteria.” *Marine Drugs* 15 (6): 1–10. https://doi.org/10.3390/md15060167.

Knight, C H, C J Wilde, and M Peaker. 1988. “1 - Manipulation Of Milk Secretion.” In , edited by PHILIP C B T - Nutrition and Lactation in the Dairy Cow GARNSWORTHY, 3–14. Butterworth-Heinemann. https://doi.org/https://doi.org/10.1016/B978-0-408-00717-7.50006-X.

Könige, Alexa M., Hans Curt Flemming, and Jost Wingender. 2015. “Nanosilver Induces a Non-Culturable but Metabolically Active State in Pseudomonas Aeruginosa.” *Frontiers in Microbiology* 6 (MAY): 1–11. https://doi.org/10.3389/fmicb.2015.00395.

Krömker, V., and S. Leimbach. 2017. “Mastitis Treatment—Reduction in Antibiotic Usage in Dairy Cows.” *Reproduction in Domestic Animals*. https://doi.org/10.1111/rda.13032.

Kunjachan, Sijumon, and Sajan Jose. 2010. “Understanding the Mechanism of Ionic Gelation for Synthesis of Chitosan Nanoparticles Using Qualitative Techniques.” *Asian Journal of Pharmaceutics* 4 (2): 148. https://doi.org/10.4103/0973-8398.68467.

Kwiatek, Magdalena, Sylwia Parasion, Lidia Mizak, Romuald Gryko, M. Bartoszcze, and Janusz Kocik. 2012. “Characterization of a Bacteriophage, Isolated from a Cow with Mastitis, That Is Lytic against Staphylococcus Aureus Strains.” *Archives of Virology*. https://doi.org/10.1007/s00705-011-1160-3.

Kyoon, Hong, Na Young, Shin Ho, and Samuel P Meyers. 2002. “Antibacterial Activity of Chitosans and Chitosan Oligomers with Different Molecular Weights” 74: 65–72.

la Fuente-Núñez, César De, Fany Reffuveille, Lucía Fernández, and Robert E W Hancock. 2013. “Bacterial Biofilm Development as a Multicellular Adaptation: Antibiotic Resistance and New Therapeutic Strategies.” *Current Opinion in Microbiology*. https://doi.org/10.1016/j.mib.2013.06.013.

Lahouassa, Hichem, Etienne Moussay, Pascal Rainard, and Céline Riollet. 2007. “Differential Cytokine and Chemokine Responses of Bovine Mammary Epithelial Cells to Staphylococcus Aureus and Escherichia Coli.” *Cytokine* 38 (1): 12–21. https://doi.org/10.1016/j.cyto.2007.04.006.

Langer, Anil, Sunanda Sharma, Narendra Kumar Sharma, and DS Nauriyal. 2014. “Comparative Efficacy of Different Mastitis Markers for Diagnosis of Sub-Clinical Mastitis in Cows.” *International Journal of Applied Sciences and Biotechnology* 2 (2): 121–25.

https://doi.org/10.3126/ijasbt.v2i2.10191.

Leland, Diane S., and Morris L. V. French. 1988. “Virus Isolation and Identification.” In *Laboratory Diagnosis of Infectious Diseases Principles and Practice*, 39–59. New York, NY: Springer New York. https://doi.org/10.1007/978-1-4612-3900-0_3.

Lewies, Angélique, Lissinda H. Du Plessis, and Johannes F. Wentzel. 2018. “The Cytotoxic, Antimicrobial and Anticancer Properties of the Antimicrobial Peptide Nisin Z Alone and in Combination with Conventional Treatments.” *Cytotoxicity*, no. July. https://doi.org/10.5772/intechopen.71927.

Lewis, L. D. 2010. “Drug-Drug Interactions: Is There an Optimal Way to Study Them?” *British Journal of Clinical Pharmacology* 70 (6): 781–83. https://doi.org/10.1111/j.1365-2125.2010.03829.x.

LI, WEIJIA, JING ZHOU, and YUYIN XU. 2015. “Study of the in Vitro Cytotoxicity Testing of Medical Devices.” *Biomedical Reports* 3 (5): 617–20. https://doi.org/10.3892/br.2015.481.

Lima, Kelbis Oliveira, Arthur Abinader Vasconcelos, José Jeosafá Vieira de Sousa Júnior, Silvia Katrine Silva Escher, Gerson Nakazato, and Paulo Sérgio Taube Júnior. 2019. “Green Synthesis of Silver Nanoparticles Using Amazon Fruits.” *International Journal of Nanoscience and Nanotechnology* 15 (3): 179–88.

M. P. Weinstein, B. L. Zimmer F. R. Cockerill M. A. Wiker J. Alder M. N. Dudley G. M. Eliopoulos M. J. Ferraro D. J. Hardy D. W. Hecht J. A. Hindler J. B. Patel M. Powell J. M. Swenson R. B. Thomson M. M. Traczewski J. D. Turnidge. 2012. *Methods for Dilution Antimicrobial Susceptibility Tests for Bacteria That Grow Aerobically ; Approved Standard — Ninth Edition*. *Methods for Dilution Antimicrobial Susceptibility Tests for Bacteria That Grow Aerobically; Approved Standar- Ninth Edition*. Vol. 32. https://doi.org/10.4103/0976-237X.91790.

Madsen, Jonas Stenløkke, Mette Burmølle, Lars Hestbjerg Hansen, and Søren Johannes Sørensen. 2012. “The Interconnection between Biofilm Formation and Horizontal Gene Transfer.” *FEMS Immunology and Medical Microbiology* 65 (2): 183–95. https://doi.org/10.1111/j.1574-695X.2012.00960.x.

Mah, Thien-Fah. 2014. “Establishing the Minimal Bactericidal Concentration of an Antimicrobial Agent for Planktonic Cells (MBC-P) and Biofilm Cells (MBC-B).” *Journal of Visualized Experiments*, no. 83. https://doi.org/10.3791/50854.

Mainau, E, D Temple, and X Manteca. 2014. “Welfare Issues Related to Mastitis in Dairy Cows.” *The Farm Animal Welfare Fact Sheet*, no. September.

Małaczewska, Joanna, and Edyta Kaczorek-Łukowska. 2021. “Nisin—A Lantibiotic with Immunomodulatory Properties: A Review.” *Peptides* 137 (December 2020). https://doi.org/10.1016/j.peptides.2020.170479.

Malcolm, Karl, David Woolfson, Julie Russell, Paul Tallon, Liam Mcauley, and Duncan Craig. 2003. “I Nfluence of Silicone Elastomer Solubility and Diffusivity on the in Vitro Release of Drugs from Intravaginal Rings” 90: 217–25.

Manyi-Loh, Christy, Sampson Mamphweli, Edson Meyer, and Anthony Okoh. 2018. *Antibiotic Use in Agriculture and Its Consequential Resistance in Environmental Sources: Potential Public Health Implications*. *Molecules*. Vol. 23. https://doi.org/10.3390/molecules23040795.

Marsh, P. D. 2004. “Dental Plaque as a Microbial Biofilm.” In *Caries Research*. https://doi.org/10.1159/000077756.

Mataraci, Emel, and Sibel Dosler. 2012. “In Vitro Activities of Antibiotics and Antimicrobial Cationic Peptides Alone and in Combination against Methicillin-Resistant Staphylococcus Aureus Biofilms.” *Antimicrobial Agents and Chemotherapy* 56 (12): 6366–71. https://doi.org/10.1128/AAC.01180-12.

McAuliffe, O., Ross, R. P., Hill, C. 2001. “Lantibiotics: Biosynthesis and Mode of Action.” *Chemical Reviews* 105 (2): 633–83. https://doi.org/10.1021/cr030105v.

McDougall, S., K. I. Parker, C. Heuer, and C. W R Compton. 2009. “A Review of Prevention and Control of Heifer Mastitis via Non-Antibiotic Strategies.” *Veterinary Microbiology* 134 (1–2): 177–85. https://doi.org/10.1016/j.vetmic.2008.09.026.

Mehuys, Els. 2004. “DEVELOPMENT OF A MATRIX-IN-CYLINDER SYSTEM FOR SUSTAINED ZERO-ORDER DRUG RELEASE.” GHENT UNIVERSITY FACULTY.

https://www.researchgate.net/publication/292349668_Development_of_a_matrix-in-cylinder_system_for_sustained_zero-order_drug_release.

Mekonnen, S. A., G. Koop, S. T. Melkie, C. D. Getahun, H. Hogeveen, and T. J.G.M. Lam. 2017. "Prevalence of Subclinical Mastitis and Associated Risk Factors at Cow and Herd Level in Dairy Farms in North-West Ethiopia." *Preventive Veterinary Medicine* 145: 23–31. https://doi.org/10.1016/j.prevetmed.2017.06.009.

Melchior, M. B. 2011. "Biofilms and Veterinary Medicine" 6. https://doi.org/10.1007/978-3-642-21289-5.

Melchior, M. B., H. Vaarkamp, and J. Fink-Gremmels. 2006. "Biofilms: A Role in Recurrent Mastitis Infections?" *Veterinary Journal* 171 (3): 398–407. https://doi.org/10.1016/j.tvjl.2005.01.006.

Meletiadis, Joseph, Spyros Pournaras, Emmanuel Roilides, and Thomas J. Walsh. 2010. "Defining Fractional Inhibitory Concentration Index Cutoffs for Additive Interactions Based on Self-Drug Additive Combinations, Monte Carlo Simulation Analysis, and in Vitro-in Vivo Correlation Data for Antifungal Drug Combinations against Aspergillus Fumi." *Antimicrobial Agents and Chemotherapy* 54 (2): 602–9. https://doi.org/10.1128/AAC.00999-09.

Metcalfe, Lucy. 2016. "Mastitis and the Link to Infertility." *Veterinary Ireland Journal* 6 (2): 95–100.

Middleton, John R., Anne Saeman, Larry K. Fox, Jason Lombard, Joe S. Hogan, and K. Larry Smith. 2014. "The National Mastitis Council: A Global Organization for Mastitis Control and Milk Quality, 50 Years and Beyond." *Journal of Mammary Gland Biology and Neoplasia* 19 (3–4): 241–51. https://doi.org/10.1007/s10911-014-9328-6.

Moon, Jin San, Hee Kyung Kim, Hye Cheong Koo, Yi Seok Joo, Hyang Mi Nam, Yong Ho Park, and Mun Il Kang. 2007. "The Antibacterial and Immunostimulative Effect of Chitosan-Oligosaccharides against Infection by Staphylococcus Aureus Isolated from Bovine Mastitis." *Applied Microbiology and Biotechnology* 75 (5): 989–98. https://doi.org/10.1007/s00253-007-0898-8.

Moran, John. 2015. "Managing Cow Lactation Cycles - The Cattle Site." 2015.

http://www.thecattlesite.com/articles/4248/managing-cow-lactation-cycles/.

More, Simon J., Tracy A. Clegg, and Finola McCoy. 2017. “The Use of National-Level Data to Describe Trends in Intramammary Antimicrobial Usage on Irish Dairy Farms from 2003 to 2015.” *Journal of Dairy Science* 100 (8): 6400–6413. https://doi.org/10.3168/jds.2016-12068.

Mulley, Geraldine, A. Tobias A. Jenkins, and Nicholas R. Waterfield. 2014. “Inactivation of the Antibacterial and Cytotoxic Properties of Silver Ions by Biologically Relevant Compounds.” *PLoS ONE* 9 (4): 2–10. https://doi.org/10.1371/journal.pone.0094409.

Nagasawa, Yuya, Yoshio Kiku, Kazue Sugawara, Fuyuko Tanabe, and Tomohito Hayashi. 2018. “Exfoliation Rate of Mammary Epithelial Cells in Milk on Bovine Mastitis Caused by Staphylococcus Aureus Is Associated with Bacterial Load.” *Animal Science Journal* 89 (1): 259–66. https://doi.org/10.1111/asj.12886.

Nallapareddy, Sreedhar R., Kavindra V. Singh, Jouko Sillanpää, Danielle A. Garsin, Magnus Höök, Stanley L. Erlandsen, and Barbara E. Murray. 2006. “Endocarditis and Biofilm-Associated Pili of Enterococcus Faecalis.” *Journal of Clinical Investigation*. https://doi.org/10.1172/JCI29021.

Namasivayam, SKR, M Preethi, ARS Bharani - Int J Biol Pharm Res, and Undefined 2012. 2012. “Biofilm Inhibitory Effect of Silver Nanoparticles Coated Catheter against Staphylococcus Aureus and Evaluation of Its Synergistic Effects with Antibiotics.” *Ijbpr* 3 (2): 259–65.

Nebel, R.L., and M.L. McGilliard. 1993. “Interactions of High Milk Yield and Reproductive Performance in Dairy Cows.” *Journal of Dairy Science*. https://doi.org/10.3168/jds.S0022-0302(93)77662-6.

“New Multi-Partner Trust Fund Launched to Combat Antimicrobial Resistance Globally.” 2019. Press Release, Noordwijk, the Netherlands. 2019. https://www.who.int/news-room/detail/19-06-2019-new-multi-partner-trust-fund-launched-to-combat-antimicrobial-resistance-globally.

Nicholas, D. Stebbins, A. Ouimet Michelle, and E. Uhrich Kathryn. 2014. “Antibiotic-Containing Polymers for Localized, Sustained Drug Delivery.” *Advanced Drug Delivery Reviews* 1 (848): 77–87. https://doi.org/10.1016/j.addr.2014.04.006.Antibiotic-containing.

Nickerson, S. C., and R. M. Akers. 2011. “Mammary Gland: Anatomy.” *Encyclopedia of Dairy Sciences: Second Edition*, no. September: 328–37. https://doi.org/10.1016/B978-0-12-374407-4.00290-9.

Nielsen, Lars K., Gordon K. Smyth, and Paul F. Greenfield. 1991. “Hemacytometer Cell Count Distributions: Implications of Non???Poisson Behavior.” *Biotechnology Progress*. https://doi.org/10.1021/bp00012a600.

Nouraei, Mehdi. 2018. “Modeling, Designing and Evaluating Fully Dilutable Self Microemulsifying Delivery System for Hydrophobic Pharmaceuticals and Nutraceuticals.” *ProQuest Dissertations and Theses*, 187. http://ezproxy.puc.cl/dissertations-theses/modeling-designing-evaluating-fully-dilutable/docview/2148289769/se-2?accountid=16788%0Ahttp://todosibuc.uc.cl/openurl/56PUC_INST/56PUC_INST_SP?url_ver=Z39.88-2004&rft_val_fmt=info:ofi/fmt:kev:mtx:dissertation&ge.

O’Brien, Bernadette. 2008. *Moorepark Dairy Levy Research Update Milk Quality Handbook Practical Steps to Improve Milk Quality Moorepark Dairy Levy Update*. www.teagasc.ie.

———. 2016. “Mastitis and SCC.” Moorepark Dairy Levy Research Update Milk Quality Handbook Practical Steps to Improve Milk Quality Moorepark Dairy Levy Update. Teagasc. 2016. https://www.teagasc.ie/media/website/animals/dairy/MilkQandMastitis.pdf.

O’Flaherty, S., Aidan Coffey, W. J. Meaney, G. F. Fitzgerald, and R. P. Ross. 2005. “Inhibition of Bacteriophage K Proliferation on Staphylococcus Aureus in Raw Bovine Milk.” *Letters in Applied Microbiology*. https://doi.org/10.1111/j.1472-765X.2005.01762.x.

O’Toole, George A. 2011. “Microtiter Dish Biofilm Formation Assay.” *Journal of Visualized Experiments*, no. 47: 10–11. https://doi.org/10.3791/2437.

Padmavathy, Nagarajan, and Rajagopalan Vijayaraghavan. 2008. “Enhanced Bioactivity of ZnO Nanoparticles - An Antimicrobial Study.” *Science and Technology of Advanced Materials* 9 (3). https://doi.org/10.1088/1468-6996/9/3/035004.

Palou, Lluís, Asgar Ali, Elazar Fallik, and Gianfranco Romanazzi. 2016. “GRAS, Plant- and Animal-Derived Compounds as Alternatives to Conventional Fungicides for the Control

of Postharvest Diseases of Fresh Horticultural Produce." *Postharvest Biology and Technology* 122: 41–52. https://doi.org/https://doi.org/10.1016/j.postharvbio.2016.04.017.

Pandian, Sureshbabu Ram Kumar, Venkataraman Deepak, Kaliniulliu Kalishwaralal, Pushpa Viswanathan, and Gurunathan Sangiliyandi. 2010. "Mechanism of Bactericidal Activity of Silver Nitrate - A Concentration Dependent Bi-Functional Molecule." *Brazilian Journal of Microbiology* 41 (3): 805–9. https://doi.org/10.1590/S1517-83822010000300033.

Pantanella, Fabrizio, Piera Valenti, Alessandra Frioni, Tiziana Natalizi, Luana Coltella, and Francesca Berlutti. 2008. "BioTimer Assay , a New Method for Counting Staphylococcus Spp . in Bio Fi Lm without Sample Manipulation Applied to Evaluate Antibiotic Susceptibility of Bio Fi Lm." *Journal of Microbiological Methods* 75 (3): 478–84. https://doi.org/10.1016/j.mimet.2008.07.027.

Pantani, Roberto, Giuliana Gorrasi, Giovanni Vigliotta, Marius Murariu, and Philippe Dubois. 2013. "PLA-ZnO Nanocomposite Films: Water Vapor Barrier Properties and Specific End-Use Characteristics." *European Polymer Journal* 49 (11): 3471–82. https://doi.org/10.1016/j.eurpolymj.2013.08.005.

Park, Hye, Min Hong, Sun Hwang, Yong Young Park, Ka Kwon, Jang Yoon, Sook Shin, Jae Kim, and Yong Young Park. 2014. "Characterisation of Pseudomonas Aeruginosa Related to Bovine Mastitis." *Acta Veterinaria Hungarica* 62 (1): 1–12. https://doi.org/10.1556/AVet.2013.054.

Pasquet, Julia, Yves Chevalier, Emmanuelle Couval, Dominique Bouvier, Gaëlle Noizet, Cécile Morlière, and Marie Alexandrine Bolzinger. 2014. "Antimicrobial Activity of Zinc Oxide Particles on Five Micro-Organisms of the Challenge Tests Related to Their Physicochemical Properties." *International Journal of Pharmaceutics* 460 (1–2): 92–100. https://doi.org/10.1016/j.ijpharm.2013.10.031.

Pasquet, Julia, Yves Chevalier, Jocelyne Pelletier, Emmanuelle Couval, Dominique Bouvier, and Marie Alexandrine Bolzinger. 2014. "The Contribution of Zinc Ions to the Antimicrobial Activity of Zinc Oxide." *Colloids and Surfaces A: Physicochemical and Engineering Aspects* 457 (1): 263–74. https://doi.org/10.1016/j.colsurfa.2014.05.057.

Patil, Hemlata, Roshan V. Tiwari, and Michael A. Repka. 2016. “Hot-Melt Extrusion: From Theory to Application in Pharmaceutical Formulation.” *AAPS PharmSciTech* 17 (1): 20–42. https://doi.org/10.1208/s12249-015-0360-7.

Peeters, Elke, Hans J Nelis, and Tom Coenye. 2008. “Comparison of Multiple Methods for Quantification of Microbial Biofilms Grown in Microtiter Plates” 72: 157–65. https://doi.org/10.1016/j.mimet.2007.11.010.

Poizat, A., F. Bonnet-Beaugrand, A. Rault, C. Fourichon, and N. Bareille. 2017. “Antibiotic Use by Farmers to Control Mastitis as Influenced by Health Advice and Dairy Farming Systems.” *Preventive Veterinary Medicine* 146 (January): 61–72. https://doi.org/10.1016/j.prevetmed.2017.07.016.

Polat, B., A. Colak, M. Cengiz, L.E. E Yanmaz, H. Oral, A. Bastan, S. Kaya, and A. Hayirli. 2010. “Sensitivity and Specificity of Infrared Thermography in Detection of Subclinical Mastitis in Dairy Cows.” *Journal of Dairy Science* 93 (8): 3525–32. https://doi.org/10.3168/jds.2009-2807.

Pormohammad, Ali, Dylan Greening, and Raymond J. Turner. 2022. “Synergism Inhibition and Eradication Activity of Silver Nitrate/Potassium Tellurite Combination against Pseudomonas Aeruginosa Biofilm.” *Journal of Antimicrobial Chemotherapy* 77 (6): 1635–44. https://doi.org/10.1093/jac/dkac094.

Porter, J., J. Anderson, L. Carter, E. Donjacour, and M. Paros. 2016. “In Vitro Evaluation of a Novel Bacteriophage Cocktail as a Preventative for Bovine Coliform Mastitis.” *Journal of Dairy Science* 99 (3): 2053–62. https://doi.org/10.3168/jds.2015-9748.

Prabhu, Sukumaran, and Eldho K Poulose. 2012. “Silver Nanoparticles : Mechanism of Antimicrobial Action , Synthesis , Medical Applications , and Toxicity Effects.” *International Nano Letters 2012,* 2: 1–10. https://doi.org/10.1186/2228-5326-2-32.

Pro-lab Diagnostics. 2012. “Microbank ™,” 1–2. https://doi.org/10.1128/JCM.00654-08.

Qin, Caiqin, Huirong Li, Qi Xiao, Yi Liu, Juncheng Zhu, and Yumin Du. 2006. “Water-Solubility of Chitosan and Its Antimicrobial Activity.” *Carbohydrate Polymers* 63 (3): 367–74. https://doi.org/10.1016/j.carbpol.2005.09.023.

Rahmatpour, Samaneh, Mehran Shirvani, Mohammad R. Mosaddeghi, Farshid Nourbakhsh, and Mehdi Bazarganipour. 2017. “Dose–response Effects of Silver Nanoparticles and Silver Nitrate on Microbial and Enzyme Activities in Calcareous Soils.” *Geoderma* 285: 313–22. https://doi.org/10.1016/j.geoderma.2016.10.006.

RAJADHYAX, ARCHANA, UJWALA SHINDE, HARITA DESAI, and SHRUSHTI MANE. 2021. “Hot Melt Extrusion in Engineering of Drug Cocrystals: A Review.” *Asian Journal of Pharmaceutical and Clinical Research* 14 (8): 10–19. https://doi.org/10.22159/ajpcr.2021.v14i8.41857.

Rajala-Schultz, P.J., Y.T. Gröhn, and C.E. McCulloch. 1999. “Effects of Milk Fever, Ketosis, and Lameness on Milk Yield in Dairy Cows.” *Journal of Dairy Science*. https://doi.org/10.3168/jds.S0022-0302(99)75235-5.

Rampersad, Sephra N. 2012. “Multiple Applications of Alamar Blue as an Indicator of Metabolic Function and Cellular Health in Cell Viability Bioassays.” *Sensors (Switzerland)* 12 (9): 12347–60. https://doi.org/10.3390/s120912347.

Reshi, Ahamad Arif, Ishraq Husain, S A Bhat, Muneeb U Rehman, Rahil Razak, S Bilal, and Manzoor R Mir. 2015. “Bovine Mastitis as an Evolving Disease and Its Impact on the Dairy Industry.” *International Journal of Current Research and Review* 7 (5): 48–55.

Rollema Hs, Kuipers Op, Both P, de Vos Wm, and Siezen Rj. 1995. “Improvement of Solubility and Stability of the Antimicrobial Peptide Nisin by Protein Engineering.” *Applied and Environmental Microbiology* 61 (8): 2873–78.

Romanazzi, Gianfranco, Franka Mlikota Gabler, Dennis Margosan, Bruce E. MacKey, and Joseph L. Smilanick. 2009. “Effect of Chitosan Dissolved in Different Acids on Its Ability to Control Postharvest Gray Mold of Table Grape.” *Phytopathology* 99 (9): 1028–36. https://doi.org/10.1094/PHYTO-99-9-1028.

Rosa, Luigi, Antimo Cutone, Monica Coletti, Maria Stefania Lepanto, Mellani Scotti, Piera Valenti, Giammarco Raponi, Maria Cristina Ghezzi, and Francesca Berlutti. 2017. “Biotimer Assay : A Reliable and Rapid Method for the Evaluation of Central Venous Catheter Microbial Colonization.” *Journal of Microbiological Methods* 143 (July): 20–25. https://doi.org/10.1016/j.mimet.2017.09.016.

Rosa, Luigi, Maria Stefania Lepanto, Antimo Cutone, Francesca Berlutti, Massimiliano De Angelis, Vincenzo Vullo, Claudio Maria Mastroianni, Piera Valenti, and Alessandra Oliva. 2019. “BioTimer Assay as Complementary Method to Vortex-Sonication- Vortex Technique for the Microbiological Diagnosis of Implant Associated Infections,” no. April: 1–10. https://doi.org/10.1038/s41598-019-44045-1.

Royster, Erin, and Sarah Wagner. 2015. “Treatment of Mastitis in Cattle.” *Veterinary Clinics of North America - Food Animal Practice* 31 (1): 17–46. https://doi.org/10.1016/j.cvfa.2014.11.010.

Ruhr, E., and H. G. Sahl. 1985. “Mode of Action of the Peptide Antibiotic Nisin and Influence on the Membrane Potential of Whole Cells and on Cytoplasmic and Artificial Membrane Vesicles.” *Antimicrobial Agents and Chemotherapy* 27 (5): 841–45. https://doi.org/10.1128/AAC.27.5.841.

Russell, A. D., and W. B. Hugo. 1994. “Antimicrobial Activity and Action of Silver.” *Progress in Medicinal Chemistry* 31 (C): 351–70. https://doi.org/10.1016/S0079-6468(08)70024-9.

Saglam, Aliye Gülmez, Mitat Sahin, Elif Çelik, Özgür Çelebi, Dogan Akça, and Salih Otlu. 2017. “The Role of Staphylococci in Subclinical Mastitis of Cows and Lytic Phage Isolation against to Staphylococcus Aureus.” *Veterinary World* 10 (12): 1481–85. https://doi.org/10.14202/vetworld.2017.1481-1485.

Saied, Habibian Dehkordi, Hosseinpour Fatemeh, and Ebrahimi Kahrizangi Azizollah. 2011. “An in Vitro Evaluation of Antibacterial Effect of Silver Nanoparticles on Staphylococcus Aureus Isolated from Bovine Subclinical Mastitis.” *African Journal of Biotechnology* 10 (52): 10795–97. https://doi.org/10.5897/AJB11.1499.

Salahpour Anarjan, Fatemeh. 2019. “Active Targeting Drug Delivery Nanocarriers: Ligands.” *Nano-Structures and Nano-Objects* 19: 100370. https://doi.org/10.1016/j.nanoso.2019.100370.

Salman, Halah Dawood. 2017. “Journal of Global Pharma Technology Evaluation and Comparison the Antibacterial Activity of Silver Nano Particles (AgNPs) and Silver Nitrate (AgNO3) on Some Pathogenic Bacteria.” *Journal of Global Pharma Technology* 10 (9): 238–48.

Sandberg, Malena E., Denise Schellmann, Gerda Brunhofer, Thomas Erker, Igor Busygin, Reko Leino, Pia M. Vuorela, and Adyary Fallarero. 2009. “Pros and Cons of Using Resazurin Staining for Quantification of Viable Staphylococcus Aureus Biofilms in a Screening Assay.” *Journal of Microbiological Methods* 78 (1): 104–6. https://doi.org/10.1016/j.mimet.2009.04.014.

Sangani, Mohammad Hassani, Mahboobeh Nakhaei Moghaddam, and Mohammad Mahdi Forghanifard. 2015. “Inhibitory Effect of Zinc Oxide Nanoparticles on Pseudomonas Aeruginosa Biofilm Formation Inhibition of Biofilm Formation by Zinc Oxide Nanoparticles.” *Nanomed J* 2 (2): 121–28. http://nmj.mums.ac.ir.

Sarker, Swapan Chandra, Mst Sonia Parvin, A. K.M.Anisur Rahman, and Md Taohidul Islam. 2013. “Prevalence and Risk Factors of Subclinical Mastitis in Lactating Dairy Cows in North and South Regions of Bangladesh.” *Tropical Animal Health and Production* 45 (5): 1171–76. https://doi.org/10.1007/s11250-012-0342-7.

Sarode, Ashish L., Harpreet Sandhu, Navnit Shah, Waseem Malick, and Hossein Zia. 2013. “Hot Melt Extrusion (HME) for Amorphous Solid Dispersions: Predictive Tools for Processing and Impact of Drug-Polymer Interactions on Supersaturation.” *European Journal of Pharmaceutical Sciences* 48 (3): 371–84. https://doi.org/10.1016/j.ejps.2012.12.012.

Savić, N. R., D. P. Mikulec, and R. S. Radovanović. 2017. “Somatic Cell Counts in Bulk Milk and Their Importance for Milk Processing.” *IOP Conference Series: Earth and Environmental Science* 85 (1). https://doi.org/10.1088/1755-1315/85/1/012085.

Schalm, O. W., and D. O. Noorlander. 1957. “Experiments and Observations Leading to Development of the California Mastitis Test.” *Jour Amer Vet Med Assoc*.

Schlich, Karsten, Martin Hoppe, Marco Kraas, Jonas Schubert, Munish Chanana, and Kerstin Hund-Rinke. 2018. “Long-Term Effects of Three Different Silver Sulfide Nanomaterials, Silver Nitrate and Bulk Silver Sulfide on Soil Microorganisms and Plants.” *Environmental Pollution* 242: 1850–59. https://doi.org/https://doi.org/10.1016/j.envpol.2018.07.082.

Schmidt, G H, and L D Van Vleck. 1974. *Principles of Dairy Science.* San Francisco: W.H. Freeman and Company. https://www.cabdirect.org/cabdirect/abstract/19740112089.

Seegers, Henri, Christine Fourichon, and François Beaudeau. 2003. “Production Effects

Related to Mastitis and Mastitis Economics in Dairy Cattle Herds." *Veterinary Research*. https://doi.org/10.1051/vetres:2003027.

Shah, Dimpalkumar, Mariam Naciri, Paul Clee, and Mohamed Al-Rubeai. 2006. "NucleoCounter - An Efficient Technique for the Determination of Cell Number and Viability in Animal Cell Culture Processes." *Cytotechnology* 51 (1): 39–44. https://doi.org/10.1007/s10616-006-9012-9.

Shanmugam, Annaian, Kandasamy Kathiresan, and Lakshman Nayak. 2016. "Preparation, Characterization and Antibacterial Activity of Chitosan and Phosphorylated Chitosan from Cuttlebone of Sepia Kobiensis (Hoyle, 1885)." *Biotechnology Reports* 9: 25–30. https://doi.org/10.1016/j.btre.2015.10.007.

Shelley, A. W., H. C. Deeth, and I. C. MacRae. 1987. "Review of Methods of Enumeration, Detection and Isolation of Lipolytic Microorganisms with Special Reference to Dairy Applications." *Journal of Microbiological Methods* 6 (3): 123–37. https://doi.org/10.1016/0167-7012(87)90008-X.

Shin, J.M., J.W. Gwak, Pachiyappan Kamarajan, J.C. Fenno, A.H. Rickard, and Y.L. Kapila. 2016. "Biomedical Applications of Nisin." *Journal of Applied Microbiology* 120 (6): 1449–65. https://doi.org/10.1111/jam.13033.

Shin, Seung Heon, Mi Kyung Ye, Hae Sic Kim, and Hyung Suk Kang. 2007. "The Effects of Nano-Silver on the Proliferation and Cytokine Expression by Peripheral Blood Mononuclear Cells." *International Immunopharmacology* 7 (13): 1813–18. https://doi.org/10.1016/j.intimp.2007.08.025.

Shivaee, Ali, Sajad Rajabi, Hamed Eraghiye Farahani, and Abbas Ali Imani Fooladi. 2021. "Effect of Sub-Lethal Doses of Nisin on Staphylococcus Aureus Toxin Production and Biofilm Formation." *Toxicon* 197 (March): 1–5. https://doi.org/10.1016/j.toxicon.2021.03.018.

Simões, Marta F., Rui M.A. Pinto, and Sérgio Simões. 2019. "Hot-Melt Extrusion in the Pharmaceutical Industry: Toward Filing a New Drug Application." *Drug Discovery Today* 24 (9): 1749–68. https://doi.org/10.1016/j.drudis.2019.05.013.

Soest, Felix J.S. van, Inge M.G.A. Santman-Berends, Theo J.G.M. Lam, and Henk Hogeveen.

2016. “Failure and Preventive Costs of Mastitis on Dutch Dairy Farms.” *Journal of Dairy Science* 99 (10): 8365–74. https://doi.org/10.3168/jds.2015-10561.

Solano, Cristina, Maite Echeverz, and Iñigo Lasa. 2014. “Biofilm Dispersion and Quorum Sensing.” *Current Opinion in Microbiology*. https://doi.org/10.1016/j.mib.2014.02.008.

Stockert, Juan C, Alfonso Blázquez-Castro, Magdalena Cañete, Richard W Horobin, and Ángeles Villanueva. 2012. “MTT Assay for Cell Viability: Intracellular Localization of the Formazan Product Is in Lipid Droplets.” *Acta Histochemica* 114 (8): 785–96. https://doi.org/https://doi.org/10.1016/j.acthis.2012.01.006.

Stoodley, P., K. Sauer, D. G. Davies, and J. W. Costerton. 2002. “Biofilms as Complex Differentiated Communities.” *Annual Review of Microbiology* 56 (1): 187–209. https://doi.org/10.1146/annurev.micro.56.012302.160705.

Sumon, S M M R, M A Ehsan, and M T Islam. 2017. “Subclinical Mastitis in Dairy Cows: Somatic Cell Counts and Associated Bacteria in Mymensingh, Bangladesh.” *J Bangladesh Agril Univ* 15 (2): 266–71. https://doi.org/10.3329/jbau.v15i2.35073.

Sun, Fengjun, Feng Qu, Yan Ling, Panyong Mao, Peiyuan Xia, Huipeng Chen, and Dongsheng Zhou. 2013. “Biofilm-Associated Infections: Antibiotic Resistance and Novel Therapeutic Strategies.” *Future Microbiology* 8 (7): 877–86. https://doi.org/10.2217/fmb.13.58.

Sutherland, I. W. 2001. “Biofilm Exopolysaccharides: A Strong and Sticky Framework.” *Microbiology*. https://doi.org/10.1099/00221287-147-1-3.

Tambe, Srushti, Divya Jain, Yashvi Agarwal, and Purnima Amin. 2021. “Hot-Melt Extrusion: Highlighting Recent Advances in Pharmaceutical Applications.” *Journal of Drug Delivery Science and Technology* 63 (March). https://doi.org/10.1016/j.jddst.2021.102452.

Tang, Jing, Krister Wennerberg, and Tero Aittokallio. 2015. “What Is Synergy? The Saariselkä Agreement Revisited.” *Frontiers in Pharmacology* 6 (SEP). https://doi.org/10.3389/fphar.2015.00181.

Thakkar, Rishi, Ruchi Thakkar, Amit Pillai, Eman A. Ashour, and Michael A. Repka. 2020. “Systematic Screening of Pharmaceutical Polymers for Hot Melt Extrusion Processing: A Comprehensive Review.” *International Journal of Pharmaceutics* 576 (January): 118989.

https://doi.org/10.1016/j.ijpharm.2019.118989.

Thompson-Crispi, Kathleen, Heba Atalla, Filippo Miglior, and Bonnie A. Mallard. 2014. “Bovine Mastitis: Frontiers in Immunogenetics.” *Frontiers in Immunology* 5 (OCT): 1–10. https://doi.org/10.3389/fimmu.2014.00493.

Thorberg, B. M., Inger Kühn, Frank Møller Aarestrup, Boel Brändström, Per Jonsson, and Marie Louise Danielsson-Tham. 2006. “Pheno- and Genotyping of Staphylococcus Epidermidis Isolated from Bovine Milk and Human Skin.” *Veterinary Microbiology* 115 (1–3): 163–72. https://doi.org/10.1016/j.vetmic.2006.01.013.

Thorne, Fiona, Emma Dillon, Trevor Donnellan, Kevin Hanrahan, Thia Hennessy, Anne Kinsella, Doris Laepple, and Michael Mckeon. 2015. *A Review of the Financial Status of Irish Farms and Future Investment Requirements*.

Tomasinsig, Linda, Gennyfer De Conti, Barbara Skerlavaj, Renata Piccinini, Maria Mazzilli, Francesca D’Este, Alessandro Tossi, and Margherita Zanetti. 2010. “Broad-Spectrum Activity against Bacterial Mastitis Pathogens and Activation of Mammary Epithelial Cells Support a Protective Role of Neutrophil Cathelicidins in Bovine Mastitis.” *Infection and Immunity* 78 (4): 1781–88. https://doi.org/10.1128/IAI.01090-09.

Tong, Zhongchun, Yuejiao Zhang, Junqi Ling, Jinglei Ma, Lijia Huang, and Luodan Zhang. 2014. “An in Vitro Study on the Effects of Nisin on the Antibacterial Activities of 18 Antibiotics against Enterococcus Faecalis.” *PLoS ONE* 9 (2). https://doi.org/10.1371/journal.pone.0089209.

Torres, Nelson S., Daniel Montelongo-Jauregui, Johnathan J. Abercrombie, Anand Srinivasan, Jose L. Lopez-Ribot, Anand K. Ramasubramanian, and Kai P. Leung. 2018. “Antimicrobial and Antibiofilm Activity of Synergistic Combinations of a Commercially Available Small Compound Library with Colistin against Pseudomonas Aeruginosa.” *Frontiers in Microbiology* 9 (OCT): 1–12. https://doi.org/10.3389/fmicb.2018.02541.

Tripura, TK, SC Sarker, SK Roy, MS Parvin, RR Sarker, AKMA Rahman, and MT Islam. 2014. “Prevalence of Subclinical Mastitis in Lactating Cows and Efficacy of Intramammary Infusion Therapy.” *Bangladesh Journal of Veterinary Medicine* 12 (1). https://doi.org/10.3329/bjvm.v12i1.20464.

U.S. Food & Drug Administraion. 2019. “CFR - Code of Federal Regulations Title 21.” https://www.accessdata.fda.gov/scripts/cdrh/cfdocs/cfcfr/CFRSearch.cfm?fr=182.8991
.

Valde, J. P., L. G. Lawson, A. Lindberg, J. F. Agger, H. Saloniemi, and O. Østerås. 2004. “Cumulative Risk of Bovine Mastitis Treatments in Denmark, Finland, Norway and Sweden.” *Acta Veterinaria Scandinavica*. https://doi.org/10.1186/1751-0147-45-201.

Vanderhaeghen, Wannes, Sofie Piepers, Frédéric Leroy, Els Van Coillie, Freddy Haesebrouck, and Sarne De Vliegher. 2015. “Identification, Typing, Ecology and Epidemiology of Coagulase Negative Staphylococci Associated with Ruminants.” *Veterinary Journal* 203 (1): 44–51. https://doi.org/10.1016/j.tvjl.2014.11.001.

Ventola, C Lee. 2015. “The Antibiotic Resistance Crisis: Part 1: Causes and Threats.” *P & T : A Peer-Reviewed Journal for Formulary Management (2015)* 40 (4): 277–83. https://doi.org/Article.

Veroli, Giovanni Y. Di, Chiara Fornari, Dennis Wang, Séverine Mollard, Jo L. Bramhall, Frances M. Richards, and Duncan I. Jodrell. 2016. “Combenefit: An Interactive Platform for the Analysis and Visualization of Drug Combinations.” *Bioinformatics* 32 (18): 2866–68. https://doi.org/10.1093/bioinformatics/btw230.

Viguier, Caroline, Sushrut Arora, Niamh Gilmartin, Katherine Welbeck, and Richard O’Kennedy. 2009. “Mastitis Detection: Current Trends and Future Perspectives.” *Trends in Biotechnology* 27 (8): 486–93. https://doi.org/10.1016/j.tibtech.2009.05.004.

Vipul, Vora, Biswajit Basu, R. Neslihan Gursoy, Simon Benita, Christopher A. Lipinski, Franco Lombardo, Beryl W. Dominy, et al. 2013. “Hydrophilic Thermoplastic Polyurethanes for the Manufacturing of Highly Dosed Oral Sustained Release Matrices via Hot Melt Extrusion and Injection Molding.” *European Journal of Pharmaceutics and Biopharmaceutics* 82 (1): 214–21. https://doi.org/10.1016/j.ijpharm.2016.04.057.

Wagner, Christof, Sara Aytac, and G. Maria Hänsch. 2011. “Biofilm Growth on Implants: Bacteria Prefer Plasma Coats.” *International Journal of Artificial Organs* 34 (9): 811–17. https://doi.org/10.5301/ijao.5000061.

Watkins, Richard R., and Robert A. Bonomo. 2016. “Overview: Global and Local Impact of

Antibiotic Resistance." *Infectious Disease Clinics of North America* 30 (2): 313–22. https://doi.org/10.1016/j.idc.2016.02.001.

Wells, S.J., S.L. Ott, and A. Hillberg Seitzinger. 1998. "Key Health Issues for Dairy Cattle—New and Old." *Journal of Dairy Science* 81 (11): 3029–35. https://doi.org/10.3168/jds.S0022-0302(98)75867-9.

WHO. 2014. "Antimicrobial Resistance. Global Report on Surveillance." *World Health Organization* 61 (3): 383–94. https://doi.org/10.1007/s13312-014-0374-3.

Wiedemann, Imke, Eefjan Breukink, Cindy Van Kraaij, Oscar P. Kuipers, Gabriele Bierbaum, Ben De Kruijff, and Hans Georg Sahl. 2001. "Specific Binding of Nisin to the Peptidoglycan Precursor Lipid II Combines Pore Formation and Inhibition of Cell Wall Biosynthesis for Potent Antibiotic Activity." *Journal of Biological Chemistry* 276 (3): 1772–79. https://doi.org/10.1074/jbc.M006770200.

Wiegand, Irith, Kai Hilpert, and Robert E W Hancock. 2008. "Agar and Broth Dilution Methods to Determine the Minimal Inhibitory Concentration (MIC) of Antimicrobial Substances." *Nature Protocols* 3 (2): 163–75. https://doi.org/10.1038/nprot.2007.521.

Wilkins, Matthew, Luanne Hall-Stoodley, Raymond N. Allan, and Saul N. Faust. 2014. "New Approaches to the Treatment of Biofilm-Related Infections." *Journal of Infection*. https://doi.org/10.1016/j.jinf.2014.07.014.

Willey, Joanne M., and Wilfred A. van der Donk. 2007. "Lantibiotics: Peptides of Diverse Structure and Function." *Annual Review of Microbiology* 61 (1): 477–501. https://doi.org/10.1146/annurev.micro.61.080706.093501.

Wilson, David J., and Rubén N. González. 2003. "Vaccination Strategies for Reducing Clinical Severity of Coliform Mastitis." *Veterinary Clinics of North America - Food Animal Practice* 19 (1): 187–97. https://doi.org/10.1016/S0749-0720(02)00070-1.

Wittebole, Xavier, Sophie De Roock, and Steven M. Opal. 2014. "A Historical Overview of Bacteriophage Therapy as an Alternative to Antibiotics for the Treatment of Bacterial Pathogens." *Virulence* 5 (1): 209–18. https://doi.org/10.4161/viru.25991.

Wooten, David J., and Réka Albert. 2021. "Synergy: A Python Library for Calculating, Analyzing

and Visualizing Drug Combination Synergy." *Bioinformatics* 37 (10): 1473–74. https://doi.org/10.1093/bioinformatics/btaa826.

Wooten, David J., Christian T. Meyer, Alexander L.R. Lubbock, Vito Quaranta, and Carlos F. Lopez. 2021. "MuSyC Is a Consensus Framework That Unifies Multi-Drug Synergy Metrics for Combinatorial Drug Discovery." *Nature Communications* 12 (1). https://doi.org/10.1038/s41467-021-24789-z.

Wooten, David, Christian Meyer, Vito Quaranta, and Carlos Lopez. 2019. "A Consensus Framework Unifies Multi-Drug Synergy Metrics." https://doi.org/10.1101/683433.

World Health Organistaion. 2015. "Global Action Plan on Antimicrobial Resistance." *Microbe Magazine* 10 (9): 354–55. https://doi.org/10.1128/microbe.10.354.1.

———. 2020. "WHO | UN Interagency Coordination Group (IACG) on Antimicrobial Resistance." *WHO*. https://www.who.int/antimicrobial-resistance/interagency-coordination-group/en/.

World Health Organization. 2019. "Antibacterial Agents in Preclinical Development." *Annual Report in Medicinal Chemistry*, 1–20.

Wu, Junqiang, Songhua Hu, and Liting Cao. 2007. "Therapeutic Effect of Nisin Z on Subclinical Mastitis in Lactating Cows." *Antimicrobial Agents and Chemotherapy* 51 (9): 3131–35. https://doi.org/10.1128/AAC.00629-07.

Wu, Yunbo, Ye Ying, Yuhong Liu, Haijiang Zhang, and Jianying Huang. 2018. "Preparation of Chitosan/Poly Vinyl Alcohol Films and Their Inhibition of Biofilm Formation against Pseudomonas Aeruginosa PAO1." *International Journal of Biological Macromolecules* 118: 2131–37. https://doi.org/10.1016/j.ijbiomac.2018.07.061.

Wylie, Matthew P., Nicola J. Irwin, David Howard, Katie Heydon, and Colin P. McCoy. 2021. "Hot-Melt Extrusion of Photodynamic Antimicrobial Polymers for Prevention of Microbial Contamination." *Journal of Photochemistry and Photobiology B: Biology* 214 (June 2020): 112098. https://doi.org/10.1016/j.jphotobiol.2020.112098.

Xie, Yanping, Yiping He, Peter L. Irwin, Tony Jin, and Xianming Shi. 2011. "Antibacterial Activity and Mechanism of Action of Zinc Oxide Nanoparticles against Campylobacter Jejuni."

Applied and Environmental Microbiology 77 (7): 2325–31. https://doi.org/10.1128/AEM.02149-10.

Yadav, Bhagwan, Krister Wennerberg, Tero Aittokallio, and Jing Tang. 2015. "Searching for Drug Synergy in Complex Dose-Response Landscapes Using an Interaction Potency Model." *Computational and Structural Biotechnology Journal* 13: 504–13. https://doi.org/10.1016/j.csbj.2015.09.001.

Yamazaki, K., M. Murakami, Y. Kawai, N. Inoue, and T. Matsuda. 2000. "Use of Nisin for Inhibition of Alicyclobacillus Acidoterrestris in Acidic Drinks." *Food Microbiology* 17 (3): 315–20. https://doi.org/10.1006/fmic.1999.0309.

Yang, Shih Chun, Chih Hung Lin, Calvin T. Sung, and Jia You Fang. 2014. "Antibacterial Activities of Bacteriocins: Application in Foods and Pharmaceuticals." *Frontiers in Microbiology* 5 (MAY): 1–10. https://doi.org/10.3389/fmicb.2014.00241.

Yoon, Hyun Joong, Myoung E. Moon, Haeng Soon Park, Suhn Young Im, and Young Ho Kim. 2007. "Chitosan Oligosaccharide (COS) Inhibits LPS-Induced Inflammatory Effects in RAW 264.7 Macrophage Cells." *Biochemical and Biophysical Research Communications* 358 (3): 954–59. https://doi.org/10.1016/j.bbrc.2007.05.042.

Zaghloul, Rashed. 2015. "Comparison of Antibacterial Activity of Fungal Chitosan and Some Preservatives Against Some Foodborne Pathogenic Bacteria." *Egyptian Journal of Microbiology* 50 (1): 31–42. https://doi.org/10.21608/ejm.2015.233.

Zeryehun, T., T. Aya, and R. Bayecha. 2013. "Study on Prevalence, Bacterial Pathogens and Associated Risk Factors of Bovine Mastitis in Small Holder Dairy Farms in and around Addis Ababa, Ethiopia." *Journal of Animal and Plant Sciences* 23 (1): 50–55. https://doi.org/10.1016/j.cub.2009.07.007.

Zgoda, J.R. R, and J.R. R Porter. 2001. "A Convenient Microdilution Method for Screening Natural Products against Bacteria and Fungi." *Pharmaceutical Biology* 39 (3): 221–25. https://doi.org/10.1076/phbi.39.3.221.5934.

Zheng, Liuhai, Yuanyuan Xu, Jinye Lu, Ming Liu, Bin Dai, Jinfeng Miao, and Yulong Yin. 2016. "Variant Innate Immune Responses of Mammary Epithelial Cells to Challenge by Staphylococcus Aureus, Escherichia Coli and the Regulating Effect of Taurine on These

Bioprocesses.” *Free Radical Biology and Medicine* 96: 166–80. https://doi.org/10.1016/j.freeradbiomed.2016.04.022.